SPECTRO-ELECTROCHEMICAL STUDIES ON LUMINESCENT COMPLEXES

LESLEY J. YELLOWLEES

PhD THESIS

UNIVERSITY OF EDINBURGH

1982

For my Family

DECLARATION

Except where specific reference is made to other sources, the work presented in this thesis is the original work of the author. It has not been submitted, in whole or in part, for any other degree. Certain of the results have already been published.

Lesley J. Yellowlees

ACKNOWLEDGEMENTS

I am deeply indebted to Dr G.A. Heath for his constant enthusiasm, encouragement and assistance throughout this work. I also wish to express my thanks to those whose help in countless ways made this work possible:

Dr P.S. Braterman of Glasgow University, our collaborator, for his substantial contribution to this work;

Dr A. Harriman of The Royal Institution, London, for recording the absorption spectrum of $*[Ru(bipy)_3]^{2+}$;

Glasgow University and Napier College of Commerce and Technology for access to their equipment;

Mr V. Coombe for the initial preparation and characterisation of iridium complexes;

the technical and academic staff and students of Edinburgh University Chemistry Department for advice and encouragement;

my parents and Peter without whose unfailing support this thesis would never have been completed.

I recall with gratitude the helpful discussions of Professor E.A.V. Ebsworth during the summer of 1980.

I am also grateful to the Science and Engineering Research Council for financial assistance and to the University of Edinburgh for the use of their facilities.

Finally, my thanks to Jean Kerr for typing this manuscript.

ABSTRACT

This thesis is devoted to the characterisation of redox-active metal-coordination complexes containing the M-bipy chromophore, where M = metal and bipy = 2,2'-bipyridine. Their electronic structural formulations have been closely defined by comparative examination of their absorption spectra in sequences of one-electron related oxidation states. We have found that such a series of related complexes offers a far greater chance of successful analysis of the absorption spectra than if the spectra are approached in isolation.

The redox changes were generally achieved by controlled electrogeneration using an optically transparent thin layer electrode (O.T.T.L.E.) directly placed in the spectrophotometer beam, so that the absorption spectra of the unstable low-oxidation state complexes could be unambiguously recorded. It was found necessary to develop such 'spectroelectrochemical techniques' because of the extreme sensitivity to oxygen of the reduced complexes.

In particular, we have shown that for reduced metal-bipyridyl complexes the spectroelectrochemical results can only be rationalised using a trapped-electron model; for example the tris-bipy complexes should be formulated as follows: $[M(bipy)_3]^{z+} = [M(bipy^{o})_3]^{z+}$, $[M(bipy)_3]^{(z-1)+} = [M(bipy^{o})_2(bipy^{-})]^{(z-1)+}$, $[M(bipy)_3]^{(z-2)+} = [M(bipy^{o})(bipy^{-})_2]^{(z-2)+}$, $[M(bipy)_3]^{(z-3)+} =$

$[M(bipy^-)_3]^{(z-3)+}$. Thus we infer that in $[M(bipy)_3]^{z+}$ and $[M(bipy)_2L_2]^{2+}$ complexes the bipy ligands are non-interacting.

We also discuss the metal-to-ligand charge transfer excited state of $[Ru(bipy)_3]^{2+}$ in which we find the optically transferred electron to be exclusively located on one ligand; best formulated as $*[Ru(III)(bipy^o)_2(bipy^-)]^{2+}$. This complex is, therefore, an example of a symmetric D_3 ground state complex giving rise to a highly unsymmetric excited state.

The detailed analysis of characteristic electrode potentials (for metal-based versus ligand-based reductions) and the spectroscopic recognition of $bipy^o$ and $bipy^-$ chromophores have provided complementary and consistent electronic structural elucidations, from which molecular orbital energy diagrams can be usefully constructed, and a simple correlation between central metal charge and ligand-based reduction potentials can be identified.

CONTENTS

LIST OF FIGURES

CHAPTER 5

CHAPTER 6

LIST OF TABLES

CHAPTER 1

INTRODUCTORY REMARKS: ELECTRODE-MEDIATED ELECTRON TRANSFER AND INTERNAL ELECTRONIC EXCITATIONS OF TRIS-BIPYRIDYL METAL COMPLEXES

This thesis is devoted to the characterisation of a remarkable and interesting family of redox-active metal-coordination complexes. Their electronic structural formulations have been closely defined by comparative examination of their absorption spectra in sequences of one-electron related oxidation states. These redox changes are generally achieved by controlled electro-generation and the detailed analysis of the corresponding electrode potentials has been of considerable importance in mapping their electronic structure.

For metal coordination complexes, as for other molecules, the electronic valence structure is generally expressed in terms of an array of independent two-electron 'orbitals', which are filled progressively by the appropriate number of electrons to yield the ground state electronic configuration. The highest occupied molecular orbital and lowest unoccupied molecular orbital in this array are sometimes termed the 'frontier orbitals'. This picture of strictly defined (quantized) occupied and unoccupied levels immediately implies the possibility of specific electronic transitions, which should occur at discrete excitation energies. Comprehensive

assignments of the various bands which may appear in the absorption spectrum of a transition metal complex is notoriously difficult because the considerable complexity of the electronic structure is only partly revealed in the observed spectrum. Thus, a unique electronic model can only be rarely determined from the available data.

In the specific area of transition-metal coordination compounds, it is helpful, though not entirely rigorous, to categorize the nature of the prominent electronic excitations in a quite simple way as 'ligand-based' or 'metal-based' or 'charge transfer' in origin as defined below:

i transitions between molecular orbitals predominantly localised on the metal centre, almost invariably concerning 'd-d transitions' otherwise referred to as ligand field transitions;

ii transitions between molecular orbitals predominantly localised on the ligands, frequently referred to as ligand-centred or intraligand transitions, and almost invariably involving π-π^* excitations; and

iii transitions between molecular orbitals of different localisation which cause the displacement of the electronic charge from the ligands to the metal or vice-versa. These transitions are generally called charge transfer (CT) transitions and more specifically can be distinguished into ligand-to-

metal charge transfer (LMCT) and metal-to-ligand charge transfer (MLCT) transitions[1].

With the increased acceptance of the delocalised molecular orbital view of coordination compounds these distinctions are in most instances an approximation.

Both the position and intensity are fundamentally important in characterising the absorption band. A ground-state molecular orbital energy diagram, populated with the appropriate number of electrons, should be very useful in predicting possible electronic transitions and may even give a semiquantitative estimation of transition energies. However, since transitions span both the ground and excited states such a diagram is ultimately inadequate for describing the geometry or lifetime or probability relative to photon-absorption and emission.

The intensity of a band is determined largely from selection rules, with more intense bands arising from transitions which are both spin and orbitally allowed. Thus bands arising from d-d transitions, which are orbitally forbidden, are orders of magnitude less intense than electronically allowed intraligand and charge-transfer transitions. For an allowed charge transfer transition to show an appreciable intensity, it must also have significant 'one-centre character'; for example a MLCT transition requires for intensity, that the nominally metal-based donor orbital should have some 'ligand character' (which is expected anyway on the basis of our commonplace understanding of molecular orbital-based

delocalisation or 'covalency' of the metal-ligand coordinate bond). In this way, the transition acquires some 'ligand/ligand' (one-centre) character. Thus the intense bands in the absorption spectra of coordinated metal complexes are highly characteristic of individual metal-ligand combinations and should reflect: (a) their propensity for molecular orbital delocalisation; and (b) the relative energies of the metal and ligand orbital arrays.

The interpretation of absorption spectra is much improved if single crystal anisotropic studies are used. Sadly, however, these are not often available and furthermore analysis still requires exacting analysis of the molecular orbitals involved in the transition. Such studies have therefore frequently proved more controversial than definitive[2], and the uv-visible solution spectra of inorganic compounds would be generally regarded as offering far less structural information than, for example, infrared or nmr spectra. In contrast, as this thesis relates, we have been able to make evidently unambiguous and detailed electronic structural formulations of complexes in a sequence of redox states sharing a common gross molecular structure, largely by dint of comparative absorption spectroscopy.

The chance to compare the spectra of complexes with differing electronic populations means that the nature of the frontier orbitals of the initial compound can be

mapped by progressive electron injection or removal. We have found that such a series of related complexes offers a far greater chance of successful analysis than has hitherto been the situation where one approaches the assignment in isolation; that is from one spectrum.

In particular, we have studied metal tris-bipyridyl complexes, consciously taking advantage of the opportunity to explore the range of stable oxidation states implied by their voltammetric behaviour. Determination of the corresponding electrode potentials provides an independent method of mapping the energies of the redox-active orbitals. Clearly there is a relationship between the internal transfer of an electron from the HOMO to LUMO by absorption of a photon and electron transfer involving an external electrode (Figure 1). The characteristic gap

FIGURE 1: Spectral/electrochemical correlations for frontier orbitals[a]

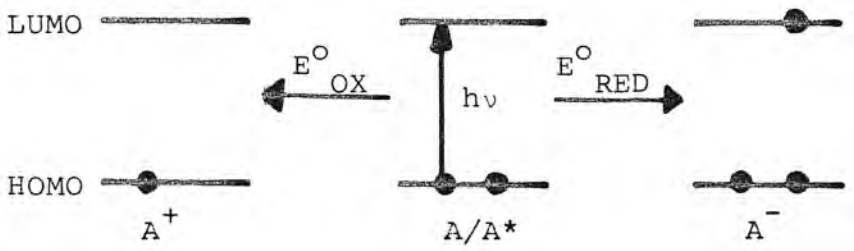

[a]LUMO = lowest unoccupied molecular orbital; HOMO = highest occupied molecular orbital.

spanned by excitation hν should also be reflected in the separation of electrode potentials for the first one-

electron oxidation and reduction steps; that is we expect hν to be related to $E_{RED}-E_{OX}$. In metal bipyridyl complexes we frequently encounter an oxidisable metal centre combined with the reducible ligand, which is just the recipe for a charge transfer transition. Thus, on oxidation we should map the energy of the metal-based HOMO and on reduction the energy of the ligand-based LUMO.

In the course of this work, very successful molecular orbital energy schemes consistent with the redox behaviour and charge transfer spectra have been constructed for these complexes by the complementary use of spectroscopic and electrochemical data. However, it is necessary to take particular note of an intrinsic difference between the two techniques. The photon absorption event, is generally described as a 'vertical' transition, which involves the immediate excited state, in which the electronically excited molecule still retains its ground state geometry (and is thus vibrationally excited), whereas the electrode potential data have thermodynamic significance and refer on all occasions to the thermally equilibrated molecules.

Thus, although molecular orbital energy schemes are very useful when envisaging electron transfer processes, more rigorous discussion should involve overall State Diagrams which represent the energetic relationship between the various states or "Spectroscopic Terms' of the molecule as a whole. Furthermore, when geometric

relaxation processes are important we must consider potential energy surfaces (one for each electronic configuration) where the energy of each state is mapped as a function of distortion coordinates. A plane section of such a surface is, of course, the familiar Morse curve.

These intensely absorbing and reversibly redox-active metal tris-bipyridyl complexes are, in general, luminescent. In principle longevity of the optically excited states offers the possibility of harnessing radiant energy and converting it to chemical energy because the excited molecule can undergo an electron or energy transfer reaction with a suitable quencher rather than relaxing by luminescence.

In this context, the complex tris-bipyridine ruthenium(II), $[Ru(bipy)_3]^{2+}$, has received the most attention. Hitherto, in spite of a great deal of research and analysis, no instinctively persuasive picture had emerged as to the reason for its long-lived excited state. In $[Ru(bipy)_3]^{2+}$, the much discussed optical excitation is acknowledged to involve transfer of an electron to the ligand set; that is, to an acceptor orbital which is essentially ligand in character. In this thesis it is demonstrated that the transferred electron is exclusively located on one ligand. Thus, remarkably the excitation of a symmetric D_3 complex can give rise to a highly unsymmetric excited state which

we regard as a significant factor in its longevity.

The popularity of the molecular orbital treatment of octahedral complexes has meant that in the excited state of tris-bipyridyl metal complexes it was assumed the promoted electron was transferred to ligand-based molecular orbitals uniformly distributed over all three ligands. Our own studies show that this is diametrically opposed to the actual situation of tris-bipy complexes and we believe that the significance of these results extends beyond this family of complexes.

Equally, we expect there to be metal-coordination complexes with a high degree of interligand delocalisation and we look forward to the identification of complexes which provide as clear cut an example of delocalised behaviour as tris-bipy complexes are an example of localised behaviour. Ultimately, then, one might hope to define the factors governing mutual interactions of ligands.

The first influential review of the coordination chemistry of the 2,2'-bipyridyl (bipy) chelating ligand was in 1954 by Brandt, Dwyer and Gyarfas[3]. Since then many reports of their properties have appeared in different branches of physical and inorganic chemistry. Stable bipy complexes are found for a wide variety of metals[4] and the tris-complexes adhere, in most cases, to a pseudo octahedral symmetry.

One of the most striking properties of bipy is its

ability to stabilise central metal low-oxidation states which, from a modern perspective, is readily attributed to the propensity of bipy to $d\pi \rightarrow \pi^*$ back-bonding. Thus in some tris-bipy metal complexes the $bipy^o$ ligands stabilise reductions of the metal ion as in the example of the redox series:

$$[Cr(III)(bipy^o)_3]^{3+} \rightarrow [Cr(II)(bipy^o)_2]^{2+} \rightarrow [Cr(I)bipy^o)_3]^{1+} \rightarrow [Cr(0)(bipy^o)_3]^{o}$$

$$d^3 \qquad\qquad d^4 \qquad\qquad d^5 \qquad\qquad d^6$$

However efficient back-bonding also implies that bipy has a low-lying acceptor orbital and hence sometimes we observe the reduction of the ligand itself, as for example in $[A\ell(III)(bipy^-)_3]^{o}$ [5] or in the continuation of the above redox series:

$$[Cr(0)(bipy^o)_3]^{o} \rightarrow [Cr(0)(bipy^o)_2(bipy^-)]^{1-} \rightarrow [Cr(0)(bipy^o)(bipy^-)_2]^{2-} \rightarrow [Cr(0)(bipy^-)_3]^{3-}$$

In our hands, the analysis of characteristic electrode potentials (for metal-based versus ligand-based reductions), and the spectroscopic recognition of $bipy^o$ and $bipy^-$ chromophores have provided complementary and consistent electronic structural elucidation. The effectiveness of the spectroscopic monitoring of low oxidation states in our work owes a great deal to the development of in situ 'spectrochemical techniques' employing a transparent electrode directly placed in the spectrophotometer beam.

REFERENCES

1. A.B.P. Lever, 'Inorganic Electronic Spectroscopy'; Elsevier Publishing Company, Amsterdam, 1968.

2. F. Felix, J. Ferguson, H.U. Gudel and A. Ludi; J. Am. Chem. Soc., 102, 4096 (1980).

3. W.W. Brandt, F.P. Dwyer and E.C. Gyarfas; Chem. Rev. 54, 959 (1954).

4. W.R. McWhinnie and J.D Miller; Adv. Inorg. Chem. and Radio Chem., 12, 134 (1969).

5. Y. Torii, S. Murasato and Y. Kaizu, Nippon Kagaku Zasshi, 91, 549 (1970).

CHAPTER 2

ABSORPTION SPECTRAL STUDIES (35,000 to 7,000 cm^{-1}) OF REDUCED TRIS-BIPYRIDINE COMPLEXES OF RUTHENIUM(II) AND IRIDIUM(III)

The photochemical, photophysical and luminescent properties of the tris-bipyridine ruthenium(II) cation, $[Ru(bipy)_3]^{2+}$, has been the subject of much attention in recent years[1-10]. Much of the work on this complex has been undertaken in search of potential solar energy conversion systems because of its spectral properties, the long life-time of the photo-excited state and the ease with which the complex undergoes oxidation and reduction.

The dye $[Ru(bipy)_3]^{2+}$ can convert light into chemical energy as shown in Equation 1. Absorption of visible

$$[Ru(bipy)_3]^{2+} + Eu^{2+} \xrightarrow{h\nu} [Ru(bipy)_3]^{+} + Eu^{3+} \qquad (1)$$

light produces a long-lived excited state, $*[Ru(bipy_3]^{2+}$, which is a strong oxidising agent, due to a hole in the metal valence core, and also a reducing agent, due to the promoted electron. The excited complex then reacts efficiently with suitable quenchers, such as europium(II), Eu^{2+}, to give reactive intermediates $[Ru(bipy)_3]^{+}$ and Eu^{3+} [11,12]. Equally, excited state $*[Ru(bipy)_3]^{2+}$ can be oxidatively quenched, for example by paraquat, PQ^{2+}, to give reactive intermediates $[Ru(bipy)_3]^{3+}$ and PQ^{+} [13,14]. Essentially then the radiation is pumping the system away from equilibrium, thereby converting light into chemical energy.

One of the potentially important aspects of $[Ru(bipy)_3]^{2+}$ is that excited state $*[Ru(bipy)_3]^{2+}$ is thermodynamically capable of splitting water (Scheme 1)[15].

Scheme 1: Splitting water by $[Ru(bipy)_3]^{2+}$

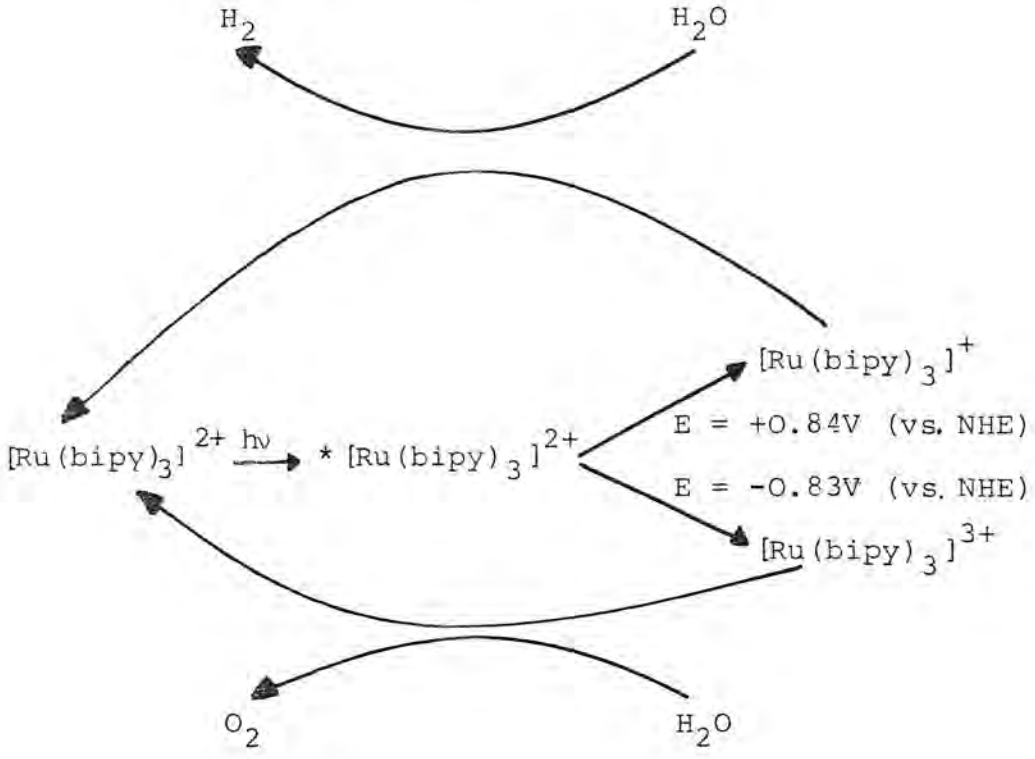

The excited state (produced by absorption of light by $[Ru(bipy)_3]^{2+}$) disproportionates to $[Ru(bipy)_3]^{+}$ and $[Ru(bipy)_3]^{3+}$ [16], which then react with water to give dihydrogen and dioxygen respectively. Although this process is thermodynamically feasible it is not efficient kinetically and only proceeds via many one-electron steps in the presence of catalysts[17-19]. Interestingly, $[Ru(bipy)_3]^{o}$ which is a two-electron donor reacts with water to give hydrogen directly[20].

Much of the interest in $[Ru(bipy)_3]^{2+}$ is directly attributable to the low-lying long-lived excited state $*[Ru(bipy)_3]^{2+}$. The ground state is fairly well understood, however the excited state requires further clarification. Although the excited state is sufficiently long-lived to undergo electron- and energy-transfer reactions it is too transient to be easily characterised by conventional means. An aspect of this thesis is the attempt to model the excited state using related ground-state species which can be characterised by spectro-electrochemistry. Direct consideration of the excited state $*[Ru(bipy)_3]^{2+}$ is taken up in Chapter 5.

This chapter is concerned with $[Ru(bipy)_3]^{2+}$ and isoelectronic $[Ir(bipy)_3]^{3+}$, and with the spectroscopic changes that accompany their stepwise one-electron reductions.

Tris-bipyridyl ruthenium(II)

In ruthenium tris-bipyridine $[Ru(bipy)_3]^{2+}$, I, the central ion has a diamagnetic electronic configuration broadly represented by $d\pi^6$. The complex shows a rich redox

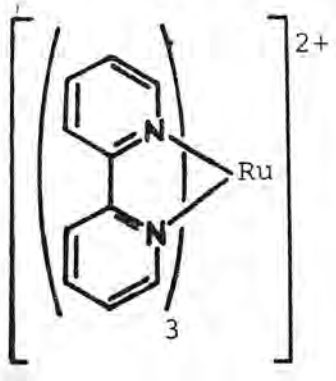

≡ I

chemistry, and voltammetric studies have established an extended sequence of reversible reduction steps at narrowly spaced potentials as well as one reversible oxidation (Table 1, Figure 1)[21,22].

Previous studies have focused on identifying the type of orbital each additional electron enters, whether essentially localised on the metal ion (within the d orbital manifold) or on the ligands (involving the π^* orbitals). Substitution of one or more bipy ligands by alternative bidentate nitrogen donors related to bipy results in little or no change in the $\underline{I}^{o/+}$ oxidation potential whereas the reduction behaviour is strongly influenced[23]. Thus it is believed that a metal $d\pi$ electron is removed by electrochemical oxidation whereas the electrons added to the complex in electrochemical reduction occupy ligand π^* orbitals. ESR evidence is also strongly indicative that the added electrons enter ligand π^* orbitals[24]. Whether such electrons are delocalised in molecular orbitals spanning all three ligands (Figure 2A) or whether they are each trapped in a π^* orbital localised on one ligand (Figure 2B) was still to be resolved. Notice that the localised description implies, perhaps unexpectedly, that the charge distribution in $\underline{I}^-$ (and $\underline{I}^{2-}$) is asymmetric unless rapid electron hopping makes the two models converge. The molecular orbital diagrams (Figure 2) illustrate the highest filled and lowest empty orbitals for the two cases. Figure 2A shows the scheme applicable for D_3 complexes ($\underline{I}$ belongs to this symmetry class[25]). Such

TABLE 1: ELECTRODE POTENTIALS FOR $\underline{I}$

$$[Ru(bipy)_3]^{3+} \xleftarrow{+0.96^a} [Ru(bipy)_3]^{2+} \xrightarrow{-1.66} [Ru(bipy)_3]^{1+} \xrightarrow{-1.83} [Ru(bipy)_3]^{0} \xrightarrow{-2.05} [Ru(bipy)_3]^{1-}$$

$\underline{I}^{+}$ $\underline{I}$ $\underline{I}^{-}$ $\underline{I}^{2-}$ $\underline{I}^{3-}$

a E^{o}/V vs. Ag/Ag^{+}; $Ep_a - Ep_c = \Delta Ep = 65$ mV in every case; Ep_a = anodic peak potential; Ep_c = cathodic peak potential.

FIGURE 1: Cyclic voltammogram of $[Ru(bipy)_3]^{2+}$ in acetonitrile

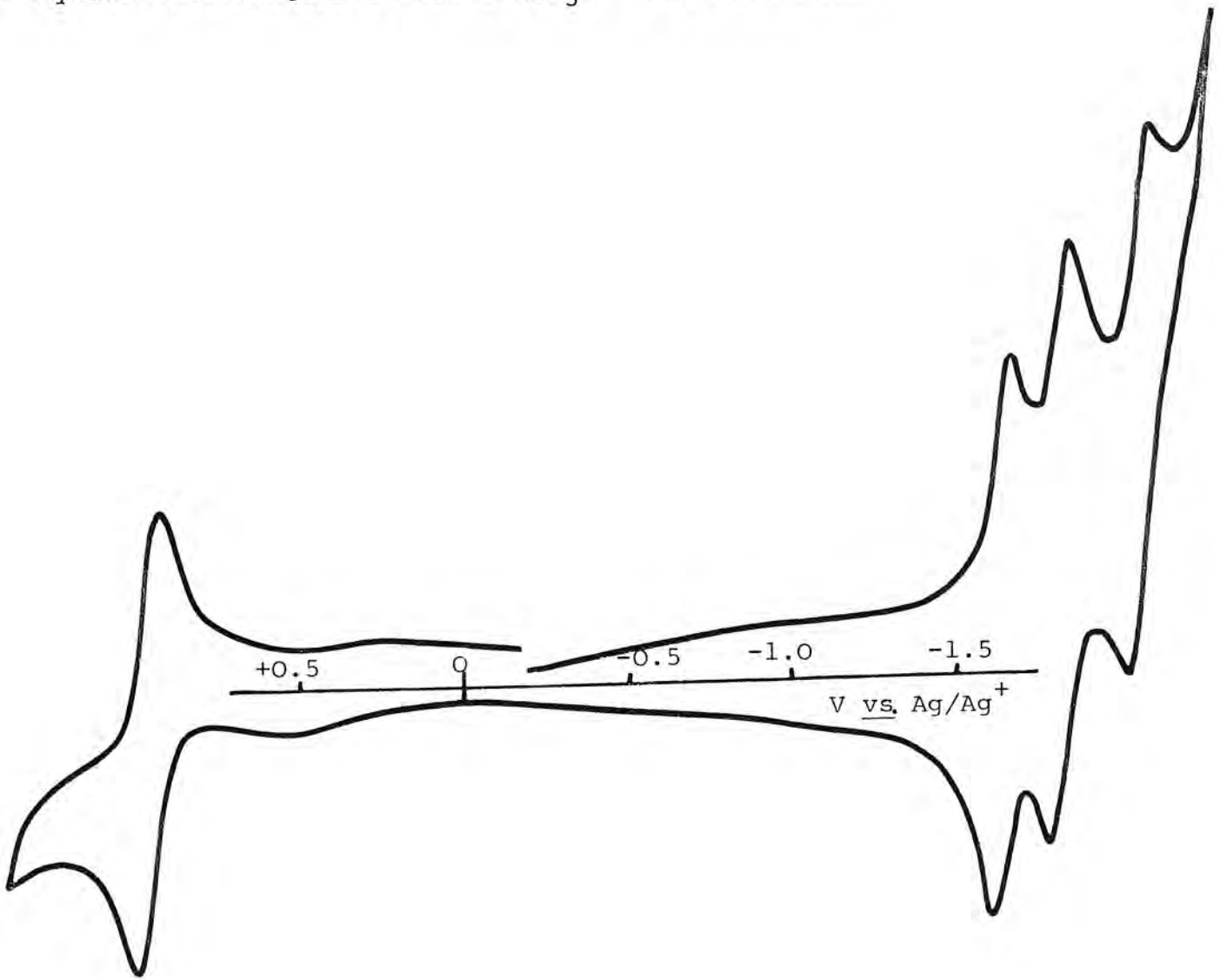

FIGURE 2: Molecular Orbital Diagrams for tris-bipy complexes

A: D_3 symmetry, delocalised model

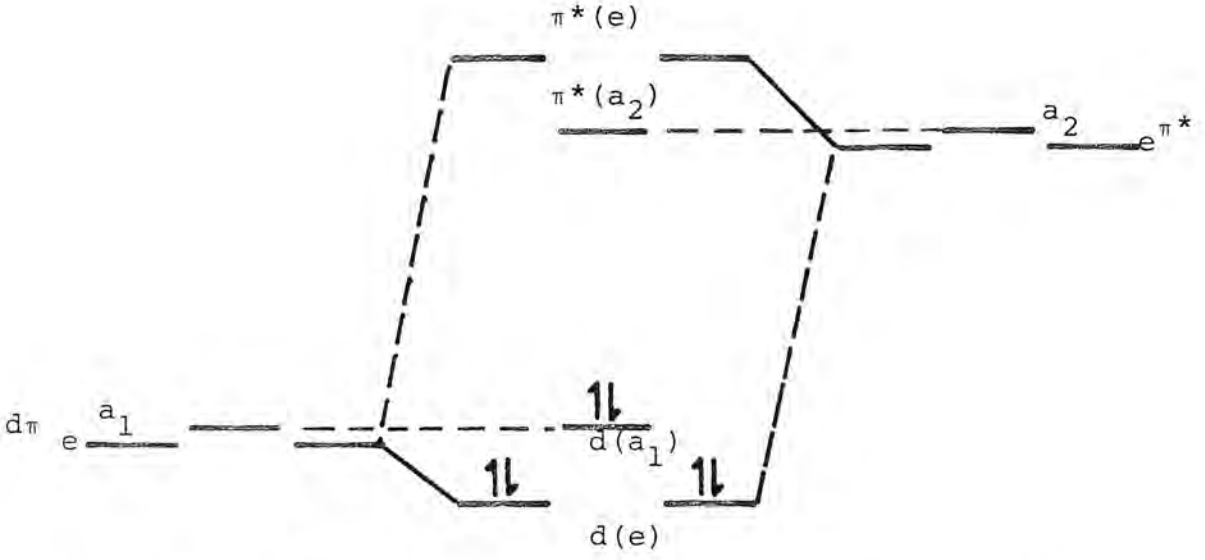

Metal Orbitals Ligand Orbitals

B: Local C_{2v} symmetry, localised model

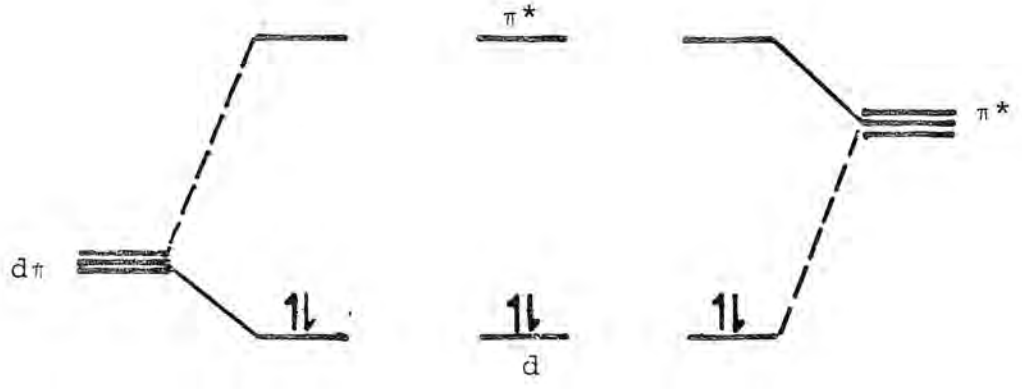

Metal Orbitals Ligand Orbitals

a diagram has been the one used until very recently to describe I and its reduced analogues[22,26,27]. Figure 2B represents the case when there is minimum interaction between the three bipy ligands[28]. This would imply that a single metal-chelate ring of local C_{2v} symmetry actually provides the characteristic chromophoric unit and redox active centre.

The absorption spectrum of I has been very extensively studied although there is still no agreement as to the exact assignment of the transitions[15,29-31]. There have been several reports of the absorption spectrum of I^- in which there are varying descriptions of the structure and origin of its intense visible absorption[11,32-35]. This is mainly because of the difficulties attending these studies, in which I^- was generated as a transient species (for example as an intermediate in the reductive quenching of *I) and characterised from the resulting difference spectra. There is one report of the absorption spectrum of electrogenerated I^- which up until now has been taken as definitive but which proves to be incorrect (vide infra)[32]. These studies are all restricted to the near-ultraviolet to visible (32,000 to 14,000 cm^{-1}) range. There are early reports of the electrogeneration of I^{2-} and I^{3-}, however no absorption spectroscopic data have been published[20,22,32].

In an effort to clarify the character of the redox-active orbitals of I, the absorption spectra of the

individual low-valent complexes $\underline{I}^{-} \rightarrow \underline{I}^{3-}$ have been determined over a wide frequency range in our laboratory. The three reduced species were isolated by electrosynthesis at controlled potentials. Firstly, however the electrochemistry of the system had to be fully characterised in a variety of solvents, at different electrode materials and in a range of temperatures. The solvents were varied to give extended potential, temperature and spectroscopic ranges and also to check there was no interaction between the complex, whether in its resting state or reduced states, and the solvent. Different electrode materials have different potential ranges and may interact with the reduced complexes to a varying degree. Altering the temperature can affect the stability of the reduced complexes, however, it can also dramatically change the electrochemistry.

A cyclic voltammogram of $\underline{I}$ in acetonitrile at room temperature on a platinum microelectrode is shown in Figure 1, peak potentials for the different waves are given in Table 1. The number of electrons involved in the electron-transfer step was determined precisely by coulometry for the oxidation wave and then by comparison of d.c. and a.c. wave heights for the three reduction waves. All four processes are confirmed to be one-electron steps. Reversible behaviour (rapid electron transfer) is observed for scan rates investigated (20 - 200 mV/s) for each of the waves. Varying the electrolyte

anion (BF_4^-, ClO_4^-, Cl^-) which is present in high concentration and using the appropriate salt of I does not affect the peak potentials. The irreversible chloride oxidation is observed before the $I^{o/+}$ oxidation[36] and hence further study of ionic chloride-containing solutions is avoided whenever possible.

Examination of the electrochemistry of I in propylene carbonate rather than acetonitrile revealed negligible change in the potentials of oxidation and the first two reductions; the third is beyond the cathodic solvent limit. In contrast dimethyl sulphoxide has a very limited positive potential range and hence the $I^{+/o}$ couple cannot be studied in this solvent. However all three reduction waves correspond closely to their position and form in acetonitrile. These results all confirm that the complex is not compromised by the solvent in any oxidation state and offer valuable freedom for pursuing spectroelectrochemical studies in differing media.

Replacing the platinum working electrode with gold, carbon or mercury makes no difference to the electrochemistry of I at any temperature investigated. It should however be remembered that the oxidation couple $I^{o/+}$ can only be studied on platinum as the other electrodes break down at sufficiently positive potentials.

In acetonitrile at $-40^{o}C$ the anodic and cathodic voltammetry peak potentials shift very slightly (40 mV) in a negative direction. A similar behaviour was noted by

Wallace and Bard[37]. This shift can be safely attributed to the temperature-induced junction potential as ferrocene's oxidation potential is found to move by the same amount. For each cyclic voltammetric wave, ΔEp decreases with decreasing temperature as expected for reversible one-electron electrode processes and diffusion-limited currents are of course smaller. A decrease in the background current and an increase in cell resistance between the working and reference electrodes are also observed at lower temperatures. Therefore although there is some shift in potentials as the temperature is altered, the spacing between adjacent redox couples remains invariant and it is in every case these separations which have intrinsic significance.

The ligand-based reductions to $\underline{I}^{-}$, $\underline{I}^{2-}$ and $\underline{I}^{3-}$ are closely spaced ($\sim$200 mV separation) but nonetheless the individual steps are resolved voltammetrically, and hence in principle each reduced species can be isolated by electrosynthesis at a precisely controlled potential at a large electrode. It would be difficult to prepare the three reduced complexes separately by any other means, however we find that they can be generated under argon in a conventional electrochemical cell. The original bright orange colour of $\underline{I}$ gives way to progressively deeper sarsparilla-brown solutions for $\underline{I}^{-}$, $\underline{I}^{2-}$ and $\underline{I}^{3-}$. The reduced species are all very air-sensitive and are oxidised instantaneously to $\underline{I}$ in the presence of oxygen. Thus, to enable unambiguous study of each reduced complex

separately, $\underline{I}^{-}$, $\underline{I}^{2-}$ and $\underline{I}^{3-}$ have been generated in the optical path of a spectrophotometer using a transparent electrode. In this case the transparent electrode was either a gold minigrid or a platinum gauze. The electrode sandwiched between quartz plates is known as an optically transparent thin-layer electrode, O.T.T.L.E.[38], and is mounted in a gas-tight teflon block (Figure 3). The cell geometry is such that only a very thin layer of solution is in contact with the electrode and exposed to the spectrophotometer beam, and in this region the reduced species are efficiently generated by rapid electrosynthesis.

The absorbance spectrum may be monitored as the complex is reduced. A typical set of curves is shown in Figure 4 for the reduction of $\underline{I}$ to $\underline{I}^{-}$. The spectra show progressive collapse of bands characterising the spectrum of $[Ru(bipy)_3]^{2+}$ and the growth of bands for the spectrum of $[Ru(bipy)_3]^{+}$. Two clear isosbestic points can be seen, implying a simple one-to-one conversion from $\underline{I}$ to $\underline{I}^{-}$. Full conversion to the reduced species is indicated by the decay of the electrosynthesis current and the achievement of a steady_state spectrum. The absorption curve for electrogenerated $\underline{I}^{-}$ described elsewhere[32] is very similar to the intermediate dotted spectrum of Figure 4, suggesting that either incomplete reduction of $\underline{I}$ to $\underline{I}^{-}$ or partial reversion of $\underline{I}^{-}$ to $\underline{I}$ had occurred. This problem is avoided using a transparent electrode in the spectrometer beam because,the controlling

FIGURE 3: Schematic representation of O.T.T.L.E.

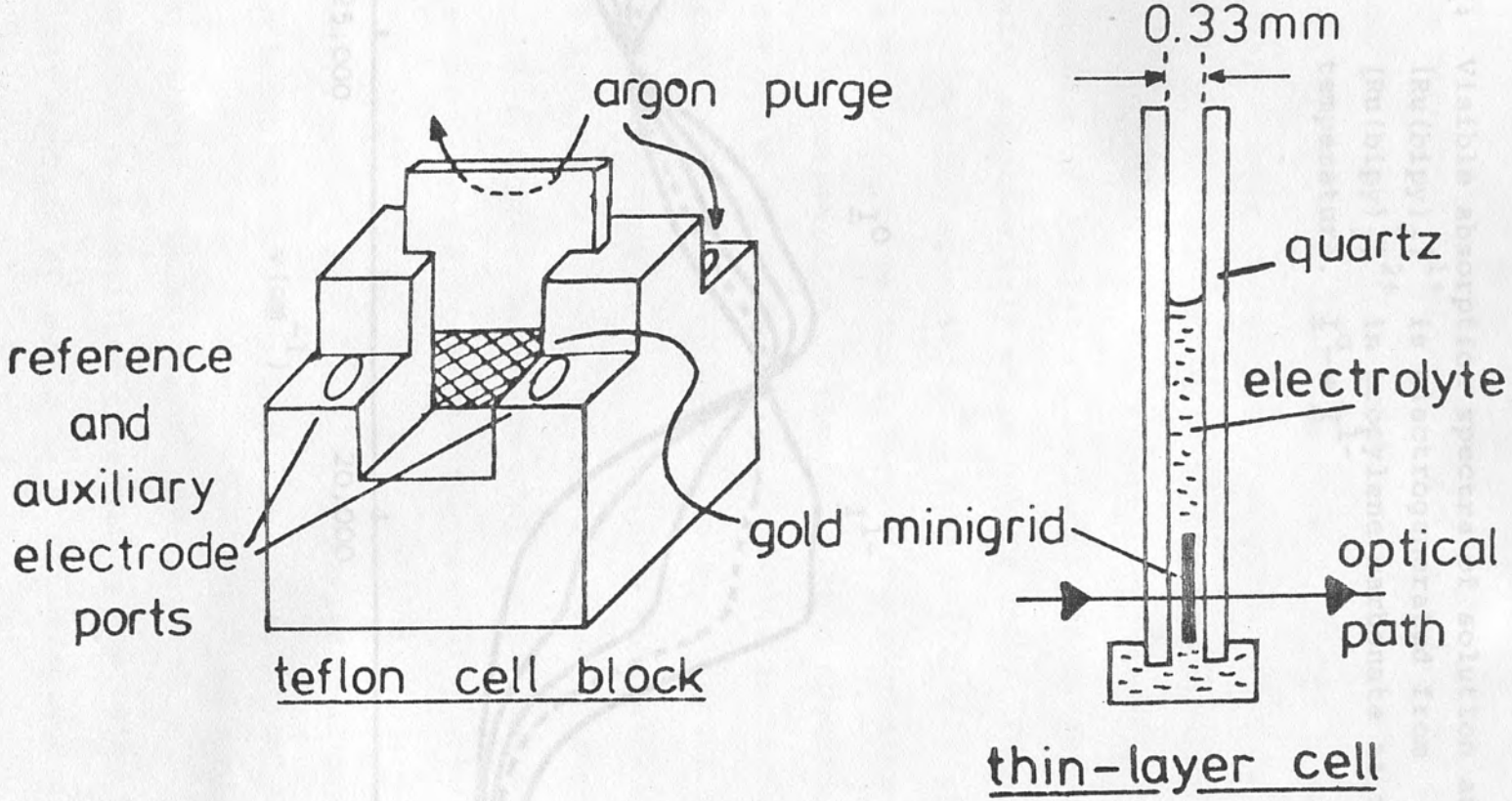

FIGURE 4: Visible absorption spectra of solution as $[Ru(bipy)_3]^{1+}$ is electrogenerated from $[Ru(bipy)_3]^{2+}$ in propylene carbonate at room temperature. $\underline{I}^{o} \rightarrow \underline{I}^{1-}$

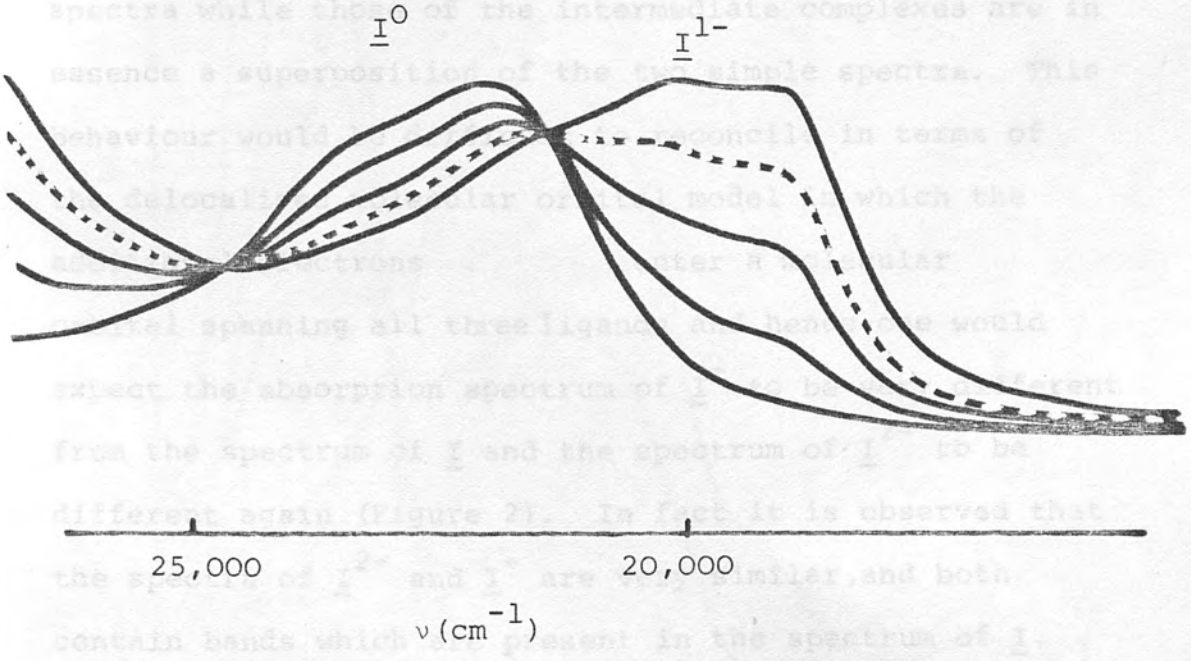

potential is applied continuously while all spectra are recorded, and the carefully designed teflon cell block does not allow ingress of oxygen or water.

The steady-state spectra for $\underline{I}$, $\underline{I}^{-}$, $\underline{I}^{2-}$ and $\underline{I}^{3-}$ generated at -1.78 V ($\underline{I}^{-}$), -2.00 V ($\underline{I}^{2-}$) and -2.30 V ($\underline{I}^{3-}$) (vs. Ag/Ag^{+}) are shown in Figure 5. The spectra were recorded over a wide spectral width, that is from 7000 cm^{-1} in the near-infrared to the ultraviolet region at around 40,000 cm^{-1}. The figure shows clearly that in this sequence of complexes some bands can be seen to be collapsing progressively while others grow. Thus $\underline{I}$ and the fully reduced species, $\underline{I}^{3-}$, have relatively simple spectra while those of the intermediate complexes are in essence a superposition of the two simple spectra. This behaviour would be difficult to reconcile in terms of the delocalised molecular orbital model in which the additional electrons enter a molecular orbital spanning all three ligands and hence one would expect the absorption spectrum of $\underline{I}^{-}$ to be very different from the spectrum of $\underline{I}$ and the spectrum of $\underline{I}^{2-}$ to be different again (Figure 2). In fact it is observed that the spectra of $\underline{I}^{2-}$ and $\underline{I}^{-}$ are very similar, and both contain bands which are present in the spectrum of $\underline{I}$.

On further examination of the spectrum of the fully reduced species a detailed resemblance was noted between it and the spectra of complexes known unambiguously to contain discrete chelated $bipy^{\cdot-}$ radical anions, for example Li bipy (Figure 6)[39]. The $bipy^{\cdot-}$ transitions in Li bipy

FIGURE 5: Absorption spectra of $[Ru(bipy)_3]^{2+/1+/0/1-}$; $\underline{I}^{0/1-/2-/3-}$ in dimethyl sulphoxide at room temperature.

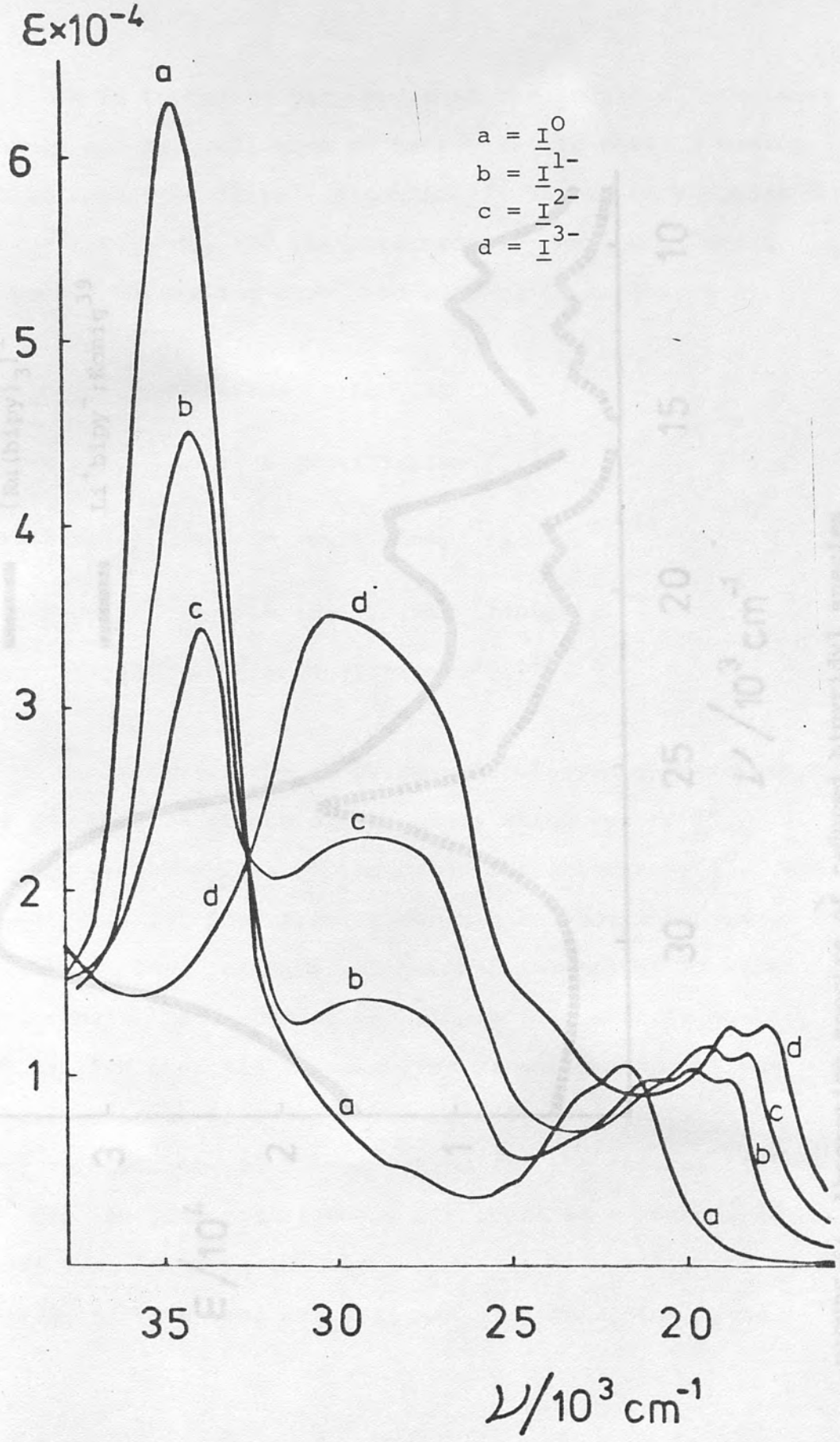

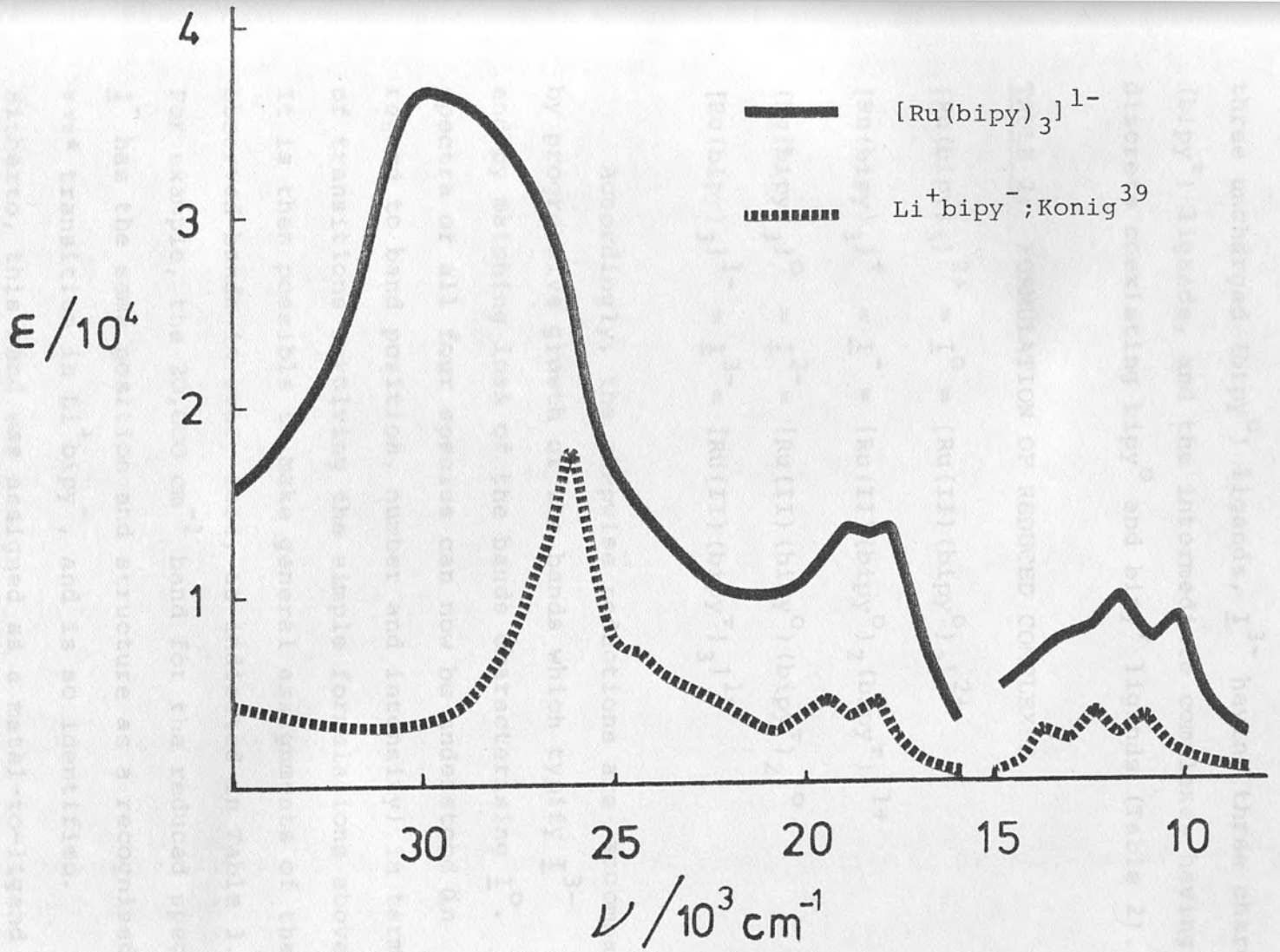

FIGURE 6: Absorption spectra of reduced bipyridyl species

are at only slightly different frequencies from those in $\underline{I}^{3-}$.

It is therefore proposed that the family of complexes should all be considered to have a Ru(II) core; $\underline{I}$ having three uncharged ($bipy^{o}$) ligands, $\underline{I}^{3-}$ having three charged ($bipy^{\cdot-}$) ligands, and the intermediate complexes having discrete coexisting $bipy^{o}$ and $bipy^{\cdot-}$ ligands (Table 2).

TABLE 2: FORMULATION OF REDUCED COMPLEXES

$[Ru(bipy)_3]^{2+} = \underline{I}^{o} = [Ru(II)(bipy^{o})_3]^{2+}$

$[Ru(bipy)_3]^{+} = \underline{I}^{-} = [Ru(II)(bipy^{o})_2(bipy^{\cdot-})]^{1+}$

$[Ru(bipy)_3]^{o} = \underline{I}^{2-} = [Ru(II)(bipy^{o})(bipy^{\cdot-})_2]^{o}$

$[Ru(bipy)_3]^{1-} = \underline{I}^{3-} = [Ru(II)(bipy^{\cdot-})_3]^{1-}$

Accordingly, the stepwise reductions are accompanied by progressive growth of the bands which typify $\underline{I}^{3-}$ and by matching loss of the bands characterising $\underline{I}^{o}$. The spectra of all four species can now be understood (in regard to band position, number and intensity) in terms of transitions involving the simple formulations above. It is then possible to make general assignments of the observed bands in every case, as indicated in Table 3. For example, the 20,000 cm^{-1} band for the reduced species $\underline{I}^{-}$ has the same position and structure as a recognised $\pi \rightarrow \pi^{*}$ transition in $Li^{+}bipy^{-}$, and is so identified. Hitherto, this band was assigned as a metal-to-ligand

TABLE 3: ABSORPTION BANDS IN TRIS-BIPYRIDYL RUTHENIUM COMPLEXES; $\nu/10^3$ cm^{-1} ($\varepsilon x 10^{-4}$)

		$\pi\rightarrow\pi^*$,bipy^0	$\pi\rightarrow\pi^*$,bipy$^-$	M→L,bipy^0	$\pi\rightarrow\pi^*$,bipy$^-$	$\pi\rightarrow\pi^*$,bipy$^-$
$[Ru(bipy)_3]^{2+}$	I	35.0(7.06)	-	22.1(1.37)	-	-
$[Ru(bipy)_3]^{+}$	I^-	34.2(5.12)	29.2(1.74)[a]	21.1(1.25)	19.9(1.35) 18.9(1.28)	13.0(0.09) 11.5(0.10) 10.2(0.09)
$[Ru(bipy)_3]^{0}$	I^{2-}	33.8(4.00)	29.0(2.50)[a]	20.8(sh)	19.5(1.48) 18.4(1.46)	12.9(0.16) 11.4(0.19) 10.1(0.18)
$[Ru(bipy)_3]^{-}$	I^{3-}	-	29.8(3.82)[a,b]	-	18.9(1.56) 18.0(1.58)	11.1(0.26) 9.9(0.27)
Na(bipy)[40,41] -tetrahydrofuran		-	25.9(2.95)	-	18.8(0.62) 17.8(0.65)	13.3(0.11) 12.0(0.15) 10.5(0.13)

(a) probably includes M→L(bipy$^-$) near 30 kK, consistent with greater breadth *cf.* Na bipy[40] and $[Al(bipy)_3]$[41].

(b) the shoulder near 24 kK is also present in Na bipy[41].

charge transfer (MLCT) band[11,32-35] by analogy with the prominent absorption at 22,000 cm^{-1} in I. However in the reduced complex, with charge accumulating on the ligands, a M→L CT transition should move to higher energy, contrary to observation. Hence the visible band of I^- is assigned principally to bipy$^-$ internal $\pi \rightarrow \pi^*$ transitions, with metal to uncharged ligand charge transfer providing only a high energy shoulder. This shoulder is also present in the I^{2-} species (it has one uncharged ligand) but is absent for the fully reduced complex which has no uncharged ligands.

This is the first report of the near-infrared spectral region of the reduced complexes. Unfortunately the lower-valent ruthenium complexes proved to be subject to continuous thermal bleaching (reversion to I) by the infrared radiation. Whereas visible and ultraviolet spectra are generally recorded using monochromatic incident radiation, in the infrared region monochromation only occurs after irradiation of the sample by the intense flux of 'white' light. In early measurements it was found that in the time necessary to complete an absorbance spectrum of the near-infrared region the solution temperature rose by approximately 50°C and the electrosynthesis current increased dramatically. The solution in the light path of the spectrophotometer had completely reverted to I during the scan. In order to overcome thermal bleaching, the transparent electrode was kept at or below room temperature for near-infrared investigations

by redesigning the cell with provision for cryostatic control based on streaming chilled nitrogen across the exterior surfaces of the O.T.T.L.E. The reduced species are then completely stable and their near-infrared spectra can be accurately recorded (Figure 7). The band centred at 11,000 cm^{-1} (and completely absent in I) is assigned to a $\pi \rightarrow \pi^*$ transition of the $bipy^{\cdot-}$ ligand. It can be seen to grow in an additive fashion with the increasing number of $bipy^{\cdot-}$ ligands. Even the detailed structure of the band is characteristic of $bipy^{\cdot-}$ as seen in its alkali metal 'salts' (see Figure 6).

The spectra of I to I^{3-} have been recorded between $20^{o}C$ and $0^{o}C$ in the concentration range 10^{-4} to 10^{-2} M and found to be invariant. The spectra are solvent independent, similar results being obtained in dimethyl sulphoxide, N,N'dimethylformamide and propylene carbonate (first reduction possible only).

It is known that, on irradiation, I can undergo substitution reactions with the solvent or counterion[42,43] and hence a standard procedure was adopted in these studies where after the steady-state spectrum of each reduced complex has been recorded, the starting material is regenerated by switching the controlling potential to 0 V. For an acceptable experiment, the initial absorption spectrum of I must be regained with minimal loss of intensity. These checks strongly indicate that the steady-state spectrum generated under potentiostatic control is indeed the designated product alone, rather than a daughter

FIGURE 7: Near-infrared absorption spectra of $[Ru(bipy)_3]^{1+/0/1-}$; $\underline{I}^{1-/2-/3-}$ in acetonitrile at 0°C

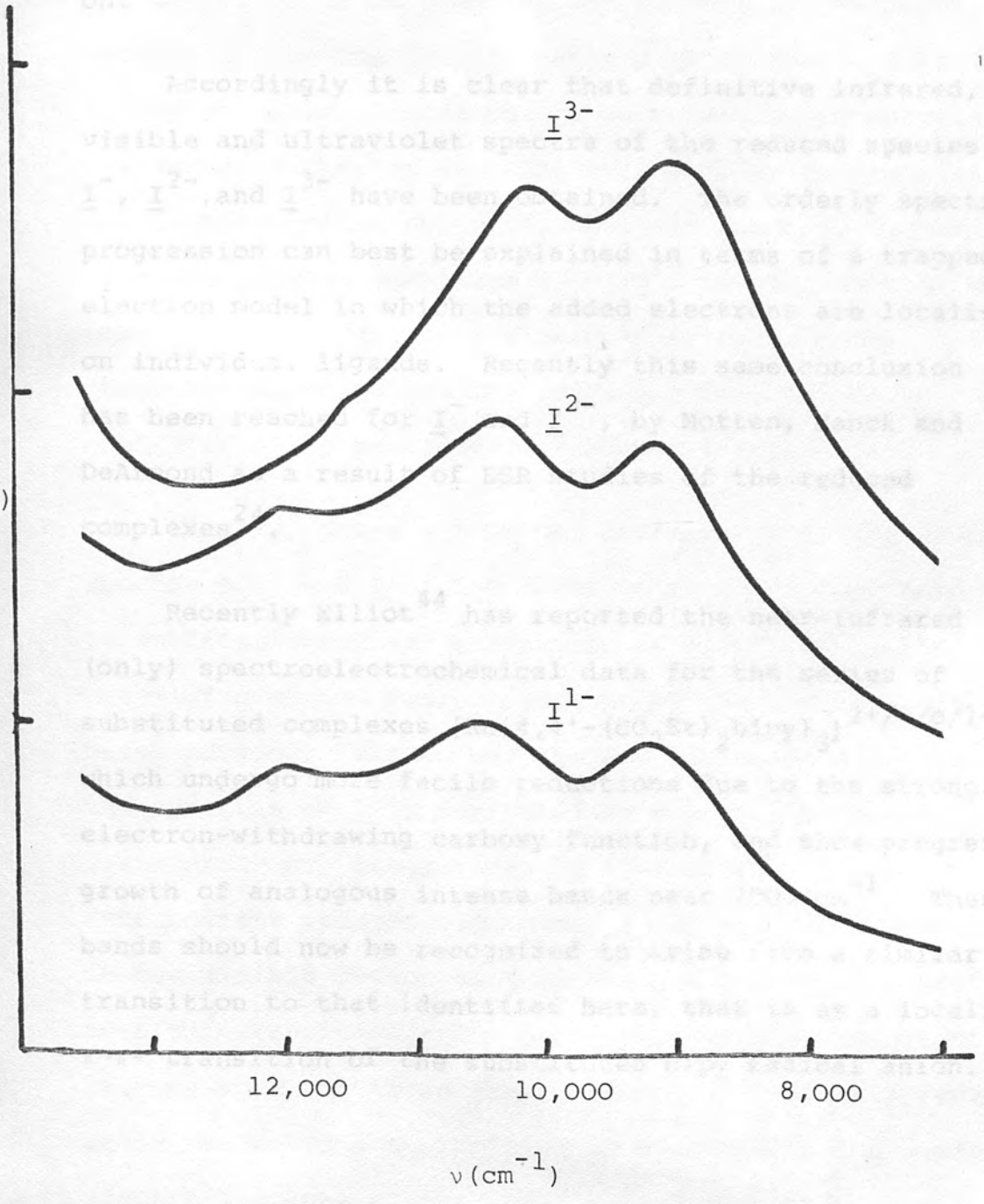

product resulting from further reaction, and that the intensity data (extinction coefficients) may be relied on.

Accordingly it is clear that definitive infrared, visible and ultraviolet spectra of the reduced species, $\underline{I}^{-}$, $\underline{I}^{2-}$ and $\underline{I}^{3-}$ have been obtained. The orderly spectral progression can best be explained in terms of a trapped-electron model in which the added electrons are localised on individual ligands. Recently this same conclusion has been reached for $\underline{I}^{-}$ and $\underline{I}^{3-}$, by Motten, Hanck and DeArmond as a result of ESR studies of the reduced complexes[24].

Recently Elliot[44] has reported the near-infrared (only) spectroelectrochemical data for the series of substituted complexes $[Ru\{4,4'-(CO_2Et)_2bipy\}_3]^{2+/+/o/1-}$ which undergo more facile reductions due to the strongly electron-withdrawing carboxy function, and show progressive growth of analogous intense bands near 7000 cm^{-1}. These bands should now be recognized to arise from a similar transition to that identified here, that is as a localised $\pi \rightarrow \pi^*$ transition of the substituted bipy radical anion.

Tris-bipyridyl iridum(III)

Tris-bipyridyl iridum(III) $[Ir(bipy)_3]^{3+}$, II, shares several general features with $[Ru(bipy)_3]^{2+}$. It is a low-spin $d\pi^6$ complex, shows a similar voltammetric

behaviour[28] (Table 4) with three successive reductions, and is relatively inert to photosubstitution[45]. However, $[Ir(bipy)_3]^{3+}$ is much easier to reduce than $[Ru(bipy)_3]^{2+}$ because of the increase in central metal charge (the effect of central metal charge on reduction potentials is discussed in Chapter 6). The very similar spacings of the cathodic redox potentials between I and II suggest that the reduced complexes II^-, II^{2-} and II^{3-} should be considered in terms of the trapped-electron model rather than the multiring delocalised one. This can be confirmed using spectroelectrochemical techniques.

Equally, there are marked differences in the electronic spectra of I and II. The first major absorption band of II is an intraligand $\pi\pi^*$ transition at 32,200 cm^{-1}; the near-infrared and visible regions of the absorption spectrum being entirely featureless whereas the visible region of the spectrum of I is dominated by a metal-to-ligand charge transfer (MLCT) transition. The absorption spectra of the intermediate reduced complexes, I^- and I^{2-}, are complicated in the visible region as they are a superposition of the Ru-$bipy^{\circ}$ transition and a $bipy^{\bar{\cdot}}$ intraligand transition. Thus we were convinced that $[Ir(bipy)_3]^{3+}$ and its reduced analogues would prove helpful in elucidating the visible spectral region, as the $bipy^-$ intraligand transitions should emerge from a featureless background.

The change in character of the lowest excited state on going from I (MLCT) to II (intraligand $\pi\pi^*$) is a direct

TABLE 4: ELECTRODE POTENTIALS FOR II, E^{o}/V vs. Ag/Ag^{+}

$$[Ir(bipy)_3]^{3+} \xrightarrow{-1.26} [Ir(bipy)_3]^{2+} \xrightarrow{-1.39} [Ir(bipy)_3]^{1+} \xrightarrow{-1.54} [Ir(bipy)_3]^{o}$$

II $\qquad$ II^{-} $\qquad$ II^{2-} $\qquad$ II^{3-}

consequence of charge, I and II having divalent and trivalent metal centres respectively. As shown in Figure 8, the separation of the π and π^* orbitals of bipy is approximately 3000 cm^{-1} less when Ir^{3+} replaces Ru^{2+}. Equally, the additional proton in the nucleus of the M^{3+} centre greatly stabilises the whole d-orbital manifold. The $[Ir(bipy)_3]^{3+/4+}$ oxidation cannot therefore be observed whereas the $[Ru(bipy)_3]^{2+/3+}$ oxidation is at a fairly moderate positive potential. Photo-emission from II* occurs from an essentially $\pi\pi^*$ state, implying that the occupied metal $d\pi$ levels have in fact dropped below the ligand π levels in energy[46] and that the lowest excited state in II is an intra-ligand $\pi\pi^*$ state whereas in I a MLCT excitation occurs at lowest energy. Thus, II* and I* are not analogous whereas II^- and I^- are expected to share a common $(bipy^o)_2(bipy^-)$ array.

As a preliminary to spectroelectrochemical studies the electrochemistry of $[Ir(bipy)_3]^{3+}$ was fully characterised, as for $[Ru(bipy)_3]^{2+}$. A cyclic voltammogram of II in acetonitrile at room temperature is shown in Figure 9. The three closely spaced ligand reductions are again evident. Comparison of wave heights of known concentrations of I and II show that the three $[Ir(bipy)_3]^{3+}$ reductions are all one-electron reductions. Extending the potential range of the voltammogram reveals a further reversible reduction. When the solution is cooled to -40^oC the four waves present at room temperature shift

FIGURE 8: Orbital correlation diagram for I and II

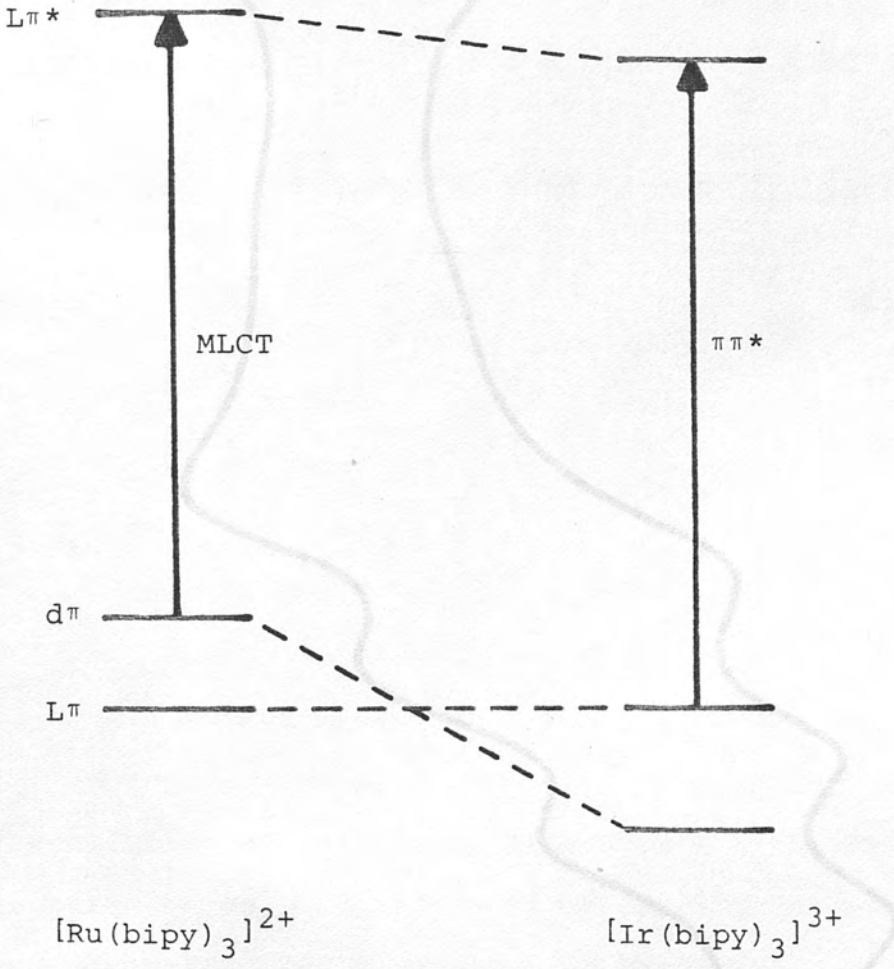

FIGURE 9: Cyclic voltammogram of $[Ir(bipy)_3]^{3+}$ in acetonitrile

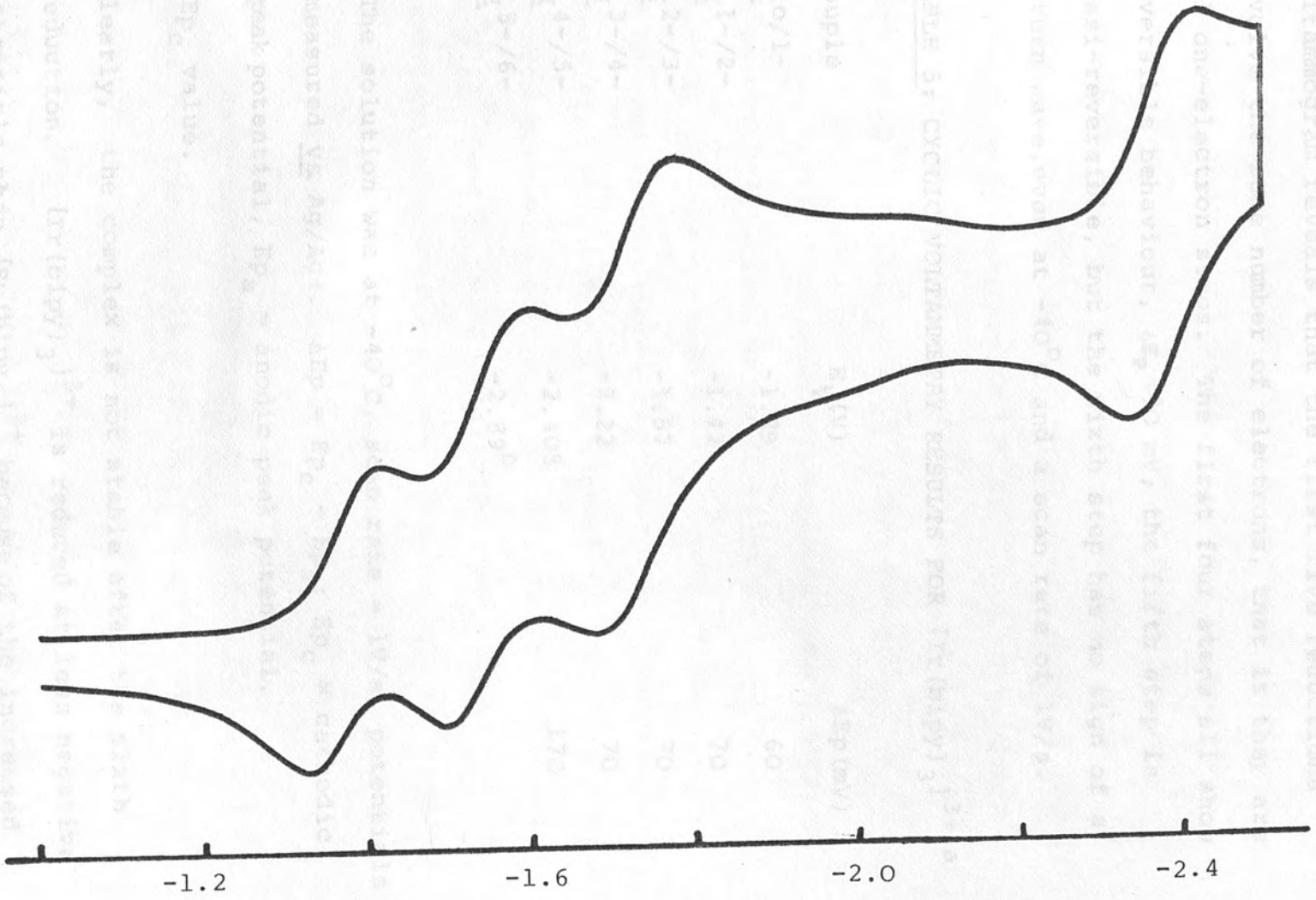

to slightly more negative potentials (as previously noted) and two more reductions, at more extreme negative potentials, may be seen (Table 5)[28]. A stirred cyclic voltammogram reveals that the first five reductions involve the same number of electrons, that is they are all one-electron steps. The first four steps all show reversible behaviour, $\Delta E_p \sim 70$ mV; the fifth step is quasi-reversible, but the sixth step has no sign of a return wave, even at -40°C and a scan rate of 1V/s.

TABLE 5: CYCLIC VOLTAMMETRY RESULTS FOR $[Ir(bipy)_3]^{3+}$ [a]

Couple	$E_{\frac{1}{2}}$ (V)	ΔEp (mV)
$\underline{II}^{o/1-}$	-1.29	60
$\underline{II}^{1-/2-}$	-1.42	70
$\underline{II}^{2-/3-}$	-1.57	70
$\underline{II}^{3-/4-}$	-2.22	70
$\underline{II}^{4-/5-}$	-2.405	170
$\underline{II}^{5-/6-}$	-2.89[b]	

[a] The solution was at -40°C, scan rate = 1V/s, potentials measured vs. Ag/Ag+. $\Delta Ep = Ep_c - Ep_a$; Ep_c = cathodic peak potential, Ep_a = anodic peak potential.

[b] Ep_c value.

Clearly, the complex is not stable after the sixth reduction. $[Ir(bipy)_3]^{3+}$ is reduced at less negative potentials than $[Ru(bipy_3]^{2+}$ because of the increased

positive charge on the metal centre. This also means, remarkably, that three further ligand-based reductions are observed in which each ligand is reduced to $bipy^{2-}$. The same electrochemical behaviour was noted in N,N'-dimethylformamide and dimethyl sulphoxide. Although the fourth reduction product, $\underline{II}^{4-}$, is stable on the voltammetric (cV, acV) timescale it proved to be unstable on an electrosynthesis timescale. After generation of $\underline{II}^{4-}$ and attempted regeneration of $\underline{II}$, at either room temperature or $-40^{o}C$, the spectrum did not return to that of the parent complex hence no further work on $\underline{II}^{4-}$ (or $\underline{II}^{5-}$ and $\underline{II}^{6-}$) was pursued.

The first three reduced complexes were generated in an OTTLE (platinum or gold) at -1.30 V ($\underline{II}^{-}$), -1.45 V ($\underline{II}^{2-}$) and -1.60 V ($\underline{II}^{3-}$) respectively *vs.* Ag/Ag^{+} reference electrode. The complete spectral range from near-infrared to ultraviolet could be studied at room temperature with no additional cooling because $\underline{II}^{-}$, $\underline{II}^{2-}$ and $\underline{II}^{3-}$ were completely stable under the experimental conditions used. The spectra are shown in Figure 10 and the general assignments of the observed bands are given in Table 6.

The successive spectra show similar features to those for the ruthenium series. Again we see the progressive growth of bands characterising $bipy^{-}$ with matching loss of $bipy^{o}$ bands as the complex is successively reduced, and once again this is compelling evidence for

FIGURE 10: Absorption spectra for $[Ir(bipy)_3]^{3+/2+/1+/0}$; $\underline{II}^{0/1-/2-/3-}$ in dimethyl sulphoxide at room temperature

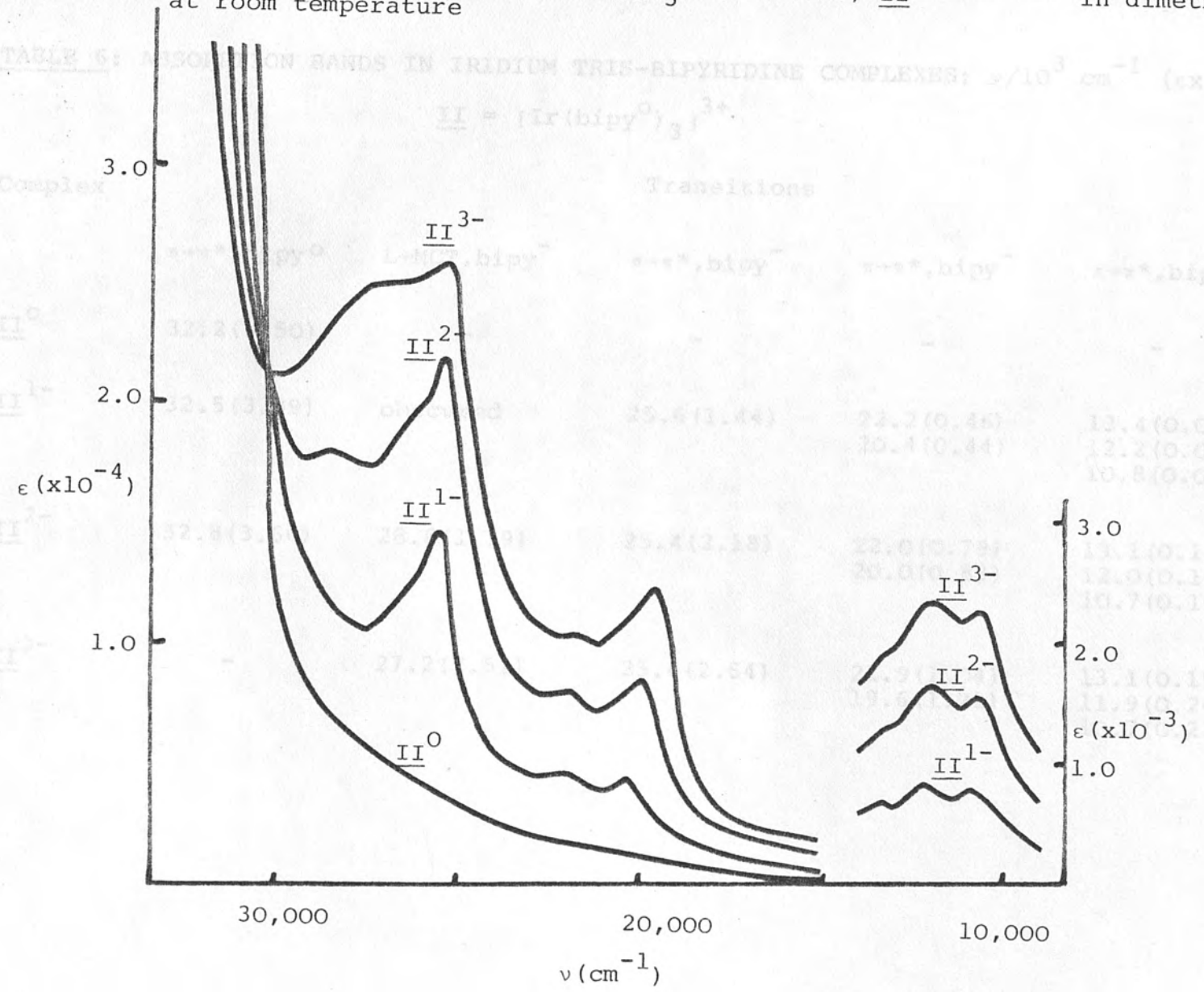

TABLE 6: ABSORPTION BANDS IN IRIDIUM TRIS-BIPYRIDINE COMPLEXES; $\nu/10^3$ cm^{-1} ($\varepsilon x 10^{-4}$)

II = $[Ir(bipy^o)_3]^{3+}$

Complex	Transitions				
	$\pi\rightarrow\pi^*$,$bipy^o$	L→MCT,$bipy^-$	$\pi\rightarrow\pi^*$,$bipy^-$	$\pi\rightarrow\pi^*$,$bipy^-$	$\pi\rightarrow\pi^*$,$bipy^-$
II^o	32.2(4.50)	-	-	-	-
II^{1-}	32.5(3.89)	obscured	25.6(1.44)	22.2(0.46) 20.4(0.44)	13.4(0.07) 12.2(0.08) 10.8(0.08)
II^{2-}	32.8(3.66)	28.6(1.79)	25.4(2.18)	22.0(0.79) 20.0(0.83)	13.1(0.13) 12.0(0.16) 10.7(0.16)
II^{3-}	-	27.2(2.51)	25.4(2.54)	21.9(1.04) 19.6(1.22)	13.1(0.19) 11.9(0.24) 10.7(0.23)

the trapped electron model. Thus the reduced complexes should be formulated as shown in Table 7.

TABLE 7: FORMULATION OF REDUCED IRIDIUM COMPLEXES

$[Ir(bipy)_3]^{3+}$ = $\underline{II}^{o}$ = $[Ir(\underline{III})(bipy^{o})_3]^{3+}$

$[Ir(bipy)_3]^{2+}$ = $\underline{II}^{1-}$ = $[Ir(\underline{III})(bipy^{o})_2(bipy^{\cdot-})]^{2+}$

$[Ir(bipy)_3]^{1+}$ = $\underline{II}^{2-}$ = $[Ir(\underline{III})(bipy^{o})(bipy^{\cdot-})_2]^{1+}$

$[Ir(bipy)_3]^{o}$ = $\underline{II}^{3-}$ = $[Ir(\underline{III})(bipy^{\cdot-})_3]^{o}$

The visible region around 20,000 cm^{-1} is much simplified in the iridium complexes compared to the corresponding ruthenium complexes because of the absence of a MLCT band. Hence the growth of the visible $\pi\pi^*$ $bipy^{\cdot-}$ band is now unambiguous and is more readily quantified. The measured extinction coefficient of the band at 20,000 cm^{-1} for $\underline{II}^{-}$ compares favourably with the similar band in $Na^{+}bipy^{\cdot-}$ (Table 3).

The highest energy $\pi\rightarrow\pi^*$ $bipy^{\cdot-}$ transition observed here at 25,500 cm^{-1} is much sharper than the corresponding band for the ruthenium system and is much more like the shape of the band in $Li^{+}bipy^{\cdot-}$. This is in accord with the suggestion that the band in $\underline{I}^{1-}$, $\underline{I}^{2-}$ and $\underline{I}^{3-}$ includes a $M\rightarrow L(bipy^{\cdot-})$ transition. We know on voltammetric evidence that the transfer of an electron <u>to</u> $bipy^{\cdot-}$ is $\sim$0.5 V (4000 cm^{-1}) more difficult than <u>to</u> $bipy^{o}$ since the

fourth reduction on Ir occurs at -2.19 V instead of -1.70 V (forward peak potentials), which suggests that the Ru→bipy^{-} charge transfer transition should occur at approximately 26,000 cm^{-1}.

The near-infrared band also increases linearly in height with the number of bipy^{-} ligands. The extinction coefficients per reduced ligand agree closely with those for the ruthenium complexes as does the structure within the band itself (note that in both cases $\underline{I}^{3-}$ and $\underline{II}^{3-}$, the highest frequency peak of the three becomes only a shoulder). The bands are all slightly shifted in position from I to II but this is almost wholly explicable in increase in central metal charge.

In every case, after recording the final spectrum for each reduced species, the potential was set at -0.6 V and the spectrum returned to that of II in its initial concentration, thus establishing that the complex was not reduced irreversibly, even in part. The family of iridium complexes II to $\underline{II}^{3-}$ were not solvent sensitive, the spectra remaining the same in acetonitrile, N,N'-dimethylformamide and dimethylsulphoxide.

The iridium system, like the ruthenium system, is then best explained using the localised orbital model. The iridium system in fact clarifies the visible and near-ultraviolet regions as there are no low-energy charge-transfer transitions masking the bipy^{-} transitions. These two systems put beyond doubt the question of the

character of the redox-active orbitals of these and related $d\pi^6$ tris-bipyridine complexes. Electrons centering such orbitals are thus effectively trapped on the individual ligands, with little or no interaction between the three neighbouring chelate rings.

These results also establish general diagnostic criteria for the presence of coordinated $bipy^-$. Spectra of complexes thought to contain such a ligand must show:

i) a near-infrared band around 10,000 cm^{-1} containing three peaks (or shoulders) separated by approximately 1000 cm^{-1};

ii) a visible doublet band around 20,000 cm^{-1}; and

iii) a near-ultraviolet band around 25,000 cm^{-1}.

Exact positions of such bands depend on the central metal charge and on the nature of the accompanying ligands.

Experimental

$Ru(bipy)_3Cl_2 \cdot 6H_2O$ was purchased from G.F. Smith & Co. The fluoroborate salt was obtained by metathesis with aqueous $NaBF_4$ and was recrystallised twice from water. $[Ir(bipy)_3](BF_4)_3$ was prepared following the method of Flynn and Demas[47], except that fluoroboric acid was used instead of nitric acid. Contaminating potassium salts were removed by dissolving the product in propanol (K^+ salts were insoluble) rather than by use of

a cation exchange resin column. Purification of the $Ir(bipy)_3(BF_4)_3$ using a Sephadex LH-20 column was performed as described by Flynn and Demas.

Acetonitrile was purified in seven stages according to Walter and Ramaley[48]. The purified acetonitrile had a transparent spectral range up to 50,000 cm^{-1} and an electrochemical range of 5 V (-2.6 to +2.4 V). Propylene carbonate, dimethylsulphoxide and N,N'dimethylformamide were used without purification. The supporting electrolyte, tetrabutylammonium tetrafluoroborate, was prepared by the method of Heath et al[49], replacing tetraethylammonium hydroxide by tetrabutylammonium hydroxide. Electrolyte concentration was 0.1 M in all media.

Voltammetric experiments were performed in a conventional cell with a three-electrode configuration consisting of a working electrode (platinum microelectrode, gold, carbon or dropping mercury electrode), Ag/Ag^+ reference electrode separated from the bulk solution by a glass frit[50] and a platinum counter electrode. Solutions were purged with argon so as to render them oxygen-free. Cyclic voltammograms were recorded using a Princeton Applied Research Model 170 with full positive-feedback IR compensation. Scan rates were in the range 20 mV/s to 1 V/s with routine measurements at 100 mV/s.

The spectroelectrochemistry of the complexes was

studied using an O.T.T.L.E. in a cell block (Figure 3) mounted in a spectrophotometer beam (Unicam SP800 and Beckman 5270). Reference and auxiliary electrodes were as above; both electrodes were shielded from the bulk solution by glass frits to prevent contamination. The solution and spectrophotometer compartment were purged with argon prior to electrogeneration experiments and constant potentials were applied by a Metrohm E506 potentiostat. Concentrations of I and II were varied to optimise the different spectral regions (however I^{2-} was found to be insoluble in acetonitrile in high concentrations[51]). At lower temperatures the apparent extinction coefficients of absorption bands all became higher. This was almost wholly due to solvent contraction at low temperature since standard solutions of I and II were uniformly prepared at 20°C, and appropriate corrections have been made in the tables.

REFERENCES

1. M. Gleria, F. Minto, G. Beggiato and P. Bertolus; J. Chem. Soc. Chem. Comm., 285 (1978).

2. P.E. Hoggard and G.B. Porter; J. Am. Chem. Soc., 100, 1457 (1978).

3. B. Durham, J.L. Walsh, C.L. Carter and T.J. Meyer; Inorg. Chem., 19, 860 (1980).

4. J. Van Houten and R.J. Watts; Inorg. Chem., 17, 3381 (1981).

5. D.M. Klassen and G.A. Crosby; J. Chem. Phys., 48, 1853 (1968).

6. F.E. Lytle and D.M. Hercules; J. Am. Chem. Soc., 91, 253 (1969).

7. R.W. Harrigan and G.A. Crosby; J. Chem. Phys., 59, 3468 (1973).

8. G.D. Hager and G.A. Crosby; J. Am. Chem. Soc., 97, 7031 (1975).

9. K.W. Hipps; Inorg. Chem., 19, 1390 (1980).

10. K. Itoh and K. Honda; Chem. Lett. 99 (1979).

11. C. Creutz and N. Sutin; J. Am. Chem. Soc., 98, 6384 (1976).

12. C. Creutz and N. Sutin; Inorg. Chem., 15, 496 (1976).

13. C.R. Bock, T.J. Meyer and D.G. Whitten; J. Am. Chem. Soc., 96, 4710 (1974).

14. B. Durham, W.J. Dressick and T.J. Meyer; J. Chem. Soc., Chem. Comm., 381 (1979).

15. V. Balzani, F. Bolletta, M.T. Gandolfi and M. Maestri; Top. Curr. Chem., 75, 1 (1978).

16. U. Lachish, M. Ottolenghi and J. Rabani; J. Am. Chem. Soc., 99, 8062 (1977).

17. K. Kalyanasundaram and M. Grätzel; Angew. Chem. Int. Ed. Engl., 18, 701 (1979).

18. D.P. Rillema, W.J. Dressick and T.J. Meyer; J. Chem. Soc. Chem. Comm., 247 (1980).

19. M. Kirch, J-M Lehn and J.P. Sauvage; Helv. Chim. Acta, 62, 1345 (1979).

20. H.D. Abruna, A.X. Teng, G.J. Samuels and T.J. Meyer, J. Am. Chem. Soc., 101, 6745 (1979).

21. T. Saji and S. Aoyagui; J. Electroanal. Chem., 58, 401 (1975).

22. N.E. Tokel-Takvoryan, R.E. Hemingway and A.J. Bard; J. Am. Chem. Soc., 95, 6582 (1973).

23. P. Belser and A. von Zelewsky; Helv. Chim. Acta, 63, 1675 (1980).

24. A.G. Motten, K. Hanck and M.K. DeArmond; Chem. Phys. Letts., 79, 541 (1981).

25. D.P. Rillema, D.S. Jones and H.A. Levy; J. Chem. Soc. Chem. Comm., 849 (1979).

26. K.W. Hipps and G.A. Crosby; J. Am. Chem. Soc., 97, 7042 (1975).

27. M.K. DeArmond, C.M. Carlin and W.L. Huang; Inorg. Chem., 19, 62 (1980).

28. J.L. Kahl, K.W. Hanck and K. DeArmond; J. Phys. Chem., 82, 540 (1978).

29. J.E. Ferguson and G.H. Harris; J. Chem. Soc., 1293 (1966).

30. F. Felix, J. Ferguson, H.U. Güdel and A. Ludi; J. Am. Chem. Soc., 102, 4096 (1980).

31. A. Ceulemans and L.G. Vanquickenborne; J. Am. Chem. Soc., 103, 2238 (1981).

32. C.P. Anderson, D.J. Salmon, T.J. Meyer, R.C. Young; J. Am. Chem. Soc., 99, 1980 (1977).

33. M Maestri and M. Grätzel; Ber. Bunsenges Phys. Chem., 81, 504 (1977).

34. D. Meisel, M.S. Matheson, W.A. Mulac and J. Rabani; J. Phys. Chem., 81, 1449 (1977).

35. Q.G. Mulazzani, S. Emmi, P.G. Fuochi, M.Z. Hoffman and M. Venturi, J. Am. Chem. Soc., 100, 981 (1978).

36. N.E. Tokel and A.J. Bard; J. Am. Chem. Soc., 94, 2862 (1972).

37. W.L. Wallace and A.J. Bard; J. Phys. Chem., 83, 1350 (1979).

38. R.W. Murray, W.R. Heineman and G.W. O'Dom; Anal. Chem., 39, 1666 (1967).

39. E. König and S. Kremer; Chem. Phys. Lett., 5, 87 (1970).

40. C. Mahon and W.L. Reynolds; Inorg. Chem., 6, 1297 (1967).

41. Y. Torii, S. Murasato and Y. Kaisu; Nippon Kagaku Zasshi, 91, 549 (1970).

42. M. Gleria, F. Minto, G. Beggiato and P. Bortolus; J. Chem. Soc., Chem. Comm., 285 (1978).

43. P.E. Hoggard and G.B. Porter; J. Am. Chem. Soc., 100, 1457 (1978).

44. C.M. Elliot; J. Chem. Soc. Chem. Comm., 261 (1980).

45. J.N. Demas, E.W. Harris, C.M. Flynn and D. Diemente; J. Am. Chem. Soc., 97, 3838 (1975).

46. M.K. DeArmond and C.M. Carlin; Coord. Chem. Rev., 36, 325 (1981).

47. C.M. Flynn and J.N. Demas; J. Am. Chem. Soc., 96, 1959 (1974).

48. M. Walter and L. Ramaley; Anal. Chem., 45, 165 (1973).

49. G.A. Heath, G.T. Hefter, T.W. Boyle, C.D. Desjardins, D.W.A. Sharp; J. Fluor. Chem. II, 399 (1978).

50. D.T. Sawyer and J.L. Roberts; Experimental Electrochemistry for Chemists, p54 (Wiley-Interscience, New York, 1974).

51. R.S. Glass and L.R. Faulkner; J. Phys. Chem., 85, 1160 (1981).

CHAPTER 3

COMPARISON WITH LOWER-SYMMETRY BIPYRIDYL COMPLEXES

In Chapter 2 we asserted that the localised model was completely sufficient to explain the absorption spectra of the complexes. The localised or trapped-electron model is essentially a one-ligand model consisting of the metal centre and an isolated ligand. Such an isolated ligand chromophore is also contained in lower-symmetry complexes $M(bipy)_2L_2^{n+}$ and $M(bipy)L_4^{m+}$. Studies then of lower-symmetry complexes should show parallel results with those in Chapter 2. The trapped-electron model also poses the question of intervalence phenomena; that is, could the $bipy^{-\cdot} \rightarrow bipy^{o}$ interligand charge-transfer transition be observed?

Replacement of bipy by L=pyridine , a ligand with similar characteristics, has enabled both lower-symmetry complexes and intervalence phenomena to be studied. The results from such spectroelectrochemical experiments can then be used to elucidate firstly the electrochemistry of another lower-symmetry bipy complex in which the replacement ligand, chloride, has a strong perturbing influence on the complex and secondly the configuration of a complex whose structure still remains open to question.

Tetrakis- and bis-pyridine ruthenium complexes

Pyridine (py) bears an obvious electronic resemblance to bipy. It is also an unsaturated ligand with empty low-lying π^* antibonding orbitals capable of π-back bonding. Hence we would predict that replacement of bipy by py should have little influence on any remaining isolated bipy-metal chromophores. Comparison of reduction potentials for the three half-reactions (1), (2) and (3) is shown in Table 1[1,2].

TABLE 1: REDUCTION POTENTIALS FOR RUTHENIUM COMPLEXES (vs. N.H.E.)

$[Ru(NH_3)_6]^{3+} + e^- = [Ru(NH_3)_6]^{2+}$ E=+0.050 V (1)

$cis\text{-}[Ru(NH_3)_4py_2]^{3+} + e^- = cis\text{-}[Ru(NH_3)_4py_2]^{2+}$ E=+0.505 V (2)

$[Ru(NH_3)_4bipy]^{3+} + e^- = [Ru(NH_3)_4bipy]^{2+}$ E=+0.505 V (3)

If we assume that back-bonding interactions are insignificant between Ru(III) and pyridine-type ligands[3] and accept that NH_3 is solely a σ-bound ligand (of similar σ-donor strength to pyridine) then the difference in redox potentials between (1) and the substituted complexes in (2) and (3) may be assigned largely to the π back-bonding contribution; that is, the change in $[Ru]^{3+/2+}$ potential can be attributed to a stabilisation of the Ru(II) oxidation state by back-bonding from the metal centre to the ligands. Moreover, the redox potentials of Table 1 indicate that the amount of back-bonding to the two py ligands is the same as that to one bipy ligand. Thus

the energy of the molecular orbitals in the Ru-bipy chromophore in pyridine-substituted complexes should be approximately the same as those in $[Ru(bipy)_3]^{2+}$.

The reduction of pyridine itself is 600 mV more difficult than that of free bipyridine[4]; that is, the π^*antibonding orbitals of py are at higher energy than those in bipy. On complexation we would expect the reductions of the py ligand to remain more difficult than those of ligated bipy, and the electrochemistry of mixed ligand complexes should be unambiguous, with the less extreme negative potential range dominated by bipy reductions.

Equally, the MLCT transitions from Ru(II) to py involve the same π^* orbitals and hence we would expect such transitions to be at higher energy than the corresponding transitions to bipy. Figure 1 shows the absorption spectra of equimolar solutions of $[Ru(bipy)_3]^{2+}$, cis-$[Ru(bipy)_2py_2]^{2+}$ and $[Ru(bipy)py_4]^{2+}$ with overall symmetries D_3, C_2 and C_{2v} respectively. Repeated replacement of bipy by py should result in a decrease in band height of those transitions involving bipy, together with an increase of those associated with py. Such an assignment of the bands is given in Table 2 with a schematic molecular orbital diagram in Figure 2.

The M→LCT band (A) at 22,100 cm^{-1} already assigned as a charge transfer to bipy in $[Ru(bipy)_3]^{2+}$ can be seen

FIGURE 1: Absorption spectra of $[Ru(bipy)_x py_{6-2x}]^{2+}$; $1 \leq x \leq 3$ in water

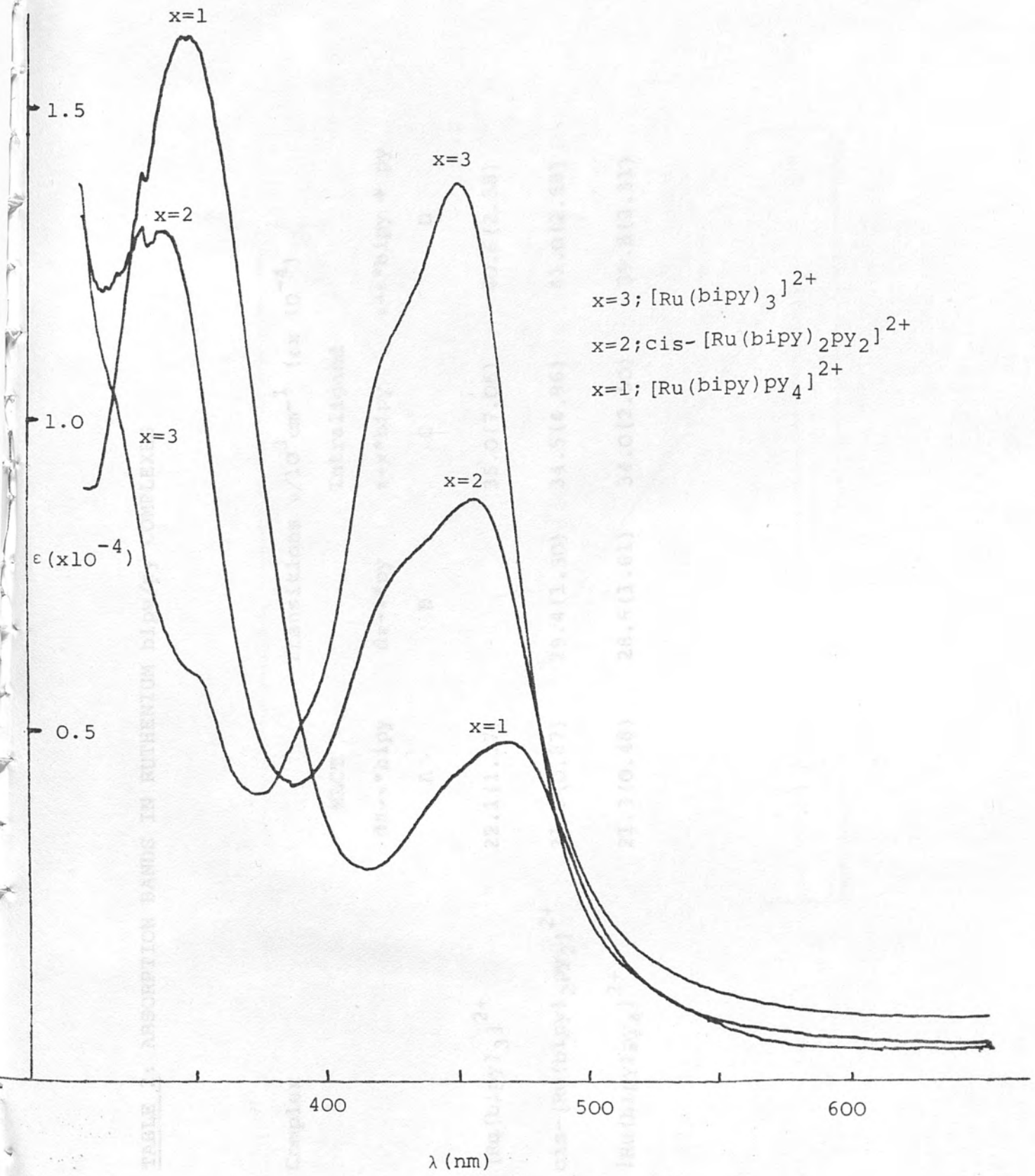

TABLE 2: ABSORPTION BANDS IN RUTHENIUM bipy/py COMPLEXES

Complex	Transitions $\nu/10^3 cm^{-1}$ ($\varepsilon \times 10^{-4}$)			
	MLCT		Intraligand	
	$d\pi \rightarrow \pi^*$bipy	$d\pi \rightarrow \pi^*$py	$\pi \rightarrow \pi^*$bipy	$\pi \rightarrow \pi^*$bipy + py
	A	B	C	D
$[Ru(bipy)_3]^{2+}$	22.1(1.37)		35.0(7.06)	40.6(2.58)
cis-$[Ru(bipy)_2py_2]^{2+}$	21.8(0.87)	29.4(1,30)	34.5(4,96)	41.0(2.58)
$[Ru(bipy)py_4]^{2+}$	21.3(0.48)	28.6(1.61)	34.0(2.50)	39.8(3.31)

FIGURE 2: Schematic molecular orbital diagram for $[Ru(bipy)_x py_{6-2x}]^{2+}$; $1 \leq x \leq 3$

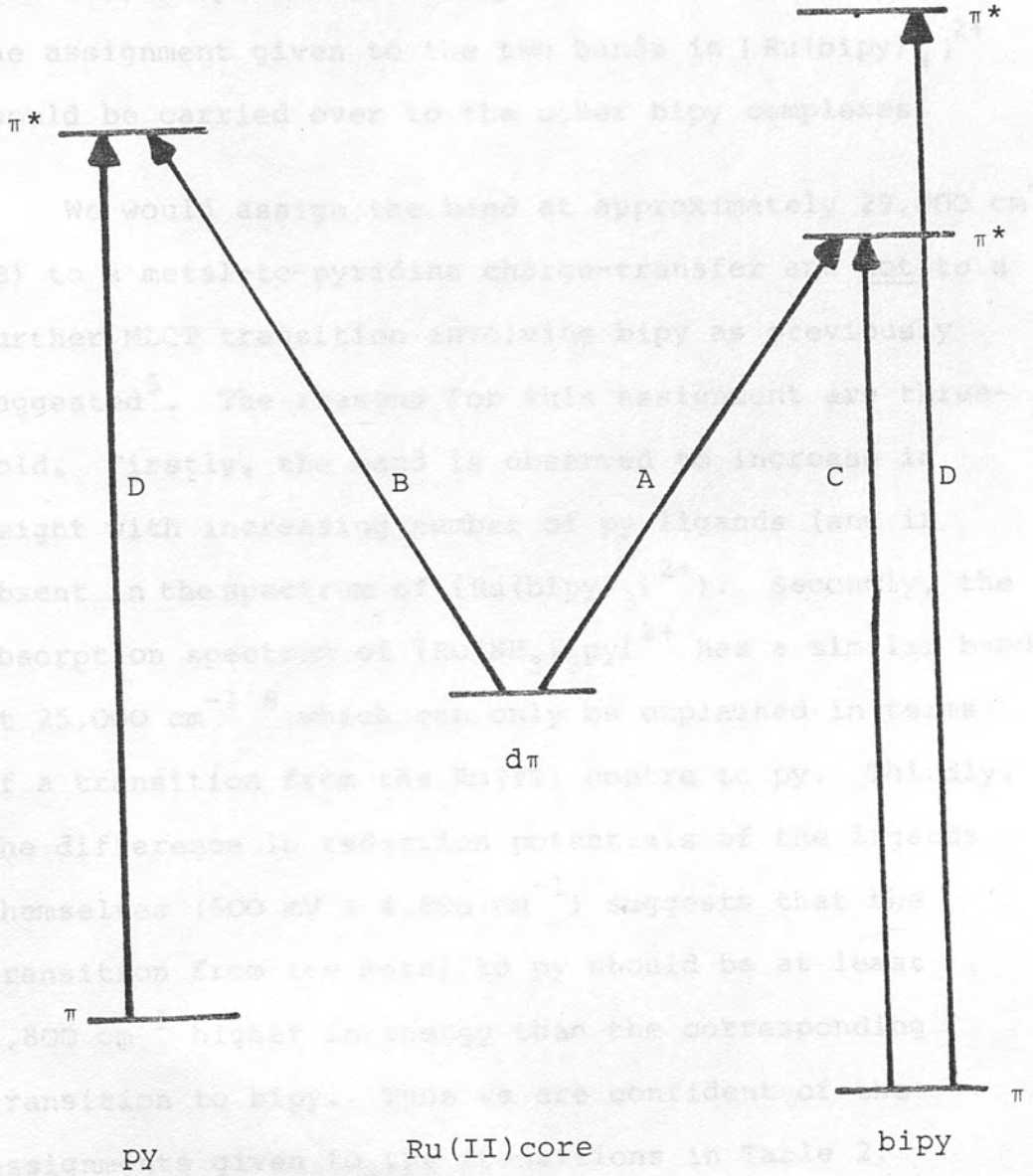

to collapse in a linear fashion with decreasing numbers of bipy ligands, as can the intraligand $\pi \rightarrow \pi^*$ band (C) at 35,000 cm^{-1}. The shapes of these bands remain unaltered for the three complexes. Thus the band position, shape and intensity lead us to conclude that the assignment given to the two bands in $[Ru(bipy)_3]^{2+}$ should be carried over to the other bipy complexes.

We would assign the band at approximately 29,000 cm^{-1} (B) to a metal-to-pyridine charge-transfer and <u>not</u> to a further MLCT transition involving bipy as previously suggested[5]. The reasons for this assignment are three-fold. Firstly, the band is observed to increase in height with increasing number of py ligands (and is absent in the spectrum of $[Ru(bipy)_3]^{2+}$). Secondly, the absorption spectrum of $[Ru(NH_3)_5py]^{2+}$ has a similar band at 25,000 cm^{-1} [6] which can only be explained in terms of a transition from the Ru(II) centre to py. Thirdly, the difference in reduction potentials of the ligands themselves (600 mV ≡ 4,800 cm^{-1}) suggests that the transition from the metal to py should be at least 4,800 cm^{-1} higher in energy than the corresponding transition to bipy. Thus we are confident of the assignments given to the transitions in Table 2.

The spectra show that replacing bipy by py has not altered the remaining metal-bipy chromophore. Hence this replacement offers the opportunity of studying this chromophore in lower-symmetry complexes where we would

expect to see directly comparable results to those obtained for the tris-complexes.

In common with the tris-bipyridyl complex, the pyridine-substituted complexes exhibit rich redox chemistries as shown in Equations 4-6 and Table 3. The cyclic voltammogram of cis-$[Ru(bipy)_2py_2]^{2+}$ is given in Figure 3.

It is immediately obvious from Table 3 that repeated replacement of bipy by py has little effect on the redox properties of any Ru-bipy chromophores in the complex. Thus the reduction processes for III and IV are primarily ligand-based whereas the oxidation is essentially a metal-based process. The characteristic spacing between the two reduction potentials of the bis-bipy complex, and the identical first ligand reduction for all three complexes, demonstrate that the trapped-electron model is indeed applicable, irrespective of the local symmetry of the complex. Accordingly further study of these lower-symmetry complexes by spectroelectrochemistry should be equally informative, particularly since the oxidations and reductions of III and IV were found to be reversible at all scan rates investigated. The spectroscopic characterisation of III^x (x = +1,0,-1) and IV^y (y = +1,0,-1,-2) is reported in this and the following chapter.

FIGURE 3: Cyclic voltammogram of cis-$[Ru(bipy)_2py_2]^{2+}$ in acetonitrile at room temperature

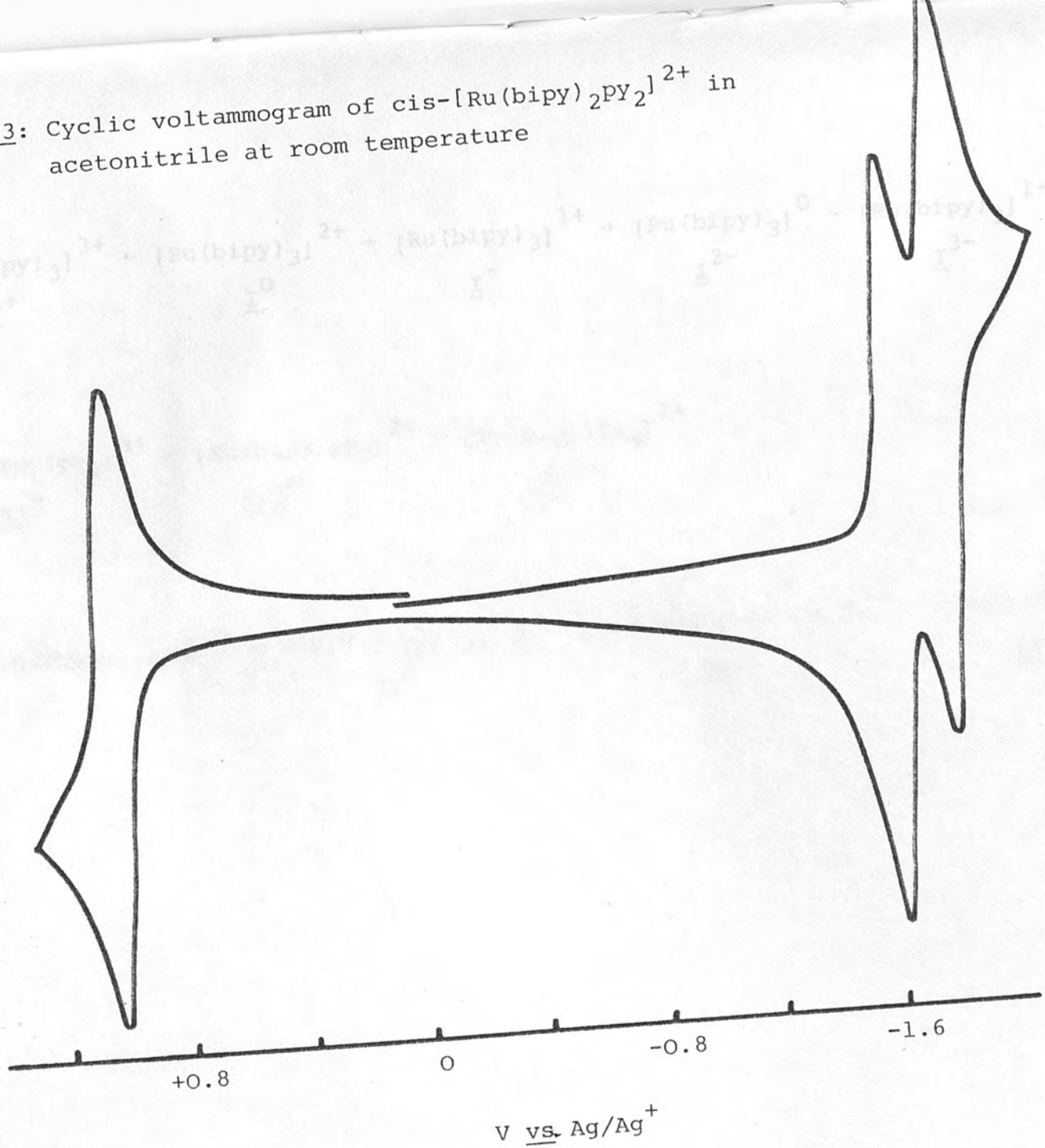

$$[Ru(bipy)_3]^{3+} \leftarrow [Ru(bipy)_3]^{2+} \rightarrow [Ru(bipy)_3]^{1+} \rightarrow [Ru(bipy)_3]^{0} \rightarrow [Ru(bipy)_3]^{1-} \quad (4)$$

$$\underline{I}^{+} \qquad \underline{I}^{O} \qquad \underline{I}^{-} \qquad \underline{I}^{2-} \qquad \underline{I}^{3-}$$

$$[Ru(bipy)py_4]^{3+} \leftarrow [Ru(bipy)py_4]^{2+} \rightarrow [Ru(bipy)py_4]^{1+} \quad (5)$$

$$\underline{III}^{+} \qquad \underline{III}^{O} \qquad \underline{III}^{1-}$$

$$cis\text{-}[Ru(bipy)_2py_2]^{3+} \leftarrow cis[Ru(bipy)_2py_2]^{2+} \rightarrow cis[Ru(bipy)_2py_2]^{1+} \rightarrow cis[Ru(bipy)_2py_2]^{0} \quad (6)$$

$$\underline{IV}^{+} \qquad \underline{IV}^{O} \qquad \underline{IV}^{1-} \qquad \underline{IV}^{2-}$$

TABLE 3: REDOX POTENTIALS FOR BIPYRIDYL COMPLEXES OF Ru(II)[a]

Couple	$E_{\frac{1}{2}}$ (V)	ΔEp (mV)
$\underline{I}^{+/O}$	+0.96	65
$\underline{I}^{O/1-}$	-1.66	65
$\underline{I}^{1-/2-}$	-1.83	65
$\underline{I}^{2-/3-}$	-2.05	65
$\underline{III}^{+/O}$	+0.95	70
$\underline{III}^{O/1-}$	-1.66	70
$\underline{IV}^{+/O}$	+0.97	65
$\underline{IV}^{O/1-}$	-1.66	70
$\underline{IV}^{1-/2-}$	-1.85	70

[a] Complexes studied in CH_3CN/0.1 M $TBABF_4$ at room temperature on platinum. Potentials quoted vs. Ag/Ag^+ reference electrode

Tetrakis-pyridine monobipyridine ruthenium(II)

The complex $[Ru(bipy)py_4]^{2+}$, III, having only one Ru-bipy chromophore, is a straightforward example of the one-ligand model; $\underline{III}^-$ must contain a discrete $bipy^-$ if our understanding is correct. Thus the visible region of the spectrum, which is dominated by a MLCT transition from Ru(II) to $bipy^O$ in III, should show only an intraligand $\pi\pi^*$ transition of $bipy^-$ in $\underline{III}^-$.

The electrochemistry of III was studied in acetonitrile, dimethylsulphoxide and propylene carbonate and the redox potentials were found to be invariant. However, the complex was found to be unstable at room temperature in these solvents over several hours, the probable reaction being solvent exchange with py. The reactivity of the complex was observed by studying the behaviour of the $\underline{III}^{0/1-}$ couple in acetonitrile as a function of time. Initially only one couple, $\underline{III}^{0/1-}$, can be seen with a half-wave potential ($E_{\frac{1}{2}}$) of -1.66 V vs. Ag/Ag^{+}. As the complex is allowed to stand in the solvent, so the height of this wave decreased while another wave, initially absent, with $E_{\frac{1}{2}}$ = -1.86 V vs. Ag/Ag^{+} grew. Equally, the wave corresponding to the oxidation couple $\underline{III}^{+/0}$ could be seen to decrease ($E_{\frac{1}{2}}$ = +0.95 V) whilst another grew ($E_{\frac{1}{2}}$ = +1.00 V) on prolonged contact of the complex with the solvent. After five hours at room temperature in acetonitrile approximately 50% of the complex had reacted as calculated by comparing the areas under the adjacent cathodic waves. As the electrochemistry changes, so too does the visible absorption spectrum with the peak at 21,300 cm^{-1} shifting gradually to higher frequencies. We know $[Ru(bipy)_2py_2]^{2+}$ undergoes solvent exchange with acetonitrile (vide infra) hence a similar suggestion may be considered here. Carlin and DeArmond noted the instability of $[Ru(bipy)py_4]^{2+}$ in methanol at room temperature[7].

The complex has far greater stability in acetonitrile if it is kept at low temperatures (cyclic voltammetric scans remained unchanged over several hours). Thus in practice $[Ru(bipy)py_4]^{2+}$ may be studied immediately at room temperature (and for as long as the visible absorption peak remains at 21,300 cm^{-1}) or examined at length at low temperatures. At $-40^{o}C$ in acetonitrile the redox couples all appear to shift by 40 mV to more negative potentials, as was noted previously.

The following spectroscopic studies of III and its reduced analogue were carried out at room temperature so that direct comparisons could be drawn between them and the other model complexes without having to make temperature/solvent contraction corrections to extinction coefficients. However the O.T.T.L.E. experiment was only judged to be successfully accomplished when the initial spectrum of III could be regenerated exactly; that is, when there was no appreciable loss of band intensity and no measurable shift of band position in the spectrum of III after regeneration of the parent complex.

The complex has only one stable reduction product, III^{-}, which was generated in an O.T.T.L.E. (platinum) at -1.82V vs. Ag/Ag^{+}. The spectrum of III^{-} was recorded from the near-infrared to the ultraviolet (7000 to 33,000 cm^{-1}) and the details of the absorption bands for III^{o} and III^{-} are given in Table 4.

TABLE 4: ABSORPTION BANDS IN MONO-BIPYRIDINE COMPLEXES OF RUTHENIUM

Complex	$\nu_{max}/10^3 cm^{-1}$ ($\varepsilon x 10^{-4}$)	
$[Ru(bipy)py_4]^{2+}$	21.3(0.48); 28.6(1.61)	
$[Ru(bipy)py_4]^{1+}$	12.8(0.11); 19.2(0.67); 11.9(0.11) 11.0(0.10)	28.2(3.61)

The absorption spectrum of $\underline{III}^-$ contains the characteristic intraligand $\pi\pi^*$ transitions for a $bipy^-$ ligand:

(i) a near-infrared band centred at 11,800 cm^{-1} containing three peaks separated by approximately 1000 cm^{-1};

(ii) a visible band at 19,200 cm^{-1}, although it is not as well defined as in previous examples probably because this band is partially masked by the very intense ultraviolet peak;

(iii) a near-ultraviolet band at 28,200 cm^{-1}.

Thus the complexes should be formulated in terms of the Ru(II)-$bipy^o$ chromophore in $\underline{III}^o$ and Ru(II)-$bipy^-$ in $\underline{III}^-$ as shown in Table 5.

TABLE 5: FORMULATION OF MONO-BIPYRIDINE RUTHENIUM COMPLEXES

$[Ru(bipy)py_4]^{2+}$ ($\underline{III}^{o}$) = $[Ru(II)(bipy^{o})py_4]^{2+}$

$[Ru(bipy)py_4]^{1+}$ ($\underline{III}^{1-}$) = $[Ru(II)(bipy^{\cdot-})py_4]^{1+}$

The measured extinction coefficients for the bands in the near-infrared and visible regions of $\underline{III}^{-}$ are in good agreement with similar bands in $\underline{II}^{-}$ and $Na^{+}bipy^{-}$, and hence must be assigned solely as intraligand $\pi\pi^*$ transitions of ligated $bipy^{\cdot-}$. The extinction coefficient of the ultraviolet band in $\underline{III}^{-}$ is much more intense than that predicted for a $\pi\pi^*$ transition of $bipy^{\cdot-}$ which for example in $\underline{I}^{-}$ has $\varepsilon = 1.74 \times 10^{4}$. We have already established however that the absorption spectrum of $\underline{III}^{o}$ has a Ru→py charge transfer transition at 28,600 cm^{-1} ($\varepsilon=1.61\times10^{4}$) and $\underline{III}^{-}$ also contains the same $Ru\text{-}py_4$ chromophore as $\underline{III}^{o}$, hence it is this transition which accounts for the anomolous intensity of the ultraviolet band in $\underline{III}^{-}$. Thus the band at 28,200 cm^{-1} in $\underline{III}^{-}$ must be thought of as composed of an intraligand $\pi\pi^*$ charge transfer of $bipy^{\cdot-}$, a Ru(II)→$bipy^{\cdot-}$ charge transfer and a Ru(II)→py charge transfer.

The electrochemical reduction $\underline{III}^{o/1-}$ is therefore a totally ligand-based reduction of bipy with no interaction from the py ligands ($\underline{III}^{o/1-}$ has the same reduction potential as $\underline{I}^{o/1-}$ and the ML(py)CT transition is at the same frequency in $\underline{III}^{o}$ and $\underline{III}^{1-}$), and the

results from the absorption spectrum of $\underline{III}^{-}$ show that $\underline{I}^{-}$, $\underline{I}^{2-}$ and $\underline{I}^{3-}$ are indeed best thought of in terms of isolated Ru-bipy chromophores.

Cis-bispyridine-bisbipyridine-ruthenium(II)

The complex cis$[Ru(bipy)_2py_2]^{2+}$, IV, is a structural analogue of I and III. Thus it should be possible to rationalise the absorption spectra of $\underline{IV}^{1-}$ and $\underline{IV}^{2-}$ in similar terms to those used for $\underline{I}^{1-}$ and $\underline{III}^{1-}$.

The cyclic voltammogram of IV in acetonitrile at room temperature is shown in Figure 2[8] and is identical in dimethylsulphoxide and propylene carbonate. The complex is more stable in all solvents than is III. However a solution of IV in acetonitrile left overnight does show marked changes in both its absorption spectrum (Figure 4) and its electrochemistry. After twenty four hours the ML(bipy)CT transition of IV in acetonitrile has shifted to 23,300 cm^{-1} (ε=8,100) and the ML(py)CT transition is no longer discernible. This suggests that the Ru(II)$(bipy)_2$ chromophore is still intact but the complex no longer contains py. The most probable reaction is solvent exchange with py to form cis-$[Ru(bipy)_2(CH_3CN)_2]^{2+}$. The acetonitrile-containing complex has been prepared and characterised by Durham and co-workers[9] and has an absorption maximum at 23,500 cm^{-1}. Equally the difference between the half-

FIGURE 4: Absorption spectra of cis-$[Ru(bipy)_2py_2]^{2+}$ in acetonitrile

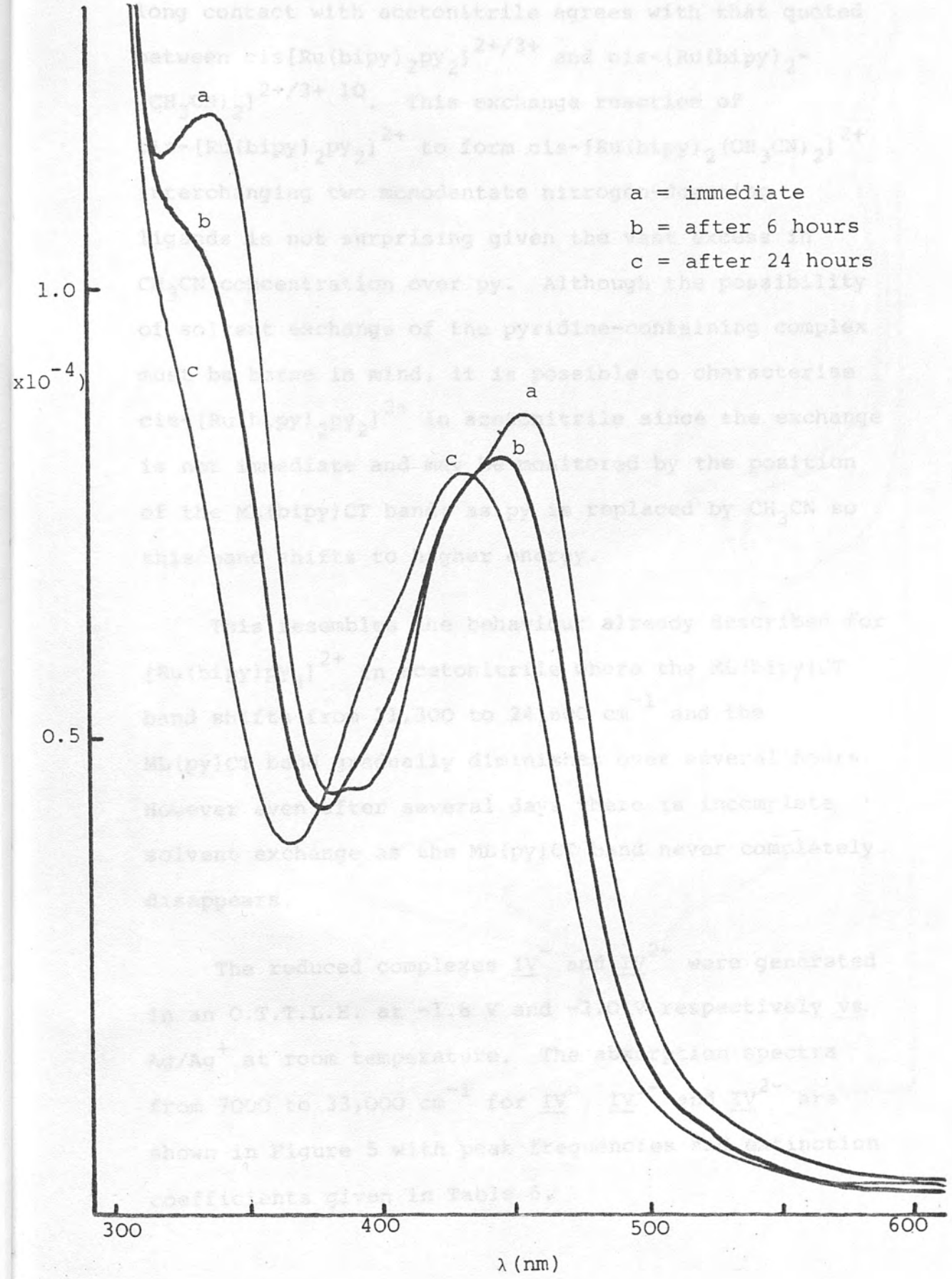

wave potential for $\underline{IV}^{O/+}$ and that of the complex after long contact with acetonitrile agrees with that quoted between cis$[Ru(bipy)_2py_2]^{2+/3+}$ and cis-$[Ru(bipy)_2(CH_3CN)_2]^{2+/3+}$ [10]. This exchange reaction of cis-$[Ru(bipy)_2py_2]^{2+}$ to form cis-$[Ru(bipy)_2(CH_3CN)_2]^{2+}$ interchanging two monodentate nitrogen-donating ligands is not surprising given the vast excess in CH_3CN concentration over py. Although the possibility of solvent exchange of the pyridine-containing complex must be borne in mind, it is possible to characterise cis-$[Ru(bipy)_2py_2]^{2+}$ in acetonitrile since the exchange is not immediate and may be monitored by the position of the ML(bipy)CT band; as py is replaced by CH_3CN so this band shifts to higher energy.

This resembles the behaviour already described for $[Ru(bipy)py_4]^{2+}$ in acetonitrile where the ML(bipy)CT band shifts from 21,300 to 24,600 cm^{-1} and the ML(py)CT band gradually diminishes over several hours. However even after several days there is incomplete solvent exchange as the ML(py)CT band never completely disappears.

The reduced complexes $\underline{IV}^{-}$ and $\underline{IV}^{2-}$ were generated in an O.T.T.L.E. at -1.8 V and -2.0 V respectively *vs.* Ag/Ag^{+} at room temperature. The absorption spectra from 7000 to 33,000 cm^{-1} for $\underline{IV}^{o}$, $\underline{IV}^{1-}$ and $\underline{IV}^{2-}$ are shown in Figure 5 with peak frequencies and extinction coefficients given in Table 6.

FIGURE 5: Absorption spectra of cis-$[Ru(bipy)_2py_2]^{2+/1+/0}$ in dimethylsulphoxide at room temperature

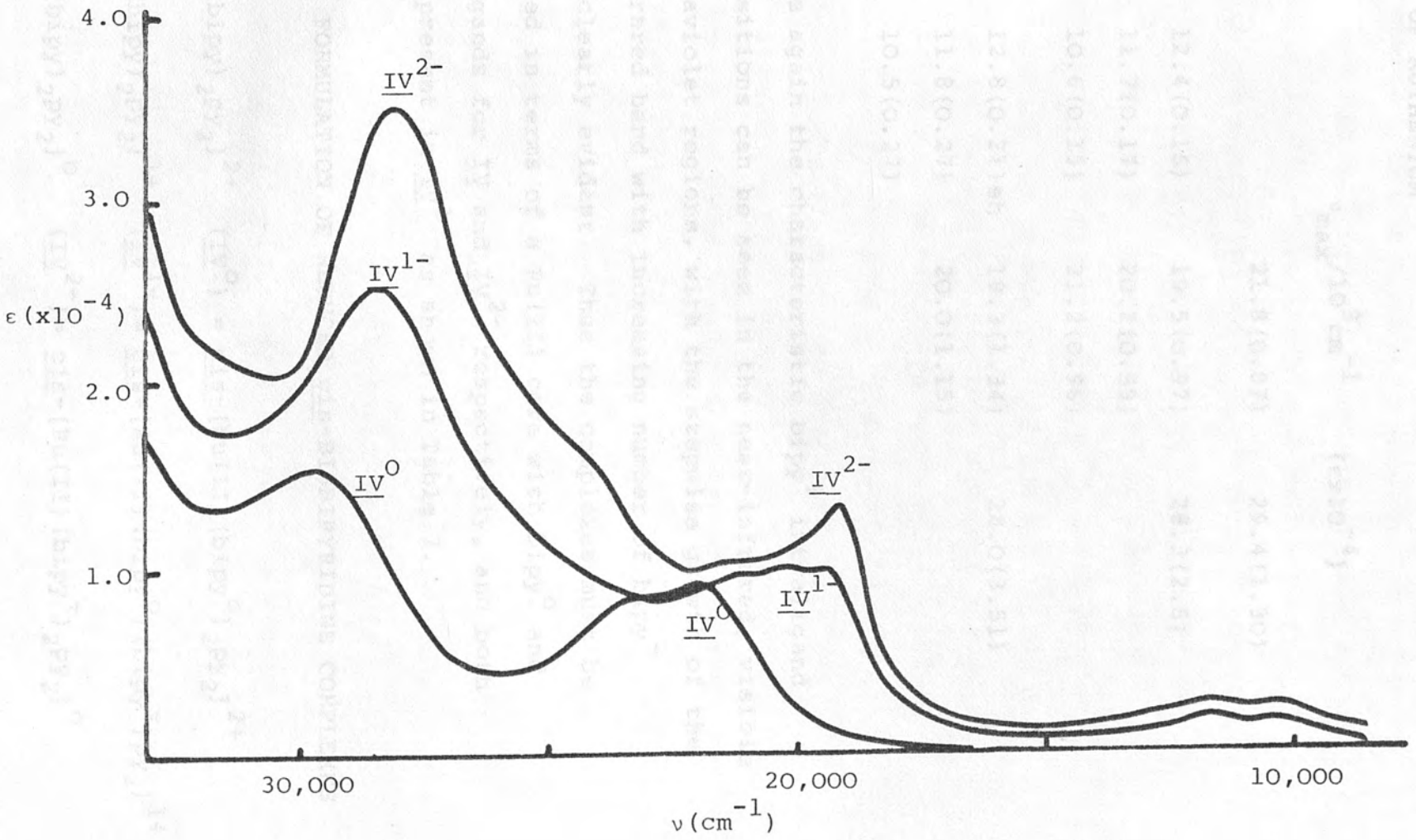

TABLE 6: ABSORPTION BANDS in cis-BISBIPYRIDINE COMPLEXES OF RUTHENIUM

Complex	$\nu_{max}/10^3 cm^{-1}$ ($\varepsilon x 10^{-4}$)		
IV^{o}		21.8(0.87)	29.4(1.30)
IV^{1-}	12.4(0.16)	19.5(0.97)	28.3(2.5)
	11.7(0.17)	20.2(0.99)	
	10.6(0.15)	21.2(0.96)	
IV^{2-}	12.8(0.21)sh	19.3(1.34)	28.0(3.51)
	11.8(0.27)	20.0(1.15)	
	10.5(0.27)		

Once again the characteristic $bipy^{\cdot-}$ intraligand $\pi\pi^*$ transitions can be seen in the near-infrared, visible and ultraviolet regions, with the stepwise growth of the near-infrared band with increasing number of $bipy^{-}$ ligands clearly evident. Thus the complexes must be formulated in terms of a Ru(II) core with $bipy^{o}$ and $bipy^{-}$ ligands for IV and IV^{2-} respectively, and both ligands present in IV^{1-} as shown in Table 7.

TABLE 7: FORMULATION OF REDUCED cis-BISBIPYRIDINE COMPLEXES

$$cis\text{-}[Ru(bipy)_2py_2]^{2+} \quad (IV^{o}) = cis\text{-}[Ru(II)(bipy^{o})_2py_2]^{2+}$$

$$cis\text{-}[Ru(bipy)_2py_2]^{1+} \quad (IV^{1-}) = cis\text{-}[Ru(II)(bipy^{o})(bipy^{\cdot-})py_2]^{1+}$$

$$cis\text{-}[Ru(bipy)_2py_2]^{o} \quad (IV^{2-}) = cis\text{-}[Ru(II)(bipy^{\cdot-})_2py_2]^{o}$$

The visible band at 21,800 cm^{-1} in $\underline{IV}^{o}$ is a Ru→$bipy^{o}$ charge transfer transition whereas the doublet at 19,300 cm^{-1} in $\underline{IV}^{2-}$ is an intraligand $\pi\pi^*$ transition of $bipy^{-}$. Thus the 20,000 cm^{-1} band in $\underline{IV}^{1-}$, which has coexisting $bipy^{o}$ and $bipy^{-}$ ligands, has a threefold structure, similar to the visible band in $\underline{I}^{1-}$ and $\underline{I}^{2-}$, due to the superposition of a Ru→$bipy^{o}$ charge transfer transition (21,200 cm^{-1}) and a doublet $bipy^{-}$ intraligand $\pi\pi^*$ transition (20,200 and 19,500 cm^{-1}). The measured extinction coefficients and band shapes for the visible and near-infrared bands of $\underline{IV}^{1-}$ and $\underline{IV}^{2-}$ are similar to those of $\underline{I}^{1-}$ (whose visible region also contains transitions due to coexisting $bipy^{o}$ and $bipy^{-}$ ligands) and $\underline{II}^{2-}$ (which has only $bipy^{-}$ transitions in its visible and near-infrared spectral region) respectively.

However, in the reduced complexes the ultraviolet band at 28,000 cm^{-1} has an anomolous intensity if assigned exclusively to a $bipy^{-}$ transition, as in $\underline{I}^{1-}$ ($\varepsilon=1.74\times10^{4}$) and $\underline{I}^{2-}$ ($\varepsilon=2.5\times10^{4}$). Thus we would suggest that this band not only contains the $bipy^{-}$ intraligand $\pi\pi^*$ transition (with $\varepsilon=1.7\times10^{4}$ and 2.5×10^{4} for $\underline{IV}^{1-}$ and $\underline{IV}^{2-}$ respectively) but also a Ru(II)→py charge transfer transition ($\varepsilon\sim1\times10^{4}$) as found in the absorption spectrum of $\underline{IV}^{o}$ (Table 6).

The absorption spectra of $\underline{IV}$, $\underline{IV}^{1-}$ and $\underline{IV}^{2-}$ are not solvent dependent for dimethylsulphoxide, N,N'-

dimethylformamide and acetonitrile on the timescale of the experiment. The possibility of solvent exchange is excluded by regenerating the spectrum of IV exactly after every spectroelectrochemical characterisation.

In summary, the behaviour of the two low-symmetry bipy-containing complexes, III and IV, complements that of the tris-bipy complex, I, and their electrochemistry and the absorption spectra of the reduced complexes can be understood and explained completely using the localised model expounded in Chapter 2.

trans-bispyridine-bisbipyridine-ruthenium(II) - V

Until recently only the cis form of complexes of the type $Ru(II)bipy)_2L_2$ were thought to be stable because of the severe steric hindrance between the mutually opposed 6,6' hydrogens in the trans geometry. However, platinum(II) and palladium(II) form stable roughly planar bis-bipy complexes whose structures have been verified by X-ray crystallography[11,12]. Krause described the preparation of trans-$[Ru(bipy)_2py_2]^{2+}$ in 1977[13] and this was verified later[10]. Earlier Durham and co-workers had synthesised trans-$[Ru(bipy)_2(OH_2)(OH)]^{2+}$, which is the starting material for trans-$[Ru(bipy)_2py_2]^{2+}$ and had characterised the trans-aquo complex by X-ray crystallography[14]. The bipy ligands were not seriously distorted but the entire ligand was slightly bowed

perpendicular to the C_2-C_2' axis.

The complex, trans-$[Ru(bipy)_2py_2]^{2+}$, V, by virtue of its trans-planar geometry, offers the possibility of direct symmetry-favoured ligand-ligand interaction and thus delocalisation of the π orbitals over the two bipy ligands. Therefore we have synthesised and characterised the trans-$[Ru(bipy)_2py_2]^{2+}$ complex in order to identify whether it belongs to the trapped-electron model class (together with all other bipyridine complexes studied to date) or departs significantly from this category.

The absorption spectra of equimolar solutions of the cis and trans complexes in dimethylsulphoxide at room temperature are compared in Figure 6, with band positions and assignments given in Table 8.

TABLE 8: ABSORPTION BANDS FOR cis- AND trans-$[Ru(bipy)_2py_2]^{2+}$; $\nu/10^3 cm^{-1}$ ($\varepsilon x 10^{-4}$)

Complex	Transitions		
	$d\pi \rightarrow \pi^*$bipy	$d\pi \rightarrow \pi^*$py	$\pi \rightarrow \pi^*$bipy
cis-$[Ru(bipy)_2py_2]^{2+}$	21.8(0.87)	29.4(1.30)	34.5(4.96)
trans-$[Ru(bipy)_2py_2]^{2+}$	21.1(0.97)	29.1(1.30)	34.4(4.96)

The absorption spectrum of trans-$[Ru(bipy)_2py_2]^{2+}$ is red-shifted compared to that of the cis-complex, with the largest shift in the visible Ru(II)→bipy charge transfer band. X-ray crystallographic studies show that

FIGURE 6: Absorption spectra of equimolar concentrations of cis- and trans-$[Ru(bipy)_2py_2]^{2+}$

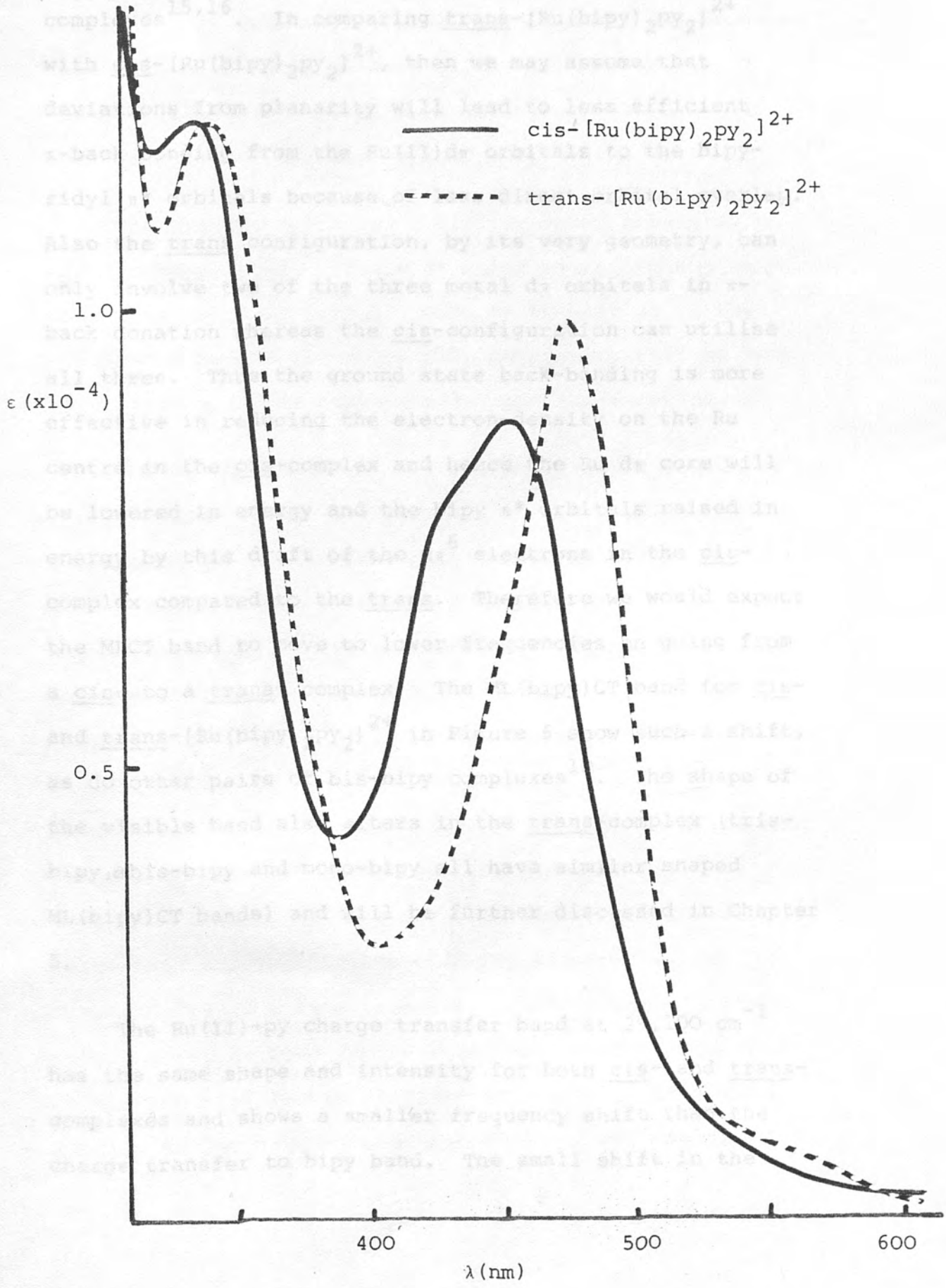

the bipy ligands in other trans-bipy complexes are not internally coplanar[11,12,14] unlike the tris-bipy complexes[15,16]. In comparing trans-$[Ru(bipy)_2py_2]^{2+}$ with cis-$[Ru(bipy)_2py_2]^{2+}$, then we may assume that deviations from planarity will lead to less efficient π-back bonding from the Ru(II)$d\pi$ orbitals to the bipyridyl π^* orbitals because of less direct orbital overlap. Also the trans configuration, by its very geometry, can only involve two of the three metal $d\pi$ orbitals in π-back donation whereas the cis-configuration can utilise all three. Thus the ground state back-bonding is more effective in reducing the electron-density on the Ru centre in the cis-complex and hence the Ru $d\pi$ core will be lowered in energy and the bipy π^* orbitals raised in energy by this drift of the $d\pi^6$ electrons in the cis-complex compared to the trans. Therefore we would expect the MLCT band to move to lower frequencies on going from a cis- to a trans- complex. The ML(bipy)CT band for cis- and trans-$[Ru(bipy)_2py_2]^{2+}$ in Figure 6 show such a shift, as do other pairs of bis-bipy complexes[10]. The shape of the visible band also alters in the trans-complex (tris-bipy, bis-bipy and mono-bipy all have similar shaped ML(bipy)CT bands) and will be further discussed in Chapter 5.

The Ru(II)→py charge transfer band at 29,100 cm^{-1} has the same shape and intensity for both cis- and trans-complexes and shows a smaller frequency shift than the charge transfer to bipy band. The small shift in the

trans-complex can be totally accounted for by the destabilisation of the Ru(II) core which may be independently estimated from electrochemical measurements (see below) and thus we must infer that the energy of the π^* orbitals of the py ligands is unaffected by the configuration of the bipy ligands.

The trans-complex has a similar redox chemistry to cis-$[Ru(bipy)_2py_2]^{2+}$ (Table 9) which therefore suggests that trans-$[Ru(bipy)_2py_2]^{2+}$ must be thought of in the same terms as all the other bipy complexes, that is the bipy ligands in the trans-complex are non-interacting.

The electrode potentials for every redox couple of V are similar to but distinct from corresponding redox couples of IV. That these differences were real and not within experimental error was confirmed by adding cis-$[Ru(bipy)_2py_2]^{2+}$ to a solution of trans-$[Ru(bipy)_2py_2]^{2+}$, and directly observing the displacement of corresponding couples: $IV^{0/1+}$-$V^{0/1+}$ = 30 mV (as was also noted by Walsh and Durham[10]); $IV^{0/1-}$-$V^{0/1-}$ = 50 mV; $IV^{1-/2-}$-$V^{1-/2-}$ = 40 mV. Note that the trans-complex is both oxidised and reduced at less extreme potentials than the cis-complex. This is exactly the behaviour predicted from the π-back bonding discussion. The electrochemical results give us a direct measure of the destabilisation of the metal $d\pi$ core (30 mV = 240 cm^{-1}) and the decrease in the $\pi\pi^*$ bipy levels (50 mV = 400 cm^{-1}) in the trans-complex as compared to the levels in the cis-complex

TABLE 9: ELECTRODE POTENTIALS FOR trans-$[Ru(bipy)_2py_2]^{2+}$ [a]

$$\underline{trans}\text{-}[Ru(bipy)_2py_2]^{3+} \xleftarrow{+0.94} \underline{trans}\text{-}[Ru(bipy)_2py_2]^{2+} \xrightarrow{-1.61} \underline{trans}\text{-}[Ru(bipy)_2py_2]^{1+} \xrightarrow{-1.81} trans\text{-}[Ru(bipy)_2py_2]^{0}$$

$\underline{V}^{1+}$ $\underline{V}^{0}$ $\underline{V}^{1-}$ $\underline{V}^{2-}$

[a] Complex studied in CH_3CN/0.1M $TBA[BF_4]$ at room temperature on platinum, E^{o}/V vs. Ag/Ag^{+}

$\Delta Ep \sim 70$ mV for every couple.

(Figure 7). The electrochemical results can therefore be used to map the energy levels of the trans- complex compared to the cis-isomer giving a predicted ML(bipy)CT of 21,160 cm^{-1} which is in close agreement with the observed value of 21,100 cm^{-1}.

The spacing between the two reduction complexes, $\underline{V}^{0/1-}$ and $\underline{V}^{1-/2-}$, of 200 mV, and the cathodic half-wave potentials themselves, suggest that trans-$[Ru(bipy)_2py_2]^{2+}$ and its reduced analogues are best thought of in similar terms to the cis- complex and other related complexes, that is in terms of the trapped-electron model. The voltammetric reversibility of the reduction processes ($\Delta Ep \sim 70$ mV) meant that this could be confirmed by spectral studies of the reduced complexes $\underline{V}^{1-}$ and $\underline{V}^{2-}$.

In common with other pyridine-containing complexes of ruthenium, the trans- complex V, is not indefinitely stable in solution. After several days in acetonitrile the visible ML(bipy)CT band had shifted from 21,100 to 22,600 cm^{-1} and the ML(py)CT band was absent, thereby implying that the complex had undergone solvent exchange to trans-$[Ru(bipy)_2(CH_3CN)_2]^{2+}$ which is confirmed by matching both spectral and electrochemical data with that of published trans$[Ru(bipy)_2(CH_3CN)_2]^{2+}$ [10]. The trans- complexes do not however isomerise, the electrochemical and spectral data remaining indicative of a trans- complex over an indefinite time period.

A solution of trans-$[Ru(bipy)_2py_2]^{2+}$ in acetonitrile

FIGURE 7: Comparative schematic molecular orbital diagram for cis- and trans-$[Ru(bipy)_2py_2]^{2+}$

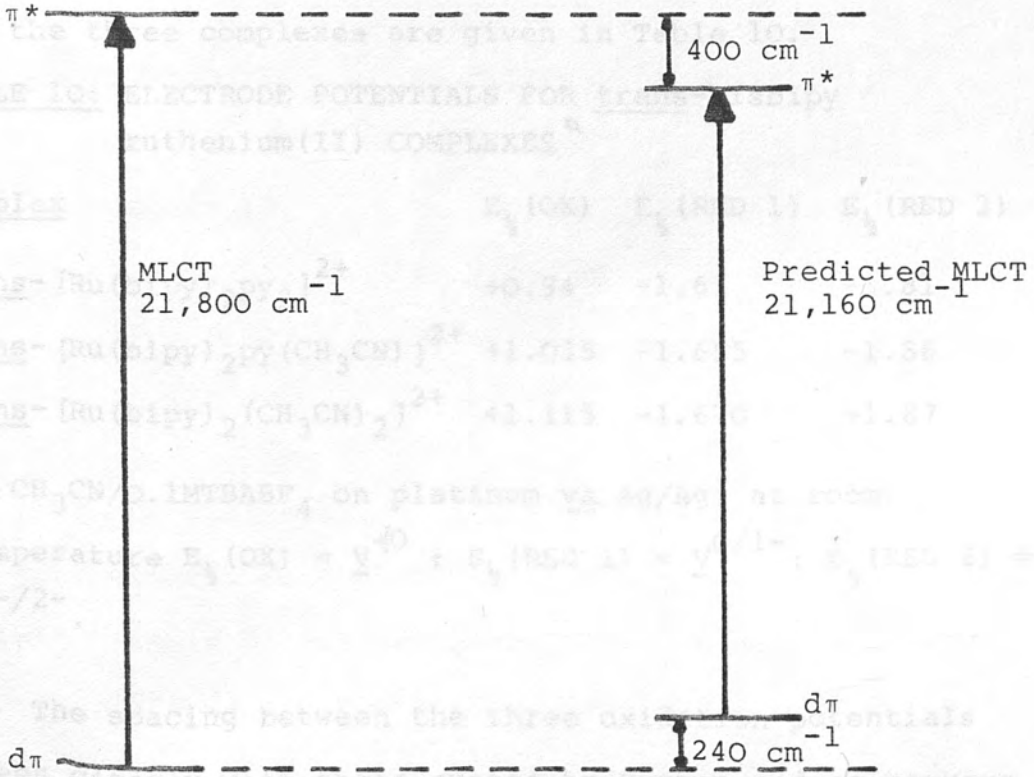

cis-$[Ru(bipy)_2py_2]^{2+}$ IV

trans-$[Ru(bipy)_2py_2]^{2+}$ V

was studied electrochemically over a period of a few days, and it became obvious that the solvent exchange occurred in a stepwise fashion: $\underline{trans}\,[Ru(bipy)_2py_2]^{2+} \xrightarrow{CH_3CN} \underline{trans}\,[Ru(bipy)_2py(CH_3CN)]^{2+} \xrightarrow{CH_3CN} \underline{trans}\,[Ru(bipy)_2(CH_3CN)_2]^{2+}$. The solution originally contained peaks due only to the bis-py complex. In time these peaks decreased in height while those of the mixed complex grew and subsequently fell as the peaks of the totally substituted complex appeared. The half-wave potentials for the three complexes are given in Table 10.

TABLE 10: ELECTRODE POTENTIALS FOR *trans*-bisbipy ruthenium(II) COMPLEXES[a]

Complex	$E_{\frac{1}{2}}$(OX)	$E_{\frac{1}{2}}$(RED 1)	$E_{\frac{1}{2}}$(RED 2)
trans-$[Ru(bipy)_2py_2]^{2+}$	+0.94	-1.61	-1.81
trans-$[Ru(bipy)_2py(CH_3CN)]^{2+}$	+1.035	-1.655	-1.86
trans-$[Ru(bipy)_2(CH_3CN)_2]^{2+}$	+1.115	-1.670	-1.87

[a] In CH_3CN/0.1MTBABF$_4$ on platinum *vs.* Ag/Ag^+ at room temperature $E_{\frac{1}{2}}(OX) = \underline{V}^{+0}$; $E_{\frac{1}{2}}(RED\ 1) = \underline{V}^{0/1-}$; $E_{\frac{1}{2}}(RED\ 2) = \underline{V}^{1-/2-}$.

The spacing between the three oxidation potentials agrees closely with those quoted by Durham and co-workers for the specified complexes[9]; however the successive reduction potentials for the *cis*- and *trans*- complexes have not been reported previously.

The solvent exchange is once again slow enough at room temperature to enable spectral studies of intact $\underline{V}^{1-}$ and $\underline{V}^{2-}$ to be accomplished. The reduced complexes

$\underline{V}^{1-}$ and $\underline{V}^{2-}$ were generated at a platinum O.T.T.L.E. at -1.78 V and -2.10 V respectively (vs. Ag/Ag^{+}); the resultant spectra are shown in Figure 8 and the absorption bands are tabulated in Table 11.

TABLE 11: ABSORPTION BANDS IN trans-$[Ru(bipy)_2py_2]^{2+/1+/0}$ ($\underline{V}^{0,1-,2-}$)

Complex	$\nu_{max}/10^3 cm^{-1}$ ($\varepsilon x 10^{-4}$)		
$\underline{V}^{0}$		21.1(0.97)	29.1(1.30)
$\underline{V}^{1-}$	13.0(0.16)	20.1(1.02)	29.1(2.51)
	12.0(0.18)	21.0(1.18)	
	10.6(0.17)		
$\underline{V}^{2-}$	12.8(0.25)	19.3(1.37)	28.6(3.54)
	11.8(0.32)	20.4(1.08)	
	10.4(0.32)		

The spectral studies of the reduced complexes, $\underline{V}^{1-}$ and $\underline{V}^{2-}$, clearly show that trans$[Ru(bipy)_2py_2]^{2+/1+/0}$ is another example of the trapped-electron model in which the bipy ligands are non-interacting; again we see the characteristic $bipy^{-}$ intraligand transitions in the near-infrared, visible and ultraviolet regions. Hence the complexes should be formulated as in Figure 8 and detailed assignments of the absorption bands, consistent with their position and intensity, can be deduced, just as for the cis-$[Ru(bipy)_2py_2]^{2+}$ complex.

The near-infrared band centred at approximately

FIGURE 8: Absorption spectra of trans-$[Ru(bipy)_2py_2]^{2+/1+/0}$ in dimethylsulphoxide at room temperature

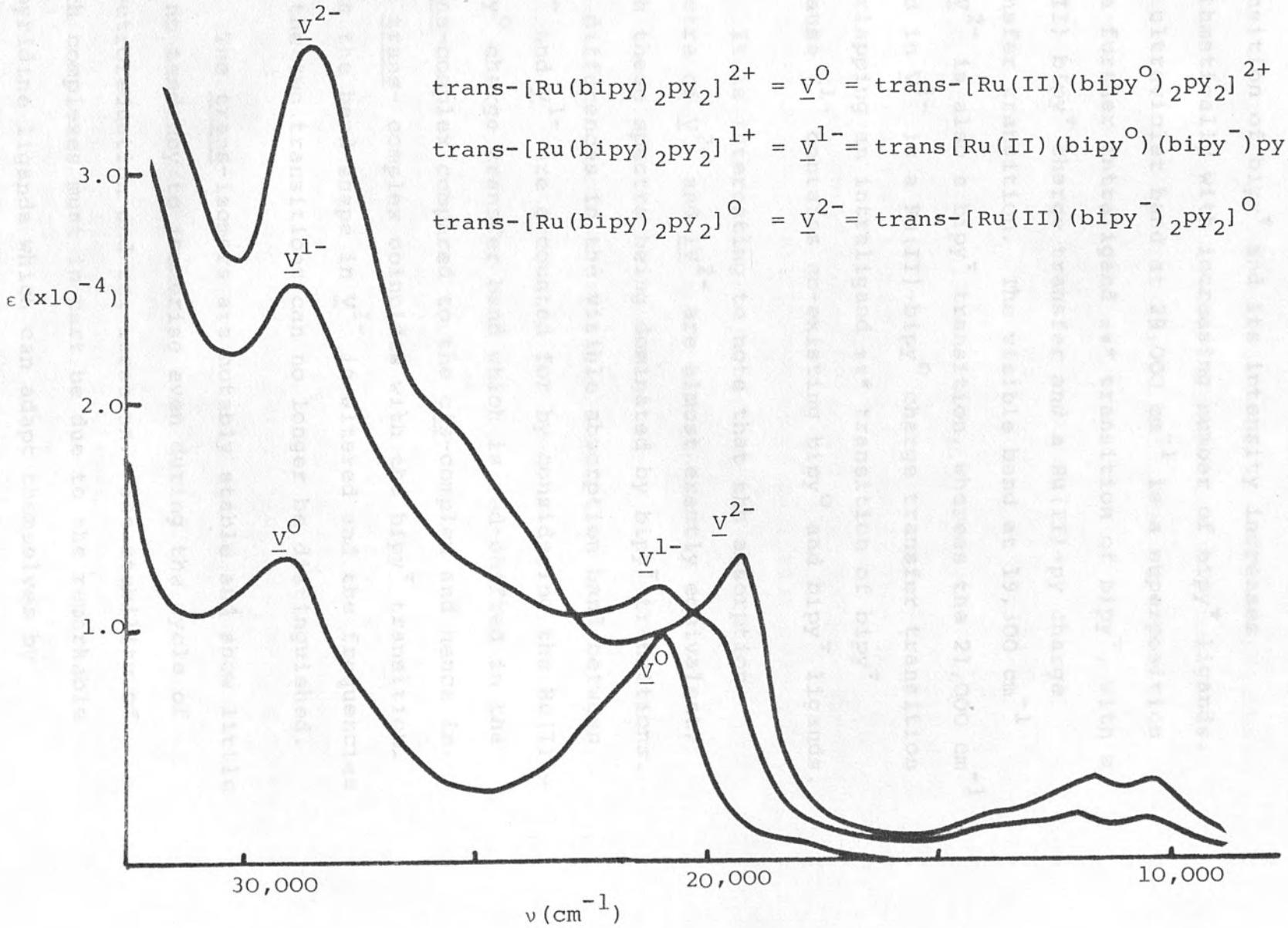

12,000 cm^{-1} in $\underline{V}^{1-}$ and $\underline{V}^{2-}$ is an intraligand $\pi\pi^*$ transition of $bipy^{\bar{\cdot}}$ and its intensity increases arithmetically with increasing number of $bipy^{\bar{\cdot}}$ ligands. The ultraviolet band at 29,000 cm^{-1} is a superposition of a further intraligand $\pi\pi^*$ transition of $bipy^{\bar{\cdot}}$, with a Ru(II) $bipy^{\bar{\cdot}}$ charge transfer and a Ru(II)→py charge transfer transition. The visible band at 19,300 cm^{-1} in $\underline{V}^{2-}$ is also a $bipy^{\bar{\cdot}}$ transition, whereas the 21,000 cm^{-1} band in $\underline{V}^{1-}$ is a Ru(II)→$bipy^{o}$ charge transfer transition overlapping an intraligand $\pi\pi^*$ transition of $bipy^{\bar{\cdot}}$ because $\underline{V}^{1-}$ contains co-existing $bipy^{o}$ and $bipy^{\bar{\cdot}}$ ligands.

It is interesting to note that the absorption spectra of $\underline{V}^{2-}$ and $\underline{IV}^{2-}$ are almost exactly equivalent, both these spectra being dominated by $bipy^{\bar{\cdot}}$ transitions. The differences in the visible absorption band between $\underline{IV}^{1-}$ and $\underline{V}^{1-}$ are accounted for by considering the Ru(II)→$bipy^{o}$ charge transfer band which is red-shifted in the *trans*-complex compared to the *cis*-complex and hence in the *trans*- complex coincides with the $bipy^{\bar{\cdot}}$ transition. Thus the band shape in $\underline{V}^{1-}$ is altered and the frequencies of the two transitions can no longer be distinguished.

The *trans*-isomers are notably stable and show little or no tendency to isomerise even during the cycle of electroreduction and regeneration. The stability of such complexes must in part be due to the remarkable bipyridine ligands which can adapt themselves by twisting or bowing to meet the constraints of the *trans*-bis-stereochemistry but remain non-mutually

interacting in all complexes studied to date. Thus the trans-$[Ru(bipy)_2py_2]^{2+}$ complex and its reduced analogues are yet another group whose electrochemistry and absorption spectra can best be rationalised using the trapped-electron model.

Ligand-ligand inter-valence charge transfer

The localised electron model implies that in principle we should observe ligand-ligand inter-valence charge transfer (IVCT) phenomena in partially reduced complexes which contain discrete co-existing $bipy^{o}$ and $bipy^{-}$ groups. Indeed Hanck and co-workers[17] have attributed the notably temperature-dependent line broadening found in their e.s.r. spectrum of $\underline{I}^{1-}$, but absent for $\underline{I}^{3-}$, to just such a process, with an estimated thermal barrier to electron hopping of about 1000 cm^{-1}.

The barrier E_{th} corresponds to the intersection of the potential energy curves of equivalent valence isomers; Hush[18] has shown that where the curves are quadratic in form and there is negligible interaction between the redox active centres the vertical (IVCT) transition energy E_{op} should be 4 E_{th}.

Accordingly spectroelectrochemical studies of the family of complexes I, III, IV and V and all their reduced analogues were extended to include the near-infrared region 7000 to 3500 cm^{-1} and the results are presented in Table 12.

TABLE 12: INTERVALENCE CHARGE TRANSFER BANDS

Species	$\nu(cm^{-1})$	ε	$10^4 F^a$
$[Ru(bipy)_3]^+$ $\underline{I}^{1-}$	4500	210	19.3
$[Ru(bipy)_3]^o$ $\underline{I}^{2-}$	4500	345	31.7
$\underline{cis}[Ru(bipy)_2py_2]^+$ $\underline{IV}^{1-}$	4350	121	8.6
$\underline{trans}[Ru(bipy)_2py_2]^+$ $\underline{V}^{1-}$	4090	100	3.2

$^a F$ = oscillator strength = $4.6 \times 10^{-9} \times \varepsilon \times$ band half-width

A weak band near 4000 cm^{-1} is detected in the tris-bipy family of complexes for the species $[Ru(II)(bipy^o)_{3-n}(bipy^-)_n]^{2-n}$ when n = 1 or 2 ($\underline{I}^{1-}$, $\underline{I}^{2-}$) but not when n = 0 or 3 ($\underline{I}^{o}$, $\underline{I}^{3-}$), and we ascribe this to the bipy/bipy$^-$ IVCT transition. As far as is known, this is the first reported direct observation of such a transition between identical ligands. A similar band can also be observed in $\underline{IV}^{1-}$ and $\underline{V}^{1-}$. Thus only those complexes which contain both bipy^o and bipy$^-$ (that is, $\underline{I}^-$, $\underline{I}^{2-}$, $\underline{IV}^{1-}$ and $\underline{V}^{1-}$) exhibit the characteristic near-infrared band. For example, $[Ru(bipy)py_4]^+$, $\underline{III}^-$, is featureless in this region in contrast to isovalent $\underline{IV}^{1-}$ and $\underline{I}^{1-}$, and $\underline{IV}^{2-}$ and $\underline{V}^{2-}$ are featureless in contrast to $\underline{I}^{2-}$.

The IVCT band is in all cases relatively broad (band width at half-height $\sim$ 2000 cm^{-1}) and weak. It is decidedly more intense in $\underline{I}^{1-}$ and $\underline{I}^{2-}$ than in $\underline{IV}^{1-}$ or $\underline{V}^{1-}$, which have only one donor and one acceptor centre. The slight but significant differences between *cis*-

and trans-$[Ru(bipy)_2py_2]^+$ are presumably due to the different mutual arrangements of the chelating ligands.

All compounds were studied in dimethylsulphoxide; in addition I and its reduction products were studied in dimethylformamide and in acetonitrile, with indistinguishable results. Careful correction for solvent background is critical, because of solvent vibrational combination bands, and was performed by direct subtraction.

We conclude that the incompletely reduced complexes $[Ru(bipy)_3]^{+/O}$ and $[Ru(bipy)_2py_2]^+$ do indeed contain Ru(II) and distinct co-existing $bipy^O$ and $bipy^-$ ligands, and exhibit low intensity IVCT transitions in accord with this formulation. These compounds are therefore mixed-valence compounds showing electron-transfer between negligibly interacting ligand sites, in general agreement with Hush's theory[18] for such systems, which has been more usually applied to adjacent metal sites in binuclear or polynuclear compounds[19].

Cis-dichloro-bisbipyridine ruthenium(II)

The replacement of a π-acceptor ligand such as bipy or py by a π-donor ligand, for example Cl^- as in cis-$[Ru(bipy)_2Cl_2]^O$, VI, is expected to be reflected in the electrochemistry and absorption spectrum. A π-donating ligand should stabilise Ru(III) relative to Ru(II) because the d^5 Ru(III) centre is a good π-

acceptor owing to the vacancy in its dπ subshell and hence the metal-based oxidation VI$^{0/1+}$ should be easier, and the ML(bipy)CT at lower energy than in cis-$[Ru(bipy)_2py_2]^{2+}$. In order to check just how much the characteristics of the Ru-bipy chromophore are altered by the spectator ligands, cis-$[Ru(bipy)_2Cl_2]^{0}$ was prepared and examined in a similar manner to cis-$[Ru(bipy)_2py_2]^{2+}$.

The absorption spectrum of VI can be understood and transitions assigned to the bands by considering several appropriate model complexes shown in Table 13.

The two ultraviolet bands at 33,700 and 41,200 cm^{-1} are assigned to intraligand ($bipy^{o}$) transitions as in all previous bipy containing complexes. Their intensities are in keeping with all other bis-bipy complexes. The bands at 18,100 and 26,400 cm^{-1} are both assigned to Ru→$bipy^{o}$ charge transfer transitions. The visible band (18,100 cm^{-1}) is the characteristic lowest-energy MLCT band previously observed (as a doublet) near 22,000 cm^{-1} in I and IV[20].

Its measured intensity is in close agreement with those of other bis-bipy complexes. The shift of this band to much lower energy (3700 cm^{-1} lower compared to IV) is indicative of the destabilisation of the metal dπ orbitals by the π-donating chloride ligand.

We assign the 26,400 cm^{-1} band as a transition from

TABLE 13: ABSORPTION SPECTRA OF BIPYRIDYL COMPLEXES OF RUTHENIUM(II); $\nu x10^{-3} cm^{-1}$ ($\varepsilon x10^{-4}$)

Complex	Transitions			
	MLCT		Intraligand	
	$d\pi \rightarrow \pi^*$bipy(1)	$d\pi \rightarrow \pi^*$bipy(2)	$\pi \rightarrow \pi^*$(1)	$\pi \rightarrow \pi^*$(2)
$cis[Ru(bipy)_2Cl_2]^{O}$	18.1(0.85)	26.4(0.93)	33.7(5.00)	41.2(2.85)
$[Ru(bipy)_3]^{2+}$	22.1(1.37)		35.0(7.06)	40.6(2.58)
$cis[Ru(bipy)_2py_2]^{2+}$	21.8(0.87)		34.5(4.96)	41.0(2.58)
$cis[Ru(bipy)_2(NH_3)_2]^{2+}$ [a]	20.2(0.93)	28.6(0.80)	34.3(5.88)	41.0(2.18)
$cis[Ru(bipy)_2(SCN)_2]^{O}$ [a]	19.4(0.82)	27.6(0.88)	33.7(4.93)	40.7(3.02)
$cis[Ru(bipy)_2Br_2]^{O}$ [a]	18.4(0.97)	26.8(1.02)	33.4(5.25)	40.8(3.32)

[a] Ref 5

the Ru(II) centre to the second vacant π^* orbital in bipy, in agreement with Bryant and co-workers[5], because this band is present in several other bis-bipy complexes of ruthenium regardless of the nature of the spectator ligand (for example, NH_3, SCN^-, Br^-). The energy difference between $d\pi\rightarrow\pi^*(1)$ and $d\pi\rightarrow\pi^*(2)$ is similar for all ruthenium bis-bipy compounds (approximately 8300 cm^{-1}) and is mirrored by the difference in energy between $\pi\rightarrow\pi^*(1)$ and $\pi\rightarrow\pi^*(2)$ internal ligand transitions. The second charge transfer transition ($d\pi\rightarrow\pi^*(2)$) is not directly observed in $[Ru(bipy)_3]^{2+}$ and $[Ru(bipy)_2py_2]^{2+}$. Using the energy difference criterion it is predicted to occur at 30,500 cm^{-1} (22,200 + 8300 cm^{-1}) for $[Ru(bipy)_3]^{2+}$. Therefore it must lie under the intense $\pi\rightarrow\pi^*(1)$ transition of bipy and its presence is indicated by the greater width of this band in I and IV compared to VI (half-band-width = 1270, 1060 and 700 cm^{-1} for I, IV and VI respectively).

The electrochemistry of VI was studied in acetonitrile (Table 14) and dimethyl sulphoxide with indistinguishable results. The redox couples are all assigned as one-electron processes, from coulometry ($VI^{1+/0}$) and then by comparison of wave heights for all other steps.

As predicted the redox couple $VI^{0/+}$ is at much less positive potentials than $IV^{1+/0}$ and is assigned in common with all the other ruthenium complexes, as a metal based $[Ru]^{2+/3+}$ process. The donation of electron density to

TABLE 14: ELECTRODE POTENTIALS FOR cis-$[Ru(bipy)_2Cl_2]^{O}$ [a]

$$cis[Ru(bipy)_2Cl_2]^{2+} \xleftarrow{+1.66} cis[Ru(bipy)_2]^{1+} \xleftarrow{+0.01} cis[Ru(bipy)_2Cl_2]^{O} \xrightarrow{-1.95} cis[Ru(bipy)_2Cl_2]^{1-} \xrightarrow{-2.06} cis[Ru(bipy)_2Cl_2]^{2-}$$

$$\underline{VI}^{2+} \qquad \underline{VI}^{1+} \qquad \underline{VI}^{O} \qquad \underline{VI}^{1-} \qquad \underline{VI}^{2-}$$

[a] Complex studied in CH_3ON/0.1M $TBA[BF_4]$ at room temperature on platinum, E^{O}/V vs. Ag/Ag^{+}

the metal centre from the σ-donor chloride ion makes oxidation of Ru(II) to Ru(III) more facile. In marked contrast the further oxidation process, $\underline{VI}^{1+/2+}$ is totally irreversible. It might be a metal-based oxidation Ru(III)→Ru(IV) or a ligand-based oxidation, but no definite assignment can be given as $\underline{VI}^{2+}$ is unstable immediately even at low temperatures (-40°C) and has not been characterised.

The spacings between redox couples for VI are in close agreement with those given by Sullivan and co-workers[8]. They state that both cathodic processes were irreversible. However the redox couple $\underline{VI}^{0/1-}$ is completely reversible if the scan is reversed before reaching the potential of the second reduction wave. If the scan continues beyond the second reduction then both this step and the first reduction are irreversible (no return wave in either case); that is, the complex $\underline{VI}^{2-}$ rapidly undergoes some sort of chemical reaction.

The electrode potential of the couple $\underline{VI}^{0/1-}$ is 290 mV more negative than the first reduction couple of I, III or IV and thus cannot be automatically assigned to a bipy reduction. However the first reduction product, $\underline{VI}^{1-}$ is stable at room temperature (in oxygen-free conditions) and hence it can be generated in an O.T.T.L.E., and its spectrum investigated. The absorption spectra of VI and $\underline{VI}^{1-}$ are shown in Figure 9 and the absorption bands are tabulated in Table 15.

FIGURE 9: Absorption spectra of cis-$[Ru(bipy)_2Cl_2]^{o/1-}$ in acetonitrile at room temperature

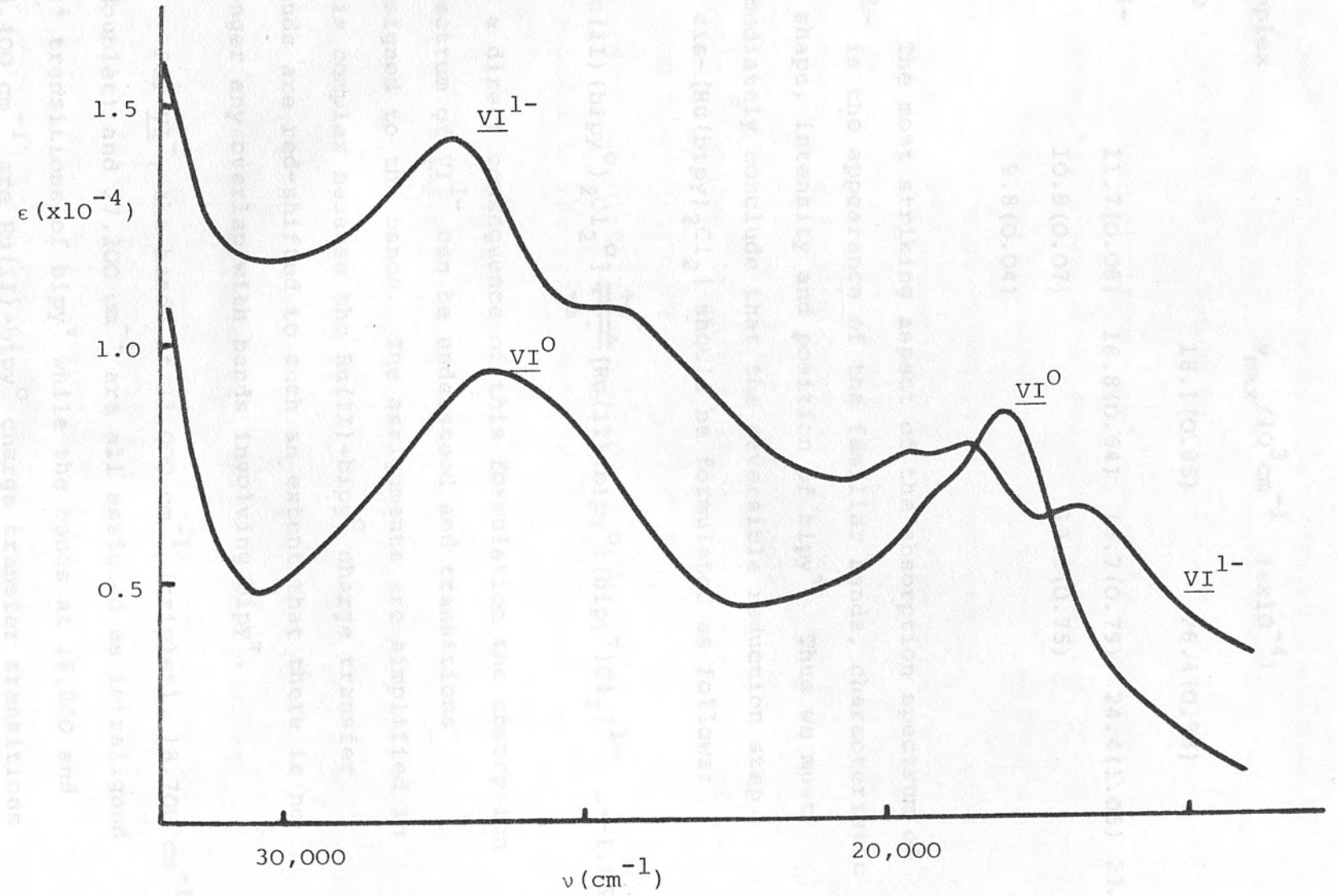

TABLE 15: ABSORPTION BANDS FOR cis-$[Ru(bipy)_2Cl_2]^{0/1-}$.

Complex	$\nu_{max}/10^3 cm^{-1}$ ($\varepsilon x10^{-4}$)				
VI^0	18.1(0.85)	26.4(0.93)			
VI^{1-}	11.7(0.08)	16.8(0.64)	18.7(0.79)	24.4(1.06)	27.2(1.42
	10.9(0.07)		19.6(0.75)		
	9.8(0.04)				

The most striking aspect of the absorption spectrum of VI^{1-} is the appearance of the familiar bands, characteristic in shape, intensity and position of bipy$^{\cdot-}$. Thus we must immediately conclude that the reversible reduction step of cis-$[Ru(bipy)_2Cl_2]$ should be formulated as follows:

$$[Ru(II)(bipy^{o})_2Cl_2{}^{o}] \underset{-e^-}{\overset{+e^-}{\rightleftharpoons}} [Ru(II)(bipy^{o})(bipy^{\cdot-})Cl_2]^{1-} \quad E=-1.95\ V$$

As a direct consequence of this formulation the absorption spectrum of VI^{1-} can be understood and transitions assigned to the bands. The assignments are simplified in this complex because the Ru(II)→bipy^o charge transfer bands are red-shifted to such an extent that there is no longer any overlap with bands involving bipy$^{\cdot-}$.

For VI$^-$, the bands at 11,000 cm^{-1} (triplet), 18,700 cm^{-1} (doublet) and 27,200 cm^{-1} are all assigned as intraligand $\pi\pi^*$ transitions of bipy$^{\cdot-}$ while the bands at 16,800 and 24,400 cm^{-1} are Ru(II)→bipy^o charge transfer transitions

as in VI^{o} (18,100 and 26,400 cm^{-1}). The movement of the remaining ML(bipy^{o})CT absorption to lower energy upon partial reduction of bipyridyl complexes has been encountered previously; for example this band is found at 22,100 cm^{-1} in I^{o} but at 21,100 cm^{-1} in I^{-}.

The spectroelectrochemical methods have therefore very effectively elucidated the electrochemistry of cis-$[Ru(bipy)_2Cl_2]$ and the nature of its reduced states. This complex is much easier to oxidise than cis-$[Ru(bipy)_2py_2]^{2+}$ because of the σ-donating chloride ligands and is more difficult to reduce because of the electrostatic effect of the negative charge on the chloride ligands. A similar electrostatic effect of negatively charged ligands on the Ru(II)→bipy^{o} chromophore is also apparent in $[Ru(bipy)_3]^{2+}$ where the third reduction is approximately 400 mV more difficult than the first, due to the presence of two bipy^{-} ligands.

The perturbation of the chloride ligand on the metal dπ levels and the bipy π* levels is shown in Figure 10. The metal dπ levels are destabilised compared to those in cis-$[Ru(bipy)_2py_2]^{2+}$ by 0.95 V (7600 cm^{-1}) and the bipy π array is raised by 0.29 V (2320 cm^{-1}) in energy. The schematic energy level diagram predicts that the ML(bipy)CT transition should shift to lower energy on going from IV to VI (predicted shift 5300 cm^{-1}) which is in very satisfactory qualitative agreement with the experimentally observed shift (MLCT IV = 21,800 cm^{-1};

FIGURE 10: Comparative schematic molecular orbital diagram for cis-bis-bipy Ru(II) complexes

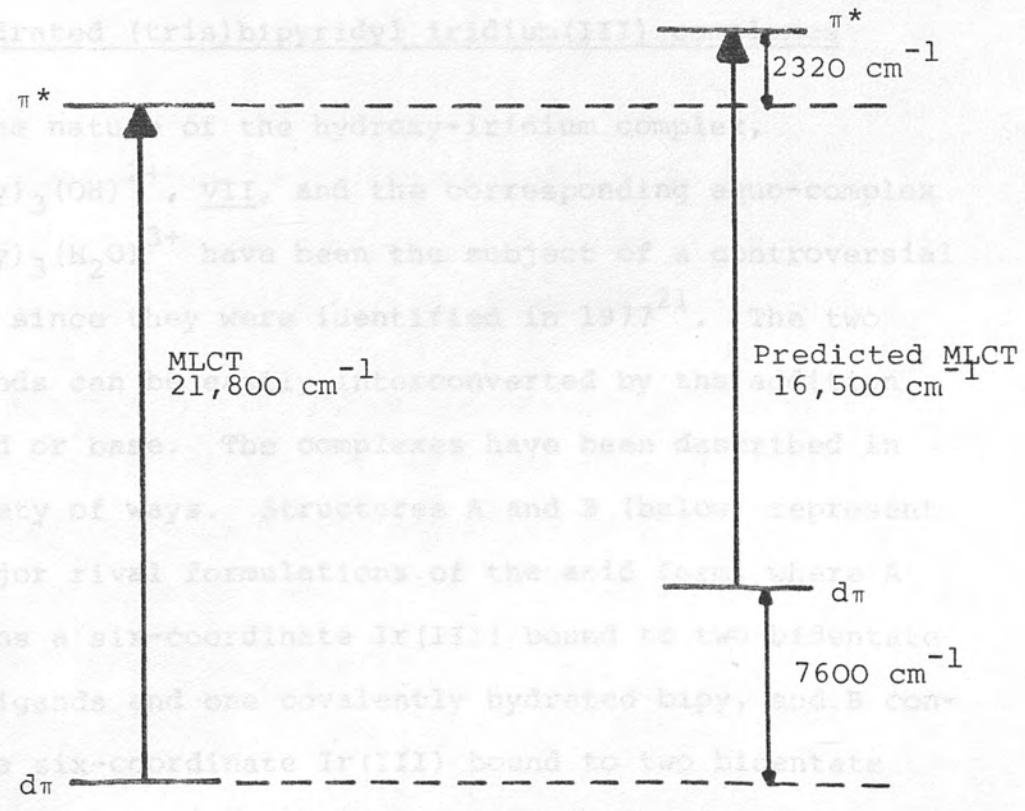

IV VI

MLCT VI = 18,100 cm^{-1}). Thus although the spectator ligand can greatly influence the behaviour of complexes of the type $Ru(II)(bipy)_2L_2$, both through its π-bonding and its electrostatic effect, the Ru-bipy chromophore still remains an isolated unit with a characteristic electrochemistry and absorption spectrum.

The hydrated (tris)bipyridyl iridium(III) complexes

The nature of the hydroxy-iridium complex, $Ir(bipy)_3(OH)^{2+}$, VII, and the corresponding aquo-complex $Ir(bipy)_3(H_2O)^{3+}$ have been the subject of a controversial debate since they were identified in 1977[21]. The two compounds can be easily interconverted by the addition of acid or base. The complexes have been described in a variety of ways. Structures A and B (below) represent two major rival formulations of the acid form, where A contains a six-coordinate Ir(III) bound to two bidentate bipy ligands and one covalently hydrated bipy, and B contains a six-coordinate Ir(III) bound to two bidentate bipy ligands, one monodentate bipy and one water molecule.

Observation of an ammonium N-H stretching band at 2650 cm^{-1} in the acidic form which disappears in basic solutions was cited as evidence for such formulations[21]. Gillard and co-workers[22] interpreted the ^1H nmr spectrum in dimethylsulphoxide in terms of structure A, whereas

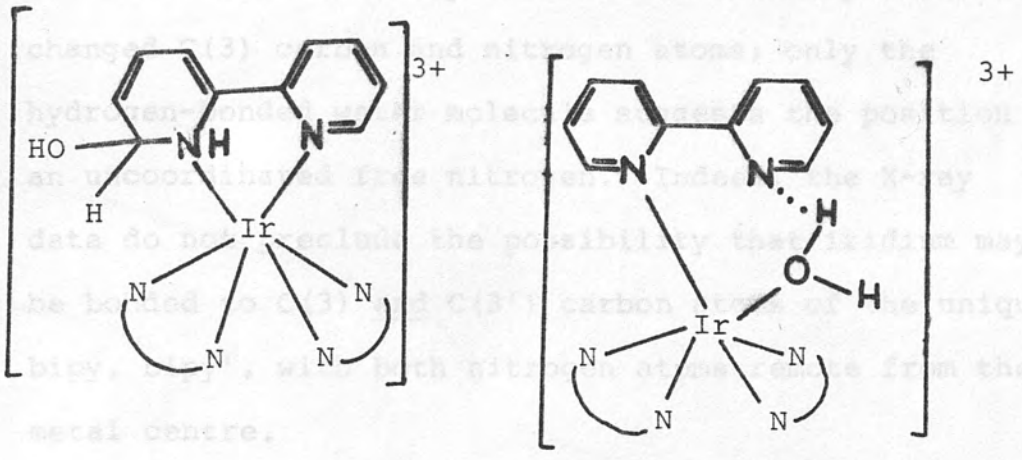

A B

Spellane and Watts[23] after examining the nmr spectrum in DCl/D_2O solutions and concluding that the water molecule is not covalently bound to bipy favoured structure B.

The X-ray crystal structure of the aquo-complex, recently published by Wickramasinghe and co-workers[24], shows that there is no monodentate bipy ligand and there is also no evidence for a covalently hydrated bipy ligand. Thus they suggest structure C.

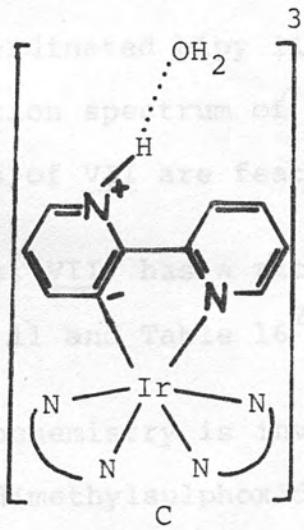

C

However, the X-ray data do not identify the interchanged C(3) carbon and nitrogen atoms; only the hydrogen-bonded water molecule suggests the position of an uncoordinated free nitrogen. Indeed, the X-ray data do not preclude the possibility that iridium may be bonded to C(3) and C(3') carbon atoms of the unique bipy, bipy', with both nitrogen atoms remote from the metal centre.

In an attempt to resolve the structural ambiguity, spectroelectrochemical studies of VII were undertaken. The deprotonated form was studied as the complex was isolated by precipitation from a basic solution.

The absorption spectrum of VII with its first major absorption band at 32,500 cm^{-1} ($\varepsilon=3.65 \times 10^4$) is very similar to that of $Ir(bipy)_3^{3+}$, II (ν_{max} = 32,200 cm^{-1}; $\varepsilon=4.50 \times 10^4$). Thus the ultraviolet bond in VII is assigned as an intraligand $\pi\pi^*$ transition of $bipy^o$. The decrease in extinction coefficient on going from II to VII is significant as it indicates that VII contains one fewer regular coordinated bipy ligand than II. In common with the absorption spectrum of II, the visible and near-infrared regions of VII are featureless.

The complex, VII, has a rich redox chemistry as is shown in Figure 11 and Table 16[25].

The electrochemistry is invariant with solvent (acetonitrile, dimethylsulphoxide, dimethylformamide and

FIGURE 11: Cyclic voltammogram of $[Ir(bipy)_2(bipy')\ OH]^{2+}$ in acetonitrile

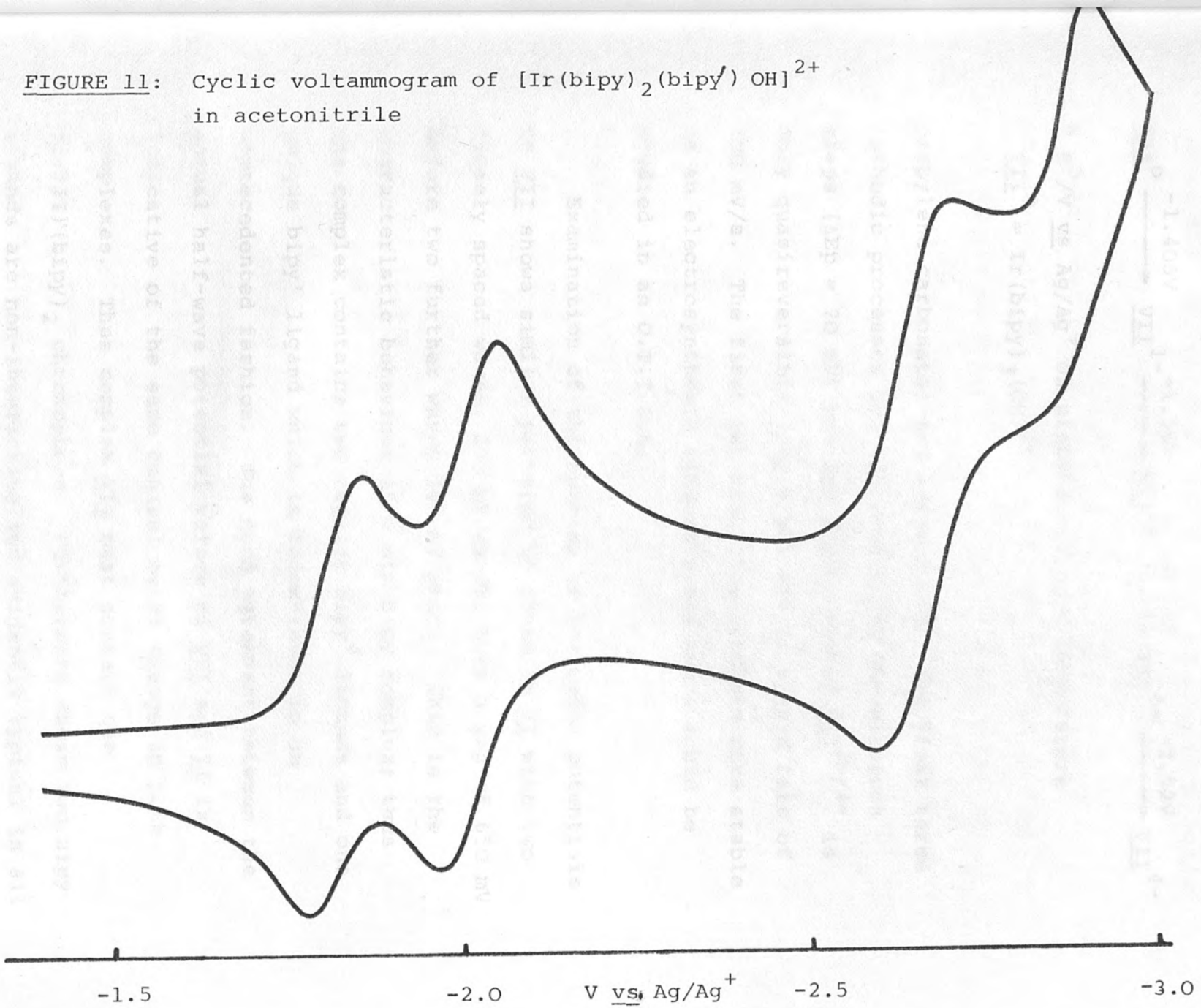

TABLE 16: ELECTRODE POTENTIALS FOR $Ir(bipy)_3(OH)^{2+}$ [a]

$$\underline{VII}^{o} \xrightarrow{-1.405V} \underline{VII}^{1-} \xrightarrow{-1.58V} \underline{VII}^{2-} \xrightarrow{-2.23V} \underline{VII}^{3-} \xrightarrow{-2.52V} \underline{VII}^{4-}$$

[a] E^{o}/V vs. Ag/Ag^{+} on platinum at room temperature

$\underline{VII}^{o} = Ir(bipy)_3(OH)^{2+}$

propylene carbonate) and temperature. The first three cathodic processes are all reversible one-electron steps (ΔEp = 70 mV) but the fourth couple $\underline{VII}^{3-/4-}$ is only quasireversible (ΔEp = 130 mV) at a scan rate of 100 mV/s. The first two reduction products were stable on an electrosynthesis timescale and hence could be studied in an O.T.T.L.E.

Examination of the spacing of the redox potentials in VII shows similar patterns to those in II with two closely spaced waves, 175 mV apart, then a gap of 650 mV before two further waves 290 mV apart. This is the characteristic behaviour of a bis-bipy complex; thus the complex contains two regular $bipy^{o}$ ligands and one unique bipy' ligand which is redox-inert in an unprecedented fashion. The good agreement between the actual half-wave potential values of VII and II is indicative of the same central metal charge in both complexes. Thus complex VII must contain the $Ir(III)(bipy)_2$ chromophore. Furthermore these two bipy ligands are non-interacting and evidently typical in all

respects. In connection with the unique ligand, we note that reduction of monodentate bipy would be expected before that of free bipy (-2.46 V). No such wave can be seen and hence structure B must be discounted.

In order to confirm that the first two cathodic processes are the reductions of non-interacting bipy ligands (in accord with the voltammetric evidence), complexes $\underline{VII}^{1-}$ and $\underline{VII}^{2-}$ were generated in an O.T.T.L.E. at -1.5 and -1.7 V vs. Ag/Ag^{+} respectively, and their absorption spectra recorded (Figure 12). The band maxima and their intensities are given in Table 17.

TABLE 17: ABSORPTION BANDS OF $Ir(bipy)_3OH^{2+}$ AND ITS REDUCED FORMS

Complexes	$\nu_{max}/10^3$ cm^{-1} (εx10^{-4})			
$\underline{VII}^{0}$			32.5(3.65)	
$\underline{VII}^{1-}$	12.9(0.14)	19.6(0.62)	25.2(1.35)	33.1(3.12)
	11.8(0.17)	20.5(0.50)	28.2(1.57)	
	10.4(0.16)			
$\underline{VII}^{2-}$	12.9(0.27)	19.3(1.31)	26.6(2.82)	
	11.7(0.32)	20.1(1.12)		
	10.5(0.31)			

Again we note the progressive growth of bands characterising $bipy^{-}$ (near-infrared, visible and ultra-violet) as the complex is successively reduced. The

FIGURE 12: Absorption spectra of $[Ir(bipy)_2bipy')OH]^{2+/1+/0}$ in dimethylsulphoxide at room temperature

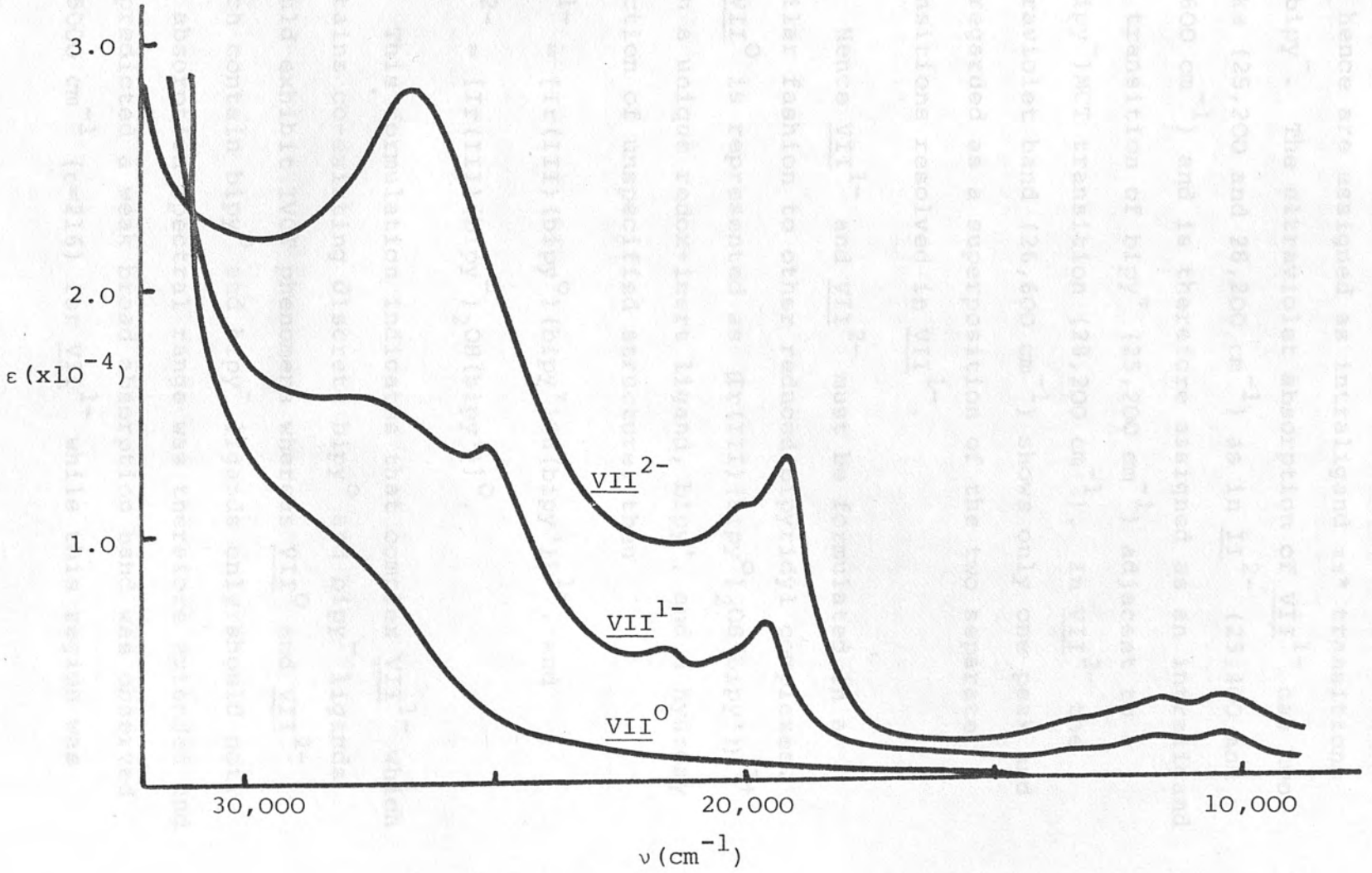

visible and near-infrared regions of the absorption spectra of $\underline{VII}^{1-}$ and $\underline{VII}^{2-}$ are very similar for band position, shape and intensity to those in $\underline{II}^{1-}$ and $\underline{II}^{2-}$ and hence are assigned as intraligand $\pi\pi^*$ transitions of $bipy^-$. The ultraviolet absorption of $\underline{VII}^{1-}$ has two peaks (25,200 and 28,200 cm^{-1}) as in $\underline{II}^{2-}$ (25,400 and 28,600 cm^{-1}) and is therefore assigned as an intraligand $\pi\pi^*$ transition of $bipy^-$ (25,200 cm^{-1}) adjacent to a $L(bipy^-)MCT$ transition (28,200 cm^{-1}). In $\underline{VII}^{2-}$ the ultraviolet band (26,600 cm^{-1}) shows only one peak and is regarded as a superposition of the two separate transitions resolved in $\underline{VII}^{1-}$.

Hence $\underline{VII}^{1-}$ and $\underline{VII}^{2-}$ must be formulated in a similar fashion to other reduced bipyridyl complexes. If $\underline{VII}^{o}$ is represented as $[Ir(III)(bipy^o)_2OH(bipy')]^{2+}$ with a unique redox-inert ligand, bipy', and a hydroxy function of unspecified structure, then

$\underline{VII}^{1-} = [Ir(III)(bipy^o)(bipy^-)OH(bipy')]^{1+}$, and

$\underline{VII}^{2-} = [Ir(III)(bipy^-)_2OH(bipy')]^{o}$.

This formulation indicates that complex $\underline{VII}^{1-}$ which contains co-existing discrete $bipy^o$ and $bipy^-$ ligands should exhibit IVCT phenomena whereas $\underline{VII}^{o}$ and $\underline{VII}^{2-}$ which contain $bipy^o$ and $bipy^-$ ligands only should not. The absorption spectral range was therefore extended and as predicted a weak broad absorption band was observed at 5000 cm^{-1} (ε=216) for $\underline{VII}^{1-}$ while this region was

featureless for $\underline{VII}^{0}$ and $\underline{VII}^{2-}$.

The unique bipy' ligand, presumed to bear the OH function, must have undergone a drastic structural rearrangement because there is no evidence of it in the absorption spectrum of $\underline{VII}^{0}$ (up to 45,000 cm^{-1}), the electrochemistry (from +1.5 V to -2.8 V), or the absorption spectra of the reduction products $\underline{VII}^{1-}$ and $\underline{VII}^{2-}$ (up to 33,000 cm^{-1}). The half-wave potentials for the redox couples $\underline{VII}^{0/1-}$ and $\underline{VII}^{1-/2-}$ agree closely with the redox couples $\underline{II}^{1-/2-}$ and $\underline{II}^{2-/3-}$ respectively. Thus the bipy' ligand is having an electrostatic effect on the two regular bipy ligands to the same degree as $bipy^{-}$, which would be consistent with the σ-bonded aryl formulation of structure C. The absence of IVCT in $\underline{VII}^{2-}$ is further powerful evidence that bipy' is <u>not</u> interchangeable with $bipy^{0}$.

In summary, the lower symmetry bipyridyl complexes of ruthenium(II) and iridium(III) follow the same spectroelectrochemical pattern as the tris-bipy complexes thereby underlining the importance of the isolated M-bipy chromophore, and the power of the trapped-electron model. The established diagnostic criteria for the presence of coordinated $bipy^{\cdot-}$ have been used to elucidate the electrochemistry of several further low-symmetry bipyridyl complexes. As a result, the nature of these compounds, and the influence of the accompanying ligands, can be understood.

Experimental

$[Ru(bipy)py_4]^{2+}$ and trans-$[Ru(bipy)_2py_2]^{2+}$ were prepared as perchlorate salts by the method of Krause[13]; cis-$[Ru(bipy)_2Cl_2]$ was prepared according to Sullivan and co-workers[26]; and cis-$[Ru(bipy)_2py_2](ClO_4)_2$ by treatment of a solution of cis$[Ru(bipy)_2Cl_2]$ in water with pyridine followed by aqueous sodium perchlorate. $[Ir(bipy)_2OH(bipy')](BF_4)_2$ was a major byproduct of the $[Ir(bipy)_3](BF_4)_3$ synthesis[27,28] and was eluted from the sephadex column directly after the $[Ir(bipy)_3]^{3+}$.

The solvents and electrolyte were exactly as described in Chapter 2, as were the electrochemical and spectral techniques.

REFERENCES

1. T. Matsubara and P.C. Ford; Inorg. Chem., 15, 1107 (1976).

2. V.E. Alvarez, R.J. Allen, T. Matsubara and P.C. Ford; J. Am. Chem. Soc., 96, 7686 (1974).

3. H. Taube; Surv. Prog. Chem., 6, 1 (1973).

4. K.B. Wiberg and T.P. Lewis; J. Am. Chem. Soc., 92, 7154 (1970).

5. G.M. Bryant, J.E. Fergusson and H.K.J. Powell; Aust. J. Chem., 24, 257 (1971).

6. P. Ford, De F.P. Rudd, R. Gaunder and H. Taube; J. Am. Chem. Soc., 90, 1187 (1968).

7. C.M. Carlin and M.K. DeArmond; Chem. Phys. Letts., 89, 297 (1982).

8. B.P. Sullivan, D J. Salmon, T.J. Meyer and J. Peedin; Inorg. Chem., 18, 3369 (1979).

9. B. Durham, J.L. Walsh, C.L. Carter and T.J. Meyer; Inorg. Chem., 19, 860 (1980).

10. J.L. Walsh and B. Durham; Inorg. Chem., 21. 329 (1982).

11. H. Endres, H.J. Keller, W. Moroni, D. Nothe and Vu Dong; Acta Cryst., B34, 1823 (1978).

12. P.C. Cheih; J. Chem. Soc., Dalton, 1643 (1972).

13. R.A. Krause; Inorg. Chim. Acta., 22, 209 (1977).

14. B. Durham, S.R. Wilson, D J. Hodgson and T.J. Meyer; J. Am. Chem. Soc., 102, 600 (1980).

15. B. Figgis, B. Shelton and A. White; Aust. J. Chem., 31, 57 (1978).

16. D.P. Rillema, D.S. Jones and H.A. Levy; J. Chem. Soc. Chem. Comm., 849 (1979).

17. A.G. Motten, K. Hanck and M.K. DeArmond; Chem. Phys. Lett., 79, 541 (1981).

18. N.S. Hush; Prog. Inorg. Chem., 8, 391 (1967).

19. G.A. Heath, A.J. Lindsay, T.A. Sephenson and D.K. Vattis; J. Organometal. Chem., 233, 353 (1982).

20. A. Basu, H.D. Gafney and T.C. Srekas; Inorg. Chem., 21, 2231 (1982).

21. R.J. Watts, J.S. Harrington and J. Van Houten; J. Am. Chem. Soc., 99, 2179, (1977).

22. R.D. Gillard, R.J. Lancashire and P.A. Williams, J. Chem. Soc. Dalton, 190 (1979).

23. P.J. Spellane and R.J. Watts; Inorg. Chem., 20, 3561, (1981).

24. W.A. Wickramasinghe, P.H. Bird and N. Serpone; J. Chem. Soc. Chem. Comm., 1284 (1981).

25. J.L. Kahl, K.W. Hanck, K. DeArmond; J. Phys. Chem., 82, 540 (1978).

26. B.P. Sullivan, D.J. Salmon and T.J. Meyer; Inorg. Chem., 17, 3334 (1978).

27. J.L. Kahl, K. Hanck and K. DeArmond; J. Inorg. Nucl. Chem., 41, 495 (1979).

28. C. Flynn and J. Demas; J. Am. Chem. Soc., 96, 1959 (1974).

CHAPTER 4

ABSORPTION SPECTRA OF Ru(III) BIPYRIDYL COMPLEXES

All of the bipyridyl complexes of ruthenium(II) studied in Chapters 2 and 3 have one reversible anodic process:

$$[Ru(bipy)_xL_{6-2x}]^{n+} \underset{+e^-}{\overset{-e^-}{\rightleftharpoons}} [Ru(bipy)_xL_{6-2x}]^{(n+1)+}; 1 \leq x \leq 3.$$

In each case the one-electron oxidation product is relatively stable (more so than the reduced species), and may be stored for several days, providing it is kept under argon in dry solvents; otherwise it reverts back to the parent complex. Thus we should be able to generate and characterise each oxidised complex in an O.T.T.L.E. cell, as with the reduced complexes previously studied.

The oxidation is essentially a metal-based process (cf. Chapter 2) in which an electron is removed from the complete metal $d\pi^6$ subshell of the Ru(II) core to give recognised Ru(III)/neutral bipyridyl complexes. Thus we would predict that the absorption spectrum of an oxidised product should contain bands due to:

i intraligand $\pi\pi^*$ transitions of bipy as in the parent complex but shifted to lower frequencies due to the higher central metal charge - such a shift is observed for internal bipy transitions on comparing $[Ru(bipy)_3]^{2+}$ and $[Ir(bipy)_3]^{3+}$;

ii ligand-to-metal charge-transfer transitions, that is (bipy)$\pi \rightarrow d\pi$(Ru(III)), due to the hole in the central metal valence core;

iii metal-to-ligand charge-transfer transitions, that is (Ru(III)$d\pi \rightarrow \pi^*$(bipy));

iv transitions corresponding to (i), (ii) and (iii) for the accompanying ligand L; these transitions may not all be visible, depending on the nature of L.

Accordingly, the oxidised complexes offer a distinctly different (and important, see Chapter 5) area in which to test our general approach, where electronic structure is interpretable in terms of individual metal-ligand chromophoric units and expressed in separate identifiable contributions to the absorption spectrum. A comparative analysis is fundamental to confident assignments. In this case we have investigated a series of isovalent complexes $[Ru(bipy)_3]^{3+}$, $\underline{I}^+$, cis-$[Ru(bipy)_2py_2]^{3+}$, $\underline{IV}^+$ and $[Ru(bipy)py_4]^{3+}$, $\underline{III}^+$ in which there is stepwise replacement of each bipy by two py ligands in contrast to the replacement of bipy by $bipy^-$ as examined in Chapter 2. Bands in the absorption spectra of $\underline{I}$, $\underline{IV}^+$ and $\underline{III}^+$, involving bipy transitions should decrease in height in going from $\underline{I}^+$ to $\underline{IV}^+$ to $\underline{III}^+$ and correspondingly the bands due to py should be absent in $\underline{I}^+$ and then increase from $\underline{IV}^+$ to $\underline{III}^+$. Such assignments can then be used to rationalise the absorption spectra of other Ru(III)-bipy

complexes, for example that of trans-$[Ru(bipy)_2py_2]^{3+}$, $\underline{V}^+$ and cis-$[Ru(bipy)_2Cl_2]^+$, $\underline{VI}^+$.

Tris-, bis- and mono-bipyridyl complexes of ruthenium-(III); $\underline{I}^+$, $\underline{IV}^+$, $\underline{III}^+$

The pale apple-green complexes $[Ru(bipy)_3]^{3+}$, cis-$[Ru(bipy)_2py_2]^{3+}$ and $[Ru(bipy)py_4]^{3+}$ were each generated in an O.T.T.L.E. (platinum gauze) all at +1.20 V vs. Ag/Ag^+ at room temperature in acetonitrile and also in propylene carbonate with indistinguishable results. The Ru(III) complexes were all stable under argon at room temperature. In every case the corresponding Ru(II) complex could be regenerated exactly after study of the oxidised product. The absorption spectra of $\underline{I}^+$, $\underline{IV}^+$ and $\underline{III}^+$ were recorded in the range 12,500 to 45,000 cm^{-1}. The intensities of the various absorption bands, designated A through F, span three orders of magnitude and hence the spectra are shown in Figures 1, 2 and 3 over successive regions, 12,5000 - 20,000 cm^{-1}, 20,000 - 29,500 cm^{-1} and 29,500 - 45,500 cm^{-1}. There is one early report of the absorption spectrum (only) of $\underline{I}^+$ in this extended spectral range[1]. Other studies of $\underline{I}^+$ and also of $\underline{IV}^+$ and $\underline{III}^+$ have centred on limited spectral regions[2,3] and contain no detailed assignment of the bands. Comparison of the absorption spectra of $\underline{I}^+$, $\underline{IV}^+$ and $\underline{III}^+$ enables us to assign transitions to the bands as in Table 1.

FIGURE 1: Absorption spectra of Ru(III) complexes (29,500-45,500 cm^{-1})

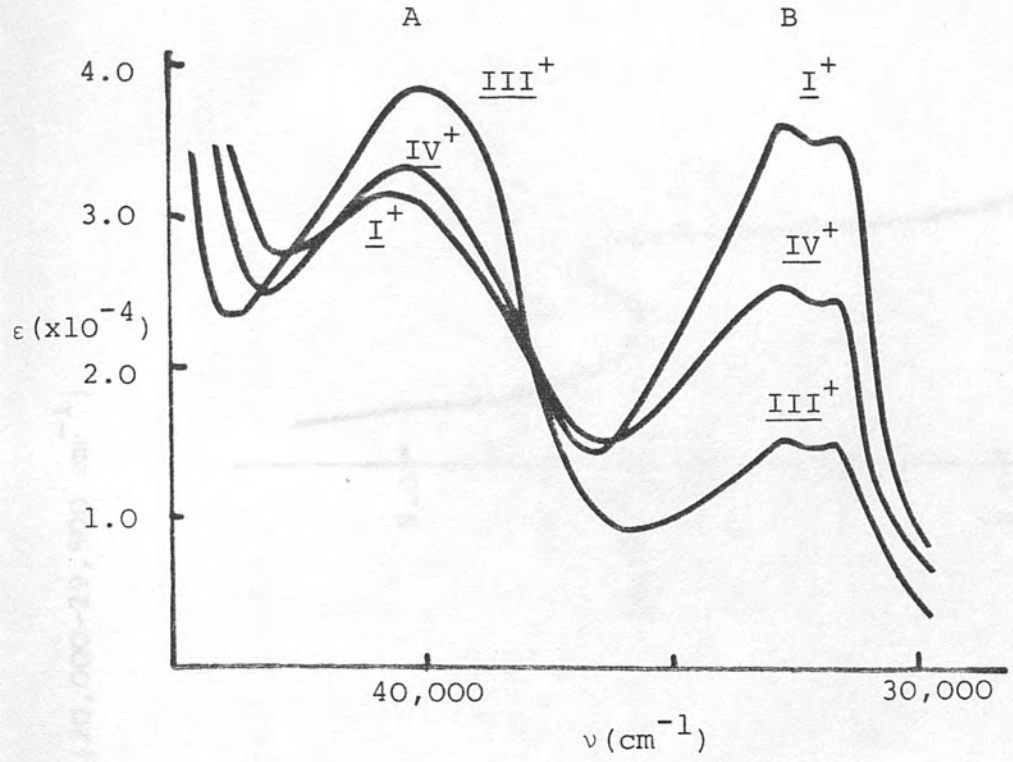

FIGURE 2: Absorption spectra of Ru(III) complexes (12,500-20,000 cm^{-1})

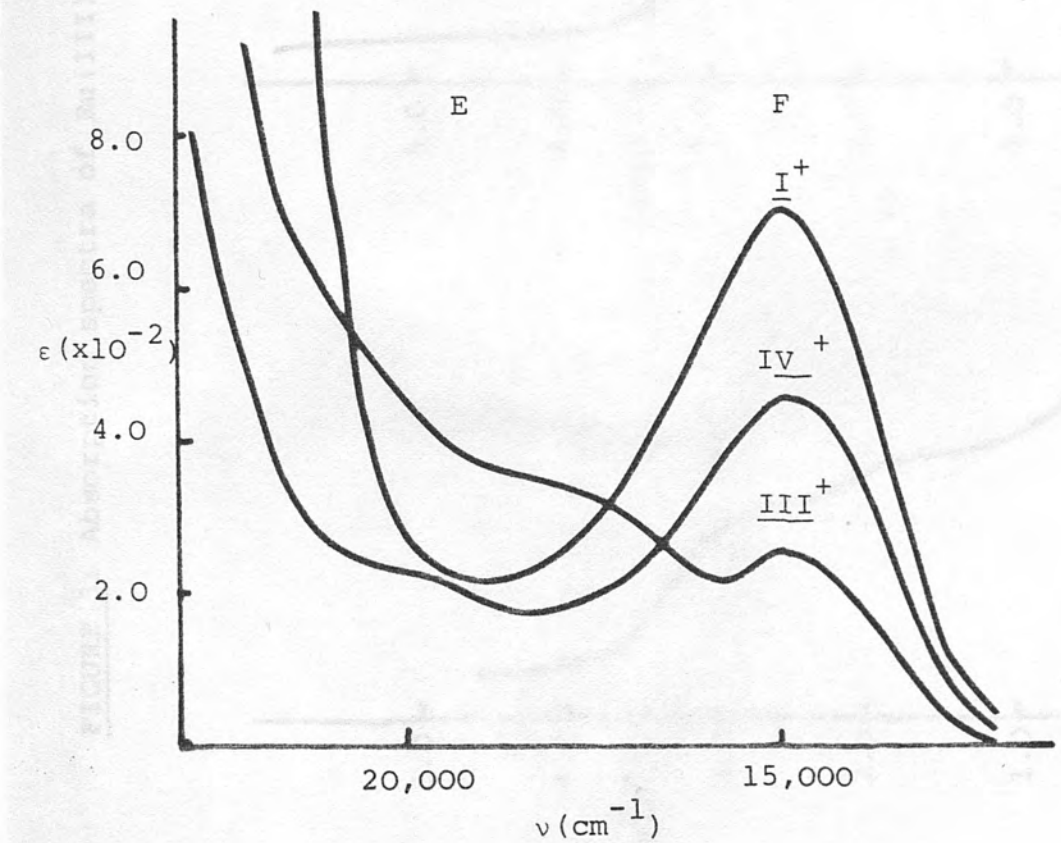

FIGURE 3: Absorption spectra of Ru(III) complexes (20,000-29,500 cm^{-1})

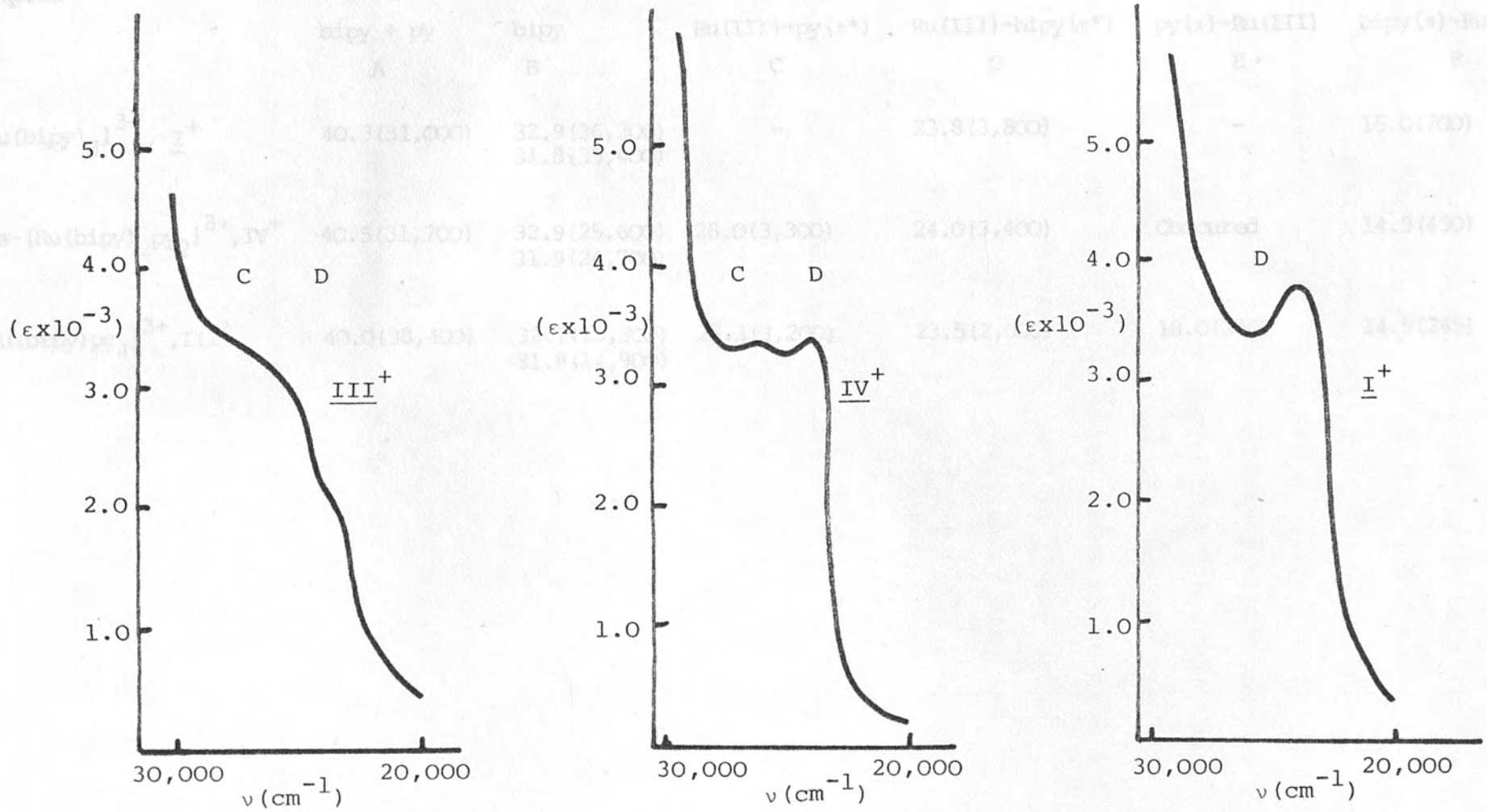

TABLE 1: ABSORPTION BANDS FOR BIPYRIDYL COMPLEXES OF RUTHENIUM(III) $\nu(x10^{-3})cm^{-1}(\varepsilon)$

Complex	Intraligand		Charge Transfer			
	$\pi\rightarrow\pi^*$	$\pi\rightarrow\pi^*$	MLCT	MLCT	LMCT	LMCT
	bipy + py	bipy	Ru(III)→py(π^*)	Ru(III)→bipy(π^*)	py(π)→Ru(III)	bipy(π)→Ru(III)
	A	B	C	D	E	F
$[Ru(bipy)_3]^{3+}$, $\underline{I}^+$	40.3(31,000)	32.9(36,300) 31.8(35,400)	-	23.8(3,800)	-	15.0(700)
cis-$[Ru(bipy)_2py_2]^{3+}$, IV^+	40.5(31,700)	32.9(25,600) 31.9(24,700)	26.0(3,300)	24.0(3,400)	Obscured	14.9(450)
$[Ru(bipy)py_4]^{3+}$, III^+	40.0(38,400)	32.7(15,300) 31.8(14,900)	26.3(3,200)	23.5(2,000)	18.0(340)	14.9(245)

The absorption band B near 32,000 cm^{-1} (Figure 1) is clearly due to a transition involving bipy. The intensity of the band falls progressively as bipy is replaced by py. The position, structure and intensity of band B in $\underline{I}^+$ corresponds closely to the ultraviolet band in $[Ir(bipy)_3]^{3+}$, $\underline{II}$, which has a central metal charge of +3. The shift of this band on going from, for example, $\underline{I}$ to $\underline{I}^+$ is further evidence that the oxidation of bipyridyl complexes of ruthenium(II) involves the removal of an essentially metal-based electron to give ruthenium(III). The ultraviolet band in $\underline{II}$ has been assigned as an intraligand $\pi\pi^*$ transition of bipy and hence the 32,000 cm^{-1} band in $\underline{I}^+$, $\underline{IV}^+$ and $\underline{III}^+$ is given a similar assignment.

Band A, near 40,000 cm^{-1}, remains at approximately the same frequency for all three species, $\underline{I}^+$, $\underline{IV}^+$ and $\underline{III}^+$ and in common with the similar band in $\underline{I}$, $\underline{IV}$ and $\underline{III}$ is assigned as a further intraligand $\pi\pi^*$ transition of bipy in $\underline{I}^+$, and as a superposition of this transition and a pyridine-based intraligand $\pi\pi^*$ transition in $\underline{IV}^+$ and $\underline{III}^+$.

The band at 15,000 cm^{-1}, F, in Figure 2 although very weak also decreases in intensity as bipy is replaced by py and thus must be assigned to a transition involving bipy. In agreement with Bryant and Ferguson[2] it is assigned as a ligand-to-metal charge transfer, that is, $(bipy)\pi \rightarrow d\pi(Ru(III))$.

Band E at 18,000 cm^{-1} is only observed in the absorption spectrum of $\underline{III}^{+}$. Its position and intensity indicate that it is due to pyridine LMCT absorption. Thus we would not expect to observe it in the spectrum of $\underline{I}^{+}$ (which contains no py) and its predicted intensity in $\underline{IV}^{+}$ (containing only two py) is such that it will be obscured by the neighbouring bands.

The intermediate regions of the spectra of $\underline{I}^{+}$, $\underline{IV}^{+}$ and $\underline{III}^{+}$ are shown in Figure 3 and, for clarity, are plotted independently as the intensities, but not the shapes, are very similar. The comparative intensities indicate that this region probably includes bands due to at least two transitions (C and D) and this is clearly suggested in the spectrum of $\underline{IV}^{+}$, whereas the visible region of $\underline{I}^{+}$ shows only one band at 23,800 cm^{-1} (D). Band D is clearly related to bipy as it decreases in intensity on going from $\underline{I}^{+}$ to $\underline{IV}^{+}$ to $\underline{III}^{+}$; that is, as the number of bipy ligands decreases in the complex so too does the intensity of this band. The band might be an internal $\pi\pi^{*}$ transition, a LMCT or a MLCT transition. The first possibility is discounted because the lowest $\pi\pi^{*}$ transition of bipy has already been assigned at higher energy (band B), the second may be neglected because the intensity of LMCT transitions in $\underline{I}^{+}$, $\underline{III}^{+}$ and $\underline{IV}^{+}$ is much lower (approximately 700 instead of 3800 in $\underline{I}^{+}$) than that observed for band D. Hence band D must be due to a MLCT and indeed the extinction coefficient of this band in $\underline{I}^{+}$ is approximately five times

that of the 15,000 cm^{-1} band which was assigned as a (bipy)$\pi \rightarrow d\pi$(Ru(III)) transition. An intensity difference of this scale may be related to the relevant electronic populations (one acceptor 'hole'on the metal ion compared to three equivalent ligand LUMO acceptor orbitals) but this is only speculation, and would demand elaborate analysis. Band D is thus assigned as a MLCT; (Ru(III))$d\pi \rightarrow \pi^*$(bipy) for all three complexes $\underline{I}^+$, $\underline{IV}^+$ and $\underline{III}^*$

Band C at 26,000 cm^{-1} in $\underline{IV}^+$ and $\underline{III}^+$ (but absent in $\underline{I}^+$) is assigned as a ML(py)CT (Ru(III)$d\pi \rightarrow \pi^*$py) by similar arguments to those used for bands E and D.

Having assigned all the bands in the absorption spectra of the oxidised product, we can now draw up a relative molecular orbital energy scheme for Ru(II) and Ru(III) bipyridine complexes using electrochemical and spectral data to test the self-consistency of the assigned transitions as in Figure 4. In both species we need only represent one Ru-bipy chromophore as it is established that the bipy ligands are non-interacting in each case. The Ru(II)-bipy molecular orbital levels are taken as the starting point and the Ru(III)-bipy levels are then mapped in relation to them. Thus the first π^* level of bipy is approximately 3,200 cm^{-1} lower in the Ru(III)-bipy system than for Ru(II) because reduction of bipy on a metal +3 centre is known to be 0.4 V (3,200 cm^{-1}) easier than on a metal +2 centre (from the difference in $E^{o}_{red}(1)$ values of $[Ru(bipy)_3]^{2+}$

FIGURE 4: Comparative molecular orbital diagram for Ru(II)-bipy and Ru(III)-bipy

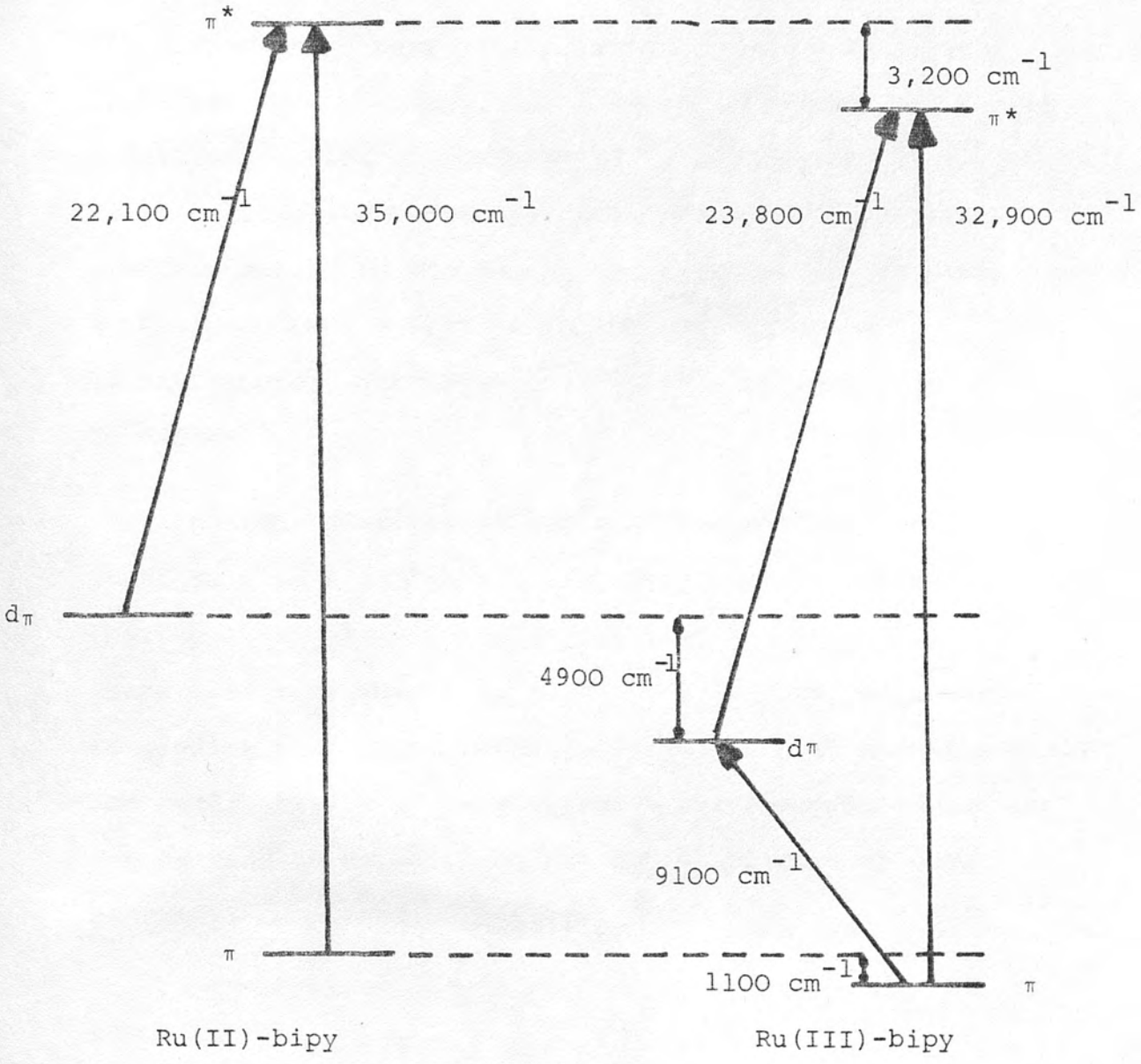

and $[Ir(bipy)_3]^{3+}$). The highest filled π-level of bipy can then be located from the $\pi\pi^*$ transition energy in $[Ru(bipy)_3]^{3+}$. Recognition of band D as the MLCT transition allows the Ru(III) $d\pi^5$ core level to be positioned. Figure 4 then predicts a separation of 9,100 cm^{-1} between the highest occupied π level of bipy and the $d\pi^5$ core of Ru(III). The experimentally measured LMCT transition energy must however also include an electron-pairing term of approximately 4,000 cm^{-1} (as evaluated from the separation between the third and fourth reduction couples of $[Ir(bipy)_3]^{3+}$, see Chapter 2) relative to all other transitions where the promoted electron enters an unoccupied orbital. This then gives a predicted LMCT energy of 13,100 cm^{-1} which is in satisfactory agreement with the measured value of 15,000 cm^{-1}.

Thus the electrochemical and spectral data are found to give a self-consistent energy-level scheme thereby strengthening the validity of the proposed transition assignments in Ru(III)-bipy. The model used to predict band assignments proves to be both quantitatively and qualitatively successful and these assignments can now be used to explain the absorption spectra of other bipyridyl complexes of Ru(III).

Trans-$[Ru(bipy)_2py_2]^{3+}$; V^+

We have already shown that trans-$[Ru(bipy)_2py_2]^{2+}$, V, behaves in a very similar fashion to the cis-complex, IV, with only minor frequency shifts in the absorption bands (Chapter 3). Hence, although the electronic considerations are different in the oxidised forms, it is not surprising that the absorption spectrum of V^+, generated at +1.1 V vs. Ag/Ag^+ in a platinum O.T.T.L.E. at room temperature, resembles very closely that of IV^+, with no anomalous bands and intensities. Thus the bands can be assigned to transitions as shown in Table 2.

TABLE 2: BAND ASSIGNMENTS FOR trans - $[Ru(bipy)_2py_2]^{3+}$

Band $\nu/10^3$ cm^{-1} (ε)	Assignment
40.3 (34,200)	$\pi\rightarrow\pi^*$(bipy) + $\pi\rightarrow\pi^*$(py)
32.7 (26,600)	$\pi\rightarrow\pi^*$(bipy)
27.4 (4,300)	ML(py)CT; (Ru(III))$d\pi\rightarrow\pi^*$(py)
24.4 (3,800)	ML(bipy)CT; (Ru(III))$d\pi\rightarrow\pi^*$(bipy)
15.1 (360)	L(bipy)MCT; (bipy)$\pi\rightarrow d\pi$(Ru(III))

Cis-$[Ru(bipy)_2Cl_2]^+$; VI^+

In comparison with the preceding complexes, the chloride ligands have a significant perturbing influence on both the Ru(II)$d\pi$ orbitals and the π orbitals of bipy in cis-$[Ru(bipy)_2Cl_2]^o$, VI, raising both to higher

energies than in cis-$[Ru(bipy)_2py_2]^{2+}$ (cf. Chapter 3). The $d\pi$ levels are affected more than the π levels of the bipy ligand and hence this should be reflected in the absorption spectrum of cis-$[Ru(bipy)_2Cl_2]^{+}$ with the L(bipy)MCT transitions moving to higher frequencies and ML(bipy)CT transitions to lower frequencies, compared to similar transitions in cis-$[Ru(bipy)_2py_2]^{3+}$.

The pale yellow oxidised product, $\underline{VI}^{+}$ can be generated in an O.T.T.L.E. at +0.35 V vs. Ag/Ag^{+} at room temperature. The absorption spectrum of $\underline{VI}^{+}$ is shown in Figure 5 and is in general agreement with earlier published data[2,4]; the band assignments are given in Table 3.

TABLE 3: BAND ASSIGNMENTS FOR cis-$[Ru(bipy)_2Cl_2]^{+}$

Band $\nu/10^3$ cm^{-1} (ε)	Assignment
41.2 (28,400)	$\pi\rightarrow\pi^*$(bipy)
33.3 (31,200) 32.1 (26,800)	$\pi\rightarrow\pi^*$(bipy)
26.5 (6,400)	L(Cl^-)MCT; (Cl^-)$\pi\rightarrow d\pi$(Ru(III))
21.9 (2,700)	ML(bipy)CT[a]; (Ru(III))$d\pi\rightarrow\pi^*$(bipy)
18.0 (500)	L(bipy)MCT[a]; (bipy)$\pi\rightarrow d\pi$(Ru(III))

a. These bands have not previously been assigned[2].

As predicted, the (bipy)$\pi\rightarrow d\pi$Ru(III) transition has moved to higher frequencies while the Ru(III)$d\pi\rightarrow\pi^*$bipy transition is at lower frequencies than in $\underline{IV}^{+}$. The assignments are, however, unambiguous due to the

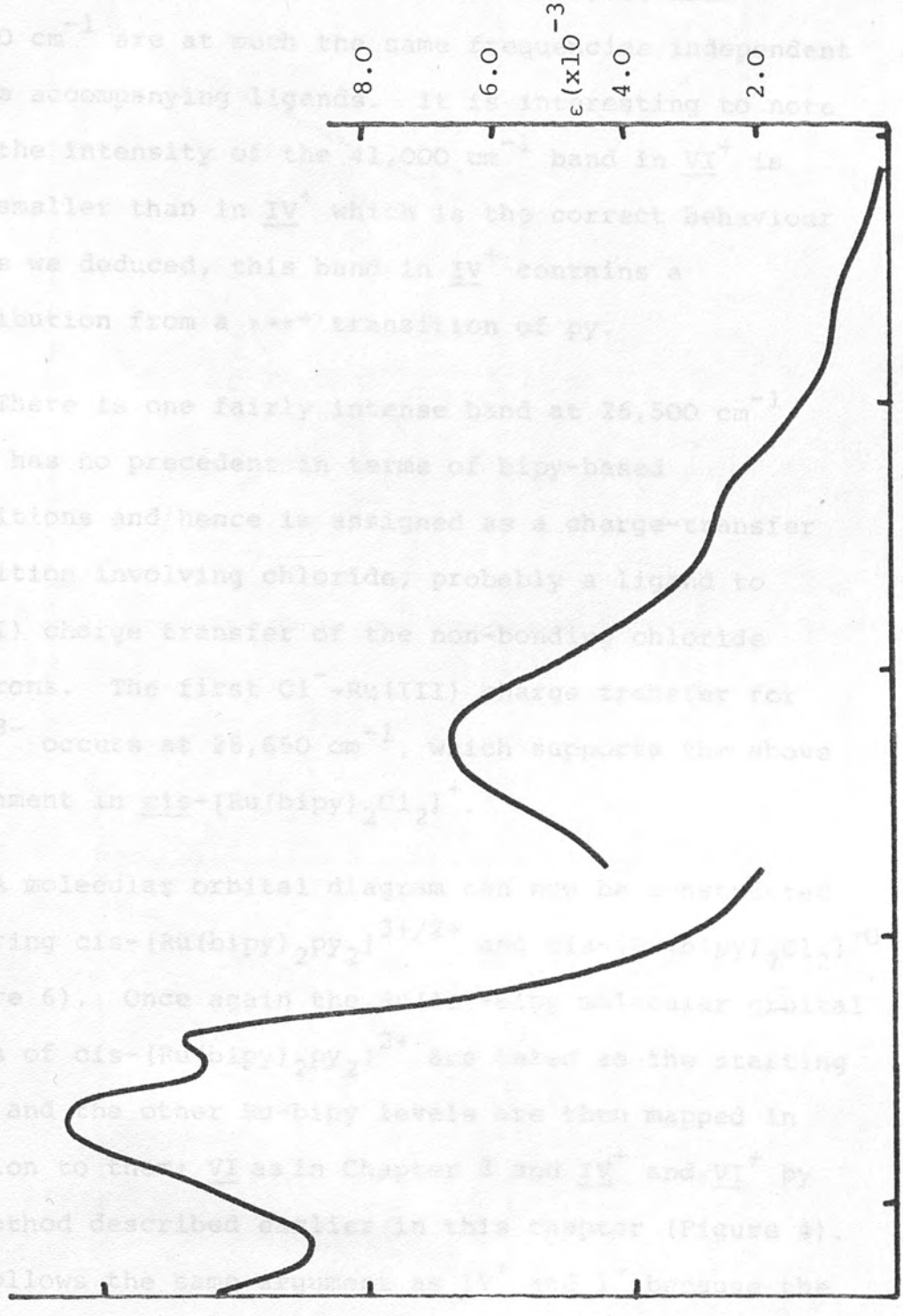

FIGURE 5: Absorption spectrum of cis-$[Ru(bipy)_2Cl_2]^+$

characteristic extinction coefficient values. The bands due to intraligand $\pi\pi^*$ transitions at 33,000 and 41,000 cm^{-1} are at much the same frequencies independent of the accompanying ligands. It is interesting to note that the intensity of the 41,000 cm^{-1} band in $\underline{VI}^+$ is much smaller than in $\underline{IV}^+$ which is the correct behaviour if, as we deduced, this band in $\underline{IV}^+$ contains a contribution from a $\pi\rightarrow\pi^*$ transition of py.

There is one fairly intense band at 26,500 cm^{-1} which has no precedent in terms of bipy-based transitions and hence is assigned as a charge-transfer transition involving chloride, probably a ligand to Ru(III) charge transfer of the non-bonding chloride electrons. The first $Cl^-\rightarrow$Ru(III) charge transfer for $RuCl_6^{3-}$ occurs at 28,650 cm^{-1}, which supports the above assignment in $\underline{cis}$-$[Ru(bipy)_2Cl_2]^+$.[5]

A molecular orbital diagram can now be constructed comparing cis-$[Ru(bipy)_2py_2]^{3+/2+}$ and cis-$[Ru(bipy)_2Cl_2]^{+o}$ (Figure 6). Once again the Ru(II)-bipy molecular orbital levels of cis-$[Ru(bipy)_2py_2]^{2+}$ are taken as the starting point and the other Ru-bipy levels are then mapped in relation to them; $\underline{VI}$ as in Chapter 3 and $\underline{IV}^+$ and $\underline{VI}^+$ by the method described earlier in this chapter (Figure 4). $\underline{VI}^+$ follows the same argument as $\underline{IV}^+$ and I^+ because the bipy π^* level of cis-$[Ru(bipy)_2Cl_2]^+$ is also stabilised by 3,200 cm^{-1} (the difference in E^ored (1) values of $[Ru(bipy)_2Cl_2]^o$ and $[Ir(bipy)_2Cl_2]^+$ is 0.4 V[6]).

FIGURE 6: Comparative molecular orbital diagram for cis-$[Ru(bipy)_2py_2]^{2+/3+}$ and cis-$[Ru(bipy)_2Cl_2]^{0/+}$

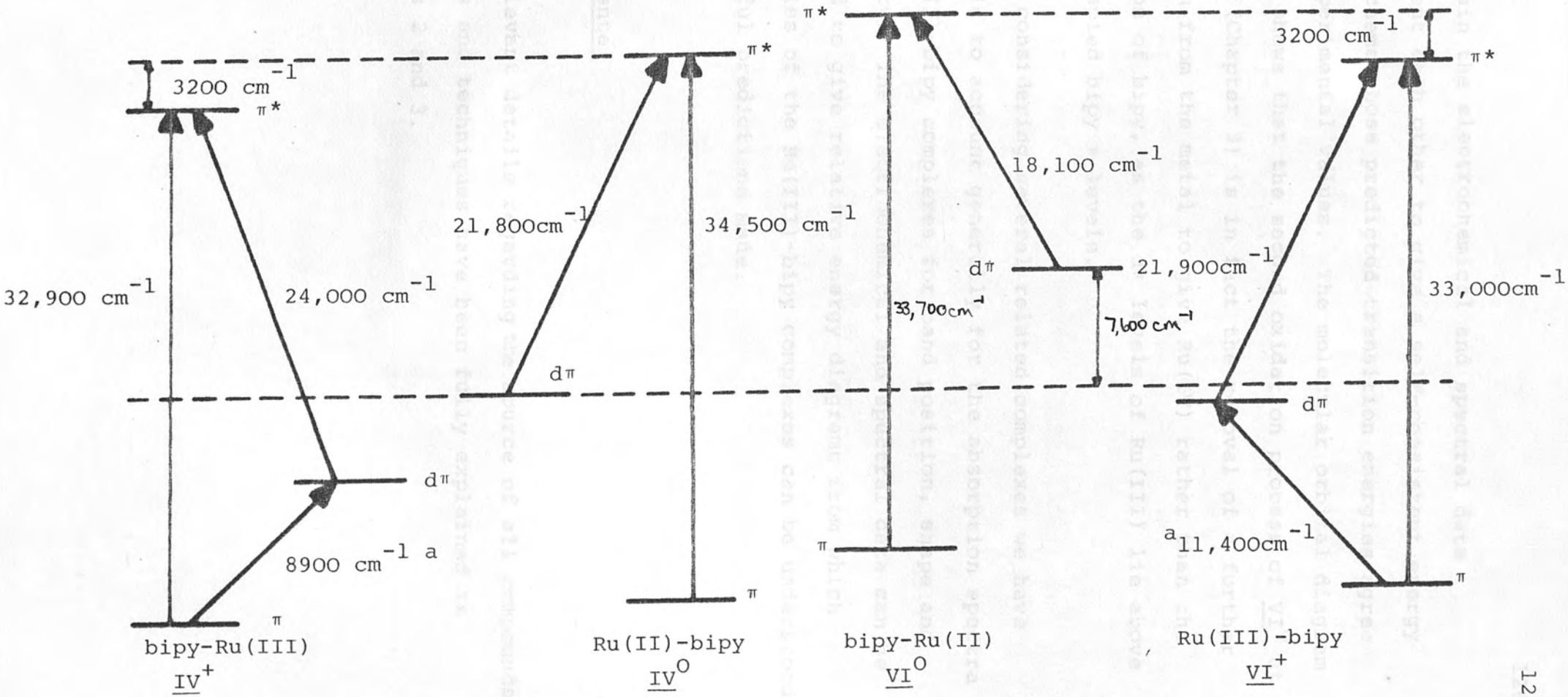

[a]MLCT transition will be augmented by mean pairing energy (ca. 5000 cm^{-1})

Once again the electrochemical and spectral data complement each other to give a self-consistent energy level scheme whose predicted transition energies agree with experimental values. The molecular orbital diagram for $\underline{VI}^{+}$ shows that the second oxidation process of $\underline{VI}^{o}$ at +1.66 V (Chapter 3) is in fact the removal of a further electron from the metal to give Ru(IV) rather than the oxidation of bipy, as the $d\pi$ levels of Ru(III) lie above the occupied bipy π levels.

By considering several related complexes we have been able to account generally for the absorption spectra of Ru(III)-bipy complexes for band position, shape and intensity. The electrochemical and spectral data can be combined to give relative energy diagrams from which properties of the Ru(III)-bipy complexes can be understood and useful predictions made.

Experimental

Relevant details regarding the source of all compounds, solvents and techniques have been fully explained in Chapters 2 and 3.

REFERENCES

1. D.J. McCaffery, S.F. Mason and B.J. Norman; J. Chem. Soc. A., 1428 (1969).

2. G.M. Bryant and J.E. Fergusson; Aust. J. Chem., 24 275 (1971).

3. J.N. Braddock and T.J. Meyer; J. Am. Chem. Soc., 95, 3158 (1973).

4. J.N. Braddock and T.J. Meyer; Inorg. Chem. 12, 723 (1973).

5. C.K. Jorgensen, Absorption spectra and chemical bonding in complexes, Pergamon Press, Oxford, 1962.

6. J.L. Kahl, K.W. Hanck and K. DeArmond; J. Phys. Chem., 82, 540 (1978).

CHAPTER 5

THE ELECTRONIC ABSORPTION SPECTRUM OF THE EMITTING STATE OF $[Ru(bipy)_3]^{2+}$ AND THE NATURE OF THE PHOTO-EXCITATION/ RELAXATION PROCESSES

We return in this chapter to direct consideration of the excited state complex $*[Ru(bipy)_3]^{2+}$, $\underline{I}^*$, which is a key intermediate in many light-driven redox processes (Chapter 2). It was for many years customary to assume that in the thermally equilibrated $\underline{I}^*$ an electron was transferred from the metal core to an acceptor orbital delocalised over all three ligands[1-4]; that is, that $\underline{I}^*$ belonged to the same D_3 point group as the ground state, $\underline{I}$[5]. In consequence there have been difficulties in explaining the photo-emission spectrum[6-8] and the behaviour of related mixed ligand complexes, which are asserted to exhibit a higher electronic than molecular geometry[2,4].

We have already shown that in the reduced species, $\underline{I}^-$, the additional electron is localised on one bipy ligand. Thus we might expect that the promoted (MLCT) electron in $\underline{I}^*$ is also localised on one of the three bipy ligands, as in the formulation $[Ru(III)(bipy^o)_2(bipy^-)]^{2+}$. After all $\underline{I}^*$ is formally derivable from $\underline{I}^-$ simply by removal of a stereochemically non-directing metal $d'a_1'$ electron. Raman studies have indicated that $\underline{I}^*$ contained an identifiable $bipy^-$ ligand[9,10]. It remained, however,

to demonstrate unequivocally the simultaneous presence of bipy^{o} together with bipy^{-} as distinct ligands in $\underline{I}^{*}$ (as we had done for $\underline{I}^{-}$) and this has recently been accomplished by Woodruff *et al*[11] in further resonance Raman studies. We have approached the problem independently by examination of the visible-ultraviolet absorption spectrum of $\underline{I}^{*}$, reasoning that, as in $\underline{I}^{-}$, bands diagnostic of separate bipy^{o} and bipy^{-} chromaphores should be evident (albeit on a Ru(III) centre in $\underline{I}^{*}$ as opposed to a Ru(II) centre in $\underline{I}^{-}$). We find this is indeed the case, though it understates the richness and complexity of the spectrum.

Previous reports of the absorption spectrum of $\underline{I}^{*}$ are incomplete in the visible region, and differ among themselves both in the shape of the bands and the reported extinction coefficients[3,12,13]. Our own results (Figure 1) agree fully with the data of Lachish *et al*[12], and confirm details discernible therein but absent in other published spectra. The present study extends through the visible region, down to 650 nm, and we have discovered at least one hitherto unsuspected absorption. In addition, our spectroelectrochemical investigations of further Group VIII bipy complexes have enlarged the range of suitable model complexes. As a result, it is now possible to offer a detailed assignment (Table 1) according to the localised charge-transfer formulation $[Ru(III)(bipy^{o})_{2}(bipy^{-})]^{2+}$, for $\underline{I}^{*}$. A semi-quantitative test of these assignments is then provided by comparison

FIGURE 1: Absorption spectrum of $^{*}[Ru(bipy)_3]^{2+}$ in water at room temperature

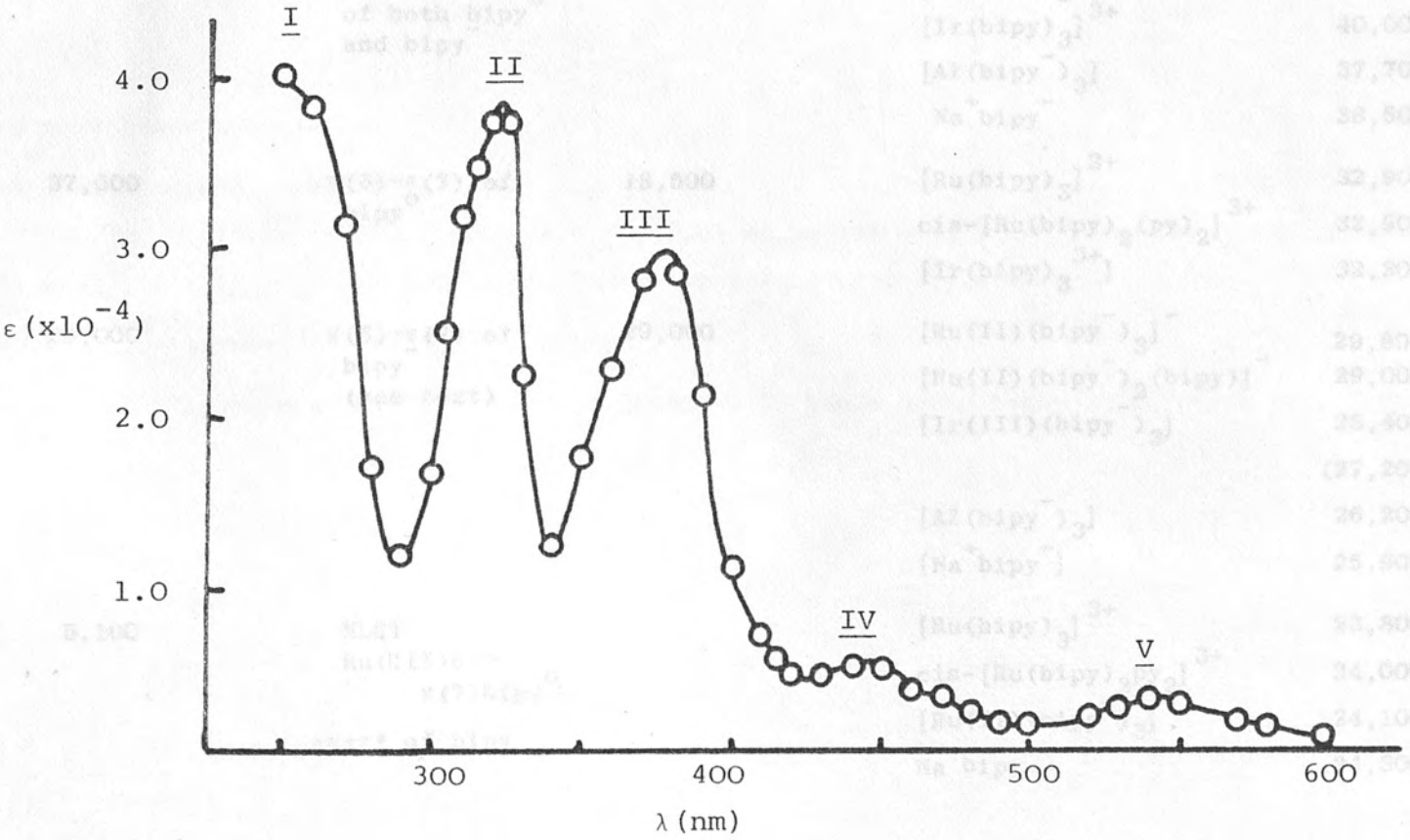

TABLE 1: PROPOSED ASSIGNMENTS FOR $*[Ru(bipy)_3]^{2+}$ WITH DATA FOR MODEL SYSTEMS

Band[a]	ν/cm^{-1}	ε[b]/dm^3 mol^{-1} cm^{-1}	Assignments[c]	ε(I*)/dm^3 mol^{-1} cm^{-1} per relevant ligand	Model Species[d]	Model Bands ν/cm^{-1}	Model Bands ε/dm^3 mol^{-1} cm^{-1} per relevant ligand
I	40,000	40,000	$\pi(6)\rightarrow\pi(8,9)$ of both bipy^o and bipy$^-$	13,300	$[Ru(bipy)_3]^{3+}$	40,300	11,000
					$[Ir(bipy)_3]^{3+}$	40,000	20,000
					$[A\ell(bipy^-)_3]$	37,700	5,400
					Na^+bipy^-	38,500	6,000
II	31,250	37,000	$\pi(6)\rightarrow\pi(7)$ of bipy^o	18,500	$[Ru(bipy)_3]^{3+}$	32,900	12,000
					cis-$[Ru(bipy)_2(py)_2]^{3+}$	32,900	12,800
					$[Ir(bipy)_3^{3+}]$	32,200	15,000
III	26,600	29,000	$\pi(6)\rightarrow\pi(7)$ of bipy$^-$ (see text)	29,000	$[Ru(II)(bipy^-)_3]^-$	29,800	12,700[e]
					$[Ru(II)(bipy^-)_2(bipy)]^-$	29,000	12,500[e]
					$[Ir(III)(bipy^-)_3]$	25,400	8,500
						(27,200	8,500[f])
					$[A\ell(bipy^-)_3]$	26,200	8,600
					$[Na^+bipy^-]$	25,900	17,000
IV	22,500	5,100	MLCT $Ru(III)d\pi\rightarrow\pi(7)bipy^o$ $+\pi\rightarrow\pi^*$ of bipy$^-$		$[Ru(bipy)_3]^{3+}$	23,800	1,300
					cis-$[Ru(bipy)_2py_2]^{3+}$	24,000	1,700
					$[Ru(II)(bipy^-)_3]^-$	24,100	4,000
					Na^+bipy^-	24,300	7,000

V	18,500	3,000	$\pi(7)\rightarrow\pi(10)$ of bipy	3,000	$[Ru(II)(bipy^-)_3]^-$	18,000	5,300
					$[Ir(III)(bipy^-)_3]$	19,600	4,000
					$[A\ell(bipy^-)_3]$	19,700	2,300
					Na^+bipy^-	18,000	4,500

[a] See Figure 1

[b] Total observed extinction coefficient

[c] $\pi(6)$ = highest energy bonding orbital of bipy

$\pi(7,8,9)$ = antibonding orbitals of bipy (elsewhere referred to as π^*). $\pi(7)$ is lowest antibonding orbital, unoccupied in $bipy^o$; singly occupied in $bipy^-$. Numbering system after reference 14

[d] Literature sources for models $[A\ell(bipy)_3]$ [15], Nabipy [14].

[e] band also contains MLCT component $Ru(II)d\pi\rightarrow\pi^*bipy^-$ (Chapter 2) hence anomolously intense for $bipy^-$ transition.

[f] LMCT($bipy^-$); see text.

of extinction coefficients (corrected as necessary for the number of chromophores); we find satisfactory agreement in each case.

Band I, 40,000 cm^{-1} (ε=40,000)

This is assigned to the overlapping $\pi(6)\rightarrow\pi(8,9)$ bands of $bipy^{o}$ and $bipy^{-}$, which we do not expect to be able to resolve separately. Model complexes containing $bipy^{o}$ or $bipy^{-}$ coordinated to a metal +3 centre show that both the band position and intensity in I* are of the correct order for such an assignment.

Band II, 31,250 cm^{-1} (ε=37,000)

We assign this band to an intraligand transition of $bipy^{o}$, in particular to $\pi(6)\rightarrow\pi(7)$. The band has shifted to lower energy on going from I to I* as is to be expected for the change in central ion valency (from +2 to +3). The band in I* is properly compared to model systems containing a tervalent central ion which it does favourably for both position and intensity (see Table I).

Band III, 26,600 cm^{-1} (ε=29,000)

This band raises interesting issues. It is assignable in large part to $bipy^{-}$ (more specifically to

$\pi(6)\rightarrow\pi(7)$ of coordinated bipy$^-$), a proposal made early by Balzani *et al*[16] but subsequently abandoned[17]. It is far too intense, however, for this alone to be a satisfactory assignment, and indeed the band shows evidence of a high energy shoulder, also discernible in the spectrum presented by Lachish *et al*[12]. We had some difficulty in assigning the extra component. There is no sign of a similar intense transition in the spectrum of $[Ru(III)(bipy^o)_3]^{3+}$ or *cis*-$[Ru(III)(bipy^o)_2py_2]^{3+}$ (the *cis*-bis complex is in some cases a better model for *I** than I^+ as both belong to the same symmetry class). The lowest $[\pi(6)\rightarrow Ru(III)]$ LMCT transition of I^+ is at 15,000 cm^{-1} and is much too weak (ε=700) to correspond to band III, as is the band in I^+ at 23,800 cm^{-1} (ε=3,800), which we suspect of contributing to band IV, discussed below. Nor is the band a property of bipy$^-$ itself or of bipy$^-$-M(III) systems in general since, for example, it is absent in $[A\ell(bipy)_3]$[15]. We must therefore look for a spin-allowed transition characteristic of the Ru(III)(bipy$^-$) chromophore (which accordingly is impossible to model) which gives rise to a triplet state *I*** 44,000 cm^{-1} above the ground state *I*, since *I*** is approximately 26,600 cm^{-1} above *I** (by absorption), and *I** is some 17,000 cm^{-1} above *I* (by emission)[6,18]. *I*** is far too energetic to be a $^3(d\rightarrow d)$ state of *I* as would be implied by a LMCT ($\pi^*\rightarrow$4de) assignment; such states are discussed below.

However, an extra band in this region is also characteristic of the Ir(III)(bipy$^-$) system. We therefore,

partly by elimination and partly on energetic grounds, assign band III to a LMCT process involving higher metal orbitals, such as 5s, 5p for Ru and 6s, 6p for Ir, which will be mixed in antibonding combinations with ligand lone pairs giving the transition some one-centre character. The proximity of these bands for the Ru(III)(bipy$^-$) and Ir(III)(bipy$^-$) chromophores is probably fortuitous and the greater intensity for the former may indicate a detailed difference in assignment within the general class proposed.

In addition, as a consequence of constructing a schematic molecular orbital diagram for I* (vide infra) like those developed in previous chapters for related complexes, we predict that a Ru(III)$d\pi \rightarrow \pi^*$(bipy$^-$) MLCT transition should occur at approximately 28,000 cm^{-1}. However, the intensity of such a transition is probably not sufficient to account for the extra intensity of band III. Therefore, although we cannot give a definitive assignment for the whole of band III we recognise two plausible transitions contributing to its anomolous intensity. A comparative study of further excited state Ru(II)-bipy complexes could prove helpful in conclusively assigning transitions to this band.

Band IV, 22,400 cm^{-1} (ε=5,100)

This band is a superposition of two transitions; it

is in part assigned to a MLCT [Ru(III)$d\pi \rightarrow \pi$(7)bipy^{o}] as in model complexes $\underline{I}^{+}$ and $\underline{IV}^{+}$. However, the band is too intense to be entirely due to this transition. The absorption spectrum of $Na^{+}bipy^{-}$ and $[Ru(bipy)_3]^{1-}$ show a pronounced shoulder in this region due to an intra-ligand $\pi\pi^*$ transition of bipy^{-} and it is these anticipated transitions taken together (MLCT + $\pi\pi^*$) which satisfactorily account for the extinction coefficient of band IV.

Band V, 18,500 cm^{-1} (ε=3,000)

Band V has not hitherto been reported, being fairly weak, located at a wavelength where photomuliplier sensitivity is mediocre, and uncomfortably close to the emission of $\underline{I}^*$. It cannot be related to the familiar visible MLCT(Ru(II)$\rightarrow$bipy^{o}) system of $\underline{I}$ since there is no Ru(II) present in $\underline{I}^*$, but it is immediately assignable as the π(7)$\rightarrow\pi$(10) transition of bipy^{-} by comparisons of position and intensity with several model complexes.

Thus we have demonstrated that the bands of Figure 1 are collectively diagnostic of distinct coexisting bipy^{o} and bipy^{-} ligands in $\underline{I}^*$ on a metal +3 centre. We therefore regard the charge-localised formulation of the emitting state, $*[Ru(III)(bipy^{o})_2(bipy^{-})]^{2+}$, (and the implied departure for D_3 molecular geometry) as established.

The assigned transitions of bands I-V can now be used to construct a molecular orbital diagram for $\underline{I}^*$ (Figure 2).

FIGURE 2: Schematic molecular orbital diagram for I*

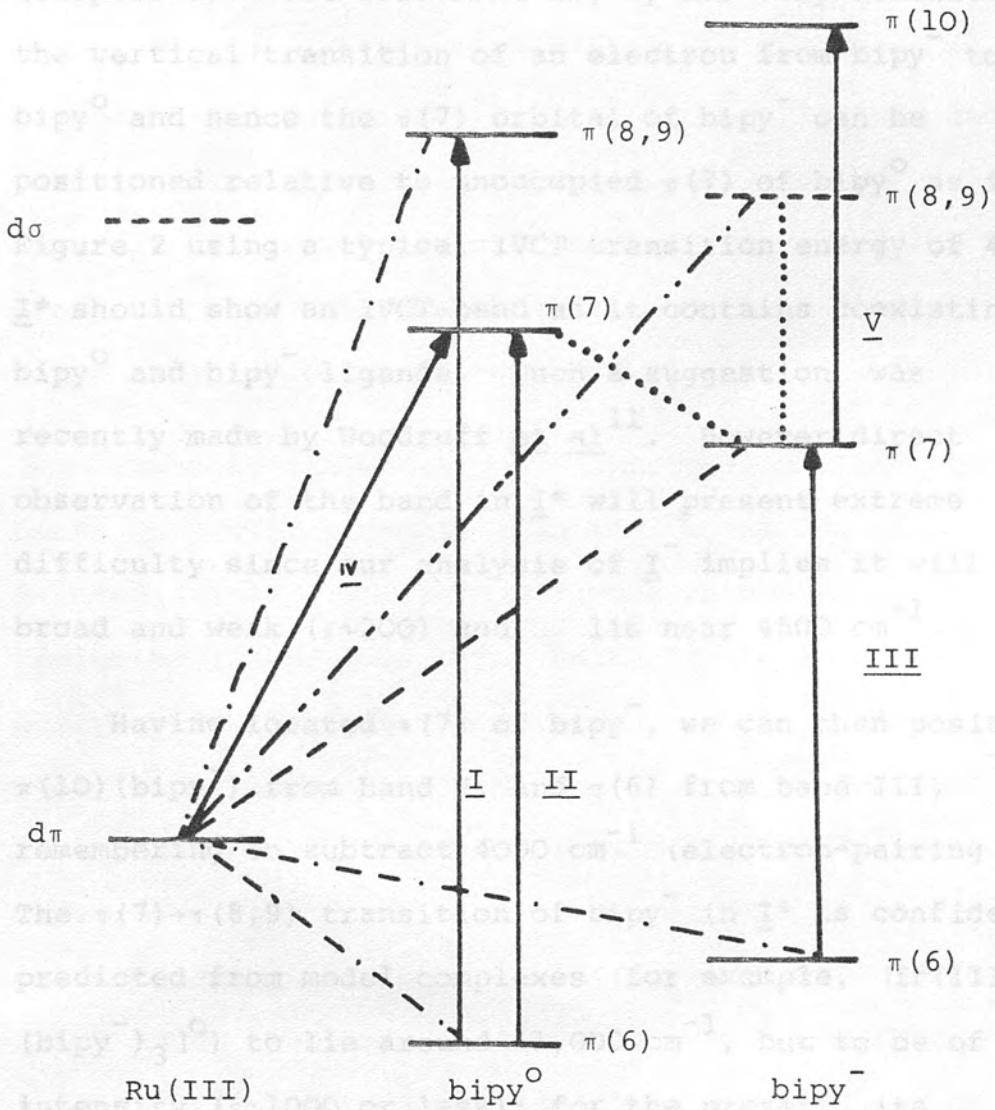

Solid lines - directly observed transitions
Broken lines- predicted transitions (see text in each case)

Bands I and II locate the HOMO, LUMO and a further anti-bonding orbital of $bipy^{o}$. The Ru(III) $d\pi^{5}$ core can then be mapped in relation to the $bipy^{o}$ π orbitals using band IV; the Ru(III)$d\pi \rightarrow \pi(7)bipy^{o}$ charge transfer transition. In order to locate the $bipy^{-}$ π orbitals in relation to the $bipy^{o}$ π orbitals, it is necessary to invoke the IVCT band previously observed in Ru(II) and Ir(III) complexes (Chapter 3). The IVCT band is, by its very definition, the vertical transition of an electron from $bipy^{-}$ to $bipy^{o}$ and hence the $\pi(7)$ orbital of $bipy^{-}$ can be positioned relative to unoccupied $\pi(7)$ of $bipy^{o}$ as in Figure 2 using a typical IVCT transition energy of 4500 cm^{-1}. $\underline{I}^{*}$ should show an IVCT band as it contains coexisting $bipy^{o}$ and $bipy^{-}$ ligands. Such a suggestion was recently made by Woodruff *et al*[11]. However direct observation of the band in $\underline{I}^{*}$ will present extreme difficulty since our analysis of $\underline{I}^{-}$ implies it will be broad and weak ($\varepsilon \sim 200$) and lie near 4500 cm^{-1}.

Having located $\pi(7)$ of $bipy^{-}$, we can then position $\pi(10)(bipy^{-})$ from band V, and $\pi(6)$ from band III, remembering to subtract 4000 cm^{-1} (electron-pairing term). The $\pi(7) \rightarrow \pi(8,9)$ transition of $bipy^{-}$ in $\underline{I}^{*}$ is confidently predicted from model complexes (for example, $[Ir(III)-(bipy^{-})_{3}]^{o}$) to lie around 11,000 cm^{-1}, but to be of low intensity ($\varepsilon \sim 1000$ or less); for the present, its position, weakness and overlap with the emission tail of $\underline{I}$ place the band below the detection limits of our measurements.

Figure 2 defines several other transitions which are not observed in the absorption spectrum of $\underline{I}^*$. The LMCT transitions $\pi(6) \rightarrow d\pi$(Ru(III) (.--.) found at 15,000 cm^{-1} (ε=700) in $\underline{I}^+$ should be observed at approximately 14,000 cm^{-1} for the Ru(III)-bipy^o chromophore and 10,000 cm^{-1} for the Ru(III)-bipy$^-$ chromophore. However both bands will be too weak and too low in frequency to be detected at present. The higher MLCT transitions ($d\pi \rightarrow \pi(8,9)$bipy^o) are predicted to lie around 31,000 cm^{-1} and will be masked by the coincident intense bipy^o $\pi\pi^*$ band; indeed this inference provides an elegant explanation of the apparent excess intensity of band II (see Table). The predicted bipy$^-$ MLCT band has already been discussed since it contributes to band III.

The spin-allowed bipy$^-$ $\pi(7) \rightarrow d(e\sigma^*)$ charge-transfer bands of $\underline{I}^*$will generate $\underline{I}$ in its $^3T_1$ or $^3T_2$ ligand-field excited states (labels in O_h), but with a slightly distorted ligand geometry. Using Figure 2 and assuming a separation between the $d\pi$ and $d\sigma$ orbitals of approximately 28,000 cm^{-1} (as in $[Ru(en)_3]^{2+}$ [19]) we can show that these LMCT transitions should lie in the near-infrared. Indeed our analysis confirms that the non-emitting decay levels, inferred to exist about 4000 cm^{-1} above $\underline{I}^*$ on the basis of temperature dependent emission studies[20,21] may be safely assigned to the lower of these d-d states of $\underline{I}$, i.e. $^3T_1$ (O_h).

Finally, we should note the self-consistency of the

molecular orbital energy diagram constructed in Figure 2, which is in some ways over-determined by independent data. Thus the charge-transfer transition (---) $Ru(III)d\pi-\pi(7)bipy^-$ corresponds, of course, to the experimentally determined emission of $\underline{I}^*$. The predicted value of the emission is 17,500 cm^{-1} which is in good agreement with the observed value of 17,000 cm^{-1} [6,18] for the emission maximum.

The charge-localised formulation of $\underline{I}^*$, $^*[Ru(III)(bipy^o)_2(bipy^-)]^{2+}$ suggests that complexes of the type $[Ru(II)(bipy)_xL_{6-2x}]$ $(1 \leqslant x \leqslant 3)$, in which there are recognised isolated $Ru(II)$-$bipy^o$ chromophores and the lowest absorption band is a ML(bipy)CT transition, should all have emission spectra with similar Franck-Condon envelopes. This is exactly what is observed experimentally[22-24]. This observation had previously been difficult to reconcile with the D_3 symmetry description of the excited state $\underline{I}^*$[2,4].

The absorption photoselection spectrum for $[Ru(bipy)_3]^{2+}$ reported first by Fiyita and Kobayashi[6] and later verified by Ferguson and co-workers[25] and DeArmond and co-workers[7] has received much attention, which led to vexed discussion until the recent emergence of localised models, because the data are frankly inconsistent with an emitter of D_3 symmetry[8]. Recently, however, Carlin and DeArmond have confirmed that the photoselection data are fully consistent with a lower

symmetry emitting state[24].

The spin multiplicity of I* has also been the subject of much debate. Crosby et al, argued that this label was meaningless due to strong spin-orbit coupling (that is, S is not a good quantum number)[18,26]. However, experimentally the spin unlabelled model has been shown to be inconsistent with the observed differences in absorption spectra of I and $[Os(bipy)_3]^{2+}$. The orthodox singlet-triplet distinction should therefore be retained as indicated below:

$$I^* = {}^3[Ru(III)(bipy^o)_2(bipy^-)]^{2+}$$

The emitting state I* is formed following the absorption of visible light by I. The character of the absorption band is universally accepted as a MLCT transition, simply described as $d\pi \rightarrow \pi^*$. The intensity of the MLCT band at 22,000 cm^{-1} indicates that the transitions are allowed by multiplicity selection rules; that is the transitions involve excitation to singlet excited states. The low intensity band at 19,100 cm^{-1} is generally regarded as equivalent transitions to the triplet states. It still remained necessary firstly to give a detailed assignment of the MLCT band, secondly to reconcile the distorted thermally equilibrated excited state I* with the D_3 symmetry ground state I and thirdly to speculate on the form of the distortion of the emitting state.

Following Orgel[27], any bipyridyl π or π* ligand orbital can be classified with respect to a twofold rotation axis bisecting the idealised metal chelate ring; each orbital is either symmetric, denoted χ, or antisymmetric, denoted ψ. The χ and ψ orbitals are antibonding or bonding respectively between the two pyridine rings. They are represented schematically in Figure 3.

FIGURE 3: Schematic representation of χ- and ψ-type orbitals in bipy

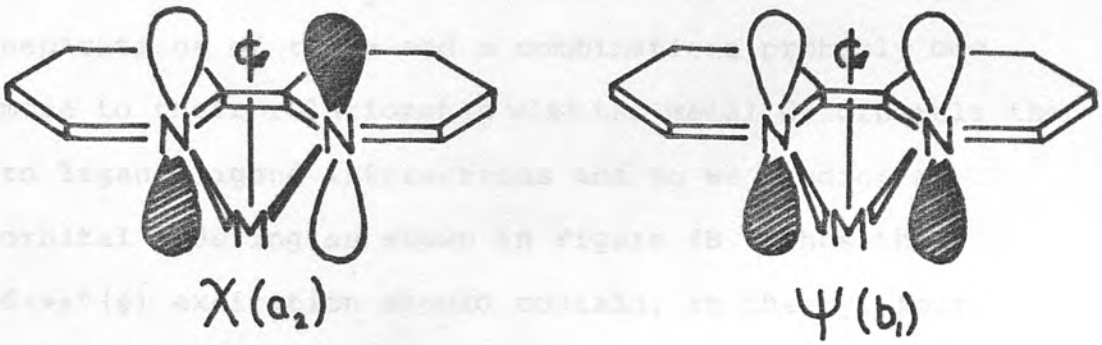

Ferguson and co-workers, investigating low-temperature spectra of oriented $M(bipy)_3^{2+}$ complexes (M = Fe, Ru and Os) in host crystals, had concluded that both types of acceptor orbitals were involved in the visible MLCT absorptions[25,28,29] which was at variance with the ψ-only model preferred by Hipps and Crosby[30]. Recently, Belser and co-workers[31] have examined the CD spectrum and their results show that the MLCT can be adequately assigned using the ψ-only model. Coulemans and Vanquickenbourne[32] have also presented compelling evidence, from energy considerations, in favour of the ψ-only proposal. Their

model was further verified by low temperature polarisation studies[33]. Thus in the following discussion we accept that in the visible MLCT transition of I (Ru(II)$d\pi \rightarrow \pi$(7)-bipy^{o}) the promoted electron is transferred to a π^* orbital of bipy^{o} (π(7)) of type ψ. The $d\pi \rightarrow \pi^*(\chi)$ absorption occurs at higher energy and is masked by the intense $\pi\pi^*$ intraligand transition of bipy (see Chapter 3).

The degeneracy of the metal $d\pi$ orbitals is lifted by the D_3 symmetry of the ground state and they transform as a_1 plus e. The π^* ligand orbitals (one ψ-only from each ligand) span a_2 and e (Figure 4A). The energetic separations of the a and e combinations probably owe more to their relationship with the metal $d\pi$ orbitals than to ligand-ligand interactions and so we predict an orbital ordering as shown in Figure 4B. Thus the $d\pi \rightarrow \pi^*(\psi)$ excitation should contain, in theory, four orbital transitions, $a_1 \rightarrow a_2$, $a_1 \rightarrow e$, $e \rightarrow a_2$ and $e \rightarrow e$ (Figure 4B). All four transitions are orbitally allowed (Table 2) and therefore no information can be derived from the solution absorption spectrum to distinguish one from another. However, single-crystal polarised-light studies can be used to distinguish between the different allowed transitions (Table 2). If the incident polarised light beam is so arranged that the electric vector is parallel to the z axis (the unique axis), absorption corresponding with the $a_1 \rightarrow a_2$ or $e \rightarrow e$ transitions should occur, but the other transitions should not. Conversely, if the electric vector lies along the x or y axes, the $a_1 \rightarrow e$, $e \rightarrow a_2$ and $e \rightarrow e$

FIGURE 4A: Schematic molecular orbitals of ψ-type ligands

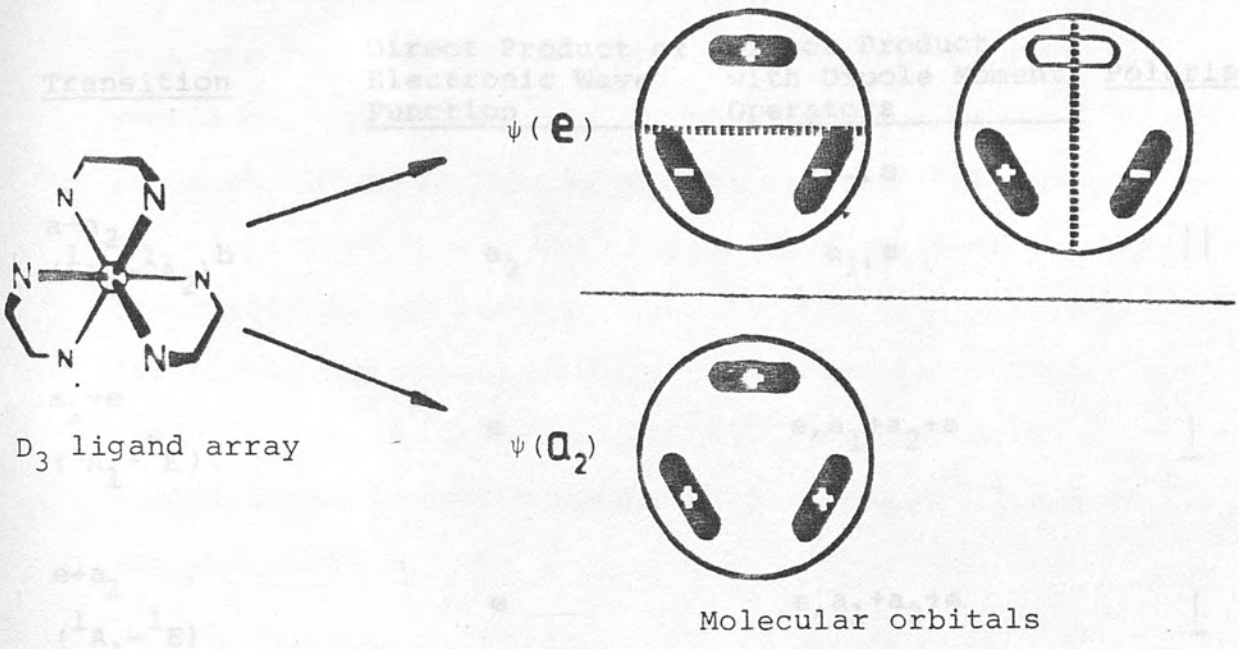

FIGURE 4B: Orbital interaction diagram of metal t_{2g}-and ligand ψ-type orbitals

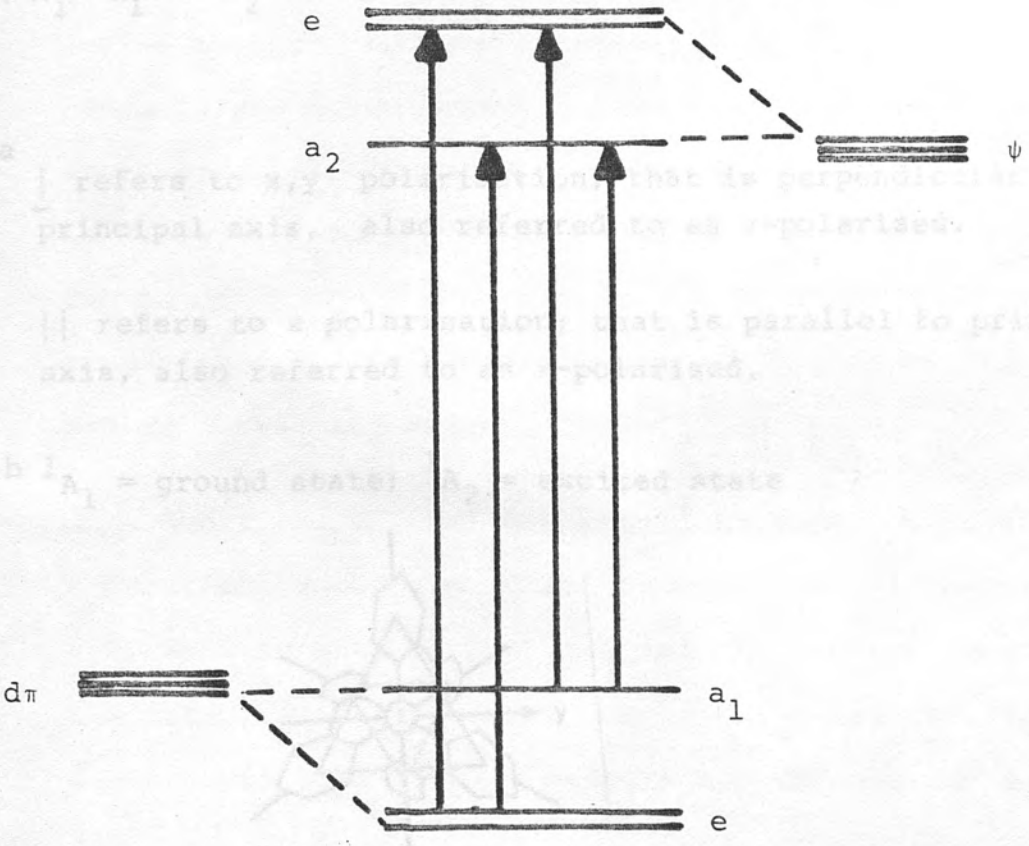

TABLE 2: ELECTRONIC SELECTION RULES FOR LOWEST CHARGE TRANSFER TRANSITION IN $[Ru(bipy)_3]^{2+}$

Transition	Direct Product of Electronic Wave Function	Direct Product with Dipole Moment Operators	Polarisation[a]
		a_2, e	
$a \rightarrow a_2$ $(^1A_1 \rightarrow {}^1A_2)$[b]	a_2	a_1, e	$\parallel$
$a_1 \rightarrow e$ $(^1A_1 \rightarrow {}^1E)$	e	e, a_1+a_2+e	$\perp$
$e \rightarrow a_2$ $(^1A_1 \rightarrow {}^1E)$	e	e, a_1+a_2+e	$\perp$
$e \rightarrow e$ $(^1A_1 \rightarrow {}^1A_1 + {}^1A_2 + {}^1E)$	a_1+a_2+e	$a_2+a_1+e, e+e+a_1+a_2+e$	$\parallel$ $\perp$

[a] $\perp$ refers to x,y polarisation; that is perpendicular to the principal axis, also referred to as σ-polarised.

$\parallel$ refers to z polarisation; that is parallel to principal axis, also referred to as π-polarised.

[b] $^1A_1$ = ground state; $^1A_2$ = excited state

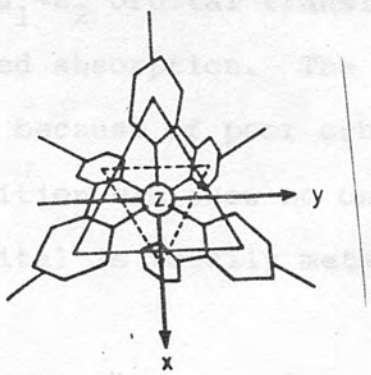

$[Ru(bipy)_3]^{2+}$ molecule showing x, y and z axes

transitions should be seen.

Ceulemans and Vanquickenbourne[32] have predicted that the two transitions $e(d\pi)\rightarrow e(\psi)$ and $e(d\pi)\rightarrow a_2(\psi)$ should each give rise to a major absorption band. The bands should be roughly of equal intensity and should be σ-polarised (Table 2). Figure 4B shows that the $e\rightarrow a_2$ transition should occur at lower energy than the $e\rightarrow e$ transition and hence, using the experimental data of Ferguson and co-workers at 8 K[25,33], we can assign transitions to the absorption bands; $e\rightarrow a_2$ at 21,900 cm^{-1} and $e\rightarrow e$ at 23,400 cm^{-1}.

The third σ-polarised transition $a(d\pi)\rightarrow e(\psi)$ carries zero 'transfer term' intensity since the $a_1(d\pi)$ orbital is not affected by interactions with the ligand orbitals and hence will be only very weakly absorbing. It will be masked by the very intense absorptions $e\rightarrow a_2$ and $e\rightarrow e$. Ferguson and co-workers indicate that only metal-centred transitions should carry circular dichroism (CD) activity in $M(bipy)_3^{2+}$ complexes (M = Fe, Ru, Os)[34] and hence the two major CD bands observed in the solution spectrum can be assigned to the transitions $a_1\rightarrow e$ (21,100 cm^{-1}) and $e\rightarrow e$ in increasing energy order[31,34].

The $a_1\rightarrow a_2$ orbital transition is expected to show π-polarised absorption. The transition will however be very weak because of poor orbital overlap and because the transition can show no one-centre character (a_1 donor orbital is totally metal-based whereas the a_2

acceptor orbital is totally ligand-based). Thus the transition will be unobserved in both the absorption and CD spectrum.

We can now reconstruct Figure 4B to scale using the results of absorption and CD spectroscopy (Figure 5A). The diagram shows that the energy difference between the principally metal-based a_1 and e orbitals (δ) is approximately 2000 cm^{-1}. The experimentally determined δ values for first row transition metal tris-bipyridyl complexes is of the order of 1000 cm^{-1} (Chapter 6) and hence the derived value of 2000 cm^{-1} for $[Ru(bipy)_3]^{2+}$ seems feasible. Absorption and CD spectral results are also available for $[Fe(bipy)_3]^{2+}$ [29,33,34] and hence we can construct a molecular orbital energy diagram for this complex in the same manner as $[Ru(bipy)_3]^{2+}$ (Figure 5B). The energies of the orbital transitions within the MLCT band are all lower in the Fe(II) complex compared to the Ru(II) complex (see Chapter 6 for explanation); however we note close similarities between the two diagrams. As expected, the separation between the metal e and a_1 orbitals is much smaller for $[Fe(bipy)_3]^{2+}$ than $[Ru(bipy)_3]^{2+}$, (δ_{Fe} = 1100 cm^{-1}; δ_{Ru} = 2300 cm^{-1}). The δ value has been calculated from e.s.r. studies for $[Fe(bipy)_3]^{3+}$ at 870 cm^{-1} [35].

Thus the analysis of the absorption and CD spectra in relation to the lowest MLCT band of $[Ru(bipy)_3]^{2+}$ has given quantitatively and qualitatively satisfactory results.

FIGURE 5A: HOMO and LUMO diagram for $[Ru(bipy)_3]^{2+}$

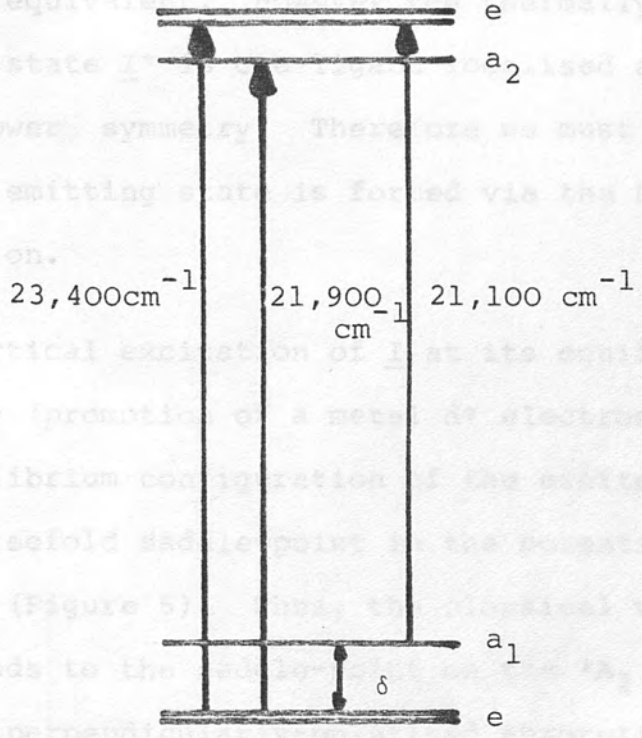

FIGURE 5B: HOMO and LUMO diagram for $[Fe(bipy)_3]^{2+}$

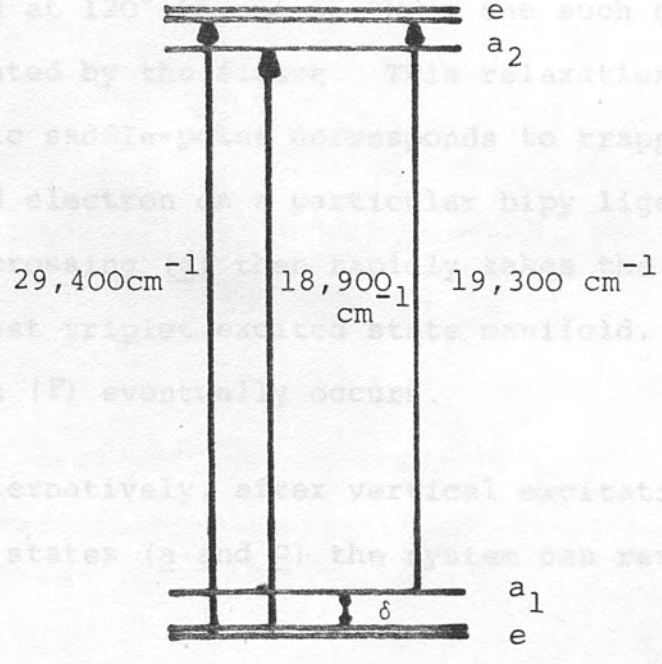

We must therefore conclude that the absorption spectrum of I is best explained in D_3 symmetry with all three bipy ligands equivalent. However the thermally equilibrated excited state I* is one-ligand localised and thus I* is of lower symmetry. Therefore we must now consider how the emitting state is formed via the D_3 MLCT transition.

Vertical excitation of I at its equilibrium D_3 geometry (promotion of a metal $d\pi$ electron) leads not to an equilibrium configuration of the excited singlet but to a threefold saddle-point in the potential energy surface (Figure 6). Thus, the classical vertical assignment leads to the saddle-point on the $^1A_2$ surface, either through perpendicularly-polarised absorption to ^1E (process a of Figure 6) followed by radiationless decay (b), or directly through parallel-polarised absorption (c). The system will then relax (d) to any one of three equivalent energy minima lying in distortion planes disposed at 120° to one another; one such plane is represented by the figure. This relaxation from the symmetric saddle-point corresponds to trapping the promoted electron on a particular bipy ligand. Intersystem crossing (e) then rapidly takes the molecule to its lowest triplet excited state manifold, I*, from which emission (F) eventually occurs.

Alternatively, after vertical excitation to the singlet states (a and c) the system can revert to a

FIGURE 6: Absorption/emission processes of $[Ru(bipy)_3]^{2+}$

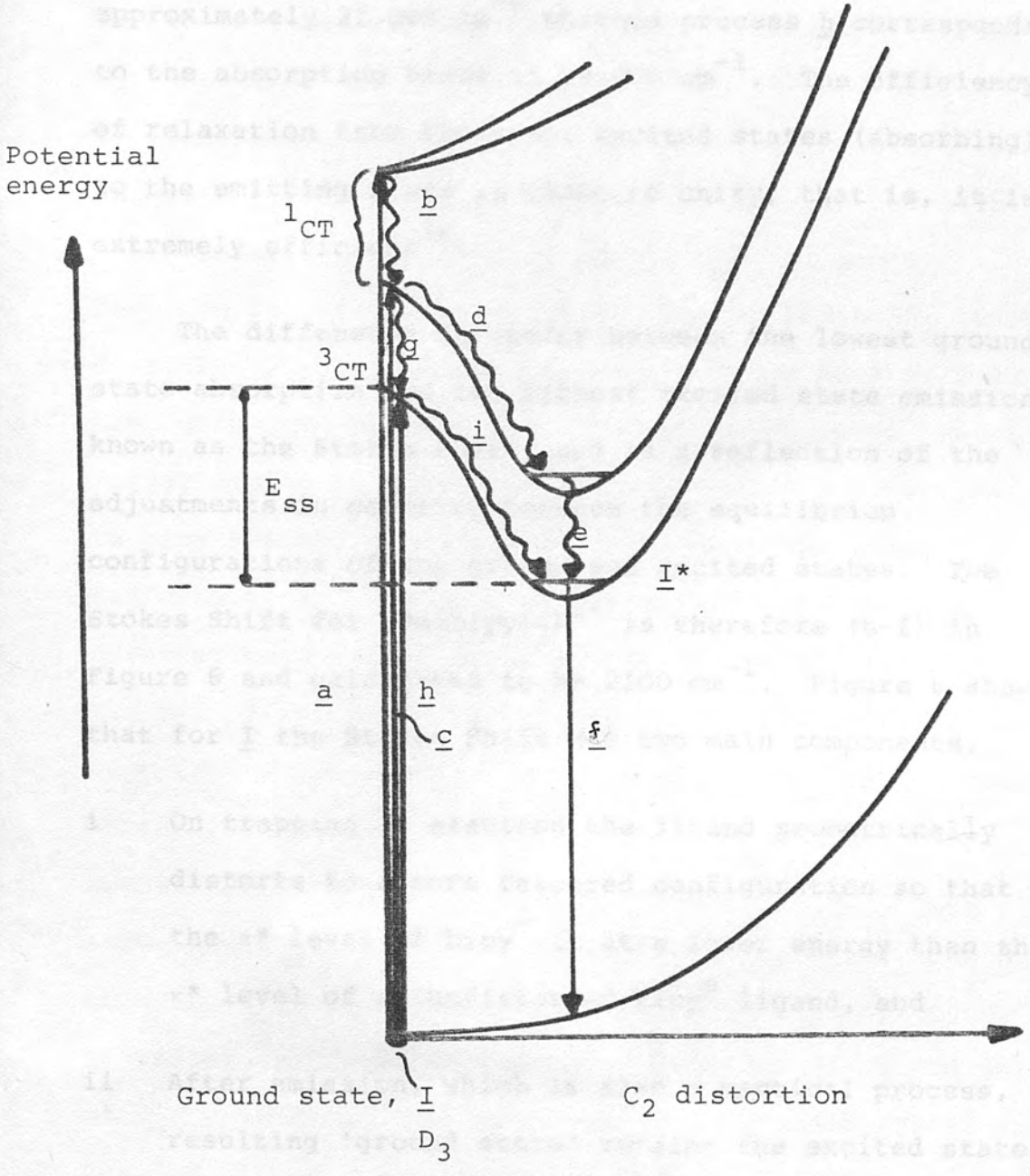

Note: transitions are not drawn to scale

E_{ss} = stabilisation energy as ligand distorts to accept charge transfer electron

triplet-excited state, ^3CT, in D_3 symmetry by rapid intersystem crossing (g). This same state could be reached by direct vertical absorption (h). In either case, ^3CT will relax (i) to the emitting state I*. Processes a and c correspond to the MLCT transition at approximately 22,000 cm^{-1} whereas process h corresponds to the absorption bands at 19,000 cm^{-1}. The efficiency of relaxation from the upper excited states (absorbing) to the emitting state is close to unity; that is, it is extremely efficient[36].

The difference in energy between the lowest ground state absorption and the highest excited state emission is known as the Stokes Shift, and is a reflection of the adjustments in geometry between the equilibrium configurations of the ground and excited states. The Stokes Shift for $[Ru(bipy)_3]^{2+}$ is therefore (h-f) in Figure 6 and calculated to be 2100 cm^{-1}. Figure 6 shows that for I the Stokes Shift has two main components:

i On trapping an electron the ligand geometrically distorts to a more favoured configuration so that the π^* level of $bipy^-$ is at a lower energy than the π^* level of an undistorted $bipy^o$ ligand, and

ii After emission, which is also a vertical process, the resulting 'ground state' retains the excited state geometry of I*. Clearly this residual energisation (relative to I) also contributes to the overall Stokes Shift between absorption (h) and emission (f).

The ligand distortion energy can be directly calculated from the ligand-based intervalence charge transfer transition (Figure 7). Hush has shown that, where the potential energy curves are quadratic in form and there is negligible interaction between the redox-active centres, the vertical (IVCT) transition energy E_{op} should be $4E_{th}$[37] where E_{th} is the thermal barrier to electron-hopping (between adjacent bipy ligands in the present case). The above conditions are found in I*. The barrier E_{th} corresponds to the thermal energy required for the electron to hop between adjacent ligands directly; however for the present purpose we also require the energy of the threefold saddle -point above the energy minima of the potential energy curve corresponding to $bipy^-$; that is, we are interested in the energy difference, E_{ss}, between the threefold saddle-point attained by vertical optical transitions and the energy minimum of the potential energy curve of the distorted bipy ligand (Figure 6). This is the stabilisation energy of the ligand as it distorts to accept the charge-transferred electron. Figures 7A and 7B (PE = E_{th}) show how E_{ss} can be calculated from E_{th} using simple trigonometry and assuming that the potential energy curve is indeed quadratic in form; $y = (x+a)^2$. Using the value of E_{op} = 4500 cm^{-1} (experimentally determined for I^- in Chapter 3), we calculate E_{th} = 1125 cm^{-1} and E_{ss} = 1560 cm^{-1}.

Figure 7 also shows that the electron remains trapped

FIGURE 7A: Vertical profile through potential energy surface as a function of the nuclear configuration for a self-exchange reaction, eg.$(bipy^{o})(bipy^{-}) \rightarrow (bipy^{-})(bipy^{o})$

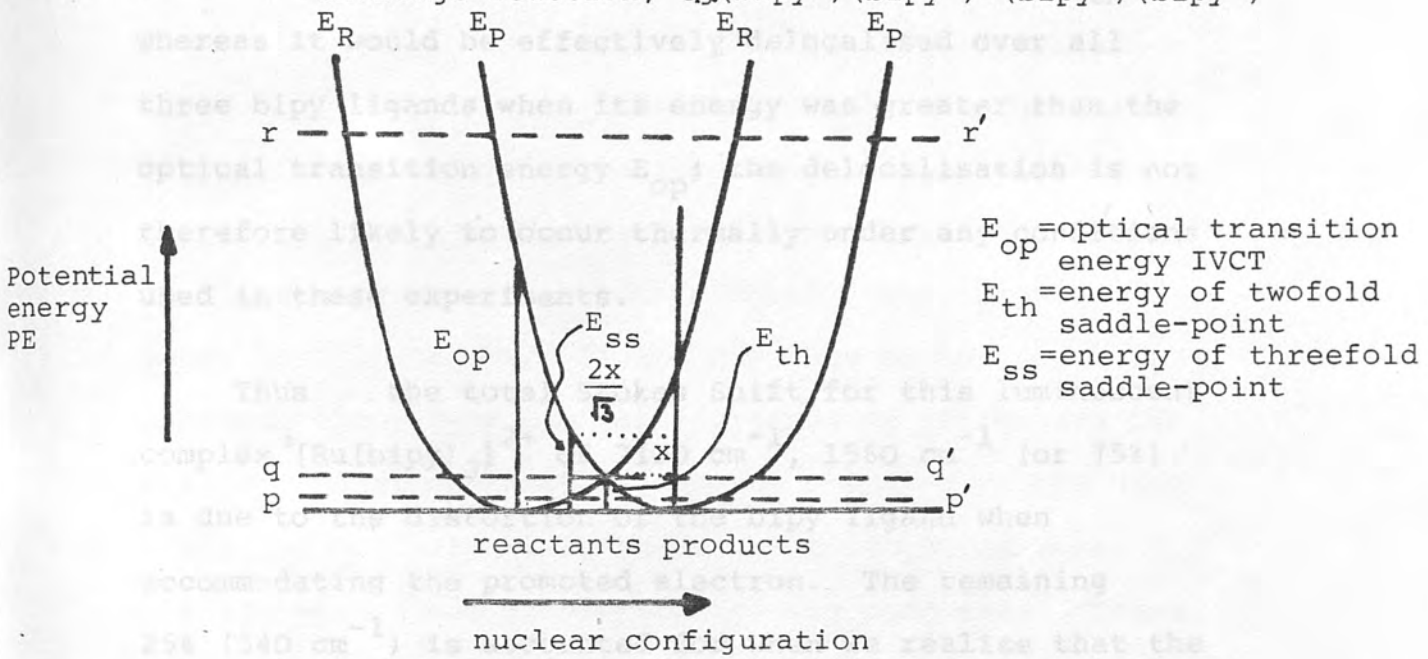

FIGURE 7B: Intersection of energy surfaces

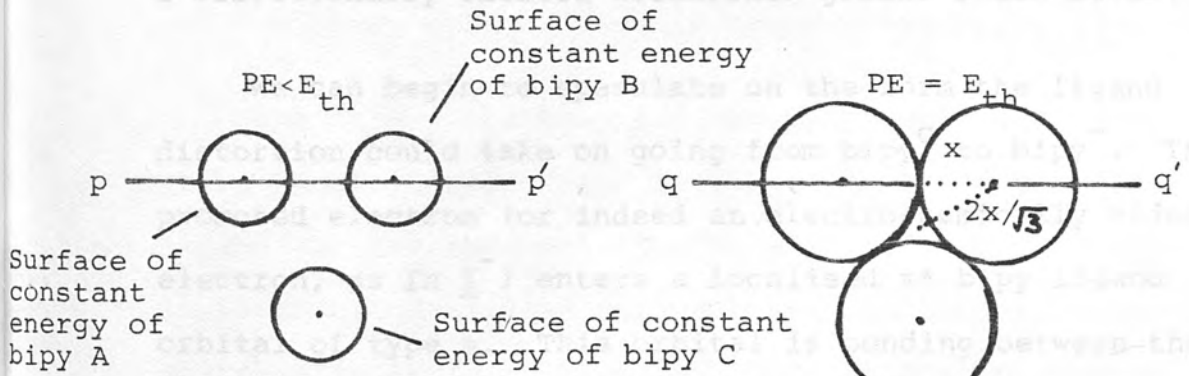

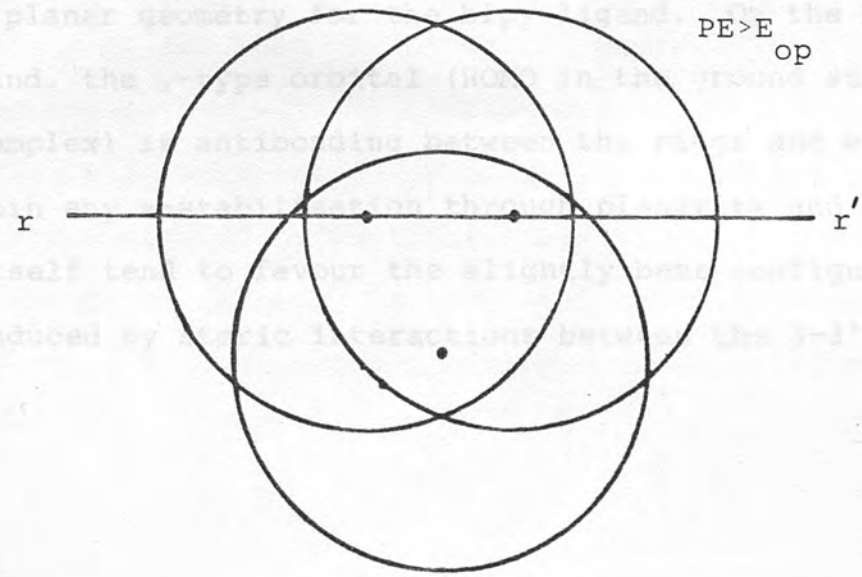

on one bipy if the molecular energy is less than E_{th}, whereas it would be effectively delocalised over all three bipy ligands when its energy was greater than the optical transition energy E_{op}; the delocalisation is not therefore likely to occur thermally under any conditions used in these experiments.

Thus the total Stokes Shift for this luminescent complex $^{*}[Ru(bipy)_3]^{2+}$ of 2100 cm^{-1}, 1560 cm^{-1} (or 75%) is due to the distortion of the bipy ligand when accommodating the promoted electron. The remaining 25% (540 cm^{-1}) is accounted for when we realise that the vertical emission process will leave the bipy ligand still in its distorted geometry; that is, it will be in a vibrationally excited electronic ground state level.

We can begin to speculate on the form the ligand distortion could take on going from $bipy^{o}$ to $bipy^{-}$. The promoted electron (or indeed an electrochemically added electron, as in $\underline{I}^{-}$) enters a localised π^* bipy ligand orbital of type ψ. This orbital is bonding between the two pyridine rings and hence its contribution to their π-interaction will be promoted by, and will greatly favour, a planar geometry for the bipy ligand. On the other hand, the χ-type orbital (HOMO in the ground state complex) is antibonding between the rings and will not gain any π-stabilisation through planarity and hence will itself tend to favour the slightly bent configurations induced by steric interactions between the 3-3' hydrogens.

Indeed the X-ray crystal structures of tris-bipy complexes show that the bipy ligands are usually twisted or bowed[5,38]. Thus we would predict that when a neutral bipy ligand accepts an electron into $\psi(7)$ it distorts towards planarity. Such a distortion should be reflected in the energy levels of both orbital types; Figure 2 shows that as the bipy ligand distorts to accept an electron the χ-type orbital increases in energy and the ψ-type orbital decreases in energy compared to the bipy^{o} orbitals. Unfortunately there are no reported X-ray crystal structures of bipy^{-}-containing complexes. There is one early report of the structure of the triplet state of biphenyl in solution which, in accord with the above reasoning, has a twisted conformation in the ground state and a planar configuration in the excited state[39].

The tris-, cis-bis- and mono-bipy complexes of Ru(II), where py is the spectator ligand, all have their bipy ligands in the same orientation and are best considered in terms of one-ligand chromophores in their reduced states (Chapter 3). Assuming that the emitting states of the cis-bis and the mono-bipy complexes should be formulated using the trapped electron model (as for the tris complex) then the potential energy curves for the excited states will be similar for all three complexes (Figure 6) with the absorption spectra of the ground state dominated by vertical transitions to non-equilibrium geometry excited states. The promoted electron will then become trapped on an isolated ligand

from which emission will occur. Thus the absorption and emission spectra will be very similar in shape and position for all three complexes (though intensities will depend on the number of bipy ligands in each). In the trans-bis-complex, however, the bipy ligands are orientated differently to one another and steric constraints between them are such that the ligands deviate from planarity in a much more dramatic fashion than in the complexes considered above. The greater deviations from planarity of the bipy ligands in the trans complexes compared to the cis are reflected in the π orbitals of the bipy. The χ orbitals will be favoured by the trans-geometry and hence should be lower in energy compared to the cis-complex. Chapter 3 shows that this is indeed what we infer experimentally.

The excited state potential energy curves will be altered and hence the absorption spectrum will have a different profile from the cis-bis-complex. However, as has been shown in Chapter 3 once the electron has been trapped on a ligand there is little difference between the two isomers and hence the emission spectra will have similar Franck-Condon envelopes[23] so long as the model of one ligand chromophores is appropriate.

The nature of the luminescent state of $[Ru(bipy)_3]^{2+}$ in which the promoted electron is trapped on one ligand thereby implying that $\underline{I}^*$ is distorted away from D_3 symmetry, is now well established having proved successful not only in explaining our own absorption

spectral results but also results obtained using different techniques.

Experimental

The spectrum of $\underline{I}^*$ was obtained by conventional room temperature flash photolysis of $\underline{I}$ (as chloride) at a concentration of 2.5×10^{-5} mol dm^{-3} in deoxygenated water in a 1 cm square cross-section cell. Data are averaged over three separate experiments, corrected for emission, and shown to be independent of laser power in the range used. Excitation was by 2.5 mJ 347 nm ruby and 3 mJ 530 nm Nd^{3+} glass lasers, both of pulse length 15 ns, and spectra were measured after 50 ns; effectively no ground state molecules are present under these conditions.

REFERENCES

1. R.W. Harrigan and G.A. Crosby; J. Chem. Phys., 59, 3468 (1973).

2. G.A. Crosby and W.H. Elfring; J. Phys. Chem., 80, 2206 (1976).

3. N. Sutin and C. Creutz; Adv. Chem. Ser., 168, 1, (1978).

4. W.H. Elfring and G.A. Crosby; J. Am. Chem. Soc., 103, 2683 (1981).

5. D.P. Rillema, D.S. Jones and H.A. Levy; J. Chem. Soc. Chem. Comm., 849 (1979).

6. I. Fujita and H. Kobayashi; Inorg. Chem., 12, 2758 (1973).

7. M.K. DeArmond, C.M. Carlin and W.L. Huang; Inorg. Chem., 19, 62 (1980).

8. K.W. Hipps; Inorg. Chem., 19, 1390 (1980).

9. R.F. Dallinger and W.H. Woodruff; J. Am. Chem. Soc., 101, 4391 (1978).

10. M. Forster and R.E. Hester; Chem. Phys. Lett., 81, 42 (1981).

11. P.G. Bradley, N. Kress, B.A.Hornberger, R.F. Dallinger and W.H. Woodruff; J. Am. Chem. Soc., 103, 7441 (1981).

12. U. Lachish, P.P. Infelta and M. Grätzel; Chem. Phys. Lett., 62, 317 (1979).

13. R.V. Bensasson, C. Salet and V. Balzani; C.R. Acad. Sci. Paris B, 289, 41 (1979).

14. E. Konig and S. Kremer; Chem. Phys. Lett., 5, 87 (1970).

15. Y. Torii, S. Murasato and Y. Kaisu; Nippon Kagaku Zasshi, 91, 549 (1970).

16. R. Bensasson, C. Salet and V. Balzani; J. Am. Chem. Soc., 98, 3722 (1976).

17. V. Balzani, F. Bolletta, M.T. Gandolfi and M. Maestri; Top. Curr. Chem., 75, 1 (1978).

18. G.D. Hager and G.A. Crosby; J. Am. Chem. Soc., 97, 7031 (1975).

19. A.B.P. Lever; Inorganic Electronic Spectroscopy; Elsevier, Amsterdam (1968).

20. J. van Houten and R.J. Watts; J. Am. Chem. Soc., 98 4853 (1976).

21. S.R. Allsop, A. Cox, T.J. Kemp and W.J. Reed; J. Chem. Soc., Faraday, Trans I, 74, 1275 (1978).

22. D.M. Klassen and G.A. Crosby; J. Chem. Phys., 48, 1853 (1968).

23. R.A. Krause and C.J. Ballhausen; Acta Chem. Scand. Ser. A, 31, 535 (1977).

24. C.M. Carlin and M.K. DeArmond; Chem. Phys. Lett., 89, 297 (1982).

25. F. Felix, J. Ferguson, H.U. Güdel and A. Ludi; J. Am. Chem. Soc., 102, 4096 (1980).

26. B.J. Pankuch, D.E. Lack y and G.A. Crosby; J. Phys. Chem., 84, 2061 (1980).

27. L.E. Orgel; J. Chem. Soc., 3683 (1961).

28. F. Felix, J. Ferguson, H.U. Güdel and A. Ludi; Chem. Phys. Lett. 62, 153 (1979).

29. S. Decurtins, F. Felix, J. Ferguson, H.U. Güdel and A. Ludi; J. Am. Chem. Soc., 102, 4102 (1980).

30. K.W. Hipps and G.A. Crosby; J. Am. Chem. Soc., 97, 7042 (1975).

31. P. Belser, C. Daul and A. von Zelewsky; Chem. Phys. Lett., 79, 596 (1981).

32. A. Ceulemans and L.G. Vanquickenbourne; J. Am. Chem. Soc., 103, 2238 (1981).

33, J. Ferguson and F. Herren; Chem. Phys. Lett. 89, 371 (1982).

34. J. Ferguson, F. Herren and G.M. McLaughlin; Chem. Phys. Lett., 89, 376 (1982).

35. J. Barker and B.N. Figgis; J. Chem. Soc., Dalton, 598 (1975).

36. J.N. Demas and D.G. Taylor; Inorg. Chem., 18, 3177 (1979).

37. N.S. Hush, Prog. Inorg. Chem., 8, 391 (1967).

38. B. Figgis, B. Shelton and A. White; Aust. J. Chem., 31, 57 (1978).

39. G. Casalone, C. Mariani, A. Mugnoli and M. Simonetta; Mol. Phys., 15, 339 (1968).

CHAPTER 6

ELECTRODE POTENTIAL/CENTRAL VALENCY CORRELATIONS OF TRIS-BIPYRIDYL COMPLEXES

In general, tris-bipyridyl complexes $[M(bipy)_3]^{z+}$ exhibit rich redox chemistries. The electrochemical behaviour of such complexes can broadly be divided into two types:

i primarily metal-based oxidations and reductions; and

ii primarily ligand-based reductions.

Uncoordinated bipy undergoes a reversible one-electron reduction at -2.47 V *vs.* Ag/Ag^+ but no oxidation processes are observed at potentials less positive than +2.00 V. Accordingly complexes tend to have at most only one metal-based oxidation step, and usually it is the extended sequence of reversible reduction steps which generate most interest. In this chapter we will therefore be primarily concerned with the reduction steps of $[M(bipy)_3]^{z+}$; firstly, whether they can be identified as either metal- or ligand-based processes, and secondly, why particular complexes undergo a ligand-based reduction as opposed to a metal-based one (or vice versa). Finally we consider whether a general understanding can be reached from which we can predict the electrochemical behaviour of other bipyridyl complexes.

In Chapter 2, the electrochemical behaviour of

$[Ru(bipy)_3]^{2+}$, I, and isoelectronic $[Ir(bipy)_3]^{3+}$, II, was reported. In both cases it was shown by spectro-electrochemical techniques that the cathodic processes were ligand-based reductions and further, that the three bipy ligands were non-interacting. Equally, in many of the complexes studied there has been no indication of interaction between the bipy ligands, irrespective of the complex geometry or the nature of any accompanying ligands. The pattern of three narrowly spaced reduction steps (with approximately equal separations of about 200 mV) in the tris-complexes were therefore recognised to be indicative of non-interacting ligand-based redox processes, hence by looking for such a characteristic grouping within the electrochemical behaviour of further $[M(bipy)_3]^{z+}$ complexes we would hope to be able to distinguish between metal- and ligand-based reductions. Recently Vlček has implicitly made use of the same criterion in his discussion of $[M(bipy)_3]^{z+}$ complexes for the limited series where M = Fe, Ru(I), Ir(II) and Cr[1].

The actual potentials for the ligand-based reductions were very different for the two complexes, I and II and it was suggested in Chapter 2 that this difference was directly attributable to the central metal charge. Thus in this chapter we investigate the electrochemical behaviour of a range of tris-bipyridyl complexes to try and correlate the potentials of the ligand-based reductions with central valence charge.

Many of the complexes are unstable towards dissociation in solution, either in their familiar oxidation state or after electrochemical reduction (even at fairly fast scan rates (5 V/s)),expelling one or more bipy ligands.

We can, however, at least slow down the expulsion by either chilling the solution or adding a substantial excess of the ligand. In the latter case it must be remembered that free bipy undergoes a reversible one-electron reduction itself at -2.47 V vs. Ag/Ag^{+}. In such cases the inherent instability of most of these complexes makes it impossible to use spectroelectrochemical techniques to characterise the short-lived products and to identify the redox processes as primarily metal- or ligand-based. However, according to the earlier discussion, such information should now be obtainable from the voltammetric data because the complexes can be stabilised on the voltammetric timescale and thus good E_o values evaluated.

Tris-bipyridine iron(II)

Dark red tris-bipyridine iron(II), $[Fe(bipy)_3]^{2+}$, VIII, is a low-spin $d\pi^6$ complex[2,3] like $[Ru(bipy)_3]^{2+}$. The cyclic voltammograms obtained at room temperature in acetonitrile for VIII are identical to those reported in the literature[4-6], and our voltammetric data are summarised in Table 1. The electrochemical behaviour is

TABLE 1: ELECTRODE POTENTIALS (V vs. Ag/Ag^+) for VIII at room temperature[a]

$$[Fe(bipy)_3]^{3+} \xleftarrow{+0.76} [Fe(bipy)_3]^{2+} \xrightarrow{-1.64} [Fe(bipy)_3]^{1+} \xrightarrow{-1.825} [Fe(bipy)_3]^{0} \xrightarrow{-2.105} [Fe(bipy)_3]^{1-}$$

VIII^{+} VIII VIII^{1-} VIII^{2-} VIII^{3-}

[a] All steps are reversible one-electron transfers ΔE_p = 70 mV

unaffected by solvent (acetonitrile, propylene carbonate, dimethylsulphoxide or dimethylformamide) or by temperature, although the electrode potentials appear to shift to more negative potentials at -40°C, as previously noted (Chapter 2).

The voltammogram traces for VIII and I (Chapter 2) are nearly superimposable for the cathodic processes, but the oxidation step $\underline{VIII}^{O/+}$ is at a different potential than $\underline{I}^{O/+}$, thereby suggesting that once again we are observing ligand-based reductions and a metal-based oxidation. Furthermore, the characteristic narrowly spaced cathodic waves are indicative of non-interacting ligand-based redox processes on a M(II) centre; that is, VIII must be formulated as $[Fe(II)(bipy^{O})_3]^{2+}$ and the reduced complexes as $[Fe(II)(bipy^{O})_2(bipy^{-})]^{1+}$, $[Fe(II)(bipy^{O}(bipy^{-})_2]^{O}$ and $[Fe(II)(bipy^{-})_3]^{1-}$. Accordingly the absorption spectrum of $\underline{VIII}^{3-}$ should be dominated by intraligand $\pi\pi^*$ transitions of $bipy^{-}$, while the partially reduced complexes $\underline{VIII}^{1-}$ and $\underline{VIII}^{2-}$ should show transitions arising from co-existing coordinated $bipy^{O}$ and $bipy^{-}$. The absorption spectrum of chemically reduced $\underline{VIII}^{3-}$ is indeed characteristic of $bipy^{-}$ [7] and that of $\underline{VIII}^{1-}$ generated electrochemically is also as predicted[2]. Noting the resemblance of the absorption spectra of VIII and $\underline{VIII}^{1-}$ in the 18,000-20,000 cm^{-1} region, Prasad and Scaife[2] suggested that the $\underline{VIII}^{1-}$ solution contained an impurity. However the trapped-electron model requires that just such a

similarity should be evident as both complexes contain the Fe(II)-bipy^{o} chromophore responsible for the band at 19,000 cm^{-1}. Motten and co-workers have shown separately by esr studies that VIII^{1-} and VIII^{3-} contain discrete bipy^{-} ligands[8].

The close agreement in ligand-based redox potentials between I and VIII suggests that the π orbital arrays are of similar energy for both complexes. However, the easier Fe(II)/Fe(III) metal-based oxidation indicates that the filled $d\pi$ orbitals of the metal are at higher energy in $[Fe(bipy)_3]^{2+}$ than $[Ru(bipy)_3]^{2+}$ ($\sim$0.2 eV = 1600 cm^{-1}). This should be reflected in the position of the MLCT transition (Fe(II)$d\pi \rightarrow \pi^*$(I)bipy), the corresponding absorption band occurring at lower frequency in $[Fe(bipy)_3]^{2+}$ than in $[Ru(bipy)_3]^{2+}$. This is indeed what is observed[9]; with MLCT, VIII = 19,000 cm^{-1} and MLCT, I = 22,000 cm^{-1}, even though the detailed shape of the MLCT bands is unaltered in I and VIII (see Chapter 5 for explanation). In fact the lowest-energy MLCT transition has shifted to such an extent in $[Fe(bipy)_3]^{2+}$ that the second MLCT (Fe(II)$d\pi \rightarrow \pi^*$(2)bipy) is clearly observed at 28,700 cm^{-1}.

There is of course a crucial difference between $[Ru(bipy)_3]^{2+}$ and $[Fe(bipy)_3]^{2+}$ which accounts for the very real interest in I as a solar energy converter, whereas VIII, which has a similar intense visible absorption and electrochemistry, does not merit such

attention. Whereas $[Ru(bipy)_3]^{2+}$ has a fairly long-lived emitting excited state (600 ns) which can undergo quenching reactions (Chapter 2), $[Fe(bipy)_3]^{2+}$ does not luminesce in absolute ethanol at room temperature or 80 K[10] and the lifetime of the non-emitting excited state at room temperature is 0.83 ns[11], which is too short for any sort of exchange reactions of the excited state. Recently, Creutz and co-workers have obtained the absorption spectrum of the thermally equilibrated excited state of $[Fe(bipy)_3]^{2+}$, *VIII, which is absolutely featureless below 300 nm; that is, there is no indication of $bipy^-$ in *VIII, in striking contrast to *I (Chapter 5)[12]. Thus they conclude that the lowest excited state of VIII is a ligand field (dd*) state, either $^3T_1$ or $^5T_2$, thereby accounting for the short-lived non-emitting excited state.

The separation between $d\pi$ and $d\sigma$ orbitals has been calculated to be 13,110 cm^{-1} for $[Fe(phen)_3]^{2+}$ [13a] which gives some indication of the splitting in VIII, since phen and bipy generally have similar ligand field strengths. Thus a molecular orbital diagram can be constructed for $[Fe(bipy)_3]^{2+}$ (Figure 1a). The diagram, constructed on the basis of absorption band energies, appears, at first sight, to be in direct conflict with electrochemical data. Figure 1A indicates that the lowest unoccupied orbitals are metal-based ($d\sigma$). On this basis we might expect metal-based reductions, whereas we know experimentally that the acceptor orbital in the electrochemical process

FIGURE 1A: Molecular orbital diagram for Fe(II)-bipy^{o} chromophore

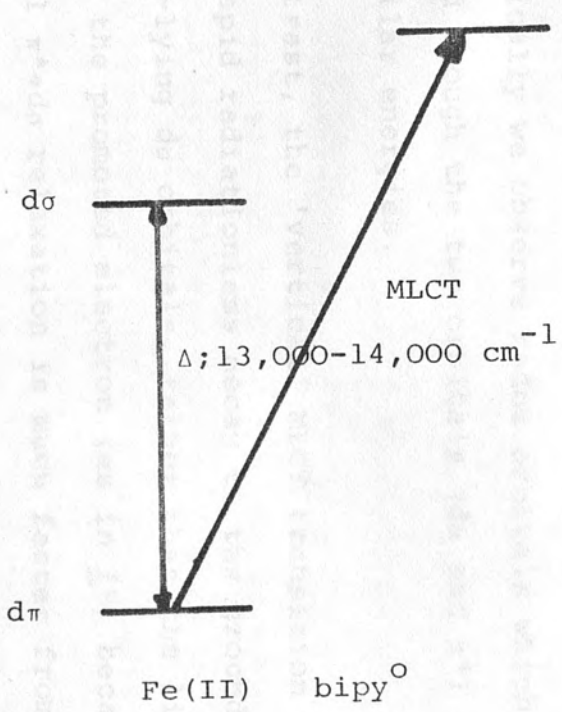

FIGURE 1B: Molecular orbital diagram for Fe(II)-bipy^{-} chromophore

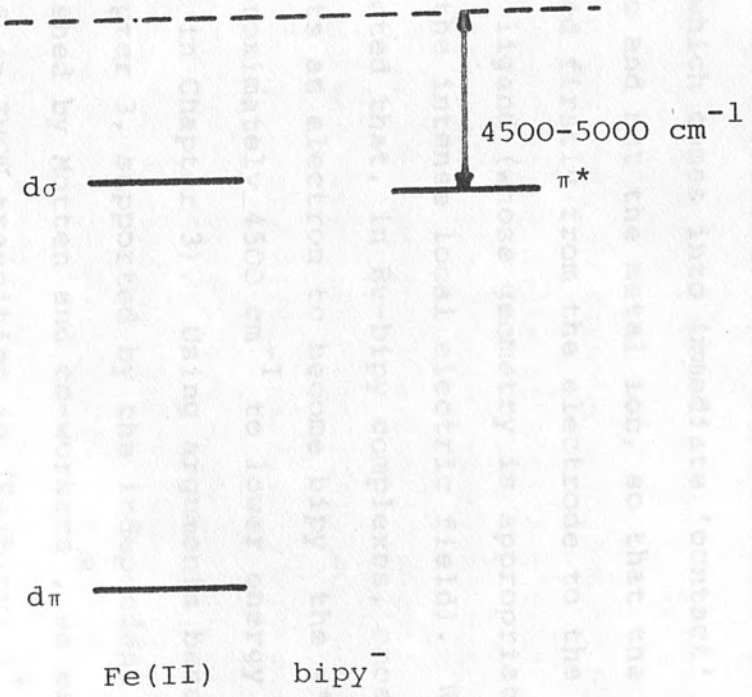

is clearly ligand-based. The arrangement of the chelating ligands around the central ion in tris-bipyridyl complexes is such that when the complex approaches an electrode, as in electrochemical experiments, it is a bipy ligand which comes into immediate 'contact' with the electrode and not the metal ion, so that the electron is transferred firstly from the electrode to the orbitals of the $bipy^{o}$ ligand (whose geometry is appropriately modified by the intense local electric field). We have previously noted that, in Ru-bipy complexes, once a $bipy^{o}$ ligand accepts an electron to become $bipy^{-}$ the π^* level falls by approximately 4500 cm^{-1} to lower energy (IVCT measurements in Chapter 3). Using arguments based on those in Chapter 3, supported by the independent value for E_{th}, established by Motten and co-workers[8], we estimate the energy of an IVCT transition in $[Fe(bipy)_3]^{+}$ to be between 4500 and 5000 cm^{-1}. Thus the π^* level of the ligand is predicted to fall to just below that of the $d\sigma$ orbital (Figure 1B) upon direct charge injection, thereby stabilising the ligand-based electrode reduction. Thus electrochemically we observe redox orbitals which are ligand-based though the two orbitals ($d\sigma$ and π^*) must be of very similar energies.

In contrast, the 'vertical' MLCT transition will result in rapid radiationless decay to the ground state via the low-lying $d\sigma$ orbitals, rather than the ligand trapping of the promoted electron (as in $\underline{I}^*$) because the internal $\pi^* \rightarrow d\sigma$ relaxation is much faster from the

potential energy saddle point than is the structural rearrangement of the acceptor ligand. Such a pathway is not available to VIII^{1-} as there is no 'hole' in the central metal ion and hence the electrochemically added electron remains trapped in the π^* orbital of bipy$^-$.

The difference between results obtained by spectral and electrochemical experiments is a direct consequence of the fact that the spectroscopic technique monitors immediate vertical transitions whereas in electrochemistry we are concerned with thermally equilibrated (geometrically adjusted) molecules. The different electronic configurations between VIII* and VIII^{1-} are also important. Usually we find that the two techniques can be used together to give information above the lowest-lying excited state (as in previous chapters); however, in this case, careful consideration is necessary to show that the results are complementary rather than inconsistent.

Tris-bipyridine osmium(II)

Tris-bipyridine osmium(II)$[Os(bipy)_3]^{2+}$, IX, is a dark green low-spin $d\pi^6$ complex[12] which exhibits a very similar redox chemistry to that of VIII and I (Table 2). We found that our electrochemical results agree with other published data[4,5,14] and did not depend on solvent (acetonitrile, dimethylsulphoxide) or temperature (usual E^o shift noted).

TABLE 2: ELECTRODE POTENTIALS FOR IX

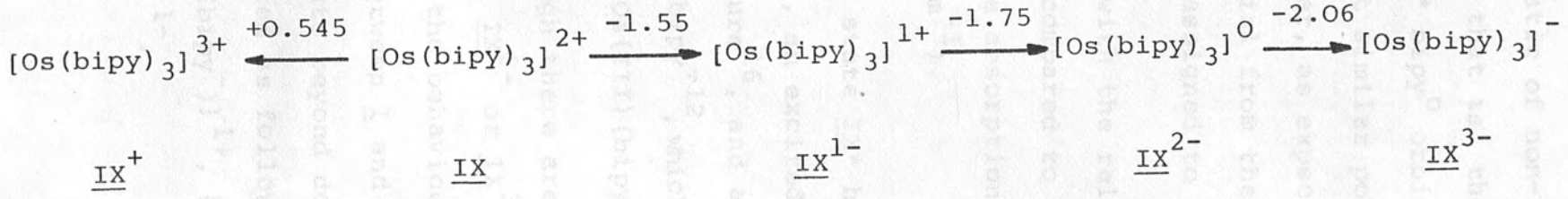

[a] E^{o}(V) vs. Ag/Ag^{+}; room temperature, all reversible one-electron steps ΔE_p = 70 mV

Again we note the three closely spaced cathodic waves characteristic of non-interacting $bipy^{o}$ ligand-based processes; that is, the LUMO available electrochemically are π^* $bipy^{o}$ orbitals. The ligand-based reductions are at similar potentials to those in I and VIII. However, as expected the anodic step is at a different potential from the corresponding couple in I and VIII and is assigned to an Os(II)/Os(III) couple.

In keeping with the relative ease of the metal-based oxidation in IX compared to I we note that the MLCT transition in the absorption spectrum of IX is at lower energy ($20,900\ cm^{-1}$).

The excited state IX* has a similar luminescence spectrum to I*[15], an excited state lifetime of 19.2 ns at room temperature[16], and an absorption spectrum of IX* clearly showing $bipy^{-}$[12], which might be provisionally formulated as $*[(Os(III)(bipy^{o})_2(bipy^{-})]^{2+}$.

Thus although there are no reports of the absorption spectra of IX^{1-}, IX^{2-} or IX^{3-} the many documented similarities in the behaviour, chemical, electrochemical and spectral, between I and IX and all their related complexes suggests beyond doubt that the reduced complexes must be formulated as follows: $[Os(II)(bipy^{o})_3]^{2+}$, $[Os(II)(bipy^{o})_2(bipy^{-})]^{1+}$, $[Os(II)(bipy^{o})(bipy^{-})_2]^{o}$, $[Os(II)(bipy^{-})_3]^{1-}$.

Tris-bipyridine zinc(II)

Tris-bipyridine zinc(II) $[Zn(bipy)_3]^{2+}$, X, is a very pale pink d^{10} complex. The absorption spectrum of X is completely dominated by ultraviolet intraligand $\pi\pi^*$ transitions of $bipy^o$, with no MLCT transitions, because the fully occupied d orbital set is well-stabilised by the high core charge and is therefore inaccessible. The emission spectrum of X* is very similar to that of $*[Ir(bipy)_3]^{3+}$ [17] which has already been established as occurring from a $\pi\pi^*$ state (Chapter 2) and hence the same conclusions as to the ordering of the orbitals must be drawn for $[Zn(bipy)_3]^{2+}$ as for II; namely, that the $d\pi$ orbitals are at lower energy than the highest filled π orbital of bipy.

The absence of empty low-energy metal orbitals means the electrochemistry of the complex, if any, should be dominated by ligand-based reductions. The cyclic voltammogram of X in acetonitrile at room temperature is shown in Figure 2. It is immediately obvious that the room temperature electrochemical behaviour of X is not that predicted for three non-interacting ligand-based reductions. There are two ill-defined forward waves at negative potentials (-1.78 V and -2.065 V vs. Ag/Ag^+). The first shows some signs of a return wave and hence is termed quasi-reversible whereas the second is completely irreversible showing no return wave.

Extending the potential range of the cyclic

FIGURE 2: Cyclic voltammogram of $[Zn(bipy)_3]^{2+}$ in acetonitrile

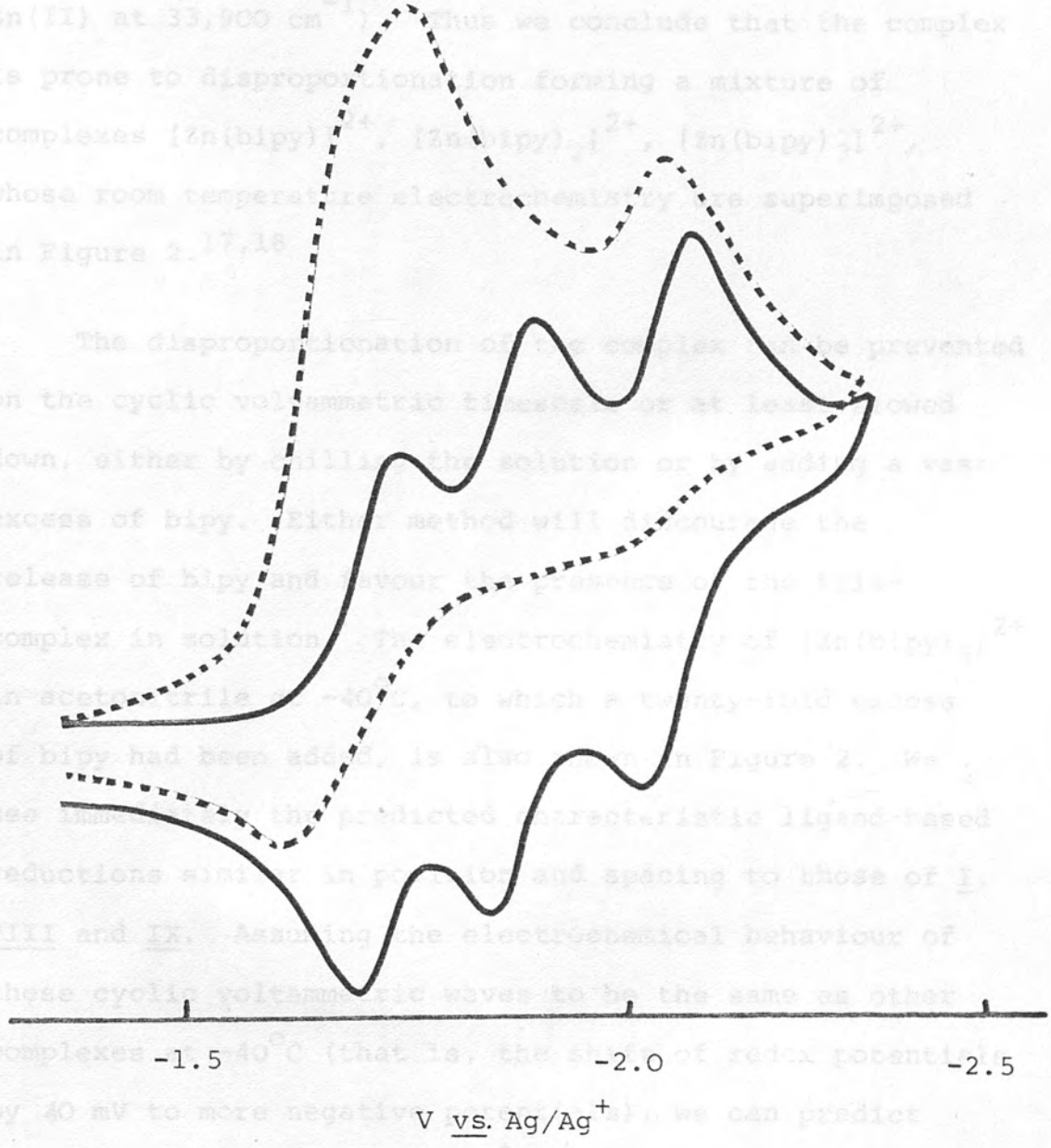

voltammogram to -2.7 V reveals the presence of uncoordinated bipy (free bipy is reduced at -2.47 V). The height of this peak, which is proportional to the concentration, grew with time. Evidence of free bipy was also observed in the absorption spectrum of solutions of X (free-bipy absorption band maximum at 35,700 cm^{-1}, bipy coordinated to Zn(II) at 33,900 cm^{-1}). Thus we conclude that the complex is prone to disproportionation forming a mixture of complexes $[Zn(bipy)]^{2+}$, $[Zn(bipy)_2]^{2+}$, $[Zn(bipy)_3]^{2+}$, whose room temperature electrochemistry are superimposed in Figure 2.[17,18]

The disproportionation of the complex can be prevented on the cyclic voltammetric timescale or at least slowed down, either by chilling the solution or by adding a vast excess of bipy. Either method will discourage the release of bipy and favour the presence of the tris-complex in solution. The electrochemistry of $[Zn(bipy)_3]^{2+}$ in acetonitrile at -40°C, to which a twenty-fold excess of bipy had been added, is also shown in Figure 2. We see immediately the predicted characteristic ligand-based reductions similar in position and spacing to those of I, VIII and IX. Assuming the electrochemical behaviour of these cyclic voltammetric waves to be the same as other complexes at -40°C (that is, the shift of redox potentials by 40 mV to more negative potentials), we can predict the E^{o} values for $[Zn(bipy)_3]^{2+}$ at room temperature (Table 3).

TABLE 3: ELECTRODE POTENTIALS FOR X

$$[Zn(bipy)_3]^{2+} \xrightarrow{-1.69^a} [Zn(bipy)_3]^{1+} \xrightarrow{-1.83} [Zn(bipy)_3]^{0} \xrightarrow{-2.00} [Zn(bipy)_3]^{1-}$$

$$\underline{X} \qquad\qquad \underline{X}^{1-} \qquad\qquad \underline{X}^{2-} \qquad\qquad \underline{X}^{3-}$$

[a] E^{o}(V) *vs.* Ag/Ag^{+}; calculated room temperature values.

The waves are all reversible one-electron processes. The same pattern is also observed at room temperature if the solution contains a large amount of free bipy or at -40°C with no excess bipy but in both cases the peaks are not as well defined as in Figure 2 (-40°C) and the return waves are smaller. Thus it requires both techniques to stabilise the complex sufficiently for electrochemical study.

The reduced complexes of $[Zn(bipy)_3]^{2+}$, although stable on a cyclic voltammetric timescale, are not stable on an electrosynthesis one and hence $\underline{X}^{1-}$, $\underline{X}^{2-}$ and $\underline{X}^{3-}$ cannot be studied spectroelectrochemically. However we conclude from the characteristic cyclic voltammetric pattern that the reduction processes are ligand-based.

Thus it becomes noticeable that all ligand-based reductions of metal +2 centres investigated so far occur at approximately the same potentials:

$$[M(II)(bipy^{o})_3]^{2+} \underset{-e^-}{\overset{+e^-}{\rightleftharpoons}} [M(II)(bipy^{o})_2(bipy^{-})]^{1+} \quad E\sim -1.65\ V$$

$$[M(II)(bipy^{o})_2(bipy^{-})]^{1+} \underset{-e^-}{\overset{+e^-}{\rightleftharpoons}} [M(II)(bipy^{o})(bipy^{-})_2]^{o} \quad E\sim -1.82\ V$$

$$[M(II)(bipy^{o})(bipy^{-})_2]^{o} \underset{-e^-}{\overset{+e^-}{\rightleftharpoons}} [M(II)(bipy^{-})_3]^{1-} \quad E\sim 2.05\ V$$

We have already noted that the ligand-based reductions of $[Ir(bipy)_3]^{3+}$ occur at more positive potentials. We

therefore decided to investigate whether this was a systematic phenomenon or peculiar to $[Ir(bipy)_3]^{3+}$.

Tris-bipyridine indium(III)

The white main-group complex tris-bipyridine indium-(III) $[In(bipy)_3]^{3+}$, XI, is also a d^{10} system and we expect only ligand-based reductions.

A cyclic voltammogram of XI in acetonitrile at room temperature on platinum gave meaningless results. After the cyclic voltammetric scan it was noted that the usually bright metallic platinum electrode had become dull and brown in colour; that is, the electrode surface was becoming contaminated and hence passivated. The brown coating could be removed by immersion in nitric acid. We did not investigate this observation further.

Further investigations of $[In(bipy)_3]^{3+}$ used a dropping mercury electrode (dme). A dme solves the electrode contamination problem as a fresh electrode surface is constantly being formed, thus enabling the electrochemistry of XI to be studied. An ac voltammogram gave three closely spaced peaks of a similar height and width (Table 4).

We must again conclude that the redox-active orbitals of $[In(bipy)_3]^{3+}$ are ligand-based, due to the characteristic spacings between the reduction potentials. We also

TABLE 4: ELECTRODE POTENTIALS FOR XI

$$[In(bipy)_3]^{3+} \xrightarrow{-1.28^a} [In(bipy)_3]^{2+} \xrightarrow{-1.46} [In(bipy)_3]^{1+} \xrightarrow{-1.675} [In(bipy)_3]^{0}$$

[a] E^{o}(V) vs. Ag/Ag^{+}; room temperature

note the effect of the metal +3 centre; the actual reduction potential values are similar to those of $[Ir(bipy)_3]^{3+}$. Thus the effect of the central metal charge on the ligand-based reductions is real. In order to investigate if there is a wider correlation between the central metal charge and the potential of the ligand-based reductions further transition metal tris-bipy complexes were selected for study.

Tris-bipyridine chromium(III)

Tris-bipyridine chromium(III) $[Cr(bipy)_3]^{3+}$, XII, is a yellow $d\pi^3$ complex which is currently of much interest in solar energy conversion systems[19,20]. The complex is relatively stable to photochemical ligand loss[19]. The lowest excited state, a metal-centred ligand-field (M(d-d)) state (^2E)[19], is both long-lived in deaerated aqueous solutions at room temperature (63 μs)[21] and highly reactive towards redox quenchers[22,23].

There is no indication of any low-lying charge transfer bands (either L→M or M→L) in the absorption spectrum of XII (Figure 4); rather the visible region of the spectrum (22,000-25.000 cm^{-1}) shows several low intensity ($\varepsilon \sim 500$) bands which have been assigned primarily to spin-allowed d→d bands[24]. Thus, the absorption spectral data and the properties of the excited state suggest that the redox-active orbitals of $[Cr(bipy)_3]^{3+}$ will be metal-based and not ligand-based.

A cyclic voltammogram of XII in acetonitrile from 0 to -2.0 V vs. Ag/Ag^{+} is shown in Figure 3 and the measured electrode potentials are listed in Table 5.

All three evenly spaced reductions correspond to one-electron steps (coulometry), are fully reversible, and the potential differences between the steps agree with previous reports[5,25,26]. The reduction potential separations are not characteristic of ligand-based reductions (200 mV separation whereas there is a 500 mV separation observed here) and the potential of the first reduction (-0.53 V) is not that predicted for a bipy-based reduction on a metal +3 centre(-1.26 V for Ir^{3+} and -1.28 V for In^{3+}). Thus we regard the three cathodic processes as metal-based reductions which should be formulated as follows:

$$[Cr(III)(bipy^{o})_3]^{3+} \underset{-e^-}{\overset{+e^-}{\rightleftharpoons}} [Cr(II)(bipy^{o})_3]^{2+} \underset{-e^-}{\overset{+e^-}{\rightleftharpoons}}$$

$d\pi^3$ $\qquad\qquad$ $d\pi^4$

$$[Cr(I)(bipy^{o})_3]^{1+} \underset{-e^-}{\overset{+e^-}{\rightleftharpoons}} [Cr(O)(bipy^{o})_3]^{O}$$

$d\pi^5$ $\qquad\qquad$ $d\pi^6$

Magnetic measurements on polycrystalline samples of $[Cr(bipy)_3]^{3+/2+/1+/O}$ show 3, 2, 1 and 0 unpaired electrons respectively[24], which is in accord with the above formulation.

In order to confirm that the redox-active orbitals of

FIGURE 3: Cyclic voltammogram of $[Cr(bipy)_3]^{3+}$ in acetonitrile, room temperature

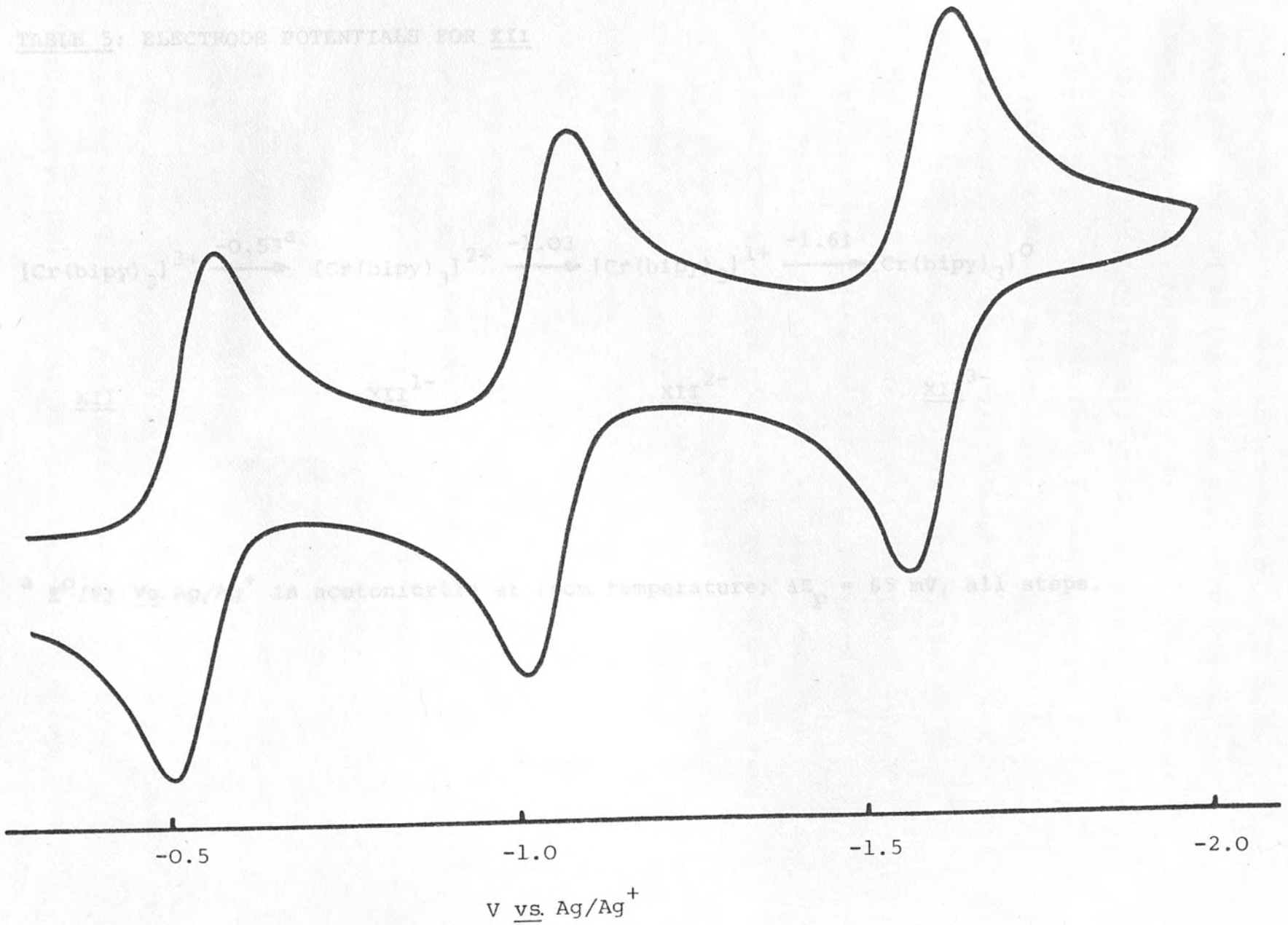

TABLE 5: ELECTRODE POTENTIALS FOR XII

$$[Cr(bipy)_3]^{3+} \xrightarrow{-0.53^a} [Cr(bipy)_3]^{2+} \xrightarrow{-1.03} [Cr(bipy)_3]^{1+} \xrightarrow{-1.61} [Cr(bipy)_3]^{0}$$

XII $\qquad$ XII^{1-} $\qquad$ XII^{2-} $\qquad$ XII^{3-}

[a] E^{o}(V) vs. Ag/Ag^{+} in acetonitrile at room temperature; ΔE_p = 65 mV, all steps.

XII are metal-based, spectroelectrochemical studies of the reduced complexes were undertaken; $bipy^-$ ligands should be detected by their characteristic intense absorption bands (Chapter 2). The ground state complex, $[Cr(bipy)_3]^{3+}$, is indefinitely stable in acetonitrile, as is $[Cr(bipy)_3]^{2+}$ providing the solution is oxygen free. The further reduced complexes XII^{2-} and XII^{3-}, although stable on a cyclic voltammetric timescale, are found to decompose giving the metal ion and bipy ligands on an electrosynthesis timescale; however addition of bipy to the solution stabilises the reduction products and enables their absorption spectra to be recorded. The vast excess of bipy does not affect the electrochemistry of XII; however it does mask the ultraviolet region of the absorption spectrum of XII^{2-} and XII^{3-}. The $\pi\pi^*$ intraligand transition of uncoordinated bipy occurs at 35,700 cm^{-1}.

The complexes XII^{1-}, XII^{2-} and XII^{3-} were all generated at room temperature in acetonitrile in a platinum O.T.T.L.E. at -0.8 V, -1.3 V and -1.9 V respectively *vs.* Ag/Ag^+. The absorption spectra of XII, XII^{1-} and XII^{2-} are shown in Figure 4. The absorption spectrum of XII^{3-} is shown in Figure 5 and is discussed later.

The absorption spectra shown in Figure 4 are in close agreement with earlier published reports[24,27]. Band assignments listed in Chapter 6 follow readily enough from

FIGURE 4: Absorption Spectra of $[Cr(bipy)_3]^{3+/2+/1+}$ in acetonitrile at room temperature

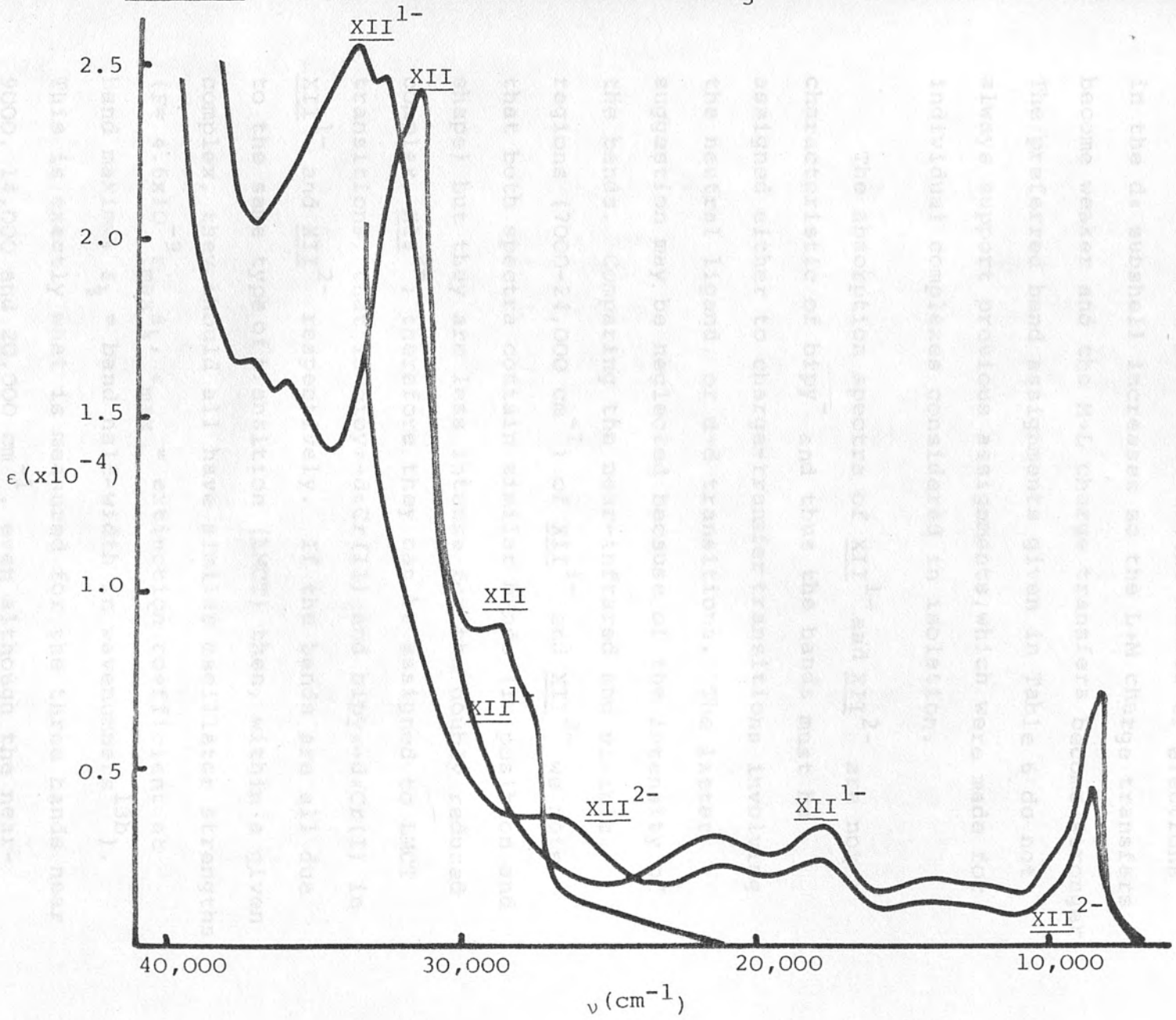

the same kind of energy and intensity arguments used in earlier chapters. Thus d→d transitions are weak ($\varepsilon \sim 500$), charge transfer transitions are intense ($1000 < \varepsilon < 15{,}000$) and intraligand transitions are very intense ($\varepsilon > 20{,}000$). Furthermore, we expect that as the number of electrons in the $d\pi$ subshell increases so the L→M charge transfers become weaker and the M→L charge transfers become stronger. The preferred band assignments given in Table 6 do not always support previous assignments, which were made for individual complexes considered in isolation.

The absorption spectra of $\underline{XII}^{1-}$ and $\underline{XII}^{2-}$ are not characteristic of $bipy^-$ and thus the bands must be assigned either to charge-transfer transitions involving the neutral ligand, or d→d transitions. The latter suggestion may be neglected because of the intensity of the bands. Comparing the near-infrared and visible regions (7000-24,000 cm^{-1}) of $\underline{XII}^{1-}$ and $\underline{XII}^{2-}$ we note that both spectra contain similar bands (in position and shape) but they are less intense for the doubly reduced complex, $\underline{XII}^{2-}$; therefore they can be assigned to LMCT transitions, that is bipyπ→dπCr(II) and bipyπ→dπCr(I) in $\underline{XII}^{1-}$ and $\underline{XII}^{2-}$ respectively. If the bands are all due to the same type of transition (LMCT) then, within a given complex, they should all have similar oscillator strengths ($F = 4.6 \times 10^{-9} \varepsilon_{max} \Delta_{\frac{1}{2}}$, ε_{max} = extinction coefficient at band maximum, $\Delta_{\frac{1}{2}}$ = band half-width in wavenumbers[13b]). This is exactly what is measured for the three bands near 9000, 14,000 and 20,000 cm^{-1}, even although the near-

TABLE 6: ABSORPTION BANDS IN $[Cr(bipy)_3]^{3+/2+/1+}$

Complex		Transitions $\nu(x10^{-3})cm^{-1}(\varepsilon x10^{-3})$				
		Intraligand $\pi\rightarrow\pi^*$bipy	M→LCT	L→MCT	L→MCT	L→MCT
$[Cr(III)(bipy^o)_3]^{3+}$	XII	31.7(24.23)				
$[Cr(II)(bipy^o)_3]^{2+}$	XII^{1-}	32.8(24.62) 33.8(25.47)	obscured	17.8(3.49) 21.6(3.10)	12.1(1.60) 13.8(1.79)	8.4(7.00) 9.6(2.75)
$[Cr(I)(bipy^o)_3]^{1+}$	XII^{2-}	obscured	26.7(3.69)	17.8(2.48) 21.0(2.37)	14.0(1.18)	8.4(4.46) 9.7(1.57)

TABLE 7: ABSORPTION BANDS IN $[Cr(bipy)_3]^{0/1-}$

Complex		Bands $\nu(x10^{-3})cm^{-1}(\varepsilon x10^{-3})$			
$[Cr(0)(bipy^o)_3]^{0}$	XII^{3-}	27.4(21.74)	22.0(10.50)sh	15.4(4.28)	10.0(2.82)
$[Cr(0)(bipy^o)_2(bipy^-)]^{1-}$	XII^{4-}	27.0(29.47)	21.6(13.43) 23.1(13.54)	15.3(3.28)	10.5(3.52) 11.4(3.24) 12.8(2.62)

infrared band has a deceptively greater extinction coefficient than the other two bands. Thus we are confident of our assignment of these bands to LMCT transitions.

The absorption spectrum of $\underline{XII}^{2-}$ contains another band, at 26,700 cm^{-1}, not observed in the spectrum of $\underline{XII}^{1-}$. We tentatively assigned it to a MLCT transfer (Cr(I)$d\pi \rightarrow \pi^*$bipy) which is masked by the intense $\pi\pi^*$ band of coordinated $bipy^{o}$ in the absorption spectrum of $\underline{XII}^{1-}$ because of its predicted low intensity (Cr(I) has five $d\pi$ electrons whereas Cr(II) has only four). The assignment can be partially substantiated by energy considerations for the Cr(I)-bipy chromophore; the highest filled bipy π orbital is 4400 cm^{-1} below the $d\pi$ orbitals (from lowest LMCT band subtracting electron pairing term) and the intraligand $\pi\pi^*$ transitions of $bipy^{o}$ will be at approximately 34,000 cm^{-1}; therefore we would predict that the lowest MLCT transition should be at roughly 29,000 cm^{-1}. Furthermore, the intensity of the band is in close agreement with the MLCT band of isoelectronic $[Ru(bipy)_3]^{3+}$.

The intraligand $\pi\pi^*$ transition of $bipy^{o}$ is clearly observed in the spectrum of $\underline{XII}^{1-}$ at 33,000 cm^{-1}; it shifts to higher energy as the charge on the metal ion decreases (Cr(III)$\rightarrow$Cr(II)). Unfortunately this band cannot be studied in the further reduced complexes because of the large amount of free bipy added to the solution

which is necessary to stabilise the lower-valent species.

The absorption spectrum of the neutral complex $[Cr(bipy)_3]^0$ is shown in Figure 5. The bands occur in the region expected for intraligand transitions of $bipy^-$ and they have indeed been so assigned by others[24,28]. However, the near-infrared and visible bands do not have the characteristic structures of intraligand transitions of $bipy^-$, and the bands are all too intense for such assignments. We favour a reassignment of the bands to MLCT transitions; that is, $Cr(O)d\pi \rightarrow \pi^*bipy$ (for further discussion vide infra). In summary, the electronic spectra extending from the near-infrared to the ultraviolet consistently indicate that the first three reductions of $[Cr(bipy)_3]^{3+}$ are strictly metal-based as suggested independently by the electrochemical data.

The ground-state complex $[Cr(bipy)_3]^{3+}$ is presumed to have D_3 symmetry and hence the $d\pi$ orbitals (degenerate in O_h) will split into a_1 and e components, with the former being at higher energy (Chapter 5). Accordingly, $[Cr(bipy)_3]^{3+/2+/1+/O}$ should have 3, 2, 1 and O unpaired electrons respectively[24] as depicted in Figure 6.

FIGURE 6: Electron distribution in tris-bipy complexes of chromium

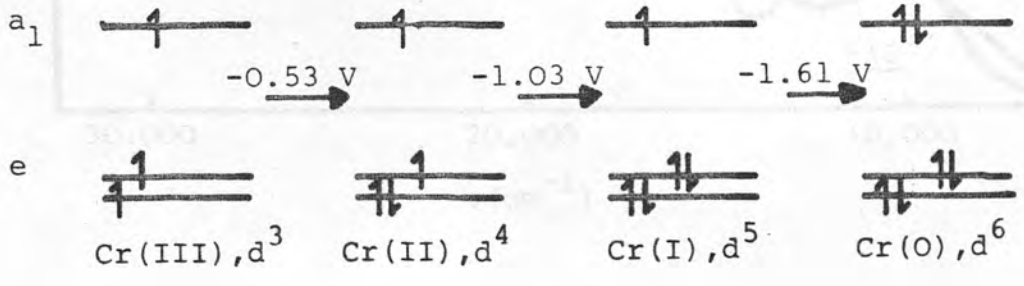

FIGURE 5: Absorption spectra of $[Cr(bipy)_3]^{0/-}$ in acetonitrile at room temperature

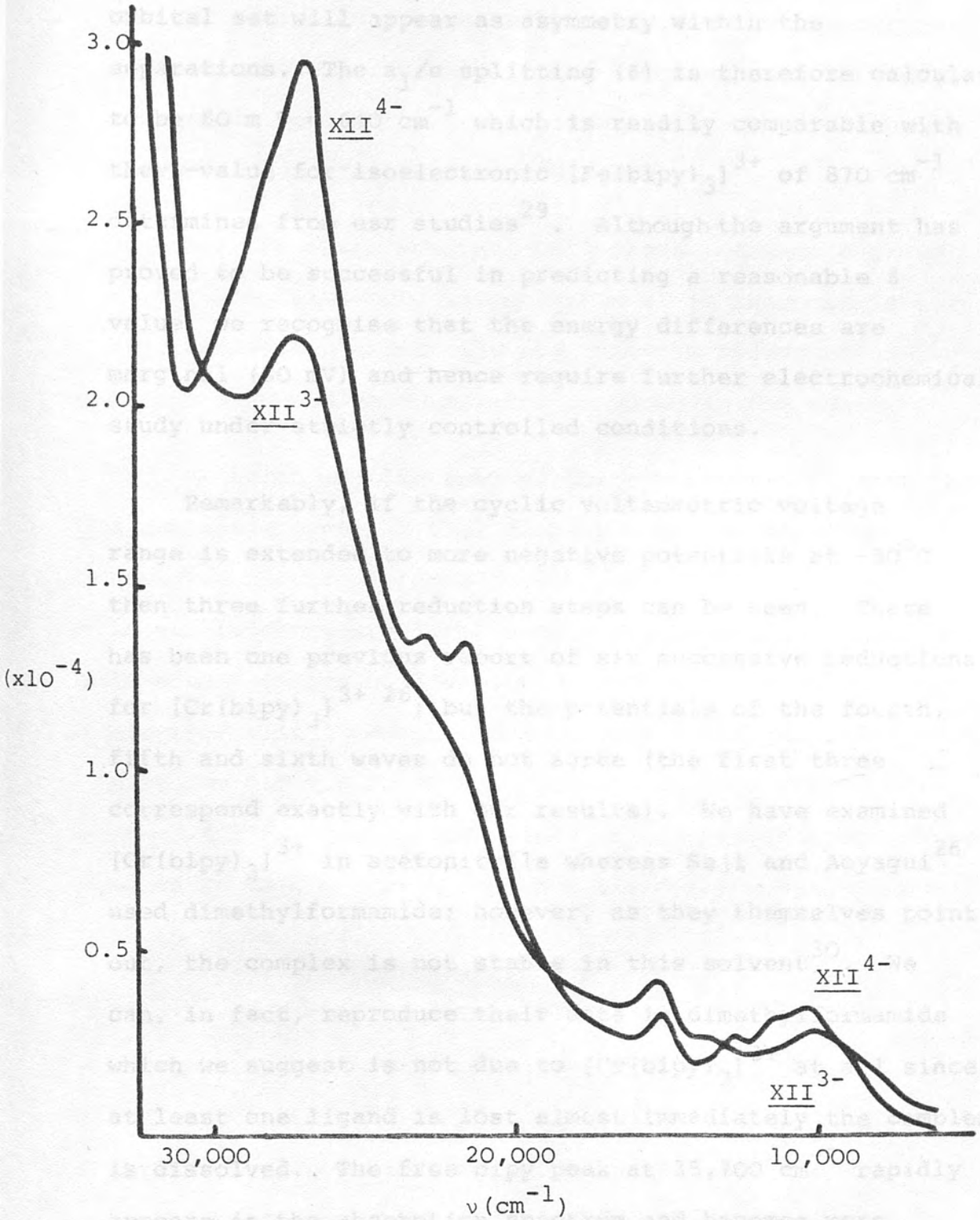

Straightforward considerations of electron correlations within a degenerate t_{2g} set establish that constant separations between the d^3/d^4, d^4/d^5 and d^5/d^6 couples are expected. Accordingly, minor splittings within this orbital set will appear as asymmetry within the separations. The a_1/e splitting (δ) is therefore calculated to be 80 m V = 640 cm^{-1} which is readily comparable with the δ-value for isoelectronic $[Fe(bipy)_3]^{3+}$ of 870 cm^{-1} determined from esr studies[29]. Although the argument has proved to be successful in predicting a reasonable δ value, we recognise that the energy differences are marginal (80 mV) and hence require further electrochemical study under strictly controlled conditions.

Remarkably, if the cyclic voltammetric voltage range is extended to more negative potentials at -30°C then three further reduction steps can be seen. There has been one previous report of six successive reductions for $[Cr(bipy)_3]^{3+}$ [26]; but the potentials of the fourth, fifth and sixth waves do not agree (the first three correspond exactly with our results). We have examined $[Cr(bipy)_3]^{3+}$ in acetonitrile whereas Saji and Aoyagui[26] used dimethylformamide; however, as they themselves point out, the complex is not stable in this solvent[30]. We can, in fact, reproduce their data in dimethylformamide which we suggest is not due to $[Cr(bipy)_3]^{3+}$ at all since at least one ligand is lost almost immediately the complex is dissolved. The free bipy peak at 35,700 cm^{-1} rapidly appears in the absorption spectrum and becomes more

intense as the dimethylformamide solution is allowed to stand. The absorption spectrum of XII in acetonitrile remains constant over twenty-four hours with no sign of release of bipy and thus further study of $[Cr(bipy)_3]^{3+}$ was restricted to acetonitrile solutions. Stirred cyclic voltammetric experiments at room temperature and $-30^{o}C$ show that the first four steps, at least, must all be considered as one-electron processes.

The potential separations between the second group of three voltammetric waves (Table 8) is characteristic of ligand-based reductions and thus the reduction products should be formulated as shown in the table.

Magnetic measurements of these complexes support the shown assignments as they display one, two and three unpaired electrons respectively[24]. The complex XII^{4-} is sufficiently stable at room temperature in the presence of a vast excess of free bipy to enable study by spectro-electrochemical methods. $[Cr(bipy)_3]^{1-}$ was generated in a platinum O.T.T.L.E. in acetonitrile at room temperature at -2.4 V *vs.* Ag/Ag^{+}; the resulting absorption spectrum is shown in Figure 5 with band positions and intensities given in Table 7.

As predicted from the electrochemical results, we observe in the absorption spectrum of XII^{4-} the characteristic band shapes of coordinated $bipy^{-}$, the threefold structure of a near-infrared band and the twofold structure of a visible band, and thus we must

TABLE 8: ELECTRODE POTENTIALS AND ELECTRONIC CONFIGURATIONS FOR $[Cr(bipy)_3]^{O}$ IN ACETONITRILE[a]

$$[Cr(O)(bipy^{O})_3]^{O} \underset{-e^-}{\overset{+e^-}{\rightleftharpoons}} [Cr(O)(bipy^{O})_2(bipy^{-})]^{1-};\ \underline{XII}^{3-/4-} \qquad E_o = -2.24\ V$$

$$[Cr(O)(bipy^{O})_2(bipy^{-})]^{1-} \underset{-e^-}{\overset{+e^-}{\rightleftharpoons}} [Cr(O)(bipy^{O})(bipy^{-})_2]^{2-};\ \underline{XII}^{4-/5-} \qquad E_o = -2.51\ V$$

$$[Cr(O)(bipy^{O})(bipy^{-})_2]^{2-} \underset{-e^-}{\overset{+e^-}{\rightleftharpoons}} [Cr(O)(bipy^{-})_3]^{3-};\ \underline{XII}^{5-/6-} \qquad E_o = -2.74\ V$$

[a] vs. Ag/Ag^{+}; calculated at room temperature values

consider XII^{4-} in terms of the trapped electron model. The positions and shapes of the bands A, B and D are as predicted for intraligand $\pi\pi^*$ transitions of bipy$^-$; however the bands are all too intense for such an assignment to be solely responsible for the bands. The absorption spectrum of the parent complex [Cr(O)(bipy^o)]^o has MLCT bands at similar frequencies and thus XII^{4-} which contains the same Cr(O)-bipy^o chromophore should also exhibit such transitions. However, band C which decreases in intensity from XII^{3-} to XII^{4-} is solely a MLCT band. Thus the position, intensity and shape of bands in the absorption spectrum of [Cr(bipy)$_3$]$^{1-}$ are all accounted for.

Strikingly therefore, although the electrochemistry of isovalent [Ir(bipy)$_3$]$^{3+}$ and [Cr(bipy)$_3$]$^{3+}$ have superficially similar cyclic voltammograms (two sets of three regularly spaced waves) we conclude that the reduction processes involved are very different. All six waves are ligand-based reductions in [Ir(bipy)$_3$]$^{3+}$ whereas in [Cr(bipy)$_3$]$^{3+}$ the first set are metal-based and the second set ligand-based reductions.

Tris-bipyridine vanadium(II)

Tris-bipyridine vanadium(II) [V(bipy)$_3$]$^{2+}$, XIII, is a dark blue complex which is isoelectronic with [Cr(bipy)$_3$]$^{3+}$. Accordingly we might ask if it would show similar electrochemical behaviour; that is, three metal-

based reductions leading to vanadium in a -1 oxidation state ($Vd\pi^6$) followed, in principle, by three ligand-based reductions.

The complex does indeed exhibit a rich electrochemistry as shown in Figure 7 and Table 9, with two groupings of three redox couples (sets A and B). The cyclic voltammogram also contains a wave due to the $bipy^{0/1-}$ couple at -2.47 V; however this wave almost completely disappears at $-35^{o}C$. That is, the complex, although indefinitely stable in acetonitrile at room temperature (no free bipy observed in ultraviolet spectrum), is prone to releasing bipy at negative potentials, but the dissociation can be inhibited at low temperatures.

The potentials of redox couples in set A are in agreement with previous reports[26,31], however those of set B are at variance. Once again the differences can be attributed to the solvents employed. Our results were obtained in acetonitrile because we found that the complex $[V(bipy)_3]^{2+}$ was liable to dissociate in dimethylformamide chosen in earlier studies.

If $[V(bipy)_3]^{2+}$ behaves electrochemically like isoelectronic $[Cr(bipy)_3]^{3+}$, then the redox processes of Set A will be metal-based and the reduction products should be formulated as follows: $[V(II)(bipy^{o})_3]^{2+}$, XIII, $[V(I)(bipy^{o})_3]^{1+}$, $XIII^{1-}$; $[V(0)(bipy^{o})_3]^{0}$, $XIII^{2-}$; and $[V(-1)(bipy^{o})_3]^{1-}$, $XIII^{3-}$. Confirmation that the first three reductions of XIII are indeed metal-based comes from

FIGURE 7: Cyclic voltammogram of $[V(bipy)_3]^{2+}$ in acetonitrile at room temperature.

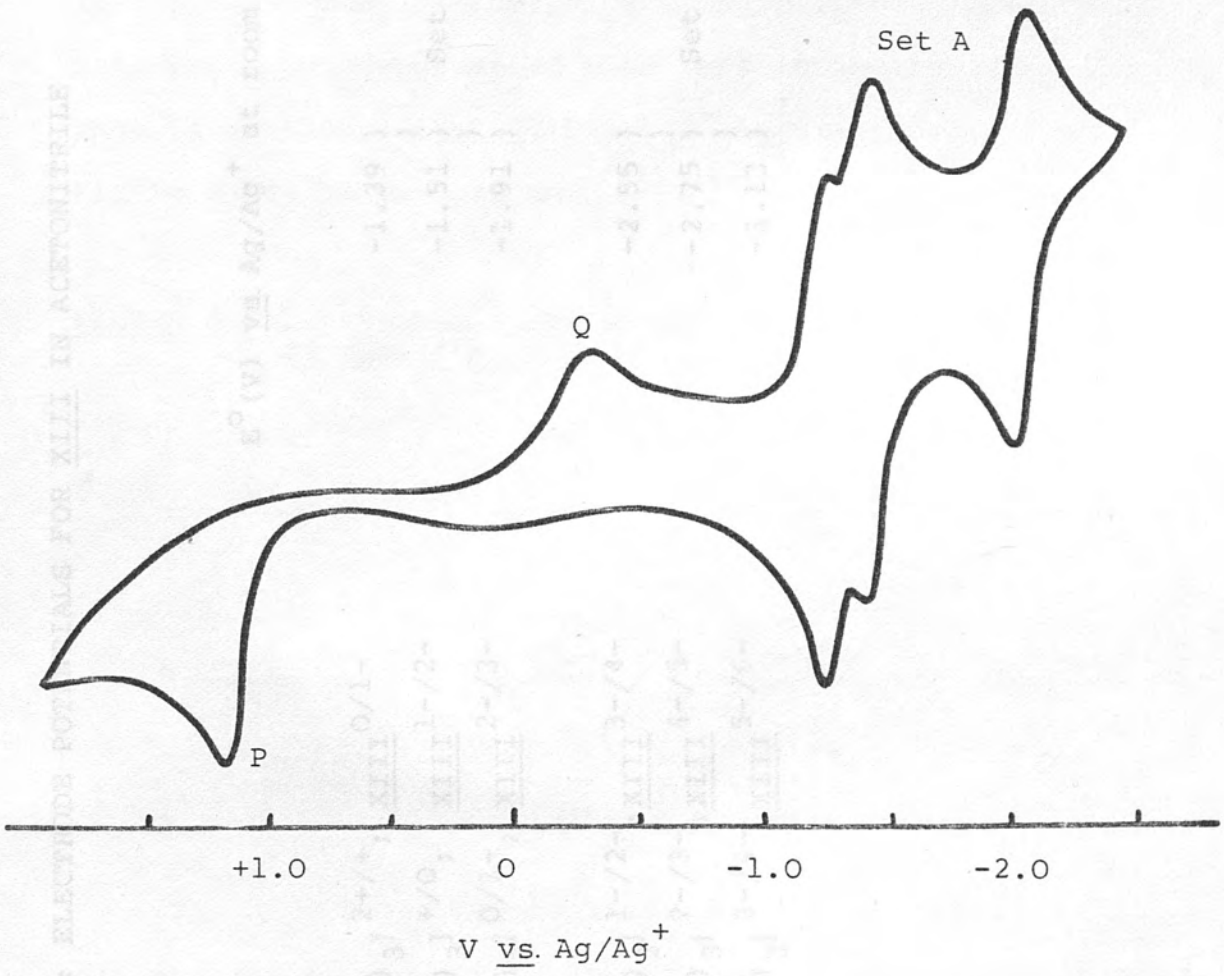

TABLE 9: ELECTRODE POTENTIALS FOR XIII IN ACETONITRILE

Couple	E^{o}(V) vs. Ag/Ag^{+} at room temperature	
$[V(bipy)_3]^{2+/+}$; $\underline{XIII}^{O/1-}$	-1.39	Set A
$[V(bipy)_3]^{+/O}$; $\underline{XIII}^{1-/2-}$	-1.51	
$[V(bipy)_3]^{O/1-}$; $\underline{XIII}^{2-/3-}$	-1.91	
$[V(bipy)_3]^{1-/2-}$; $\underline{XIII}^{3-/4-}$	-2.55	Set B
$[V(bipy)_3]^{2-/3-}$; $\underline{XIII}^{4-/5-}$	-2.75	
$[V(bipy)_3]^{3-/4-}$; $\underline{XIII}^{5-/6-}$	-3.13	

the absorption spectral studies of the reduced complexes in which there is no indication of coordinated bipy[28, 32, 33].

In $[Cr(bipy)_3]^{3+}$ the separations between the three metal-based reductions were both approximately 500 mV. In $[V(bipy)_3]^{2+}$ however the first two metal-based reductions are only 120 mV apart while the potential difference between the second and third metal-based reductions is 400 mV. It is documented that a solution of $[V(bipy)_3]^{+}$ does not exhibit esr signals while $[V(bipy)_3]^{2+}$ and $[V(bipy)_3]^{0}$ are known to be paramagnetic with three and one unpaired electrons respectively[31]. Thus if we accept that $[V(bipy)_3]^{+}$ is diamagnetic then Figure 8 may be constructed.

FIGURE 8: Electronic distribution in tris-bipy complexes of vanadium

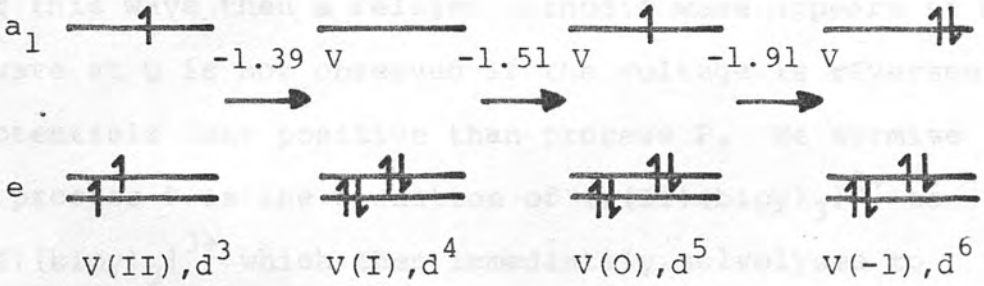

The only cogent explanation for the striking differences in the metal-based reduction potentials between $[Cr(bipy)_3]^{3+}$ and $[V(bipy)_3]^{2+}$ seems to be spin pairing of the d^4 metal ion in $[V(bipy)_3]^{+}$. It is curious and

unusual that the d^4 ion is spin paired but the d^3 ion is not. The spin pairing could, however, be associated with a favoured distortion of d^4. Unfortunately the magnetic data required to secure this are only available for solid state $[V(bipy)_3]^+$ whereas the solution data are most desirable.

The different behaviour noted for the metal-based reductions between isoelectronic $[V(bipy)_3]^{2+}$ and $[Cr(bipy)_3]^{3+}$ is probably a direct consequence of the less positive core charge in $[V(bipy)_3]^+$ compared to $[Cr(bipy)_3]^{2+}$, which will result in more diffuse $d\pi$ electrons (smaller mutual repulsion within the t_{2g} subshell) which could encourage the formulation of diamagnetic $[V(bipy)_3]^+$ and paramagnetic $[Cr(bipy)_3]^{2+}$.

Extending the cyclic voltammetric scan in an anodic direction reveals a completely irreversible one-electron oxidation process (P) - Figure 7. If the scan is reversed after this wave then a related cathodic wave appears at Q. The wave at Q is not observed if the voltage is reversed at potentials less positive than process P. We surmise that process P is the oxidation of $[V(II)(bipy)_3]^{2+}$ to $[V(III)(bipy)_3]^{3+}$ which then immediately solvolyses to give V(III) and bipy. Electrochemical investigation of a solution containing V(III) ions, but no bipy, shows a wave similar to Q at the same potential, but these speculations have not been pursued further.

The group of redox processes at more extreme negative

potentials (set B) are assigned to stepwise ligand-based reductions of $[V(-1)(bipy)_3]^{1-}$, from the characteristic spacings between the adjacent couples. The ligand-based reductions are only stable on a voltammetric timescale at low temperatures or if a large concentration of bipy is added to the solution. Under no experimental conditions available at present are they stable enough for spectro-electrochemical study.

Tris-bipyridine copper(II)

Tris-bipyridine copper(II) $[Cu(bipy)_3]^{2+}$, XIV, is a pale turquoise complex which is unlike all other familiar tris-bipy complexes as it does not belong to the D_3 symmetry class. The d^9 electronic configuration of the central ion is responsible for a Jahn-Teller splitting of the $d\sigma$ orbitals related to a tetragonal distortion of the complex with four shorter than usual metal-ligand bonds and two longer axial bonds[34].

Electrochemical study of the complex in either acetonitrile or dimethylformamide solutions at $-40^{o}C$ gives four reduction steps as shown in Table 10.

The second, third and fourth redox couples are all reversible but can only be observed at low temperatures. Even then, the fourth wave, corresponding to the $XIV^{3-/4-}$, couple has a negative potential shoulder attributable to the unbound $bipy^{0/1-}$ couple; that is, the Cu system is

TABLE 10: ELECTRODE POTENTIALS FOR $[Cu(bipy)_3]^{2+}$

$$[Cu(bipy)_3]^{2+} \xrightarrow{-0.21^a} [Cu(bipy)_3]^{+} \xrightarrow{-1.98} [Cu(bipy)_3]^{0} \xrightarrow{-2.12} [Cu(bipy)_3]^{1-} \xrightarrow{-2.29} [Cu(bipy)_3]^{2-}$$

XIV $\quad$ XIV^{1-} $\quad$ XIV^{2-} $\quad$ XIV^{3-} $\quad$ XIV^{4-}

$^a E_{\frac{1}{2}}$ vs. Ag/Ag^+; calculated room temperature values.

ultimately unstable to electrochemical reduction even at low temperature, releasing bipy. Interestingly, in this case the potential differences between the second, third and fourth couples are characteristic of ligand-based reductions and hence are so assigned.

The first redox process also corresponds to a one-electron step (by comparison of wave heights). The shape of the cyclic voltammetric wave of $\underline{XIV}^{0/1-}$ is, however, characteristic of a slow charge transfer step; with a relatively large potential separation between forward and return waves which increases with increasing scan rate (and as the temperature decreases). The ligand-based processes have already been located and hence we infer that the $\underline{XIV}^{0/-}$ couple involves a metal-based process. Reduction of the metal centre from Cu(II) to Cu(I) will probably return the complex to a regular D_3 symmetry as there is no favoured distortion of a d^{10} system. This molecular rearrangement is therefore responsible for the sluggish charge transfer profile of the first cyclic voltammetric wave.

Thus the electrochemical behaviour of $[Cu(bipy)_3]^{2+}$ can be satisfactorily accounted for by the following scheme:

$$[Cu(II)(bipy^{o})_3]^{2+} \xrightarrow{+e^-} [Cu(I)(bipy^{o})_3]^{+} \underset{-e^-}{\overset{+e^-}{\rightleftharpoons}} [Cu(I)(bipy^{o})_2(bipy^{-})]^{o} \underset{-e^-}{\overset{+e^-}{\rightleftharpoons}} [Cu(I)(bipy^{o})(bipy^{-})_2]^{1-} \underset{-e^-}{\overset{+e^-}{\rightleftharpoons}} [Cu(I)(bipy^{-})_3]^{2-}$$

Tris-bipyridine nickel(II)

Tris-bipyridine nickel(II) $[Ni(bipy)_3]^{2+}$, XV, is a pale pink d^8 complex. Magnetic measurements indicate that the metal centre has two unpaired electrons and hence the electronic configuration of the nickel(II) ion is $d\pi^6 d\sigma^2$. The $d\sigma$ orbitals must be degenerate in XV because the complex has strict D_3 symmetry[35].

Electrochemical studies of $[Ni(bipy)_3]^{2+}$ were first undertaken in acetonitrile (Figure 9), however the cyclic voltammograms did not correspond with previous reports[36,37] as the first cathodic wave was completely irreversible (no return wave) and the second wave was too close to the first. The addition of excess bipy or decreasing the temperature did not alter this behaviour; however if the solvent was replaced by propylene carbonate, dimethyl-sulphoxide or dimethylformamide, then the cyclic voltammograms were in perfect accord with the published data. Margel and co-workers had reported that the electrochemical behaviour of $[Co(bipy)_3]^{3+}$ was compromised by acrylonitrile[38], which is a major impurity in acetonitrile. When acrylonitrile was deliberately added to a solution of $[Ni(bipy)_3]^{2+}$ in dimethylformamide the cyclic voltammogram reverted to that observed previously in acetonitrile. Ultimately the electrochemical results were found to be independent of solvent after strict purification of the acetonitrile. We conclude that one bipy ligand of $[Ni(bipy)_3]^{2+}$ is efficiently replaced by acrylonitrile and the observed electrochemistry

FIGURE 9: Cyclic voltammograms of $[Ni(bipy)_3]^{2+}$ in acetonitrile at room temperature

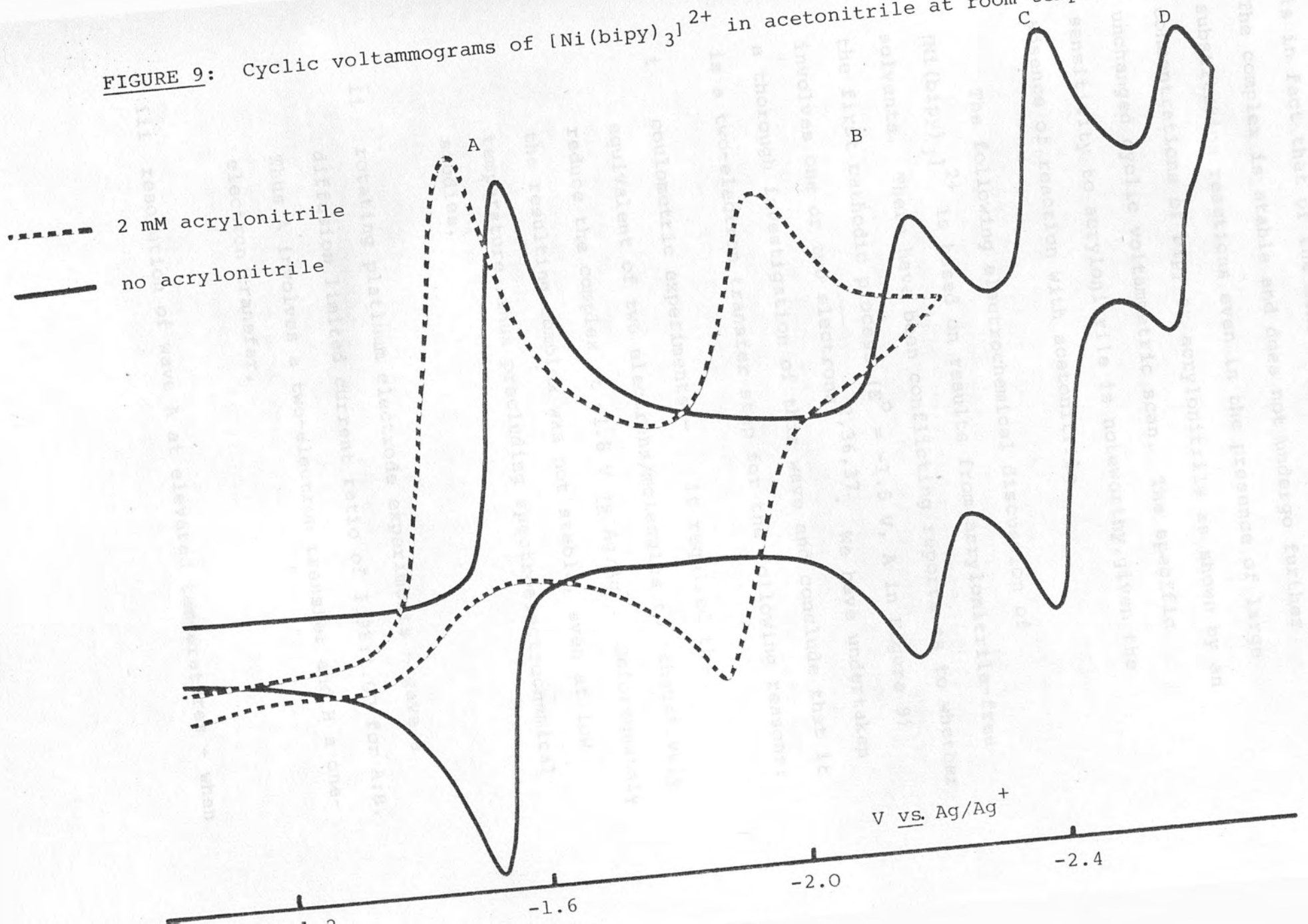

is in fact that of the mixed complex, $[Ni(bipy)_2(CH_2CHCN)]^{2+}$. The complex is stable and does not undergo further substitution reactions even in the presence of large concentrations of bipy or acrylonitrile as shown by an unchanged cyclic voltammetric scan. The specific sensitivity to acrylonitrile is noteworthy, given the absence of reaction with acetonitrile.

The following electrochemical discussion of $[Ni(bipy)_3]^{2+}$ is based on results from acrylonitrile-free solvents. There have been conflicting reports as to whether the first cathodic process (E^o = -1.5 V, A in Figure 9) involves one or two electrons[2,36,37]. We have undertaken a thorough investigation of this wave and conclude that it is a two-electron transfer step for the following reasons:

i coulometric experiments - it required the equivalent of two electrons/molecules to exhaustively reduce the complex at -1.8 V vs. Ag/Ag^+. Unfortunately the resulting complex was not stable, even at low temperature, thus precluding spectroelectrochemical studies.

ii rotating platinum electrode experiments - gave a diffusion limited current ratio of 1.98:1.00 for A:B. Thus A involves a two-electron transfer and B a one-electron transfer.

iii resolution of wave A at elevated temperatures - when

wave A was examined by cyclic voltammetry as a function of temperature in propylene carbonate or dimethylsulphoxide it was observed to split into two one-electron steps at elevated temperature (Figure 10). The half wave potentials at $+60^{o}C$ for the two waves are -1.39 V and -1.52 V. As the solution cools so the potentials of the two waves move closer together. At $+40^{o}C$ wave A is very broad and the two components are no longer resolved; at room temperature only one apparently reversible wave can be observed, and at $-40^{o}C$ the forward and reverse peaks of the wave are widely separated indicating perhaps a slow charge transfer reaction. The reproducible splitting of this wave would be hard to account for if wave A were a one-electron transfer process.

The three further reversible waves B, C and D have the characteristic potential separations of ligand-based reductions and indeed the esr data for $[Ni(bipy)_3]^{1-}$ is indicative of a ligand-based reduction[37]. The anomalous height of wave C at room temperature is due to the coincident reductions of $[Ni(bipy)_3]^{-}$ and $bipy^{o}$, free bipy being present because the reduced complexes are not indefinitely stable. At low temperatures ($-40^{o}C$) the height of wave C approaches that of B as does wave D; that is, the complex has a smaller tendency to dissociate at low temperatures. Excess ligand has little effect on waves A and B; however C and D are completely masked.

FIGURE 10: Cyclic voltammograms of $Ni(bipy)_3^{2+}$ at different temperatures in propylene carbonate

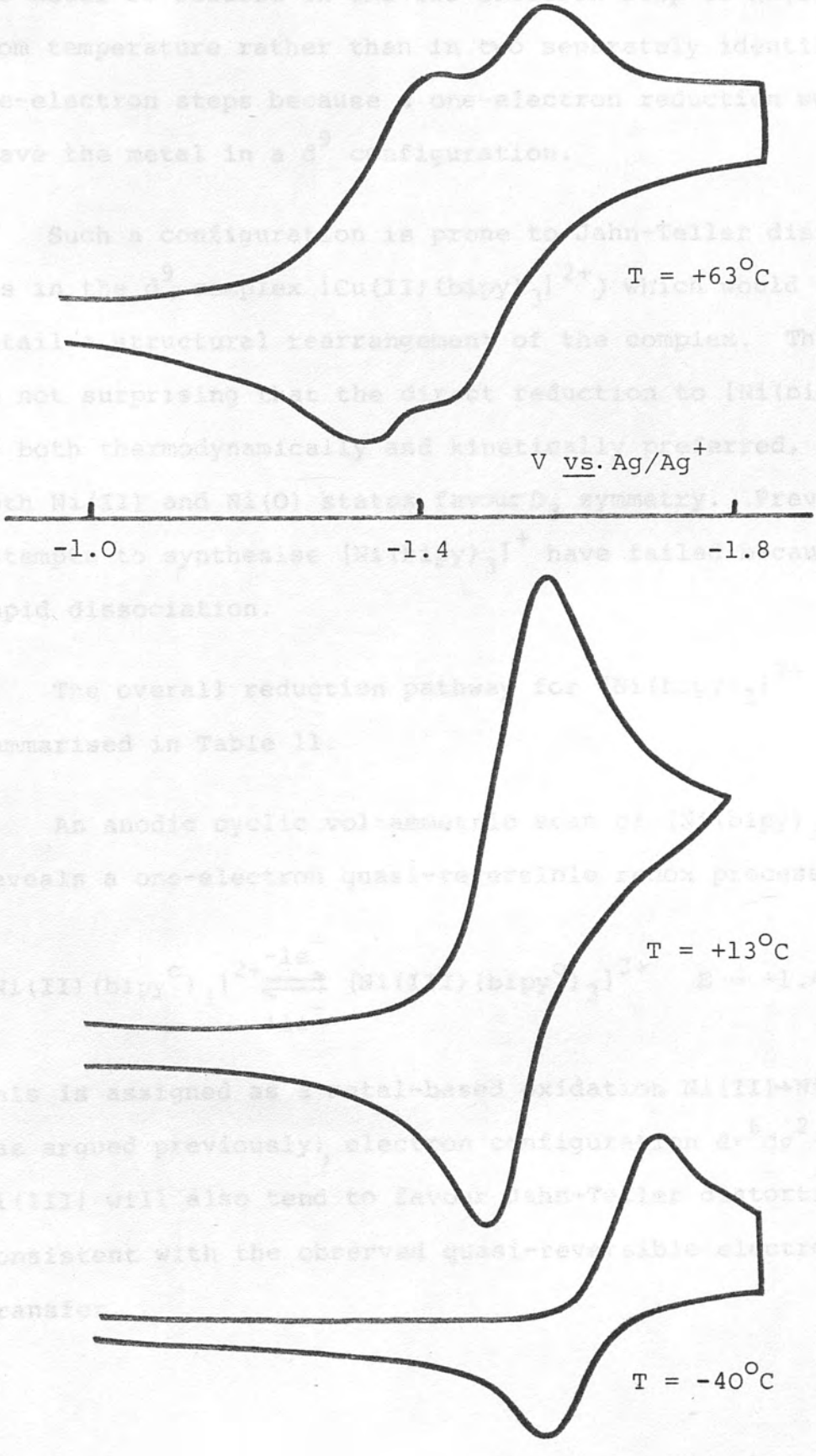

Since waves B, C and D have been assigned as ligand-based processes then A must be metal-based; Ni(II) $\underset{-2e^-}{\overset{+2e^-}{\rightleftharpoons}}$ Ni(O). The metal is reduced in one two-electron step to Ni(O) at room temperature rather than in two separately identifiable one-electron steps because a one-electron reduction would leave the metal in a d^9 configuration.

Such a configuration is prone to Jahn-Teller distortion (as in the d^9 complex $[Cu(II)(bipy)_3]^{2+}$) which would then entail a structural rearrangement of the complex. Thus it is not surprising that the direct reduction to $[Ni(bipy)_3]^{O}$ is both thermodynamically and kinetically preferred, since both Ni(II) and Ni(O) states favour D_3 symmetry. Previous attempts to synthesise $[Ni(bipy)_3]^{+}$ have failed because of rapid dissociation.

The overall reduction pathway for $[Ni(bipy)_3]^{2+}$ is summarised in Table 11.

An anodic cyclic voltammetric scan of $[Ni(bipy)_3]^{2+}$ reveals a one-electron quasi-reversible redox process:

$$[Ni(II)(bipy^{O})_3]^{2+} \underset{+1e^-}{\overset{-1e^-}{\rightleftharpoons}} [Ni(III)(bipy^{O})_3]^{3+} \qquad E = +1.46\ V$$

This is assigned as a metal-based oxidation Ni(II)→Ni(III) (as argued previously), electron configuration $d\pi^6 d\sigma^2 \rightarrow d\pi^6 d\sigma^1$. Ni(III) will also tend to favour Jahn-Teller distortions consistent with the observed quasi-reversible electron transfer.

TABLE 11: CATHODIC REDOX PROCESSES OF $[Ni(bipy)_3]^{2+}$ [a]

$$[Ni(II)(bipy^{o})_3]^{2+} \underset{-2e^-}{\overset{+2e^-}{\rightleftharpoons}} [Ni(O)(bipy^{o})_3]^{o} \qquad E = -1.54\ V$$

$$[Ni(O)(bipy^{o})_3]^{o} \underset{-1e^-}{\overset{+1e^-}{\rightleftharpoons}} [Ni(O)(bipy^{o})_2(bipy^{-})]^{1-} \qquad E = -2.23\ V$$

$$[Ni(O)(bipy^{o})_2(bipy^{-})]^{1-} \underset{-1e^-}{\overset{+1e^-}{\rightleftharpoons}} [Ni(O)(bipy^{o})(bipy^{-})_2]^{2-} \qquad E = -2.47\ V$$

$$[Ni(O)(bipy^{o})(bipy^{-})_2]^{2-} \underset{-1e^-}{\overset{+1e^-}{\rightleftharpoons}} [Ni(O)(bipy^{-})_3]^{3-} \qquad E = -2.65\ V$$

[a] $E(V)$ *vs.* Ag/Ag^+ at room temperature

Tris-bipyridine cobalt(II)

Tris-bipyridine cobalt(II) $[Co(bipy)_3]^{2+}$, XVI, is a tan d^7 ($d\pi^5 d\sigma^2$) complex. The electronic configuration is deduced from magnetic measurements which show three unpaired electrons[2]. The electrochemistry of $[Co(bipy)_3]^{2+}$ parallels closely that of $[Ni(bipy)_3]^{2+}$, for example small concentrations of acrylonitrile are found to drastically change the cyclic voltammetric scans[38,40].

The electrochemical behaviour of $[Co(bipy)_3]^{2+}$ in acrylonitrile-free acetonitrile is presented in Figure 11 and Table 12. Data for waves A, B and C agree with published reports[4,5,40]. However, in addition to these we observe three further waves, and free bipy (near -2.47 V), due to complex dissociation at negative potentials. Waves D, E and F are characteristic of successive ligand-based one-electron reductions so that the oxidation A and the reductions, B and C, are assigned to the metal centre.

Stirred linear voltammograms confirm that A and B are one-electron transfer steps while C is a two-electron step. $[Co(bipy)_3]^{+}$ is isoelectronic with $[Ni(bipy)_3]^{2+}$ and hence it is consistent that the reduction process is also a two-electron step. However the electrochemical behaviour differs for the isoelectronic $[Co(bipy)_3]^{2+/+}$ and $[Ni(bipy)_3]^{3+/2+}$, the former being reversible while the latter is only quasi-reversible. The explanation should be in the electronic configuration of the central metal

FIGURE 11: Cyclic voltammogram of $[Co(bipy)_3]^{2+}$ in acetonitrile at room temperature

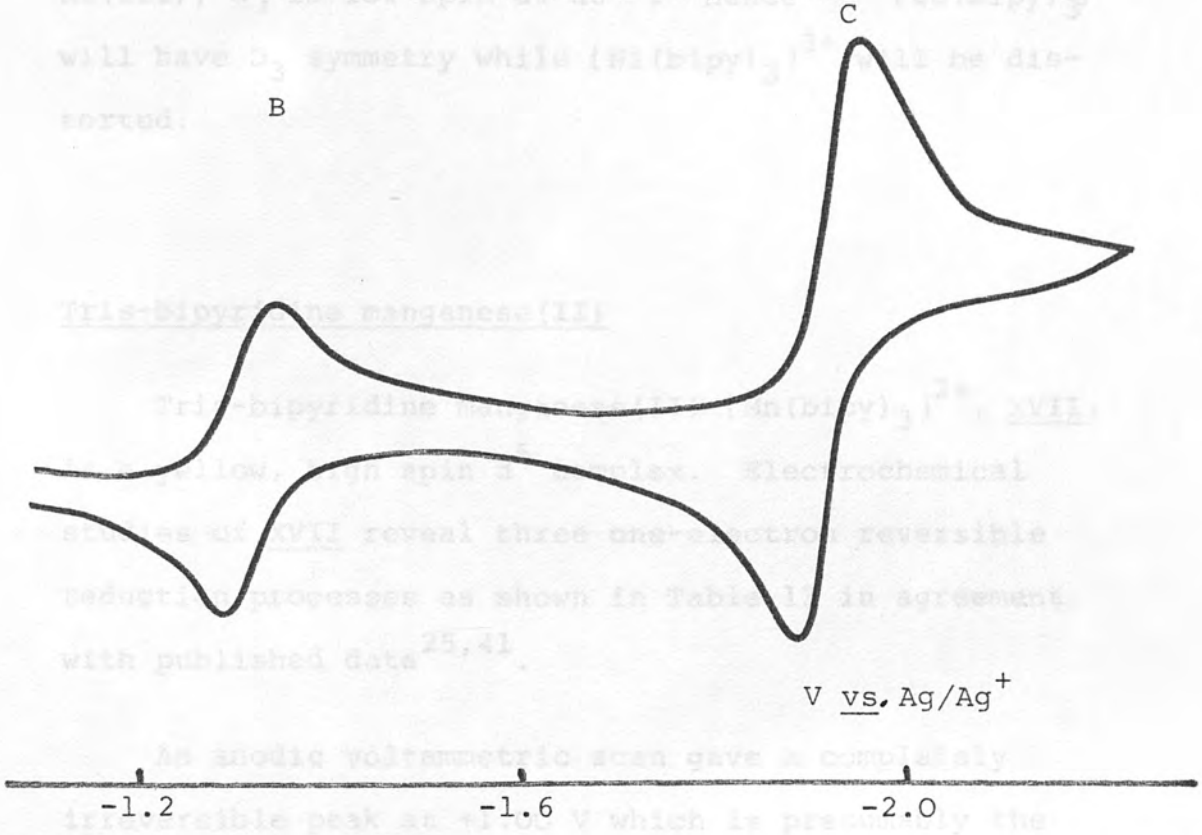

TABLE 12: REDOX COUPLES OF $[Co(bipy)_3]^{2+}$

A $[Co(II)(bipy^{o})_3]^{2+} \underset{+e^-}{\overset{-e^-}{\rightleftharpoons}} [Co(II)(bipy^{o})_3]^{3+}$ E = 0.00 V[a]

B $[Co(II)(bipy^{o})_3]^{2+} \underset{-e^-}{\overset{+e^-}{\rightleftharpoons}} [Co(I)(bipy^{o})_3]^{1+}$ E = -1.275 V

C $[Co(I)(bipy^{o})_3]^{1+} \underset{-2e^-}{\overset{+2e^-}{\rightleftharpoons}} [Co(I-)(bipy^{o})_3]^{1-}$ E = -1.89 V

D $[Co(I-)(bipy^{o})_3]^{1-} \underset{-e^-}{\overset{+e^-}{\rightleftharpoons}} [Co(I-)(bipy^{o})_2(bipy^{-})]^{2-}$ E = -2.72 V

E $[Co(I-)(bipy^{o})_2(bipy^{-})]^{2-} \underset{-e^-}{\overset{+e^-}{\rightleftharpoons}} [Co(I-)(bipy^{o})(bipy^{-})]^{3-}$ E = -2.92 V

F $[Co(I-)(bipy^{o})(bipy^{-})]^{3-} \underset{-e^-}{\overset{+e^-}{\rightleftharpoons}} [Co(I-)(bipy^{-})_3]^{4-}$ E = -3.21 V

[a] vs. Ag/Ag^+; A,B,C and D directly measured at room temperature; E and F measured at -40°C then corrected for room temperature values.

ion; Co(II), d^7, has the configuration $d\pi^5, d\sigma^2$ whereas Ni(III), d^7, is low spin $d\pi^6 d\sigma^1$[1,2]. Hence $[Co(bipy)_3]^{2+}$ will have D_3 symmetry while $[Ni(bipy)_3]^{3+}$ will be distorted.

Tris-bipyridine manganese(II)

Tris-bipyridine manganese(II) $[Mn(bipy)_3]^{2+}$, XVII, is a yellow, high spin d^5 complex. Electrochemical studies of XVII reveal three one-electron reversible reduction processes as shown in Table 13 in agreement with published data[25,41].

An anodic voltammetric scan gave a completely irreversible peak at +1.00 V which is presumably the oxidation of the metal centre, $Mn(II) \rightarrow Mn(III) + e^-$. This behaviour was previously noted by Morrison and co-workers[42].

The complex was also studied in dimethylformamide and dimethylsulphoxide, but it was found to be unstable in both, releasing bipy. This was confirmed by studying the absorption spectrum of XVII in these solvents in which only free bipy peaks could be distinguished and hence further study in these solvents was not pursued.

Returning to Table 13, the redox couple $XVII^{1-/2-}$ was anomalously intense (independent of temperature); however addition of excess ligand meant that all three

TABLE 13: ELECTRODE POTENTIALS FOR XVII IN ACETONITRILE[a]

$$[Mn(bipy)_3]^{2+} \xrightarrow{-1.67} [Mn(bipy)_3]^{1+} \xrightarrow{-1.855} [Mn(bipy)_3]^{0} \xrightarrow{-2.045} [Mn(bipy)_3]^{1-}$$

[a] E_o (V) vs. Ag/Ag^+; room temperature

waves were equally well defined. Under these conditions, the overall cyclic voltammogram closely parallels that of $[Fe(bipy)_3]^{2+}$, despite the very different central ion d-arrangement. (However both high spin Mn^{2+} and low spin Fe^{2+} ions are spherically symmetric). The waves are therefore assigned to ligand-based processes and the complexes should be formulated accordingly. The absorption spectrum of XVII^{2-} is dominated by bipy^{-} transitions[28], in keeping with the charge-localised model.

The very similar cathodic electrochemical behaviour of $[Fe(bipy)_3]^{2+}$ and $[Mn(bipy)_3]^{2+}$ shows that the energies of the ligand π,π^* orbitals are not much perturbed by central ion electronic structure; that is, the potentials of the ligand-based reductions are primarily dependent on the charge of the metal ion, see next section.

Electrode potential/central valency correlations

All of the tris-bipy complexes studied in the thesis exhibited a rich redox chemistry. The cathodic processes could be divided into two distinct types: (a) metal-based reductions; and (b) ligand-based reductions (Table 14). The ligand-based reductions were invariably identified by their characteristic cyclic voltammograms, which contain three closely spaced reversible one-electron steps. The spacings between the waves are approximately constant at 200 mV (Table 14). This pattern can often be observed only at low temperatures and/or using a fast scanning

technique because the reduced complexes are not stable, releasing bipy in many cases. All other cathodic steps (prior to the recognisable coordinated $bipy^{0/-}$ reductions) have been assumed so far to involve metal-based redox processes, even when extremely low oxidation states are involved.

A definite trend can be discerned from Table 14 in the electrode potential behaviour of the tris-bipy complexes; namely as the formal charge on the central metal ion decreases the potentials of the ligand-based reductions become more negative and, furthermore, complexes with the same central metal charge (Q_m in Table 14) have the same ligand-based reduction potentials, most often within a few mV.

We are now in a position to correlate the character of the redox-active orbitals in tris-bipy complexes with the electronic configuration of the central metal ion. We now formulate a general rule, as follows. Reduction of coordinated bipyridyl is only observed on metal centres which have complete d orbital shells or subshells; that is ligand-based reductions only occur on a metal centre with an electronic configuration $d^6(d\pi^6)$ or d^{10} $(d\pi^6 d\sigma^4)$, for example in $[V(II)(bipy)_3]^{2+}$ and $[Ni(bipy)_3]^{2+}$.

TABLE 14: REDUCTION POTENTIALS FOR $[M(bipy)_3]^{z+}$ [a] COMPLEXES AT ROOM TEMPERATURE

Metal	Metal-based reductions			Q_m [b]	Ligand-based reductions			Separations of ligand-based reductions	
					X	Y	Z	Y-X	Z-Y
Ru(II)				+2	-1.66	-1.83	-2.05	0.17	0.22
Fe(II)				+2	-1.64	-1.825	-2.105	0.185	0.28
Os(II)				+2	-1.55	-1.75	-2.06	0.20	0.31
Zn(II)				+2	-1.69	-1.83	-2.00	0.14	0.17
Ir(III)				+3	-1.26	-1.39	-1.54	0.13	0.15
In(III)				+3	-1.28	-1.46	-1.675	0.18	0.215
Cr(III)	-0.53	-1.03	-1.61	0	-2.24	-2.51	-2.74	0.27	0.23
V(II)	-1.39	-1.51	-1.91	-1	-2.55	-2.75	-3.13	0.20	0.38
Cu(II)		-0.21		+1	-1.98	-2.12	-2.29	0.14	0.17
Ni(II)		-1.54		0	-2.23	-2.47	-2.65	0.24	0.18
Co(II)	-1.275	-1.89		-1	-2.72	-2.92	-3.21	0.20	0.29
Mn(II)				+2	-1.67	-1.855	-2.045	0.185	0.19

[a] z = overall charge on complex

[b] Q_m = charge on metal ion after metal-based reductions

FIGURE 12: Electrode potential/central valency correlation for bipy complexes

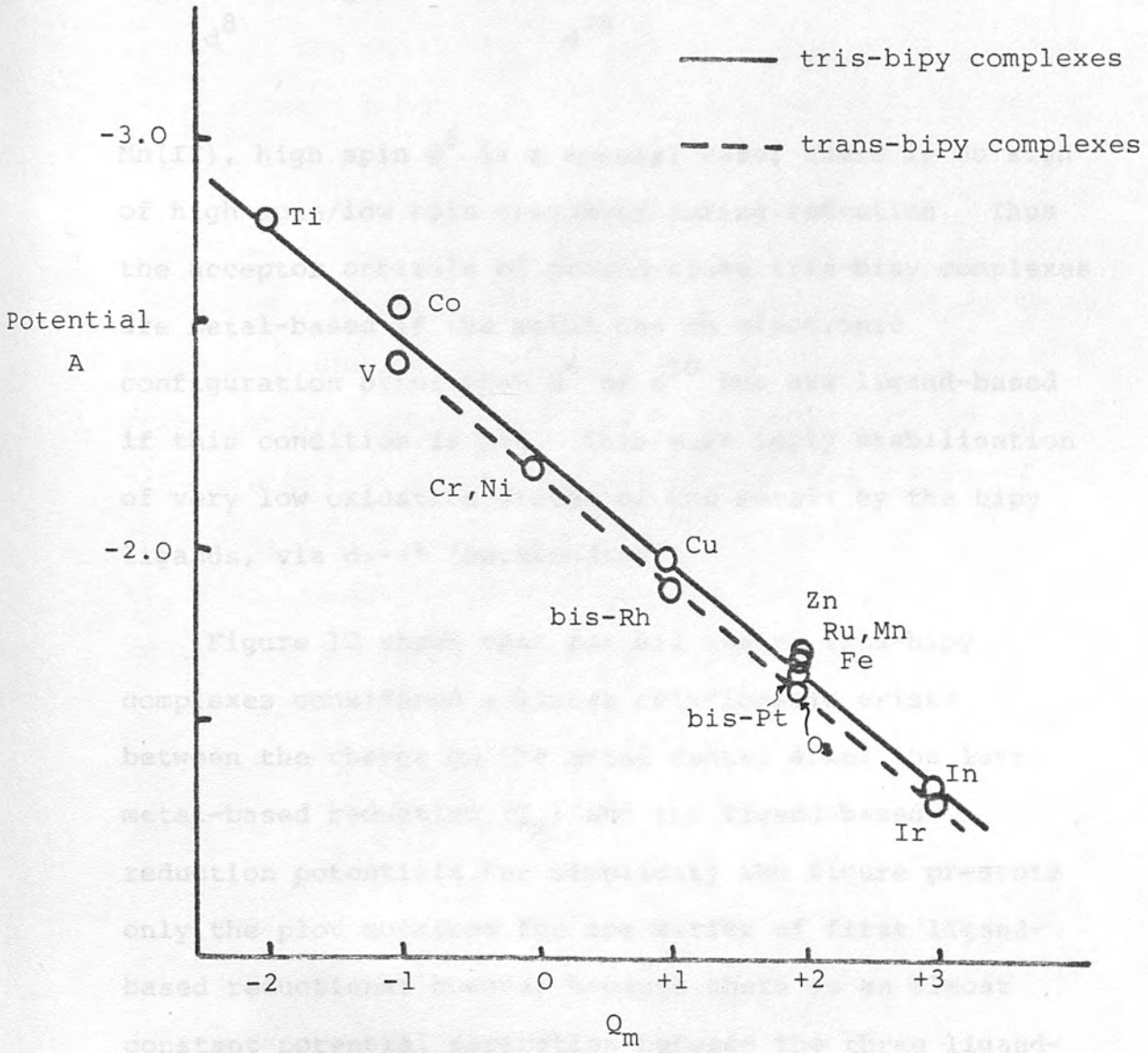

Potential A = potential of first ligand-based reduction, V vs. Ag/Ag^+

Q_m = charge on metal ion after metal-based reductions

$[V(II)bipy)_3]^{2+}$ $\rightarrow [V(I)bipy)_3]^{+}$ $\rightarrow [V(O)(bipy)_3]^{O}$ $\rightarrow$
d^3 d^4 d^5

$[V(1-)(bipy)_3]^{1-}$ $\rightarrow$ ligand based reductions
d^6

$[Ni(II)(bipy)_3]^{2+}$ $\rightarrow$ $[Ni(O)(bipy)_3]^{O}$ $\rightarrow$ ligand based reductions
d^8 d^{10}

Mn(II), high spin d^5 is a special case; there is no sign of high spin/low spin crossover during reduction. Thus the acceptor orbitals of ground-state tris-bipy complexes are metal-based if the metal has an electronic configuration other than d^6 or d^{10} but are ligand-based if this condition is met. This must imply stabilisation of very low oxidation states of the metals by the bipy ligands, via $d\pi \rightarrow \pi^*$ 'backbonding'.

Figure 12 shows that for all twelve tris-bipy complexes considered a linear relationship exists between the charge on the metal centre after the last metal-based reduction (Q_m) and the ligand-based reduction potentials.For simplicity the figure presents only the plot obtained for the series of first ligand-based reductions; however because there is an almost constant potential separation between the three ligand-based reductions, the linear correlation is actually independently established by three parallel lines of best fit, corresponding to the successive ligand reductions. Such a linear relationship has also been observed recently for the restricted set of $d\pi^6$-only tris-bipy

complexes[43]. The absorption spectra of tris-bipy complexes of lower-valent metals (for example $[V(O)(bipy_3)]^O$ and $[Cr(O)(bipy)_3]^O$) gave no indication of $bipy^-$. Thus we can deduce that although the low-lying π^* orbitals on the ligand are important in stabilising the low oxidation states of the metal, the primary influence on the ligand-based reduction potentials is the electrostatic effect of the charge on the central metal ion.

The electrochemical behaviour of other tris-bipy complexes can now be identified and explained using these results; ligand-based reductions only occur on d^6 or d^{10} metal centres and the appropriate potential of the first ligand-based reduction is determinable from Figure 12. Consider, for example, the complex $[Ti(O)(bipy^O)_3]^O$. The metal centre has the electronic configuration d^4; thus we predict two metal-based reductions, taking the metal to the d^6 configuration and a central metal charge of -2, followed by a first ligand-based reduction at -2.96 V *vs.* Ag/Ag^+.

The potentials of the metal-based reductions cannot be predicted although their separation is expected to be approximately 500 mV (see discussion on $[Cr(bipy)_3]$). Saji and Aoyagui[26] quote the potentials for three one-electron reductions of $[Ti(bipy)_3]^O$. The separation between the first two cathodic redox processes is 540 mV and the third reduction potential is at -2.98 V *vs* Ag/Ag^+. Therefore the predicted electrochemical behaviour has been

verified by experimental results.

Complexes which contain less than three bipy ligands (the other spectator ligands being non-interfering), but with bipy in a geometrically undistorted configuration as in, for example, cis-$[Ru(bipy)_2py_2]^{2+}$ have the same ligand-based reduction potentials as tris-complexes with the same central metal charge. Therefore the linear relationship expressed in Figure 12 does not apply solely to tris-bipy complexes. However trans-$[Ru(bipy)_2py_2]^{2+}$, in which bipy is in a distorted geometric configuration, has easier ligand-based reductions. Square planar tris-bipy complexes having a similar mutual arrangement of ligands might also be expected to show such behaviour. Indeed $[Pt(II)(bipy)_2]^{2+}$ has two reversible one-electron redox processes at -1.60 V and -1.74 V vs. Ag/Ag^+ and $[Rh(I)(bipy)_2]^+$ has two reversible one-electron redox processes of -1.89 V and -2.10 V vs. Ag/Ag^+ [44]. Plotting these results on Figure 12 gives an almost parallel straight line to the one appropriate to the tris-bipy complexes displaced by approximately 70 mV.

The straight line relationship developed above has been used in previous chapters in constructing comparative molecular orbital energy diagrams when considering the effect of the central metal charge on the energy of the π^* bipy orbitals.

Finally, consider the following redox process:

$$*[Ru(III)(bipy^{o})_2(bipy^{-1})]^{2+} \underset{+e^-}{\overset{-e^-}{\rightleftharpoons}} [Ru(III)(bipy^{o})_3]^{3+}.$$

Figure 12 would predict the electrode potential for such a process to be -1.26 V vs. Ag/Ag^+ which is in excellent agreement with the experimentally determined value of -1.22 V vs. Ag/Ag^+ [45]. Thus the present correlations, remarkably enough, are also applicable to deduction of excited state redox behaviour.

Experimental

All complexes were prepared by standard literature methods; $[Fe(bipy)_3]^{2+}$ [46], $[Os(bipy)_3]^{2+}$ [47], $[Zn(bipy)_3]^{2+}$ [48], $[In(bipy)_3]^{3+}$ [49], $[Cr(bipy)_3]^{3+}$ [50], $[V(bipy)_3]^{2+}$ [51], $[Cu(bipy)_3]^{2+}$ [34], $[Ni(bipy)_3]^{2+}$ [52], $[Co(bipy)_3]^{2+}$ [46], $[Mn(bipy)_3]^{2+}$ [25]. Experimental procedures are adequately described in preceding chapters.

REFERENCES

1. A.A. Vlcek; Coord. Chem., 21, 99 (1980).

2. R. Prasad and D.B. Scaife; J. Electroanal. Chem., 84, 373(1977).

3. N. Tanaka, T. Ogata and S. Niizuma; Bull Chem. Soc. Jpn., 46, 3299 (1973).

4. T. Saji and S. Aoyagui; J. Electroanal. Chem.,58, 401 (1975).

5. T. Saji and S. Aoyagui; J. Electroanal. Chem.,60, 1 (1975).

6. J.M. Rao, M.C. Hughes and D.J. Macero; Inorg. Chim. Acta, 35, L369 (1979).

7. C. Mahon and W.L. Reynolds; Inorg. Chem., 6, 1927 (1967).

8. A.G. Motten, K. Hanck and M.K. DeArmond; Chem. Phys. Lett., 79, 541 (1981).

9. G.M. Bryant, J.E. Ferguson and H.K.J. Powell; Aust. J. Chem., 24, 257 (1971).

10. D.W. Fink and W.E. Ohnesorge; J. Am. Chem. Soc., 91, 4995 (1969).

11. A.D. Kirk, P.E. Hoggard, G.B. Porter, M.G. Rockley and M.W. Windsor; Chem. Phys. Lett., 37, 199 (1976).

12. C. Creutz, M. Chou, T L. Hetzel, M. Okumura and N. Sutin; J. Am. Chem. Soc., 102, 1309 (1980).

13. A.B.P. Lever; Inorganic Electronic Spectroscopy; Elsevier Publishing Company, Amsterdam, 1968a, p305b, p124.

14. T. Matsumura-Inoue and T. Tominaga-Morimoto; J. Electroanal. Chem., 93, 127 (1978).

15. I. Fujita and H. Kobayashi; Z. Phys. Chem. Neue Folge, 79, 309 (1972).

16. C.T. Lin and N. Sutin; J. Phys. Chem., 80, 97 (1976).

17. M.K. DeArmond, C.M. Carlin and W.L. Huang; Inorg. Chem., 19, 62 (1980).

18. S. Utsumo and F. Uchida; Rep. Fac. Sci., Shizuoka Univ., 7, 57 (1972).

19. N. Serpone, M.A. Jamieson, M.S. Henry, M.Z. Hoffman, F. Bolletta and M. Maestri; J. Am. Chem. Soc., 101, 2907 (1979).

20. V. Balzani, F. Bolletta, M.T. Gandolfi and Maestri; Top. Curr. Chem., 75, 1 (1978).

21. M. Maestri, F. Bolletta, L. Moggi, V. Balzani, M.S. Henry and M.Z. Hoffman; J. Am. Chem. Soc., 100, 2694 (1978).

22. A. Juris, M.F. Manfrin, M. Maestri and N. Serpone; Inorg. Chem., 17, 2258 (1978).

23. R. Ballardini, G. Varani, M.T. Indelli, F. Scandola and V. Balzani; J. Am. Chem. Soc., 100, 7219 (1978).

24. E. Konig and S. Herzog; J. Inorg. Nucl. Chem., 32, 585 (1970).

25. M.C. Hughes, J.M. Rao and D.J. Macero; Inorg. Chim. Acta, 35, L321 (1979).

26. T. Saji and S. Aoyagui; J. Electroanal. Chem., 63, 405 (1975).

27. I. Fujita, T. Yazaki, Y. Torii and H. Kobayashi; Bull. Chem. Soc. Jpn., 45, 2156 (1972).

28. Y. Kaisu, T. Yazaki, Y. Torii and H. Kobayashi; Bull. Chem. Soc. Jpn., 43, 2068 (1970).

29. J. Baker and B.N. Figgis; J. Chem. Soc. Dalton, 598 (1975).

30. T. Saji and S. Aoyagui; J. Electroanal. Chem., 63, 31 (1975).

31. T. Saji and S. Aoyagui; Chem. Lett., 203 (1974).

32. E. Konig and S. Herzog; J. Inorg. Nucl. Chem., 32, 601 (1970).

33. R. Pappalardo; Inorg. Chim. Acta, 2, 209 (1968).

34. O. Anderson; J. Chem. Soc. Dalton, 2597 (1972).

35. A. Wada, N. Sakabe and J. Tahaka; Acta. Cryst., B32, 1121 (1976).

36. N. Tanaka and Y. Sato; Inorg. Nucl. Chem. Lett., 4, 487 (1968).

37. N. Tanaka, T. Ogata and S. Niizuma; Inorg. Nucl. Chem. Lett., 8, 965 (1972).

38. S. Margel, W. Smith and F.C. Anson; J. Electrochem. Soc., 125, 241 (1978).

39. D.G. Holah, A.N. Hughes and B.C. Hui; Can. J. Chem., 55, 4048 (1977).

40. N. Tanaka and Y. Sato; Bull. Chem. Soc. Jpn., 41, 2059 (1968).

41. Y. Sato and N. Tanaka; Bull. Chem. Soc. Jpn, 41, 2064 (1968).

42. M.M. Morrison and D.T Sawyer; Inorg. Chem., 17, 333 (1978).

43. T. Saji and S. Aoyagui; J. Electroanal. Chem., 108, 223 (1980).

44. G. Kew, K. DeArmond and K. Hanck; J. Phys. Chem., 78, 728 (1974).

45. N. Sutin and C. Creutz; Adv. Chem. Ser., 168, 1 (1978).

46. F.H. Burstall and R.S. Nyholm, J. Chem. Soc., 3570 (1952).

47. D.A. Buckingham, F.P. Dwyer, H.A. Goodwin and A.M. Sargeson; Aust. J. Chem., 17, 325 (1964).

48. R.G. Bray, J. Ferguson and C.J. Hawkins; Aust. J. Chem., 22, 2091 (1969).

49. G.J. Sutton; J. Proceed. Aust. Chem. Inst., 16, 115 (1949).

50. F. Hein and S. Herzog; Z. Anorg. Allg. Chem., 267, 337 (1952).

51. S. Herzog; Z. Anorg. Allg. Chem., 294 , 155 (1958).

52. G.T. Morgan and F.H. Burstall; J. Chem. Soc., 2213 (1931).

APPENDIX I

ABBREVIATIONS

bipy	2,2'-bipyridine
CH_3CN	acetonitrile
CH_2CHCN	acrylonitrile
esr	electron spin resonance
nmr	nuclear magnetic resonance
py	pyridine
$TBABF_4$	tetrabutylammonium tetrafluoroborate
I	$[Ru(bipy)_3]^{2+}$
II	$[Ir(bipy)_3]^{3+}$
III	$[Ru(bipy)py_4]^{2+}$
IV	cis-$[Ru(bipy)_2py_2]^{2+}$
V	trans$[Ru(bipy)_2py_2]^{2+}$
VI	cis-$[Ru(bipy)_2Cl_2]$
VII	$[Ir(bipy)_2OH(bipy')]^{2+}$
VIII	$[Fe(bipy)_3]^{2+}$
IX	$[Os(bipy)_3]^{2+}$
X	$[Zn(bipy)_3]^{2+}$
XI	$[In(bipy)_3]^{3+}$
XII	$[Cr(bipy)_3]^{3+}$
XIII	$[V(bipy)_3]^{2+}$
XIV	$[Cu(bipy)_3]^{2+}$
XV	$[Ni(bipy)_3]^{2+}$
XVI	$[Co(bipy)_3]^{2+}$
XVII	$[Mn(bipy)_3]^{2+}$
ε	extinction coefficient ($l\,mol^{-1}\,cm^{-1}$)
ν	wavenumber (cm^{-1})
λ	wavelength (nm)

Spectro-electrochemical Studies on Tris-bipyridyl Ruthenium Complexes; Ultra-violet, Visible, and Near-infrared Spectra of the Series $[Ru(bipyridyl)_3]^{2+/1+/0/1-}$

By Graham A. Heath* and Lesley J. Yellowlees
(*Department of Chemistry, University of Edinburgh, Edinburgh* EH9 3JJ)
and Paul S. Braterman*
(*Department of Chemistry, University of Glasgow, Glasgow* G12 8QQ)

Reprinted from the Journal of The Chemical Society
Chemical Communications 1981

J.C.S. CHEM. COMM., 1981

Spectro-electrochemical Studies on Tris-bipyridyl Ruthenium Complexes; Ultra-violet, Visible, and Near-infrared Spectra of the Series $[Ru(bipyridyl)_3]^{2+/1+/0/1-}$

By GRAHAM A. HEATH* and LESLEY J. YELLOWLEES
(*Department of Chemistry, University of Edinburgh, Edinburgh* EH9 3JJ)
and PAUL S. BRATERMAN*
(*Department of Chemistry, University of Glasgow, Glasgow* G12 8QQ)

Summary The *in situ* electrochemical reduction of $[Ru(bipy)_3]^{2+}$ allows comparison of absorption spectra for the series of tris-bipyridyl complexes $[Ru(bipy)_3]^z$ with $z = 2+$, $1+$, 0, and $1-$.

IN common with other tris-bipyridyl complexes, $[Ru(bipy)_3]^{2+}$ (**1**, $z = 2+$) shows a rich redox chemistry, and voltammetric studies have established an extended

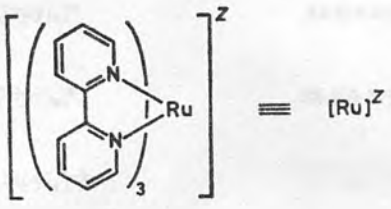

(1)

sequence of reversible one-electron reduction steps at narrowly spaced potentials, as well as a metal-based oxidation (Table 1).[1,2] The absorption and luminescence spectra of $[Ru(bipy)_3]^{2+}$ have received considerable study, partly owing to this compound's prominence in discussion of suitable redox-active dyes for photogalvanic devices, and in the photocatalysed splitting of water.[3] $[Ru(bipy)_3]^{1+}$ is an intermediate in the reductive quenching of $^*[Ru(bipy)_3]^{2+}$ and there are varying descriptions of the structure and origin of its intense visible absorption.[4-8] $[Ru(bipy)_3]^0$ efficiently reduces H_2O to H_2, in contrast to $[Ru(bipy)_3]^+$,[9] and there is an earlier report of electrogeneration of $[Ru(bipy)_3]^0$ and $[Ru(bipy)_3]^{1-}$.[2] However, no spectroscopic data have been published for these lower-oxidation state species.

TABLE 1. Electrode potentials for $[Ru(bipy)_3]^z$, $E°$/V.[a]

$[Ru]^{3+}$	$\longrightarrow$	$[Ru]^{2+}$	$\longrightarrow$	$[Ru]^{1+}$	$\longrightarrow$	$[Ru]^0$	$\longrightarrow$	$[Ru]^{1-}$	$\longrightarrow$	$[Ru]^{2-}$ [b]
	−1·06		−1·24		−1·49		−2·17			

[a] *Vs.* standard hydrogen electrode (S.H.E.). [b] $[Ru(bipy)_3]^{2-}$ is short-lived, releasing bipy.[2]

We now report that controlled electrochemical reduction of $[Ru(bipy)_3]^{2+}$ in an optically transparent cell has enabled us to determine the absorption spectra of the individual low-valent complexes over a wide range. A very simple progression in the spectra emerges, and provides fresh insight into the electronic structure of the reduced species.

Solutions of $[Ru(bipy)_3][BF_4]_2$ (1 mmol l^{-1}) in dry acetonitrile, propylene carbonate, or dimethyl sulphoxide containing 0·1 M Bu_4NBF_4 were purged with argon and reduced at a gold minigrid optically transparent thin-layer electrode[10] mounted in a gas-tight poly(tetrafluoroethylene) cell block in the spectrometer beam (Unicam SP800 and Beckman 5270). Steady-state spectra for (**1**) with $z = 1+$, 0, and $1-$, at applied potentials of −1·2, −1·4, and −1·7 V respectively (*vs.* S.H.E.), were recorded in the range 40,000—7,000 cm^{-1} using a Metrohm E506 potentiostat.

A notable finding in the present study is that the fully reduced species $[Ru(bipy)_3]^{1-}$ shows a detailed resemblance

in band positions and structure to $[Mo(CO)_4(bipy)]^{1-}$ and Na(bipy), which both contain the chelated $bipy^-$ radical anion.[11,12] It is also apparent from the tabulated data, and particularly from the Figure, that the stepwise reduction is accompanied by *progressive* growth of the bands which typify $[Ru(bipy)_3]^{1-}$, and by matching loss of the bands characterising $[Ru(bipy)_3]^{2+}$, with only minor frequency shifts. In the richer spectra associated with the intermediate complexes, both sets of bands are evidently present. This behaviour is difficult to reconcile with charge-averaged models arising from population of delocalised molecular orbitals spanning three ligands in D_3 symmetry.

On the evidence of the number, position, structure, and intensity of the observed spectral features the reduced ruthenium complexes are most realistically formulated with distinct bipy and $bipy^-$ ligands, *i.e.* as $[Ru(bipy)_2(bipy^-)]^{1+}$, $[Ru(bipy)(bipy^-)_2]^0$, and $[Ru(bipy^-)_3]^{1-}$, respectively. It is then possible to make general assignments of the observed bands in every case, as indicated in Table 2. For example, the prominent band envelope near 20,000 cm^{-1} for $[Ru(bipy)_3]^{1+}$ is dominated by $bipy^-$ internal $\pi\rightarrow\pi^*$ transitions with M→L($bipy^0$) charge transfer providing only a high energy shoulder,† contrary to previous assignments.[4-8] It also follows that a trapped-electron model $[Ru^{III}(bipy)_2(bipy^-)]^{2+}$ deserves consideration in relation to the spectrum of $^*[Ru(bipy)_3]^{2+}$ which resembles that of Na(bipy) in crucial respects, though a delocalised model has been preferred.[13]

Our observations indicate that $[Ru(bipy)_3]^0$ is a diradical, contrary to the diamagnetic formulation proposed on the basis of early e.s.r. results and a delocalised model.[2] In the case of successive reductions of $[Ir(bipy)_3]^{3+}$, Hanck and his co-workers have drawn similar conclusions from the spacing of the electrode potentials.[14] We note that a similar E^0 sequence exists for $[Ru(bipy)_3]^{2+}$.‡

Interestingly, the lower-valent ruthenium complexes are subject to continuous thermal bleaching (reversion to $[Ru(bipy)_3]^{2+}$) under the experimental conditions of near-i.r. irradiation. Studies are continuing in order to provide extinction coefficients and a definitive near-i.r. spectrum of $[Ru(bipy)_3]^{1-}$, though the trend in spectral features is

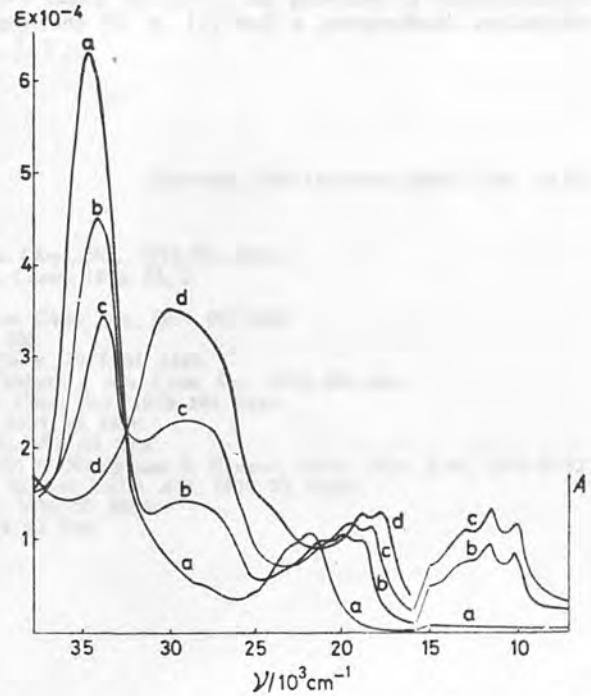

FIGURE. Absorption spectra of $[Ru(bipy)_3]^z$ complexes: (a) $z = 2+$; (b) $z = 1+$; (c) $z = 0$; (d) $z = 1-$; complexes dissolved in dimethyl sulphoxide (u.v.–visible region, ϵ = optical extinction coefficient in $mol^{-1}\ dm^3\ cm^{-1}$) and propylene carbonate (near-i.r. region, A = relative absorbance in arbitrary units).

TABLE 2. Absorption bands in tris-bipyridyl ruthenium complexes; $\nu/10^3\ cm^{-1}$ ($\epsilon \times 10^{-4}$).

	$\pi\rightarrow\pi^*$, bipy	$\pi\rightarrow\pi^*$, $bipy^-$	M→L, bipy	$\pi\rightarrow\pi^*$, $bipy^-$	$\pi\rightarrow\pi^*$, $bipy^-$
$[Ru(bipy)_3]^{2+}$	35·0(6·12)	—	22·0(1·11)	—	—
$[Ru(bipy)_3]^{+}$	34·2(4·44)	29·2(1·43)[a]	21·1(1·01)	19·9(1·09) 18·9(1·04)	12·8 11·5 10·1
$[Ru(bipy)_3]^{0}$	33·8(3·47)	29·0(2·29)[a]	20·8(sh)	19·5(1·20) 18·4(1·18)	12·7 11·1 10·0
$[Ru(bipy)_3]^{-}$[b]	—	29·8(3·50)[a]	—	18·9(1·26) 18·0(1·28)	not established
Na(bipy)–tetrahydrofuran[12c]	—	25·9(2·95)	—	18·8(0·62) 17·8(0·65)	13·3(0·11) 12·0(0·15) 10·5(0·13)

[a] Probably includes M→L($bipy^-$) near 30,000 cm^{-1}, consistent with greater breadth *cf.* Na(bipy)[12] and $[Al(bipy)_3]$.[12c] [b] The shoulder near 24,000 cm^{-1} is also present in Na(bipy).[12]

† The absorption curve for electrogenerated $[Ru]^{1+}$ described elsewhere[5] can be simulated by incomplete reduction or by controlled partial reversion to $[Ru]^{2+}$; isosbestic points coincide exactly with those reported.

‡ *Added in proof:* Independent e.s.r. studies for $[Ru]^z$ ($z < 2$) now support a localised model (K. W. Hanck, A. G. Motten, and K. DeArmond, to be published). We thank Professor Hanck for his personal communication.

clear. Very recently, Elliot has reported near-i.r. (only) spectro-electrochemical data for the more stable series of substituted complexes $[Ru\{4,4'\text{-}(CO_2Et)_2bipy\}_3]^z$ (z = 2+, 1+, 0, 1−) which show progressive growth of analogous intense bands near 7,000 cm^{-1}.[15] An unusual inter-ligand charge-transfer was suggested but these bands should now be reassigned as localised $\pi \rightarrow \pi^*$ transitions of the radical bipyridyl anion, as in the parent compounds.

We thank the S.R.C. for provision of electrochemical equipment (G. A. H.) and a postgraduate studentship (L. J. Y.).

(*Received, 29th December* 1980; *Com.* 1372.)

[1] T. Saji and S. Aoyagui, *J. Electroanal. Chem.*, 1975, **58**, 401.
[2] N. E. Tokel-Takvoryan, R. E. Hemingway, and A. J. Bard, *J. Am. Chem. Soc.*, 1973, **95**, 6582.
[3] V. Balzani, F. Bolletta, M. T. Gandolfi, and M. Maestri, *Top. Curr. Chem.*, 1978, **75**, 1.
[4] C. Creuz and N. Sutin, *J. Am. Chem. Soc.*, 1976, **98**, 6384.
[5] C. P. Anderson, D. J. Salmon, T. J. Meyer, and R. C. Young, *J. Am. Chem. Soc.*, 1977, **99**, 1980.
[6] M. Maestri and M. Gratzel, *Ber. Bunsenges. Phys. Chem.*, 1977, **81**, 504.
[7] D. Meisel, M. S. Matheson, W. A. Mulac, and J. Rabani, *J. Phys. Chem.*, 1977, **81**, 1449.
[8] Q. G. Mulazzani, S. Emmi, P. G. Fuochi, M. Z. Hoffman, and M. Venturi, *J. Am. Chem. Soc.*, 1978, **100**, 981.
[9] H. D. Abruna, A. X. Teng, G. J. Samuels, and T. J. Meyer, *J. Am. Chem. Soc.*, 1979, **101**, 6745.
[10] R. W. Murray, W. R. Heineman, and G. W. O'Dom, *Anal. Chem.*, 1967, **39**, 1666.
[11] Y. Kaizu, I. Fujita, and H. Kobayashi, *Z. Phys. Chem.* (*Frankfurt*), 1972, **79**, 298.
[12] (a) C. Mahon and W. L. Reynolds, *Inorg. Chem.*, 1967, **6**, 1297; (b) E. König and S. Kremer, *Chem. Phys. Lett.*, 1970, **5**, 87; (c) Y. Torii, S. Murasato, and Y. Kaizu, *Nippon Kagaku Zasshi*, 1970, **91**, S49; *Chem. Abs.*, 1970, **73**, 93426.
[13] Reference **3**, p. 35; G. A. Crosby and W. H. Elfrin, *J. Phys. Chem.*, 1976, **80**, 2206.
[14] J. L. Kahl, K. W. Hanck, and K. DeArmond, *J. Phys. Chem.*, 1978, **82**, 540.
[15] C. M. Elliot, *J. Chem. Soc., Chem. Commun.*, 1980, 261.

LIGAND-LIGAND INTER-VALENCE CHARGE TRANSFER ABSORPTION IN REDUCED RUTHENIUM(II) BIPYRIDINE COMPLEXES

G.A. HEATH* and L.J. Yellowlees

Chemistry Department, King's Buildings,
University of Edinburgh, Edinburgh EH9 3JJ

P.S. BRATERMAN

Chemistry Department, University of
Glasgow, Glasgow G12 8QQ

Chemical Physics Letters - 92, 646 (1982)

An electronic absorption band at 4000 cm^{-1} in incompletely reduced Ru(II)-bipyridine and Ru(II)-bipyridine-pyridine complexes is characteristic of co-existing bpy^{o} and bpy^{-} ligands and assigned to bpy^{-}/bpy^{o} IVCT.

1. Introduction

Recent spectro-electrochemical studies [1] have provided convincing evidence that stepwise reduction of $[Ru(bpy)_3]^{2+}$ (I) according to Equation 1 yields complexes with localised charge distributions, viz, $[Ru(II)bpy^{o})_2(bpy^{-})]^{+}$ (I^{-}), $[Ru(II)(bpy^{o})(bpy^{-})]^{o}$ (I^{2-}), and ultimately $[Ru(II)(bpy^{-})_3]^{-}$ (I^{3-}).† Thus electronic transitions are observed which are due separately to coordinated bpy^{o} and bpy^{-} (I^{-}, I^{2-}), or to coordinated bpy^{-} alone (I^{3-}), and these conclusions are supported by independent e.s.r. data for I^{-} and I^{3-} [2].

(Equation 1 here please)

The simultaneous presence of discrete bpy^{o} and bpy^{-} groups implies the possibility of ligand-ligand inter-valence charge transfer (IVCT) phenomena. Indeed Hanck and co-workers [2] have attributed the notably temperature-

† bpy = 2,2'-bipyridine; py = pyridine.

dependent line broadening found in their e.s.r. spectrum of $\underset{\sim}{I}^-$, but absent for $\underset{\sim}{I}^{3-}$, to just such a process, with an estimated thermal barrier to electron hopping of ca. 1000 cm^{-1}.

This barrier E_{th} corresponds to the intersection of the potential energy curves of equivalent valence isomers; Hush [3] has shown that where the curves are quadratic in form and there is negligible interaction between the redox active centres the vertical (IVCT) transition energy E_{op} should be $4E_{th}$.

Accordingly, we have extended our spectro-electrochemical studies to encompass the near-i.r. absorption spectra (7000-3500 cm^{-1}) of the sequence $\underset{\sim}{I}$ to $\underset{\sim}{I}^{3-}$, and other, closely related, species.

2. Results and Discussion

A weak band near 4000 cm^{-1} (see Table) is detected for the species $[Ru(II)(bpy^{o})_{3-n}(bpy^{-})_{n}]^{2-n}$ when n = 1 or 2 ($\underset{\sim}{I}^-$, $\underset{\sim}{I}^{2-}$), but <u>not</u> when n = 0 or 3($\underset{\sim}{I}$, $\underset{\sim}{I}^{3-}$), and we ascribe this to the bpy/bpy^- IVCT transition. As far as we know, this is the first reported direct observation of such a transition between identical ligands.

We have also examined the behaviour of partly-substituted analogues of $\underset{\sim}{I}$, <u>cis</u>-$[Ru(bpy)_2(py)_2]^{2+}$ (<u>cis</u>-$\underset{\sim}{II}$) and $[Ru(bpy)(py)_4]^{2+}$ ($\underset{\sim}{III}$), and of the structurally distinct <u>trans</u>-$[Ru(bpy)_2(py)_2]^{2+}$ (<u>trans</u>-II), and their corresponding reduced forms, according to Equations 2 and 3. These species are all inert to

(Equations 2, 3 near here please)

solvolysis and geometric isomerism on our electrochemical timescales, and the voltammetric data and u.v.-visible absorption spectra [4] are again fully consistent with separately absorbing coordinated bpy^{o} and bpy^{-} chromophores. We find (see Table) that only those complexes containing <u>both</u> bpy^{o} and bpy^{-} (i.e. I^-, I^{2-}, <u>cis</u>-$\underset{\sim}{II}^-$ and <u>trans</u>-$\underset{\sim}{II}^-$) exhibit the characteristic near-infrared band. For example, $\underset{\sim}{III}^-$ is featureless in this region in contrast to isovalent II^- and I^-, and II^{2-} is featureless in contrast to I^{2-}.

The IVCT band is in all cases relatively broad (FWHM $\sim$ 2000 cm^{-1}) and weak. It is decidedly more intense in I^- and I^{2-} than in cis- or trans-II^-, which have only one donor and one acceptor centre. The slight but significant differences between cis- and trans-II^- are presumably due to the different mutual arrangements of the chelating ligands.

We conclude that the incompletely reduced complexes $[Ru(bpy)_3]^{+,o}$ and $[Ru(bpy)_2(py)_2]^+$ do indeed contain Ru(II) and distinct co-existing bpy^o and bpy^- ligands and exhibit low intensity IVCT transitions in accord with this formulation. These complexes are therefore mixed-valence compounds showing electron-transfer between negligibly interacting ligand sites, in general agreement with Hush's theory [3] for such systems, which has been more usually applied to adjacent metal sites in binuclear or polynuclear compounds.

We have recently shown [5] that the absorption spectrum of the thermally equilibrated excited state, I^*, in the range 250-650 nm can be understood in terms of the formulation $[Ru(III)(bpy^o)_2(bpy^-)]^{2+}$ with distinct bpy^o and bpy^- chromophores. Accordingly there is an analogy between electrochemical and MLCT reduction of the ligand array, and our detection of the intervalence process in I^- lends qualified support to Woodruff's hypothesis [6] that I^* could show such a band. By characterising typical IVCT transitions near 4000 cm^{-1}, with $\varepsilon \sim 200$ $\ell mol^{-1} cm^{-1}$ (and particularly since Ir(III) reduced-bipyridyl complexes give similar results [4]), the present data make clear that observation of the intervalence absorption band in I^* itself will present extreme difficulty.

3. Experimental

$Ru(bpy)_3Cl_2$ was purchased from G.F. Smith Inc., converted to the BF_4^- salt, and recrystallised from acetonitrile, while trans-II and III perchlorates were prepared by the method of Krause [7], and pure cis-II perchlorate by treatment of cis-$[Ru(bpy)_2Cl_2]$ [8] with pyridine followed by aqueous $NaClO_4$. Spectroelectrochemical data were collected as in our earlier work [1], using a Metrohm E506 potentiostat and an optically transparent thin layer electrode

cell. Careful correction for solvent background is critical, because of solvent vibrational combination bands, and was performed by direct subtraction. All compounds were studied in dimethylsulphoxide; in addition, I and its reduction products were studied in dimethylformamide and in acetonitrile, with indistinguishable results.

Acknowledgements

We thank Napier College, Edinburgh for access to their Beckman 5270 spectrometer, and S.E.R.C. for a postgraduate studentship (to LJY) and provision of electrochemical equipment.

References

[1] G.A. Heath, L.J. Yellowlees, and P.S. Braterman, J. Chem. Soc., Chem. Commun. (1981) 287.

[2] A.G. Motten, K. Hanck, and M.K. DeArmond, Chem. Phys. Lett. 79 (1981) 541.

[3] N.S. Hush, Prog. Inorg. Chem. 8 (1967) 391.

[4] G.A. Heath, L.J. Yellowlees, and P.S. Braterman, to be published.

[5] P.S. Braterman, A. Harriman, G.A. Heath, and L.J. Yellowlees, in preparation.

[6] P.G. Bradley, N. Kress, B.A. Hornberger, R.F. Dallinger, and W.H. Woodruff, J. Am. Chem. Soc., 103 (1981) 7441.

[7] R.A. Krause, Inorg. Chim. Acta 22 (1977) 209.

[8] B.P. Sullivan, D.J. Salmon, and T.J. Meyer, Inorg. Chem. 17 (1978) 3334.

Equations

$$\underset{\underset{\sim}{I}}{[Ru(bpy)_3]^{2+}} \overset{\pm e^-}{\rightleftharpoons} \underset{\underset{\sim}{I^-}}{[Ru(bpy)_3]^{+}} \overset{\pm e^-}{\rightleftharpoons} \underset{\underset{\sim}{I^{2-}}}{[Ru(bpy)_3]^{o}} \overset{\pm e^-}{\rightleftharpoons} \underset{\underset{\sim}{I^{3-}}}{[Ru(bpy)_3]^{-}} \qquad (1)$$

$$\underset{\underset{\sim}{II}}{[Ru(bpy)_2(py)_2]^{2+}} \overset{\pm e^-}{\rightleftharpoons} \underset{\underset{\sim}{II^-}}{[Ru(bpy)_2(py)_2]^{+}} \overset{\pm e^-}{\rightleftharpoons} \underset{\underset{\sim}{II^{2-}}}{[Ru(bpy)_2(py)_2]^{o}} \qquad (2)$$

$$\underset{\underset{\sim}{III}}{[Ru(bpy)(py)_4]^{2+}} \overset{\pm e^-}{\rightleftharpoons} \underset{\underset{\sim}{III^-}}{[Ru(bpy)(py)_4]^{+}} \qquad (3)$$

Table. Intervalence Charge Transfer Bands in $[Ru(II)(bpy^{o})_{x-n}(py)_{6-2x}]^{2-n}$ Complexes ($x = 2, 3$; $o<n<x$)

Species	ν (cm^{-1})	ε ($\ell mol^{-1} cm^{-1}$)	$10^4 f$ [a]
$[Ru(bpy)_3]^{+}$	4500	210	19.3
$[Ru(bpy)_3]^{o}$	4500	345	31.7
cis-$[Ru(bpy)_2(py)_2]^{+}$	4350	121	8.6
trans-$[Ru(bpy)_2(py)_2]^{+}$	4090	100	3.2

(a) Taking $f = 4.6 \times 10^{-9}$ ε x FWHM

COURSES ATTENDED

Inorganic Chemistry - Third Year Undergraduate Lectures

Inorganic Chemistry - Fourth Year Undergraduate Lectures

Elementary Computer Programming Methods - Dr C. Pounder

Mathematical Methods - Dr C. Pounder

Homogeneous Catalysis - Dr T.A. Stephenson

Photoelectrochemistry - The Royal Society of Chemistry, Faraday Division, General Discussion No. 70, 1980.

University of Strathclyde Inorganic Club Conferences, 1980, 1981, 1982.

Departmental and Research Seminars and Colloquia